The physiological and epigenetic effects of dynamic light acclimation in *Arabidopsis thaliana*

Robyn Abigail Emmerson

A thesis submitted for the degree of Doctor of Philosophy in Biological Sciences

School of Life Sciences

University of Essex

October 2022

Abstract

The majority of the world's crops are grown outdoors, covering 1.6 billion hectares of land, where they are subjected to dynamic light conditions. Plant light acclimation has been extensively studied, but lesser understanding on physiological processes from the impact of dynamic light fluctuations. Understanding the impact of fluctuating light on photosynthesis, and how plants acclimate is key for improving plant light responses and could allow identification of novel targets for crop improvements.

Previous work demonstrated that naturally fluctuating regimes reduced photosynthetic efficiency and increased net CO_2 assimilation in *Arabidopsis thaliana*. Utilising these same regimes, results were replicated to demonstrate phenotypic consistency. This was key to investigating epigenetic change where a consistent phenotype indicated consistent epigenetic change. Assessment of differential methylation between square and fluctuating light regimes, more typical in field environments, demonstrated widespread changes in DNA methylation, with a subset of these methylated regions also relating to changes in transcription.

The oxidation and reduction state have a role in regulating photosynthesis. To further understand this regulation under fluctuating light *cp12-1/2/3* knockdown/knockout lines were grown under differing light regimes and the reduced expression of CP12 assessed. The physiological assessment of these plants showed reduction in CP12 expression which negatively impacted fluctuating light acclimation, with reductions in assimilation rates and increased non-photochemical quenching.

These findings illustrate that naturally fluctuating light has multiple consequences for plants which can be regulated by DNA methylation. Importantly, it further demonstrates that square light regimes are not reflective of field environments, with changes in DNA methylation and expression providing some explanation to these mechanisms. Furthermore, it suggests the need to consider how plants are grown, particularly if translating results into agricultural settings. Finally, this work provides a suite of genes which could be targeted to improve responses to fluctuating light, potentially improving crop yields.

Acknowledgements

Firstly, I would like to thank my supervisors Prof Tracy Lawson and Dr Radu Zabet. Tracy, without your guidance, patience, and kindness, I do not think I could have done this. You changed my life by giving me this opportunity and I will be forever grateful. Radu, you have always been so encouraging with my genomics progress and understanding whenever I hit a wall. Without you both, this thesis would not be what it is.

To the rest of the Lawson lab, past and present, without your support this would not have been as fun at it was. During the pandemic, you were my encouragement and only contact with the real world and made a bad situation just a little bit easier. Special thanks for Dr Phil Davey, for always being there to help with anything and being an all-round lab dad to me, and to Dr Jack Matthews and Dr Martin Battle for all their help and advice over the years. I am proud to have had you as colleagues, and lucky to have you as my friends. This work also benefitted hugely from the advice and help of Olivia Grant- your bioinformatics guidance was invaluable, particularly in the moments where I felt like I'd tried everything, I can't thank you enough for your help. My thanks to the rest of the Plant Group at Essex, for always asking the difficult questions and pushing me to be a better scientist, this experience would not be complete without you.

I would also like to thank all my friends and family for their support. My mum for always encouraging me to follow what I wanted (no matter how far away that takes me), and my grandparents for their continued support. To Liam for understanding and supporting me through everything and joining me on every adventure. To Holly for always being there when I need her the most and being the best friend I could have ever asked for. Finally, my gratitude to everyone else who has helped me through the years to reach this point- this would not have been possible without all of you.

I am grateful to the University of Essex for their generous financial support throughout this project

Table of Contents

Abstract i
Acknowledgements ii
Table of Contents iii
List of Abbreviations vi
List of Figures ix
List of Tables xi
1. Chapter 1: Introduction 12
1.1. Introduction 13
1.2. Epigenetics in Plants 20
1.2.1. DNA methylation 20
1.2.2. Histone Modification 32
1.2.3. Transgenerational Epigenetic Inheritance 37
1.2.4. Epigenetics in Context 43
1.2.5. Whole Genome Bisulfite Sequencing 50
1.3. Impacts of Light on Plant Physiology 52
1.3.1. Effects of Light Acclimation 52
1.3.2. Photoinhibition 62
1.3.3. Fluctuating Light 65
1.4. Aims and Objectives 68
2. Chapter 2: General Materials and Methods 69
2.1. Plant Materials 70
2.2. Arabidopsis Growth Conditions 70
2.2.1. Germination Conditions 70
2.2.2. Fluctuating Light Acclimation 70
2.3. Physiological Measurements 71
2.3.1. Chlorophyll Fluorescence Imaging 71
2.3.2. Leaf Gas Exchange 72
2.4. DNA Methylation Analysis 73
2.4.1. DNA extraction- CTAB method 73
2.4.2. Whole Genome Bisulfite Sequencing 74
2.4.3. Computational Analysis 75
2.5. RNA Sequencing Analysis (RNAseq) 76
2.5.1. RNA extraction 76
2.5.2. RNA sequencing 76
2.5.3. Computational Analysis 77

2.6. Quantitative Reverse Transcriptase PCR (RT-qPCR) 77
2.6.1. RNA Extraction 77
2.6.2. RT-qPCR 78
2.7. Statistical Analysis 78
3. Chapter 3: Characterising the photosynthetic phenotype of Arabidopsis thaliana grown under fluctuating light 79
3.1. Introduction 80
3.2. Materials and Methods 87
3.2.1. Plant Material and Growth Conditions 87
3.2.2. Tracking Plant Growth 87
3.2.3. Stomatal Impressions 87
3.2.4. Leaf Gas Exchange 88
3.2.5. Chlorophyll Fluorescence Imaging 88
3.3. Results 89
3.3.1. Impact of light regime on growth and stomatal density 89
3.3.2. Chlorophyll Fluorescence analysis revealed ongoing acclimation of photosynthesis 92
3.3.3. Differences in photosynthetic capacity show impact of acclimation to fluctuating light 100
3.3.4. Light regime effects carbon assimilation under changing light 102
3.4. Discussion 106
4. Chapter 4: The effects of fluctuating light acclimation on DNA methylation in Arabidopsis thaliana 115
4.1. Introduction 116
4.2. Materials and Methods 120
4.2.1. Plant Material 120
4.2.2. DNA methylation data analysis 120
4.2.3. RNA analysis 121
4.3. Results 123
4.3.1. Acclimation to fluctuating light results in global changes to the methylome 123
4.3.2. Transposable element methylation is affected by light acclimation 131
4.3.3. RNA sequencing reveals a role of DNA methylation in light acclimation 135
4.3.4. Differential methylation and gene expression resulting from growth light acclimation are correlated 139

4.3.5. Differential transcription of photosynthetic genes was revealed in RNA sequencing data 159
4.4. Discussion 161
5. Chapter 5: Acclimation of Arabidopsis thaliana mutant *cp12-1/2/3* to fluctuating light 171
5.1. Introduction 172
5.2. Materials and Methods 177
5.2.1. Plant Material and Growth Conditions 177
5.2.2. Fluctuating Light Plant Material and Growth 177
5.2.3. Leaf Gas Exchange 178
5.2.4. Chlorophyll fluorescence imaging 178
5.2.5. cp12-1/2/3 RNA extraction and qPCR 180
5.2.6. Statistics 180
5.3. Results 181
5.3.1. RT-qPCR confirms knockout or severe knockdown of all three CP12 genes 181
5.3.2. Chlorophyll fluorescence imaging suggest lack of CP12 affects acclimation to fluctuating light 183
5.3.3. CP12 knockdown results in high levels of energy dissipation via NPQ 189
5.3.4. Infrared gas exchange shows significant differences in carbon assimilation in CP12 knockdowns and those acclimated to fluctuating light 193
5.4. Discussion 199
6. Chapter 6: General Discussion 204
7. Chapter 7: Bibliography 219
8. Chapter 8: Supplementary Data 258

List of Abbreviations

A/Ci	Curve measuring the change in carbon assimilation as a function of changing internal carbon dioxide
A_{max}	Maximum assimilation
Anova	Analysis of variance
A/Q	Curve measuring the change in carbon assimilation as a function of increasing light intensity in PPFD (µmol m^{-2} s^{-1})
ATP	Adenosine Triphosphate
CBB cycle	The Calvin-Benson-Bassham cycle
CpG	Cytosine [C] in context where cytosine is next to guanine [G]
CpHpG	Cytosine [C] in context where it precedes any base other than guanine [G] (i.e., H= thymine [T] or adenine [A]) which is followed by a G
CpHpH	Cytosine in the context where it is followed by two non-guanine [G] bases, i.e., adenine [A] or thymine [T]
CO_2	Carbon dioxide
Col-0	*Arabidopsis thaliana* ecotype Colombia-0
CP12	Small redox sensitive protein, localised to the chloroplast
cp12-1/2/3	Triple knockdown of CP12-1, 2, and 3
DEG	Differentially Expressed Gene

DMR	Differentially Methylated Region
DNA	Deoxyribonucleic Acid
EEE	Excess Excitation Energy
ETC	Electron transport chain
FL	Fluctuating light
FLH	Fluctuating high light
FLL	Fluctuating low light
$F_q'/F_{m'}$	Maximum PSII operating efficiency
F_q'/F_v'	Photochemical Quenching
F_v/F_m	Maximum quantum efficiency of PSII in the dark
F_v'/F_m'	Maximum quantum efficiency of PSII in the light
g_{sw}	Stomatal Conductance to water
HL	High light
IRGA	Infrared Gas Analyser
LL	Low light
log2FC	Log2 Fold Change
NADPH	Nicotinamide adenine dinucleotide phosphate
NPQ	Non-Photochemical Quenching
PPFD	Photosynthetic Photon Flux Density, measured in μmol m^{-2} s^{-1}
PSI	Photosystem I

PSII	Photosystem II
qP	Photochemical Quenching
SE	Standard Error
SQ	Square light
SQH	Square high light (460 µmol m^{-2} s^{-1})
SQL	Square low light (230 µmol m^{-2} s^{-1})
TEs	Transposable elements
Trxs	Thioredoxins
RdDM	RNA directed DNA Methylation
RNA	Ribonucleic Acid
RNAi	RNA interference
RNAseq	mRNA sequencing
RT-qPCR	Quantitative reverse transcriptase PCR
RuBP	Ribulose 1,5-bisphosphate
WGBS	Whole Genome Bisulfite Sequencing
WT	Wild type, *Arabidopsis thaliana* Col-0

List of Figures

Figure 1.1: Generic signalling pathway resulting in epigenetic change. 18
Figure 1.2:Schematic demonstrating possible chemical modifications to DNA and histones, ultimately resulting in modified gene expression.) 19
Figure 1.3: Cytosine can be methylated on the 5' carbon by a DNA methyltransferase 20
Figure 1.4: The three different methylation pathways that result in cytosine methylation in plants. 21
Figure 1.5: Schematic of the RNA directed DNA methylation pathway. 22
Figure 1.6: The wrapping of DNA around the core histone octamer to form a nucleosome. 33
Figure 1.7: Amino acid sites of the core histones which are susceptible to covalent modification. 34
Figure 1.8: Sexual vs asexual reproduction and the retention of methylation from parental tissues. 41
Figure 1.9: Schematic of whole genome bisulfite sequencing. 51
Figure 1.10: Demonstrated increase in the Rubisco content with increased irradiance in *Arabidopsis thaliana*. From Bailey *et al.*, 2001 54
Figure 1.11: Leaf cross sections demonstrating the effect of low and high light on leaf morphology in wild type *Arabidopsis thaliana*. 59
Figure 1.12: Simple proposed model of the inhibition and damage caused by ROS on PSII 63
Figure 1.13: Diurnal light regimes utilised by Vialet-Chabrand *et al*. (2017) 67
Figure 2.1: Diurnal light regimes utilised in this study. 71
Figure 3.1: Schematic of the field of view (1mm^2) movement used to measure stomatal density. 88
Figure 3.2: Growth phenotypes of *Arabidopsis thaliana* under square and fluctuating light regimes after 16 days if light exposure. 90
Figure 3.3: Growth of *Arabidopsis* exposed to each of the four light regimes in terms of visible leaf area of the whole rosette 91
Figure 3.4: Variation (box and whiskers plot showing the distribution of replicates) of stomatal densities per mm^2 92
Figure 3.5: Chlorophyll fluorescence imaging of *A.thaliana* on day 0 and day 18 of light regime exposure. 94
Figure 3.6: Chlorophyll fluorescence imaging on day 0 and day 18 of the time series indicates that light regime alters photosynthetic efficiency 95
Figure 3.7: Variation (box and whiskers plot showing the variation of replicates) of the maximum quantum efficiency of PSII (F_v/F_m) after the first pulse in chlorophyll fluorescence imaging 96
Figure 3.8: Time series of chlorophyll fluorescence over a 21-day period at PPFD=1000 µmol m^{-2} s^{-1} (**A-C**) and t=12 (**D**). 99
Figure 3.9: The effects of changing internal carbon dioxide concentration on photosynthesis in plants grown under four light treatments 101
Figure 3.10: The effect of changing Photosynthetic Photon Flux Density (PPFD; µmol m^{-2} s^{-1}) on photosynthesis in plants grown under one of four light treatments; SQH, SQL, FLH, FLL 105
Figure 4.1: Low resolution profiles for *Arabidopsis thaliana* chromosome in each sequence context. 124

Figure 4.2: Results of differential methylation analysis using DMRcaller, demonstrating genome wide changes in methylation 126
Figure 4.3: Heatmaps of differentially methylated genes in each regime comparison 129
Figure 4.4: Venn diagram of all differentially methylated coding genes and transposable elements 131
Figure 4.5: Proportion of transposable element genes differentially methylated, separated by Class 132
Figure 4.6: Pie charts of transposable element (TEs) which were differentially methylated under different light regimes grouped by family 133
Figure 4.7: Enrichment analysis of each transposable element family subject to differential methylation under different growth light comparisons. Data shows the log_2[observed/expected]. 134
Figure 4.8: Principal component analysis (PCA) plot of RNAseq data demonstrating the similarity in transcription between replicates of plants exposure to each of the four light regimes 136
Figure 4.9: Heatmap of differentially expressed genes in transcripts per million (TPM) between samples of each light regime 137
Figure 4.10:: Volcano plots of RNAseq data for each context comparison 138
Figure 4.11: Venn diagram of differentially expressed genes according to RNAseq data. 139
Figure 4.12: Venn diagrams of the overlaps between differentially methylated regions (DMRs) and differentially expressed genes (DEGs). 140
Figure 4.13: Venn diagrams of the differentially methylated and expressed genes between light regimes according to WGBS and RNAseq respectively. 141
Figure 4.14: Heatmap of the log2-fold change in expression of photosynthetic genes according to RNA sequencing data 160
Figure 5.1: The role of CP12, PRK, and GAPDH in the Calvin-Benson Cycle. 173
Figure 5.2: Diurnal light regimes utilised in this study 178
Figure 5.3: qRT-PCR analysis of *cp12-1/2/3* lines and associated genes to determine knockdown status and the effect of light regime relative to the respective wild type 182
Figure 5.4: Chlorophyll fluorescence imaging of photosynthetic induction (F_q'/F_m') and relaxation (F_v/F_m) in CP12 *RNAi* knockdown *A.thaliana*. 184
Figure 5.5: Chlorophyll fluorescence imaging of light response curve at day 7 of exposure to square (SQL) or fluctuating (FLL) light in *cp12-1/2/3* knockdown line 186
Figure 5.6: Breakdown of F_q'/F_m' (Fig. 5.5) into its constituent parameters 188
Figure 5.7: Induction and relaxation of non-photochemical quenching (NPQ) in *cp12-1/2/3* mutant lines 190
Figure 5.8: The effect of fluctuations in light from 200 µmol m^{-2} $s^{-1}$to 1000 µmol m^{-2} s^{-1} on NPQ of *cp12-1/2/3* knockdown and wild type lines acclimated to square and fluctuating light. 192
Figure 5.9: Photosynthesis as a function of internal CO_2 concentration (C_i) of wild type and *cp12-1/2/3* mutants acclimated to square (SQL) and fluctuating light (FLL) 194
Figure 5.10: Photosynthesis as a function of light (PPFD) of wild type and *cp12-1/2/3* mutants acclimated to square and fluctuating light 196
Figure 5.11: Box and whisker plots of showing the variation across replicates of parameters extracted from the *A/Q* curves 198

List of Tables

Table 1.1: The classification of transposable elements into class and superfamily . 27
Table 2.1: Calculations of chlorophyll fluorescence parameters obtained from imaging 72
Table 3.1: Parameters of chlorophyll fluorescence imaging and their description ... 84
Table 3.2: Summary of studied parameters in plants exposed to one of four light regimes 106
Table 4.1: Preprocessing data showing the raw read data, data removed by the trimming (Trimmomatic), mapping (Bismark –bowtie2), and deduplication (Deduplicate) of Whole Genome Bisulfite Sequencing data. 121
Table 4.2: Processing data showing the alignment scores (hisat2), and the quality control (QC) and reference genome mapping (flagstat) for RNAseq data. 122
Table 4.3: Reduced list of differentially methylated genes that are differentially expressed in RNA sequencing data. 142
Table 4.4: List of differentially methylated and differentially expressed transposable elements.. 148
Table 4.5: Subset of differentially expressed genes within 1kb of a differentially methylated transposable element (TE)..... 150
Table 5.1: Protocol for chlorophyll fluorescence imaging with successive step changes.. 179
Table 5.2: Forward and reverse primer sequences utilised in qPCR of CP12 180
Table 6.1: Summary of key results across the chapters in both square versus fluctuating light comparisons..... 205

Chapter 1: Introduction

1.1. Introduction

Plants are constantly exposed to dynamic environments, where changes in light intensity, temperature, and humidity happen on a second to minute basis, requiring systems to alter physiology and molecular biology in order to cope with such changes. This process, commonly known as acclimation, allows plants to cope with fluctuations to both biotic and abiotic stress, and has become increasingly well characterised. Understanding the molecular consequences of acclimation, in terms of how DNA methylation and gene expression change, may facilitate the manipulation of photosynthesis via changing light regimes, allowing for enhanced biomass, and flowering time to be altered, potentially allowing for improvement to crop production and increased yield, in a bid to contribute to feeding the expanding global population under changing climate conditions. Here, acclimation has been defined as “a physiological, structural, or biochemical adjustment by an individual plant in response to an environmental stimulus that is manifested as alterations in the short-term response function of a physiological process” (Smith and Dukes, 2013).

Plants sense changes in light via a range of receptors, triggering a response at the morphological, physiological, and molecular level, acting to improve tolerance to changing light (Murchie and Horton, 1997; Terashima *et al.*, 2006), known as light acclimation. When plants are consistently exposed to suboptimal conditions, developmental acclimation occurs in which new tissues generated by the plant, particularly the leaves (Murchie *et al.*, 2005), exhibit acclimation (Walters, 2005; Athanasiou *et al.*, 2010), aiding in improved survival. To meet requirements for global food security, photosynthetic productivity and efficiency has become a key

research target (Ort *et al.*, 2015), so understanding the underlying mechanisms of acclimation and its possible benefits is essential.

Light is essential for photosynthesis and an important environmental cue, with variations in quantity, quality, and timing effecting plant growth and development (Kami *et al.*, 2010; Zhang, Maruhnich and Folta, 2011; Bayat *et al.*, 2018). However, the light available to a plant depends on where the plant is found and the type of environment in which it grows, meaning light fluctuations can vary in multiple different ways. For example, desert plants regularly experience light intensities of over 2000 μmol m^{-2} s^{-1} (Liu *et al.*, 2022), while plants grown in the Northern Hemisphere rarely experience light over 1500 μmol m^{-2} s^{-1} during the summer (Poorter *et al.*, 2019), demonstrating the range of light environments that plants experience globally. Differences in light are also dependent on season, especially away from the equator where much arable land is located (Botta *et al.*, 2000; Masson *et al.*, 2013). Such seasonal change results in reduced natural light availability during the winter, due to shorter days and increased cloud cover, with the opposite being observed during the summer (Bhandary *et al.*, 2021). However, light availability can also vary daily due to weather conditions, sunrise and set, and the position of the sun (Berry and Smith, 2012), meaning plants must cope with changes in their light environment that can vary on a second-by-second basis. Understanding how these rapid variations impact plant growth and development is an important step in improving productivity. Recently, there has been interest in understanding how these daily fluctuations in light impact upon plant physiology, utilising a real light regime for a summer day in the East of England (Vialet-Chabrand *et al.*, 2017), where many of the UK's crops are grown (DEFRA, 2023).

Fluctuating light has been demonstrated to have important implications for plant physiology and morphology. Dynamic light has been noted to effect photosynthesis, with its efficiency theoretically dependent on the speed at which non photochemical quenching (NPQ) can be reduced in shade conditions (Kaiser, Galvis and Armbruster, 2019), as the transfer from high to low light can result in carbon assimilation losses due to the slow response of PSII (Zhu *et al.*, 2004). Photo-protective mechanisms, such as thermal dissipation, decreases in the maximum quantum efficiency of photosystem II (F_v/F_m) and CO_2 assimilation, with modelling demonstrated a decreased maximum efficiency of photosynthesis in high light results in a delayed reversal of thermal energy dissipation once the leaf is shaded (Zhu *et al.*, 2004), demonstrating that dynamic light can have a significant impact on crop productivity.

The impacts of dynamic light and sun flecks on photosynthesis were primarily investigated in tropical plant and forests (Chazdon and Pearcy, 1986b, 1986a; Pearcy, Chazdon and Kirschbaum, 1987). This work provided early evidence for the detrimental effects that the sun-shade transition can have on photosynthetic efficiency and carbon gain (Chazdon and Pearcy, 1986a, 1986b). Early models predicted that, under natural patterns of sun flecks, there would be a 12-50% reduction in photosynthesis compared to the steady state in *Alocasia macrorrhiza* (Pearcy, Gross and He, 1997). Later, field studies into the impacts of dynamic light on yield and productivity have revealed important implications of light environment. In wheat, it was noted that it took around 15 minutes for maximum photosynthetic efficiency to be reached following the sun to shade transition (Taylor and Long, 2017). This was linked to the activation of Rubisco, the primary carboxylase in C3 plants, and a delay in stomatal opening, ultimately resulting in a 21% reduction in

potential assimilation at the flag leaf (Taylor and Long, 2017). Similar was noted in soybean, with delays in adjustment to light fluctuation related to a 13.5% loss in carbon assimilation on a sunny day, related to both Rubisco activation and NPQ (Wang *et al.*, 2020). This demonstrates the importance of understanding the effects of fluctuating light and investigate possible avenues to reduce losses in productivity.

The process of acclimation is key in ensuring survival and occurs under multiple scenarios including fluctuating light. Light is essential for plant processes, however too much or too little light can cause stress to the plant (Demmig-Adams and Adams, 1992; Kalaji *et al.*, 2012). In the field environment fluctuating light occurs naturally due to changes in cloud cover, season, and time of day. Although fluctuating light intensity is experienced by all plants grown in the field, little research has been conducted investigating the effect of naturally dynamic light on physiological processes. Several studies have simulating fluctuating light as a series of square waves (Yin and Johnson, 2000; Thormählen *et al.*, 2017; Kaiser, Walther and Armbruster, 2020) however, few have used regimes with true peaks and troughs such as thought found in the field (Lawson, von Caemmerer and Baroli, 2010; Matthews, Vialet-Chabrand and Lawson, 2018). A handful of field studies have demonstrated that dynamic light impacts upon crop performance in wheat and soybean (Taylor and Long, 2017; Wang *et al.*, 2020), demonstrating the importance of understanding the impacts of fluctuating light on plant physiology. Acclimatory responses have been correlated with epigenetic changes as both a response to the stress (Grativol, Hemerly and Ferreira, 2012; Sahu *et al.*, 2013; Crisp *et al.*, 2016; Thiebaut, Hemerly and Ferreira, 2019)and as a priming effect (Hilker and Schmülling, 2019; Godwin and Farrona, 2020). DNA and histones are chemically modified, providing evidence for molecular control of plant's ability to acclimate and

change phenotype to cope with varying environmental conditions. An epigenetic change is established because of signalling pathways, in which signal transduction from an epigenator, the stimulus associated with epigenetic change, triggers the assembly of epigenetic machinery in the nucleus (Figure ***1.1***). Epigenetic regulation refers to chemical modifications of DNA and histones, alongside the insertion of histone variants, resulting in changes to gene expression (Figure **1.2**). This differs from genetic mutation, as there is no change to the DNA base sequence, instead with reversible chemical modification resulting in alterations to phenotype but not genotype (Slotkin, 2016). Such modification acts to affect the packaging of DNA by altering the charge interactions of DNA with itself, as well as with histones, the proteins around which DNA wraps to compact and regulate gene expression. Modification to the DNA or histones can act to alter the chromatin status of DNA, for example establishing heterochromatin, a more condensed form of chromatin. The formation of heterochromatin results in transcriptional repression by blocking the binding of RNA polymerase, and affecting the binding of a handful transcription factors to the DNA (Hughes and Lambert, 2017), often guided by DNA methylation patterns (Yin *et al.*, 2017). This results in phenotypic changes enabling the plant to survive by reversibly modifying gene expression by altering transcription factor and RNA polymerase binding. However, epigenetics can also refer to heritable change not caused by changes to the DNA base sequence which can be maintained across

several generations or until the stimulus changes (Eichten, Schmitz and Springer, 2014), providing another layer of complexity when discussing epigenetic changes.

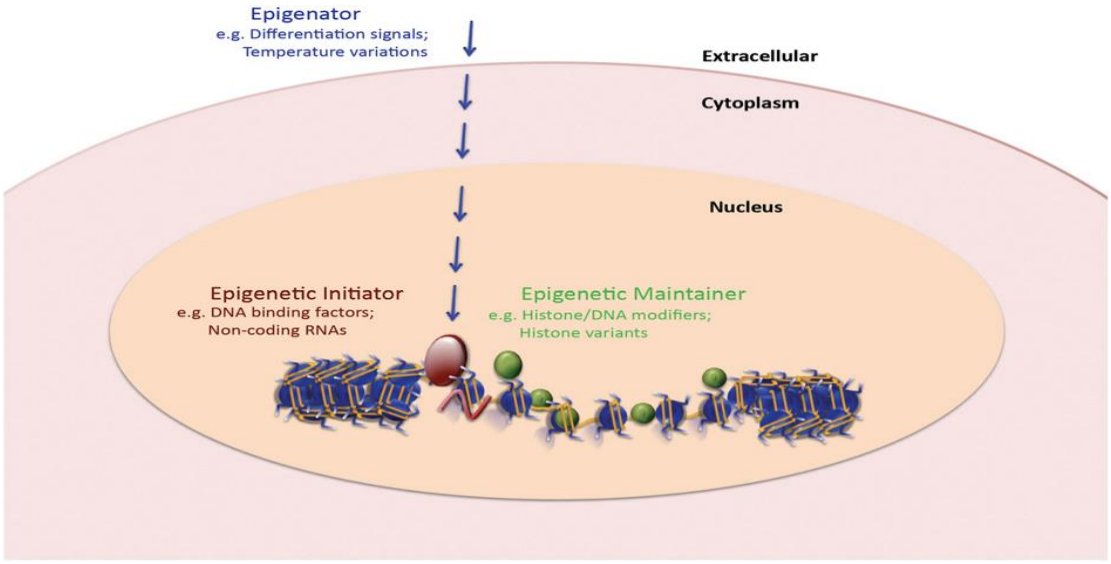

Figure 1.1: Generic signalling pathway resulting in epigenetic change. An extracellular signal, the epigenator, is perceived by the cell at the cell membrane, resulting in a signalling cascade. This cascade ultimately signals within the nucleus to epigenetic initiator machinery, including enzymes and DNA binding factors, which act to establish the epigenetic mark, e.g., cytosine methylation. These marks can then be maintained across replications and cellular divisions by epigenetic maintainers, allowing for the epigenetic code to be propagated. Taken from Berger et al., 2009

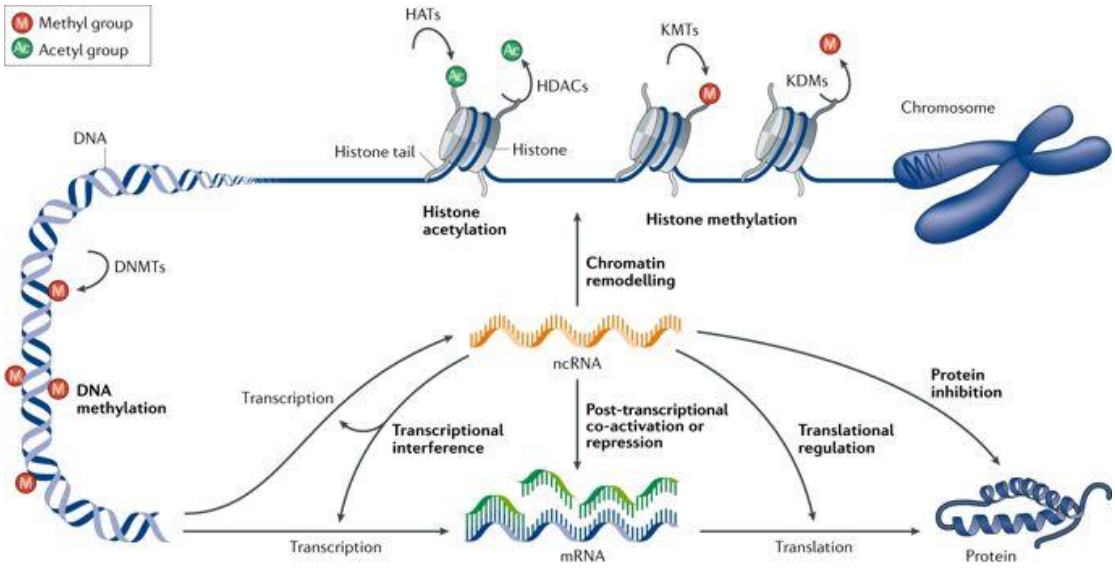

Figure 1.2:Schematic demonstrating possible chemical modifications to DNA and histones, ultimately resulting in modified gene expression. DNA is condensed into chromatin by wrapping around nucleosomes consisting of histones. These histones have tail with can be methylated, by lysine methyltransferases (KMTs) or acetylated by histone acetyl transferases (HATs), altering the interaction between DNA and the nucleosome. Both modifications are reversible- methylation can be removed from lysine by lysine demethylases (KDMs), and acetylation removed by histone deacetylases (HDACs). DNA can also be chemically modified by DNA methylation via DNA methyltransferases (DNMTs). Both histone modification and DNA methylation can alter transcription, ultimately impacting gene expression. Figure copied from Joosten *et al.* (2018)

Epigenetic change, and the exact effects of modification on transcription, has been implicated in plant stress responses. Characterising these epigenetic changes could lead to greater understanding of how stress responses are regulated, and potentially aiding stress tolerance. This application is of particular importance in relation to the changing climate conditions plants currently experience, and those which are expected in the future. With increases in greenhouse gas concentrations and temperature many plant species will experience a shift in their growth ranges and seasonal activity (IPCC, 2019). This means plants will have to cope with more extreme stress conditions to maintain crop yields required to feed the global population. Understanding the possible epigenetic link between light and phenotype

may be particularly important in providing novel targets for manipulating these processes that can be feed into on-going breeding programmes.

1.2. Epigenetics in Plants

1.2.1. DNA methylation

DNA methylation is a key epigenetic mechanism with roles in repressing transposable elements (TEs) and regulating gene expression. This methylation occurs on cytosine residues on carbon 5 (Figure **1.3**), via the action of a set of DNA methyltransferases. DNA methylation in plants can occur at cytosines in the sequence contexts CpG, CpHpG, and CpHpH by three different pathways (Figure **1.4**), where H is Adenine, Thymine, or Cytosine (Law and Jacobsen, 2010). In comparison, DNA methylation in mammals can occur only in the CG sequence context (Law and Jacobsen, 2010). These methylation patterns occur at different distributions. Most CHH sites have little methylation (10-20%), with the majority of CpHpG sites unmethylated, while ~40% of CpG sites show a high level of methylation (Cokus *et al.*, 2008; Catoni and Zabet, 2021), demonstrating that methylation of these residues are under separate control mechanisms.

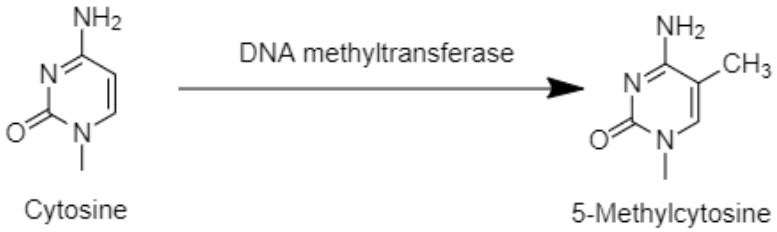

Figure 1.3: Cytosine can be methylated on the 5’ carbon by a DNA methyltransferase

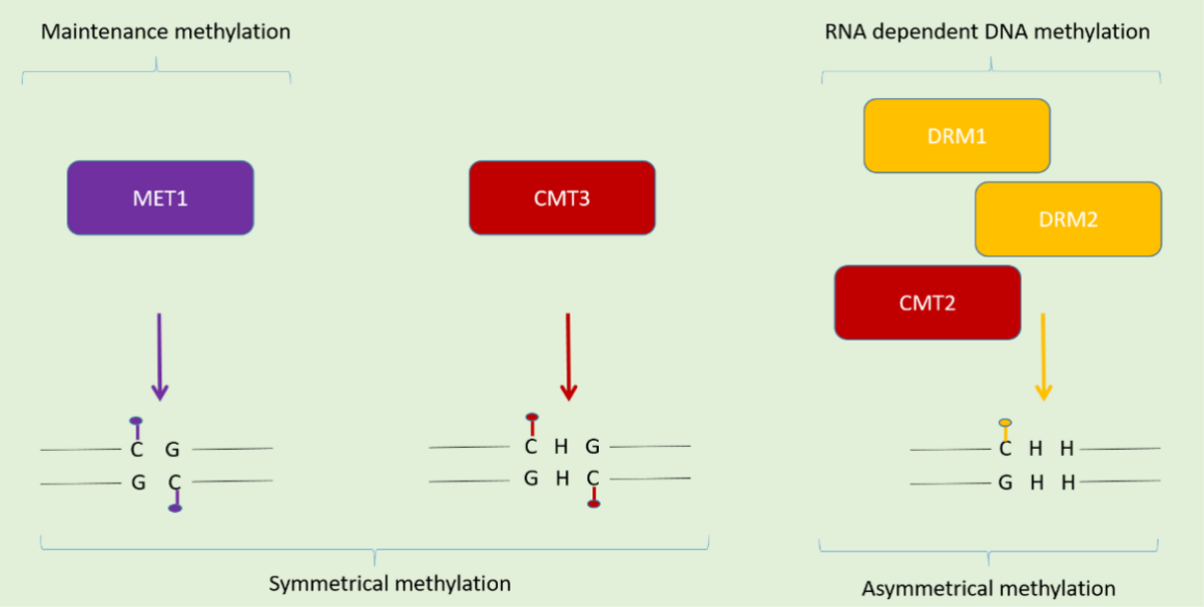

Figure 1.4: The three different methylation pathways that result in cytosine methylation in plants. CpG methylation is maintained by methyltransferase MET1, while Chromomethylase 3 (CMT3) acts to maintain CpHpG methylation. Chromomethylase 2(CMT2) acts with DNA methyltransferases DRM1 and DRM2 to establish all cytosine methylation and maintain methylation in the CpHpH contexts. Methylation by CMT3 and the RdDM pathway are unique to plants

The RNA-directed DNA methylation (RdDM) pathway is responsible for establishing methylation in all three sequence contexts (Figure **1.4**) and is known to induce transcriptional silencing of repetitive DNA elements , including transposons (Matzke and Mosher, 2014). The RdDM pathway requires two plant-specific RNA polymerases, RNA pol IV and V, which have a role in development and genome defence (Haag and Pikaard, 2011), for example in silencing transposable element insertions. In the canonical RdDM pathway (Figure **1.5**), RNA pol IV is recruited by SHH1, a nuclear homeodomain protein, when it binds to methylated lysine 9 of histone H3, and acts to transcribe double stranded RNA transcripts of nuclear DNA, which are processed by RNA-dependent RNA polymerase 2 (RDR2), then cleaved by Dicer Like 3 (DCL3) to produce a 24 nucleotide long small interfering RNA (siRNA) (Gebert and Rosenkranz, 2015). The generated siRNAs are methylated by RNA methyltransferase HEN1 and exported from nucleus to cytoplasm where one

strand can be loaded into Argonaute 4/6, with assistance from HSP90 to form the RNA-induced silencing complex (RISC), which is then imported back into the nucleus. DNA methyltransferase DRM2 is recruited to the complex (Matzke and Mosher, 2014), which acts to methylate cytosines on DNA as directed by the siRNA. The recruitment of DRM2 to the RISC first requires the recruitment of RNA pol V, dictated by methylation already present on the DNA backbone. Following this *de novo* establishment of methylation, CG methylation can be maintained by MET1, and CHG by CMT3 (Wendte *et al.*, 2019) as described below, while CHH methylation is maintained via the RdDM pathway through the same mechanism as establishes methylation (Feng, Jacobsen and Reik, 2010), indicating the importance of this pathway in establishing and maintaining epigenetic changes.

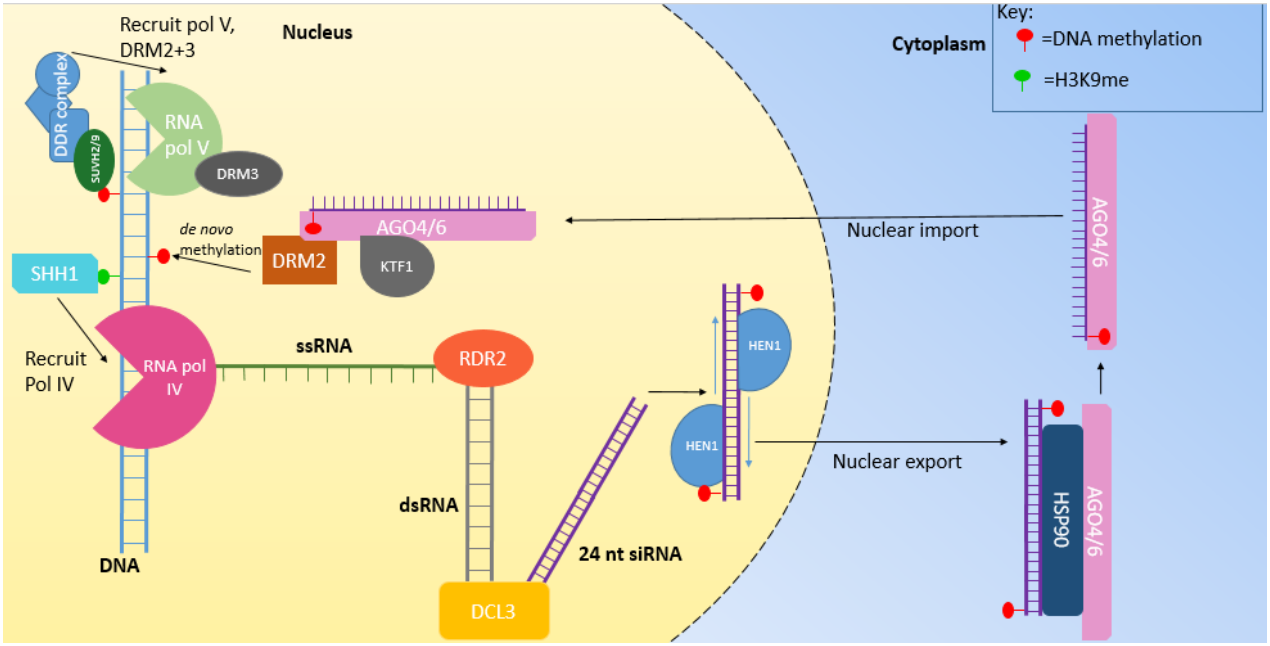

Figure 1.5: Schematic of the RNA directed DNA methylation pathway**.** Single stranded RNA transcripts (ssRNA) from RNA polymerase IV are processed to form 24 nucleotide double stranded small interfering RNAs (siRNAs) which, when loaded onto Argonaut 4/6, form the RNA induced silencing complex (RISC). This can then be imported into the nucleus where the RISC targets directs the activity of cytosine methyltransferase DRM2 to establish *de novo* DNA methylation.

Of the three methylation pathways in plants (Figure **1.4**), only CG methylation is evolutionarily conserved across eukaryotes. DNA METHYLTRANSFERASE 1 (MET1), a homolog of mammalian DNMT1, acts to maintain CG methylation with the aid of a co-factor VARIATION IN MEHTYLATION (VIM) in higher plants (Kim *et al.*, 2014; Shook and Richards, 2014). The pathway can detect hemi methylated DNA, i.e., where one strand of DNA is methylated such as after DNA replication. MET1 recognises the hemi-methylation, and the methylated strand is used as a template as it marks the methylation pattern to be maintained on the new strand (Law and Jacobsen, 2010), allowing the epigenetic code to remain complete. Mutations in the *met1* gene have a range of effects, which demonstrate the importance of CG methylation. For example, partial loss of function of met1 (*met1-1*) in *Arabidopsis* results in a 70% reduction in methylation, referred to as hypomethylation, particularly of repetitive DNA elements (Kankel *et al.*, 2003). This results in a distinct morphological phenotype, with *met1-1* mutants displaying a delay in flowering time associated with increased rosette and aerial leaf production, with juvenile rosette leaves lacking abaxial trichomes (Kankel *et al.*, 2003). Total loss of met1 function in *Arabidopsis* (*met1-3*) causes almost complete loss of CpG methylation, also resulted in delayed flowering, small rosette size and short stature, increasing in severity with each generation, and is not viable by the fourth generation (Mathieu *et al.*, 2007; Catoni *et al.*, 2017). Such phenotypes can be due to the activity of transposable elements and repetitive genome elements no longer silenced by methylation (Lippman *et al.*, 2004), which are free to move around the genome and insert at sites not observed in wild type, therefore affecting development.

Another DNA methyltransferase, CHROMOMETHYLASE 3 (CMT3), a plant specific DNA methyltransferase, works alongside KRYPTONITE (KYP), a histone

methyltransferase, to maintain CHG methylation in a feedforward loop (Boyko and Kovalchuk, 2008; Feng, Jacobsen and Reik, 2010). In 2002, the action of KYP was first characterised, which demonstrated that it binds to methylated CHH and CHG residues, acting to recruit CMT3 to hemi methylated sites (Jackson *et al.*, 2002; Malagnac, Bartee and Bender, 2002) and so propagating methylation. KYP is a histone lysine methyltransferase, acting specifically on lysine 9 of histone H3 (H3K9), to recruit CMT3 which is targeted to H3K9me-containing nucleosomes (Du *et al.*, 2014) . In turn, CMT3 can methylate CHG residues to create more binding sites for KYP (Du *et al.*, 2014). The activity of this pathway has important implications in growth and physiology. Mutation of *kyp* has been shown to significantly enhance seed dormancy in *Arabidopsis* (Zheng *et al.*, 2012), possibly linked to the loss of some non-CG methylation as CMT3 activity is dependent on signalling for KYP Functional loss of kyp and CMT3 is also associated with altered WUSCHEL (WUS) expression (Li *et al.*, 2011), a key transcription faction in shoot regeneration. Such evidence indicates the fundamental importance of epigenetic regulation, as without the activities of KYP and CMT3, there would be dysregulation of growth. However, the activity of these enzymes is not always clearly delimited, as it has been shown that CHG methylation is also dependent on MET1 methylation at CCG sites (Zabe*t et al*, 2017).

Methylation of nuclear DNA is well documented but the occurrence of DNA methylation in the chloroplasts of higher plants has been shown not to occur. No chloroplast-localised DNA methyltransferases have been identified in higher plants (Pavlopoulou and Kossida, 2007), and demonstrated that the introduction of DNA methyltransferases had no effect on chloroplast gene expression (Ahlert *et al.*, 2009). This suggests that DNA methylation is unlikely to occur in chloroplasts. The

occurrence of mitochondrial genome methylation is currently unclear, with conflicting evidence as to whether it occurs. In mammalian systems, mitochondrial DNA (mtDNA) methylation is considered to occur, and has been correlated with a range of diseases (Iacobazzi *et al.*, 2013), suggesting the potential for mtDNA methylation to occur. However, in plant systems, the data is conflicting, and may be dependent on the plant species investigated. For example, mtDNA cytosine methylation has been noted in *Sequoia sempervirens* (Huang *et al.*, 2012), a red wood tree species, and rice (Muniandy *et al.*, 2020), where differential methylation between old and new leaf mtDNA was observed(Muniandy *et al.*, 2020). However, other studies have suggested that no methylation takes place in the plant mitochondria , demonstrating a requirement for further investigation (Ward, Anderson and Bendich, 1981; Bailey-Serres *et al.*, 1987; Yan *et al.*, 2010). This means, when considering DNA methylation in relation to photosynthesis

1.2.1.1. Transposable Elements

Transposable elements (TEs) are mobile, repetitive DNA sequences (Quesneville, 2020) capable of replicating independently from the host genome (Wells and Feschotte, 2020). They are present across eukaryotes, as well as prokaryotes, and often make up a large portion of the genome, representing ~21% of the genome in *Arabidopsis thaliana* according to TAIR10 (Quesneville, 2020). Their activity can be regulated by cytosine methylation, with methylation in all three contexts across the majority, if not all, cytosines required for repression (Ahmed *et al.*, 2011), which is important to maintain genome stability (Fedoroff, 2012). Activity of the above three pathways in unison is important to maintain silencing of repetitive elements of the genome, including transposable elements. This is the best understood role for DNA methylation. Silencing of TEs occurs via the RdDM pathway, with maintenance

occurring via RdDM, MET1, and CMT3 (Law and Jacobsen, 2010). In tomato and *Arabidopsis*, knock out of CMT3 and KYP reduced CHG and CHH methylation of TEs at specific loci in chromatin (Wang and Baulcombe, 2020), indicating the importance of all three methylation pathways being functional to maintain genome stability. It has been proposed that there is an age effect for such transposon methylation, with younger repeats, in terms of the evolutionary timeline, appearing to be preferentially methylated at CHG (Wang and Baulcombe, 2020), indicating these pathways have distinct roles to play at different stages of development.

Class I TEs, also known as retrotransposons transpose via an RNA intermediate which is reverse transcribed to DNA and inserted at a new regions in the genome, often referred to as a "copy-and-paste" mechanism (Quesneville, 2020; Wells and Feschotte, 2020). Class II TEs, also known as DNA transposons, mostly transpose as DNA in a "cut-and-paste" mechanism (Quesneville, 2020), where the element is excised and moved to a new genomic location (Wells and Feschotte, 2020). Approximately 32,000 TE copies are present in the *Arabidopsis thaliana* genome (Ahmed *et al.*, 2011), with retroelements representing the largest group (10Mb) (Kaul *et al.*, 2000; Ahmed *et al.*, 2011), demonstrating the potential significance of TEs and their regulation in genomic studies. The classes can be further categorized into orders and superfamilies depending on the structure of the transposable element (summarized in Table **1.1**).

Table 1.1: The classification of transposable elements into class and superfamily, and the number of TEs present within the subsequent families in *Arabidopsis thaliana*. Defining features summarizes the sequence features specifically associated with the order. Adapted from Quesneville (2020)

Class	Order	Superfamily	Family numbers	Defining features
I	Long terminal repeat (LTR) retrotransposons	Copia	109	• Have three functional areas: - U3, may contain regulatory motifs and promoter region at 3' end - R contains start and termination sites for transcription - U5 • Have a potential tRNA primer binding site • Copia and Gypsy distinguished according to position of integrase in the polyprotein *pol*
		Gypsy	32	
	LINE	L1	11	• Encode: - an endonuclease - a reverse transcriptase - a non-sequence specific RNA binding protein that contains zinc finger, leucine zipper, and coiled-coil motifs • Terminated by polyA or A/T-rich 3' tail
		Unknown	1	
	SINE	tRNA	5	• Transcribed by RNA polymerase III rather than II • Contain 2, well conserved motifs (box A and box B) which acts as internal promoter for transcription • Do not encode any protein
II	TIR	En-Spm	12	• Use "cut-and-paste" mechanism
		MuDR	70	

		Harbinger	3	• Encode a transposase with a DDE or DDD domain • Bordered by an inverted repeat
		hAT	22	
		Pogo	4	
		Mariner	2	
		Tc1	1	
		Unknown	12	
	Helitron	Helitron	34	• Transpose via a roll circle mechanism • Generally, contain: - a Y2-type tyrosine recombinase - hairpin structure in second half of sequence • Insert into AT dinucleotide

The majority (~74%) of TEs are densely methylated, while the remaining ~26% are either unmethylated at most or all sites, or show significant methylation in only one or two of the three contexts (Ahmed *et al.*, 2011), indicating the importance of DNA methylation for controlling transposition. Loss of cytosine methylation at TE sites is known to result in TE activation. Treatment with zebularine and α-amanitin, drugs which transiently reduce DNA methylation in plants (Baubec *et al.*, 2009), resulted in activation, and new insertions, of multiple types of transposable elements when applied to *A. thaliana*, including those in CACTA, LINE, and Copia (Baubec *et al.*, 2009; Roquis *et al.*, 2021). Such evidence suggests that widespread changes to DNA methylation, such as hypomethylation resulting from drug treatment, may allow for TE activation and therefore insertion into new sites which could cause disruption or change regulation of coding genes.

TE methylation is also known to impact on nearby genes. DNA methylation of TEs has the potential to spread into nearby genes. High levels of CG methylation within

TEs and a high TE density has been negatively correlated with gene expression in multiple plant species including *Arabidopsis thaliana* (Hollister and Gaut, 2009; Wang, Weigel and Smith, 2013) and maize (Eichten *et al.*, 2012). In several accessions of *Arabidopsis thaliana,* genes flanked by a TE within 2kb were found to have reduced expression compared to genes with no TEs within 2kb (Wang, Weigel and Smith, 2013), suggesting TE proximity impacts gene expression. This has been attributed to both the spreading of DNA methylation from TEs into nearby genes(Ahmed *et al.*, 2011) or TE activation, where transcription of the TE can result in synthesis of the antisense transcript of near-by genes (Kashkush, Feldman and Levy, 2003). Such evidence demonstrates that TE methylation can have consequences for gene expression and therefore potentially impact upon how plants respond to their environments. However, not all plant species demonstrate the correlation between TEs and decreased gene expression. In *Brachypodium distachyon,* a wild relative of many cereal crops including wheat and barley, limited spreading of methylation from TEs to genes was noted, with limited impact of TE presence on nearby gene expression (Wyler et al., 2020). This demonstrates that the results obtained in *Arabidopsis* cannot necessarily be applied to all plant species, so investigation into other species is required.

Transposable element activation can have consequences for gene expression. A range of TEs, including VANDAL21 in *A.thaliana*, are known to target 5' upstream regions of genes, which may modulate expression of adjacent genes (Wells and Feschotte, 2020). Furthermore, Ty1/Copia-like TEs have been noted to preferentially insert at sites enriched in H2A.Z, a histone variant primarily associated with environmentally responsive genes (Quadrana *et al.*, 2019). Insertion of ATCOPIA93 at H2A.Z enriched sites in 4 environmentally responsive genes lead to reduction in

transcript levels (Quadrana *et al.*, 2019), providing evidence that TE insertion could contribute to environmental responses and adaptation. Supporting this, TE ATCOPIA78, known as ONSEN, is known to undergo heat activation (Ito *et al*, 2011; Sanchez *et al*, 2017), resulting in accumulation of transcripts and extrachromosomal DNA, linked to loss of DNA methylation but also recruitment of heat shock transcription factor, HSFA2 (Cavrak *et al.*, 2014). This demonstrated that environmental influences, including abiotic factors which are known to impact the methylome, may impact upon TE expression, and that host molecular machinery may also contribute to TE expression and insertion. However, it is important to note that these TE activations are often reliant on very specific stress scenarios, so activation may be unlikely under natural conditions.

There are several well-known examples of transposable element activity in commercially significant plants. TE activity was first identified in maize plants with broken chromosomes, resulting in kernel variegation (McClintock, 1950, 1953). When the chromosomes of the parental and experimental generation were compared, it was noted that parts of the chromosomes had switched position consistently at the same loci (McClintock, 1950), indicating that these mobile elements had some insertion preference. It was later found that insertion was occurring in anthocyanin-related genes, altering the expression, and therefore resulting in variegated plants (McClintock, 1953). Similarly, retrotransposon activity in grapes has been related to changes in grape-skin colour. Insertion into the gene *VvmybA1*, a regulator of anthocyanin biosynthesis, was found in white-skinned cultivars, resulting in no transcript detection (Kobayashi, Goto-Yamamoto and Hirochika, 2004). This demonstrates the prevalence of active TEs within

commercially significant crops, and that much of our understanding of TEs has been derived from plant models.

1.2.1.2. Gene Body Methylation

Methylation can act to alter interactions between DNA and proteins (Razin and Cedar, 1991) including transcription factors, and proteins which promote gene repression (Moore, Le and Fan, 2013). This gene body methylation (gbM) often primarily refers to methylation in the CpG context rather than CpHpG and CpHpH, which usually refers to transposon and transposon-like methylation (Muyle *et al.*, 2022). Modelling of selection for populations containing gbM versus those that do not has indicated there is some role for gbM in natural selection, with ancestrally methylation CG and unmethylated CG displaying selection pressure to maintain this methylation (Muyle *et al.*, 2022). This indicates a possible role for gbM in evolution and section, suggesting the methylation status of certain loci may confer a competitive advantage. However, the impacts of gbM on gene expression are not well known. There are two conflicting views as to how gbM may impact gene expression; the first being that gbM might effect expression, and the second that active transcription may drive gbM (Teixeira and Colot, 2009; Muyle *et al.*, 2022). It is known that many highly expressed genes do not display gbM (Zilberman *et al.*, 2007; Muyle *et al.*, 2022), which suggests the second hypothesis is not the case. Furthermore, in *Arabidopsis* plants with mosaic patterns of methylation, generated from cross of Col-0 wild types and *met1* knockouts, while multiple genes were noted to have differential DNA methylation, only a small subset were found to be differentially expressed (Bewick *et al.*, 2016), further indicating only a small role for gbM in gene expression regulation. However, it may be that gbM instead has small effects on expression which may not be detectable with current differential

expression analysis techniques, and further work would be required to fully understand the role of gbM.

1.2.2. Histone Modification

There are four conserved core histone proteins in eukaryotes which come together to form the histone octamer.147 base pairs of DNA wraps around this octamer to form a nucleosome (Figure **1.6**), contributing to the regulation of gene expression (Deal and Henikoff, 2011). A higher number of histones within a given region of DNA often results in more compact chromatin, which less accessible to RNA polymerases (Deal and Henikoff, 2011), known as heterochromatin. This placement of histones acts to dictate the condensing of DNA into chromatin, with the more densely packed heterochromatin associated with a greater histone density and reduced transcriptional activity. Less compact chromatin is termed euchromatin. DNA wrapping also blocks other DNA binding proteins from binding (Bowman and Poirier, 2015), acting to further alter gene expression. Posttranslational modification of histones tails can contribute to altered gene expression by effecting the interactions of the histone octamer with DNA, therefore influencing the degree to which DNA is packed. Furthermore, variants of the core histones can be incorporated into the histone octamer under specific scenarios including stress, acting to alter to transcriptional profile by modifying the interaction within the histone octamer.

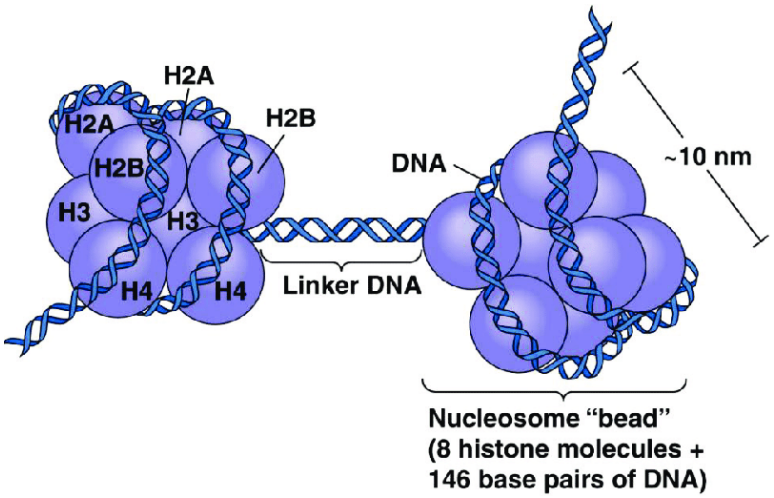

Figure 1.6: The wrapping of DNA around the core histone octamer to form a nucleosome. There are two of each of the core histones present in the core octamer, which DNA associated with to wrap around. Taken from (Caputi, Candeletti and Romualdi, 2017)

Modification of the core histones has been noted to alter the interaction of the histone octamer with DNA. Modelling has predicted that charge-altering Posttranslational Modifications (PMTs) affect nucleosome stability and therefore changes in DNA accessibility (Fenley *et al.*, 2018), so consequently affecting gene expression. Histone tails are susceptible to a variety of modifications, including acetylation, methylation, phosphorylation, and ubiquitination (Figure ***1.7***). These modifications result in dynamic changes to the interactions of histone with allowing DNA binding complexes to access their binding sites (Bowman and Poirier, 2015). If these modifications did not occur, such complexes would be unable to bind, so preventing expression.

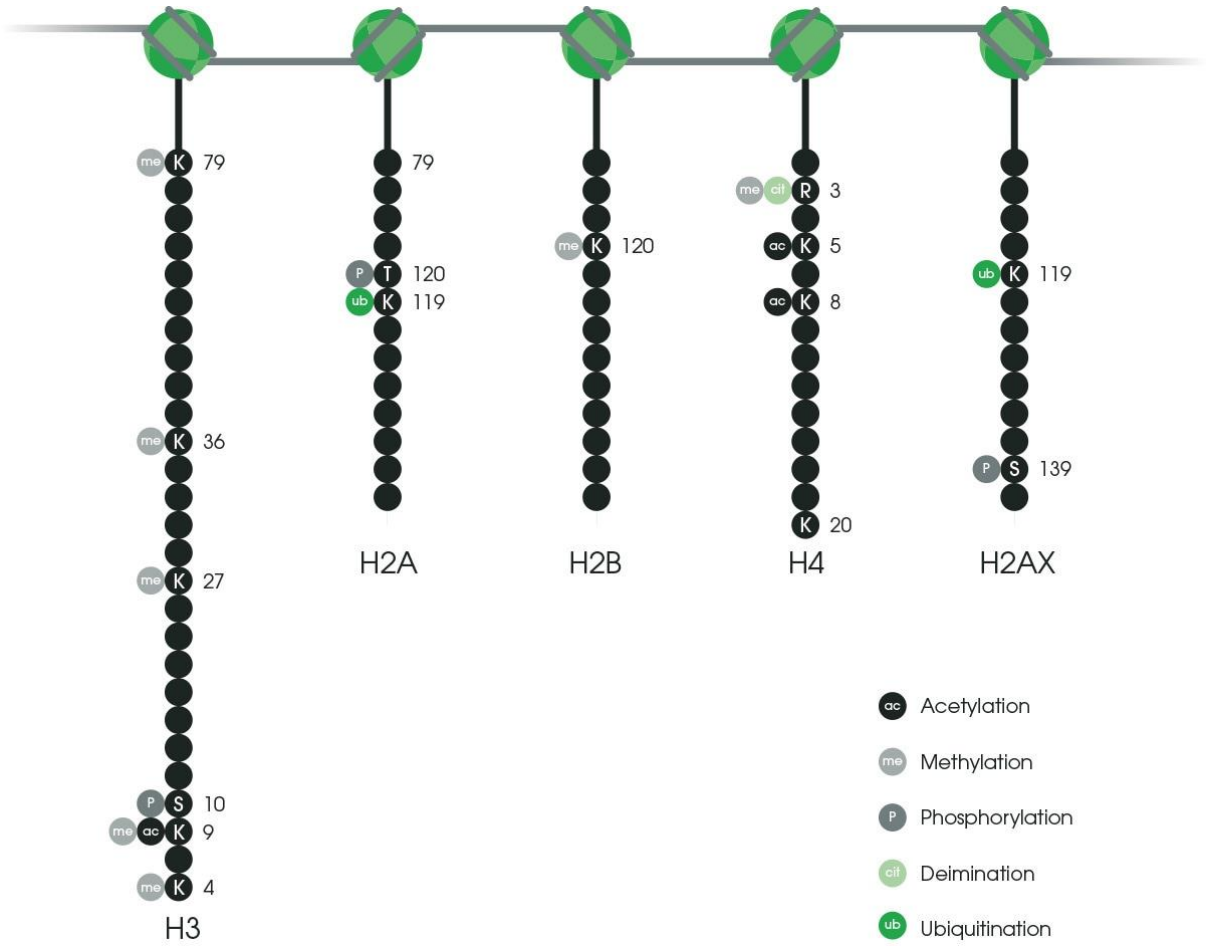

Figure 1.7: Amino acid sites of the core histones which are susceptible to covalent modification. Taken from Histone modifications | Abcam (2022)

In the case of stress responses, histone acetylation and methylation appear most relevant. Histone acetylation is a PMT that occurs when acetyl groups are transferred to lysine (Lys) residues present in the histone core or histone tail. This acts to counteract the positive charge on Lys, which normally would to counteract the negative charge of DNA (Carrozza *et al.*, 2003), resulting in relaxation of chromatin due to repulsion of DNA with itself and increasing gene expression, meaning acetylation can act as a marker for euchromatin. This modification can also form recognition sites for factors involved in transcriptional activation (Carrozza *et al.*, 2003), indicating that histone acetylation is important in activation of gene expression. In *Arabidopsis*, there are four families of histone acetyltransferase

(Benhamed *et al.*, 2006) catalysing this reaction, which has been particularly correlated with acetylation of lysine (K) on histones H3 and H4 (Boycheva, Vassileva and Iantcheva, 2014). Similarly, histone methylation can be observed on both arginine and lysine resides in histone H3 and H4, directed by a set of 10 SUVH proteins, but is usually correlated with both gene silencing and activation (Naumann *et al.*, 2005). The amino group of lysine can accept up to three methyl groups, meaning it can be mono-, di-, or tri- methylated (Grewal and Rice, 2004), but do not act to affect charge interactions as acetylation does as methyl groups are neutral (Pontvianne, Blevins and Pikaard, 2010). It appears that again, the residue methylated, rather than the number of methyl groups, is significant in controlling chromatin status. For example, mono-, di- or tri-methylation of H3K4 is correlated with active genes, whereas methylation of H3K9 is correlated with inactive genes within euchromatin, i.e. active transcription, as well as heterochromatin (Pontvianne, Blevins and Pikaard, 2010). Immunoprecipitation of modified histones has demonstrated the different distributions of histone acetylation and methylation in heterochromatin and euchromatin. Methylation of H3 lysine 4, 9, 20, and 27, acetylation of H3 lysine56, and ubiquitination of H2B are most commonly found within euchromatin (Roudier *et al.*, 2011), where genes are actively transcribed, and subject to differential expression. In heterochromatin, methylation of H4 lysine 20 and 9 are particularly enriched, as well as in transposable elements and other repetitive elements of the genome (Roudier *et al.*, 2011), acting to repress expression**. I**mportantly, these histone PMTs are dynamic, so are easily reversible via a separate set of enzymes. Histone Demethylases and Histone Deacetylases act to remove the chemical groups from modified residues, often with specificity based up the modified amino acid (Cheung and Lau, 2005). The dynamic nature of these

modifications provides a mechanism by which the plants can alter gene expression depending on their surroundings, providing a potential acclamatory mechanism.

Histone modification can also result in DNA methylation. For example methylation of CHG sequences by CMT3 depends on demethylation of H3K9, and has been reported to occur via the stable interaction of CMT3 with nucleosomes containing the methylated histone H3 (Du *et al.*, 2012). CMT3 is highly enriched in the pericentromeric regions, the DNA flanking the centromere on a chromosome, of the *Arabidopsis* genome and found to be co-localised with H3K9me2, such as in heterochromatic patches in the euchromatin of chromosome arms (Du *et al.*, 2012). This demonstrates the complex interactions between DNA methylation and histone modifications, as each can affect the other.

Variants in the core histones H2A and H3 provide a further level of regulation. In plants, core histone H2 has two main variants; H2AX and H2A.Z, each with specific roles in the cell. H2AX has a unique C-terminal serine residue which is phosphorylated at sites of DNA damage (van Attikum and Gasser, 2009). The role of H2A.Z is less clear, appearing to be incorporated into histones marking transcriptional start sites, possibly mediating transcriptional activity (Deal and Henikoff, 2011). Histone H3 also has multiple variants, including CenH3, present at centromeres, and H3.3, found mainly within promotor regions and transcribed regions of expressed genes (Deal and Henikoff, 2011). Both are found across eukaryotes. However, H3.3 in plants is less well understood than in animals, having evolved independently (Shu *et al.*, 2014). Shu et al (2014) found that H3.3 was present within transcribed regions and strongly correlated with transcriptional activity, but its presence at promoters appeared to be independent of transcription. Furthermore the H3 variant H3.1, which differs from H3.3 in only 4 residues, is

enriched at silenced regions of the genome, including regions of heterochromatin and transposable elements (Stroud *et al.*, 2012; Lu *et al.*, 2018).

The exact content of histone modifications and DNA binding proteins can be assessed using chromatin immunoprecipitation followed by a sequencing step (ChIP-seq). The technique relies on cross-linking protein-DNA interactions using formaldehyde, which results in covalent fixation (Park, 2009; Schmidt *et al.*, 2009). The DNA is then sheared via sonication and incubated with magnetic beads to which an antibody specific to the protein or modification of interest is attached (Schmidt *et al.*, 2009). These are washed and eluted, and cellular proteins and RNA are digested to purify the sample, and the samples are run through PCR for DNA base sequencing. The data can then be analysed by mapping the fragments back to the sequence genome (Raha, Hong and Snyder, 2010), with peaks at the DNA sequences of interest indicating an enrichment of the modification.

1.2.3. Transgenerational Epigenetic Inheritance

In plants, unlike mammals, DNA methylation can be stably inherited over multiple generations and can persist in reproductively isolated populations (Williams and Gehring, 2017). These transgenerational effects (TGEs) allow phenotypic changes resulting from epigenetic modification to be expressed in later generations, in theory improving the fitness of the next generation as they may be acclimated to the environment experience by their parents (Rendina Gonzále*z et al*, 2018). Since plants can reproduce clonally and via the germline there are two possible routes by which epigenetic modification can be inherited. One of the earliest examples of transgenerational epigenetic inheritance was seen in floral symmetry of *Linaria vulgaris*, in which methylation of *Lcyc* gene resulted in altered dorsoventral symmetry

and was noted to be stability heritable and co-segregates (Cubas, Vincent and Coen, 1999). This provided an early indication that epigenetic change could be heritable, leading to investigation into the mechanisms and causes of such heritability.

The germline in plants arises from somatic tissue, at the shoot apical meristem which is environmentally exposed, providing a possible explanation as to why transgenerational heritability has been noted in plants and not animals (Feng, Jacobsen and Reik, 2010). During gametogenesis and fertilisation, methylation marks which were present in early fertilisation are removed in mammalian cells, but in plants some epigenetic marks avoid removal in the germline (Hauser *et al.*, 2011). In pollen, >80% of methyl cytosine is suggested to be retained, with CpHpH methylation specifically reduced (Calarco *et al.*, 2012) by the action of the DEMETER DNA glycosylase, which excises 5-methylcytosine (Ibarra *et al.*, 2012). DEMETER is highly expressed in the central cells of the egg, with much of the endosperm genome demethylated, accompanied by increased CHH methylation of embryo transposable elements (Hsieh *et al.*, 2009). The central cell of the egg displays global demethylation, possibly producing small RNAs capable of migrating to the egg cell and embryo to induce *de novo* methylation (Köhler and Lafon-Placette, 2015). Extensive demethylation in the endosperm has been noted in multiple plant species, with transposable element genes and gene-flanking regions seen to be less methylated in the endosperm than the embryo (Lauria *et al.*, 2004; Gehring, Bubb and Henikoff, 2009), suggesting a role for transposable elements within the endosperm. Such demethylation may represent potential loss of regions methylated because of environmental pressures.

Differences in the methylation pattern between two plants allows for imprinting to occur. This is the phenomena by which genetically identical alleles are differentially

expressed depending on the parent-of origin (Bai and Settles, 2015). This does not follow Mendelian genetics, instead either the maternal or paternal allele will be expressed despite being genetically identical (Bai and Settles, 2015). Differential methylation between the two copies results in contrasting chromatin states (Bai and Settles, 2015), which can then result in differential expression between the maternal and paternal copies due to difference in transcription. Therefore, the degree of epigenetic inheritance may depend on the parent of origin.

The propagation of TGEs may depend on whether a plant has clonally or sexually reproduced (Figure **1.8**), as sexual reproduction involves two parents, whereas clonal plants reproduce asexually from vegetative tissue, meaning clonal plants may inherit a greater degree of epigenetic modification. In clonal plant *Trifolim repens*, parental drought stress triggered DNA methylation changes, many of which were present in the clonal offspring (Rendina González *et al.*, 2018). Apomictic dandelions (*Taraxacum officinale*) may also display transgenerational epigenetic inheritance. When droughted, an increase in DNA methylation was noted in some accessions, but no stable inheritance of this methylation was noted (Preite *et al.*, 2018). In contrast, chemical induction of biotic stress defences induced an increase in DNA methylation compared to non-exposed plants, with between 74% and 92% of methylation observed in the first generation faithfully transmitted to the second, with the second generation displaying reduced variance in methylated regions (Verhoeven *et al.*, 2010). This suggests transmission could be species and stress dependent and may not be enhanced in clonal species. Despite the possibility that sexual reproduction results in loss of methylation, transgenerational epigenetic inheritances have been noted in multiple plant species. *Polygonum persicaria* is known to show transgenerational phenotypic plasticity, and when drought stressed

methylation has been correlated with this phenomena (Herman and Sultan, 2016). Removal of methylation from seed of drought parents using zebularine resulted in a 17% lower biomass, shorter roots, and lower leaf area compared to non-zebularine treated seed, while also resulting reduced root system length and leaf area compared to seed of non-droughted parents (Herman and Sultan, 2016). This indicates that methylation has a role in both stress phenotypes and maintaining “normal” development under optimal conditions, demonstrating its importance.

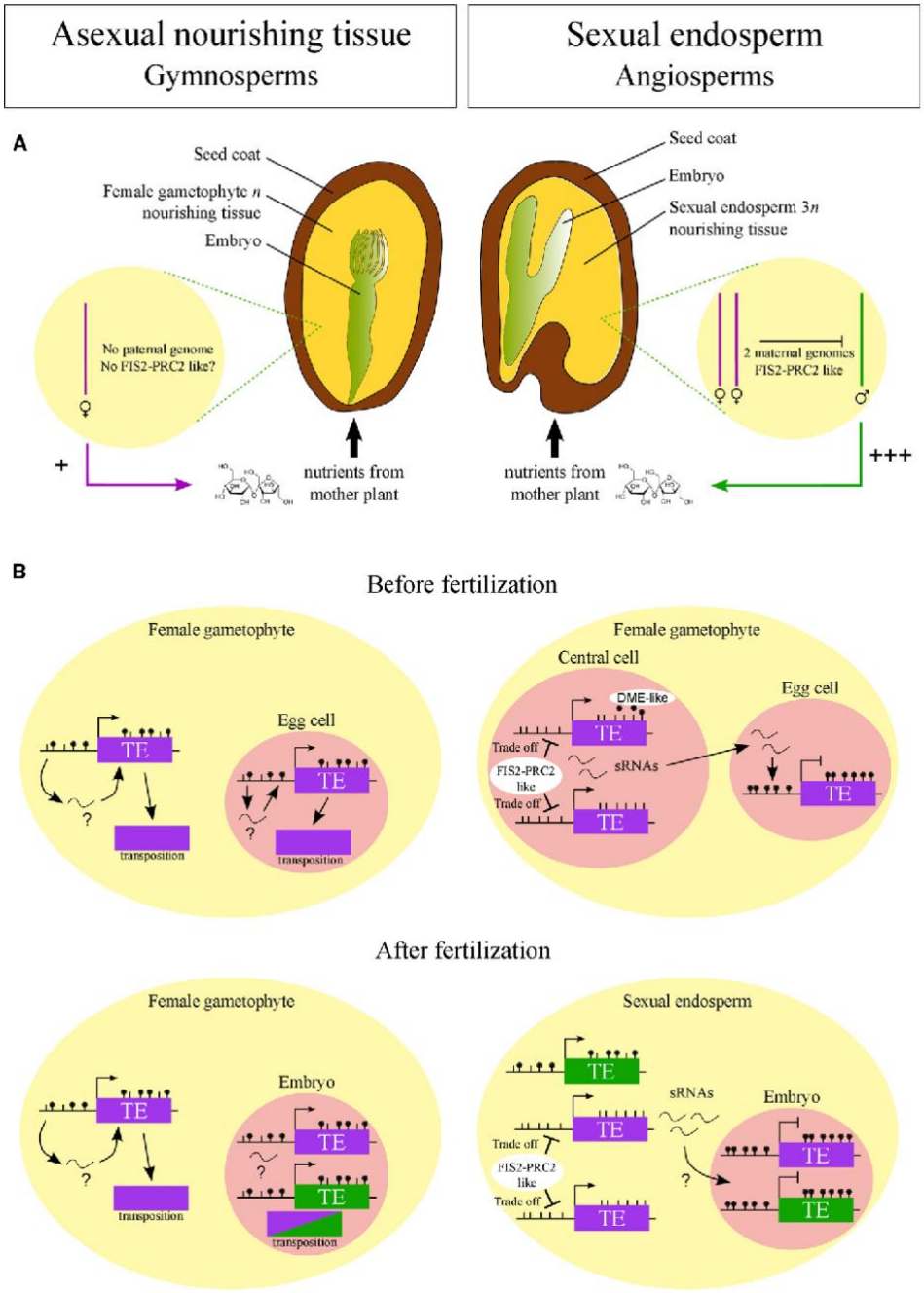

Figure 1.8: Sexual vs asexual reproduction and the retention of methylation from parental tissues. When reproducing asexually, there is no conflict between the maternal and paternal genome, suggesting much of the maternal phenotype from the egg cell. In contrast, the presence of paternal genome and methylation patterns requires some form of control mechanism, proposed to be FIS2-PRC2. FIS2-PRC2 is targeted to hypomethylated regions of the genome, acting to supress transposition Taken from Köhler and Lafon-Placette (2015)

The exact mechanisms for transgenerational inheritance are unclear but appears to have some relation to epialleles. Epialleles are heritable alternative expression

states of a gene not caused by genetic variation (Rakyan et al., 2002; Casas and Vavouri, 2020). In *Arabidopsis* mutants displaying loss of MET1 (*met1-3*) which have been backcrossed into wildtype Ler, there is regain of methylation at only some loci, while others appears unable to do so (Catoni *et al.*, 2017).Here, the regain of methylation appeared dependent on the epiallele, indicating that DNA methylation and epigenetics has an impact upon inheritance. For example, the study reported that increased numbers of CG residues was correlated with the activity of transposable elements (Catoni *et al.*, 2017), a phenomenon that has also been reported in human cells (Onuchic *et al.*, 2018). The observation that some loci did not regain methylation after backcrossing, where methyltransferase activity was regained, was linked to the requirement of maintenance of the original methylation (Catoni *et al.*, 2017). Even with re-establishment of the required machinery, methylation could not occur as the mark needed to be inherited in order to be maintained (Catoni *et al.*, 2017). This suggests there may be a degree of conservation in epigenetic inheritance, despite differences in the ability to pass epigenetic modification along the germline. Furthermore, stable inheritance of parental DNA variants (epialleles) was noted in *Arabidopsis* crossed of wild type and DDM1, an ATPase chromatin remodelled involved in DNA methylation maintenance, deficient mutants. These parents have little variation in base sequence but contrasting DNA methylation profiles, and were used to generated a panel of epigenetic Inbred Recombinant Lines (epiRILs), with the F1 backcrossed into Col-wt plants (Johanne*s et al*, 2009). By analysing the methylation of 11 loci, including *FWA*, whose hypomethylation and ectopic expression is associated with delayed flowering, 5 loci were noted to be inherited in a Mendelian, or near-Mendelian, fashion, while the other 6 were found to be fully methylated in all lines. This suggests

that the methylation state can be variable, as methylation was regained in 6 sequence contexts following DDM1 restoration, while others are stably methylated (Johannes *et al.*, 2009), indicating that some sequences are able to retain methylation pattern better than others across generations. They noted a heritability value of ~30%, close to that used in traditional breeding programs (Johannes *et al.*, 2009), meaning the identification of epialleles could be significant in breeding of agronomic traits. Under stress, epigenetic inheritance may represent an evolutionary advantage by producing more stress-tolerant offspring without altering the underlying genetic code, and there is possibility of utilising this mechanism to create more stress tolerant crops.

1.2.4. Epigenetics in Context

1.2.4.1. Plant Stress Responses

How can these mechanisms be applied to plant stress? Epigenetic regulation has been increasingly investigated to explain altered phenotypes. They are thought to have an important role under fluctuating conditions, associated with plant phenotypic plasticity as epigenetic changes are more likely to be reversible (Kooke *et al.*, 2015). As such, epigenetic changes have been implicated in both biotic and abiotic responses. Although there are possible transgenerational effects, here the immediate response of stress exposed plants is discussed.

There is increasing evidence for the role of epigenetic modification in abiotic stress responses in a range of species, including salt stress (Kaldis *et al.*, 2011; Karan *et al.*, 2012; Mousavi *et al.*, 2019), heat stress (Liu *et al.*, 2015, 2021; Qian *et al.*, 2019), and cold stress (Steward *et al.*, 2002; Shan *et al.*, 2013; Tong *et al.*, 2021). Salt

stress has been correlated with both DNA and histone modification in multiple species, including olive, *Arabidopsis*, and rice (Kaldis *et al.*, 2011; Karan *et al.*, 2012; Mousavi *et al.*, 2019). Increased methylation at CG sites was noted in olive treated with 200mM salt compared to the wildtype, with some of these differentially methylated regions within coding regions of key genes associated with salt tolerance, including aquaporin and a cytochrome b6 (Mousavi *et al.*, 2019). In rice, salt stress caused decreases in methylation in salt resistant cultivars, while less resistant cultivars showed increased methylation (Karan *et al.*, 2012), suggesting increased methylation is a key step in salt tolerance unless already resistant. Heat stress has also been demonstrated to induce epigenetic changes in *Arabidopsis thaliana*. Sanchez and Paszkowski (2014) demonstrated that genes silencing by DNA methylation can be induced by heat stress. They observed that *SDC*, a gene epigenetically silenced in somatic tissue, is activated during vegetative growth under 12-hour cycles at 37°C in light and 21°C in the dark, contributing to the recovery of biomass following stress. The ability of such stress to undo silencing suggests the potential to force activation of genes if plants are exposed to the correct scenario, with the genes likely to be linked in some way to stress tolerance or recovery.

Biotic stress has been most extensively linked to epigenetic change. Inoculation of mutant *Arabidopsis* lacking CG or non-CG methylation with *Pseudomonas syringae* (*Pst*) resulted in hypomethylation of pathogen responsive genes, with mutants showing improved resistance compared to wildtype plants (Dowen *et al.*, 2012). This indicates that methylation has a role in regulating resistance genes, which may act as a reversible mechanism to regulate energy use in wildtype plants. Histone modifications have also been linked to biotic stress resistance. Rymen *et al.*, 2019 found that histone acetylation resulted in induced expression of key wound-induced

genes in *Arabidopsis*. Utilising ChIP-seq, in which the genome wide distribution of histone modifications can be assessed and compared between samples, they assessed the enrichment of histone H3 modifications, including tri-methylation of lysine 27 (H3K27me3), lysine 36 (H3K36me3), and lysine 4 (H3K4me3), as well as acetylation of lysine 9/14 (H3K9/14ac) and lysine 27 (H3K27ac). They noted an association between increases in H3K9/14ac and H3K27ac and transcriptional activation of wound-induced genes as early as 1 hour after artificial wounding (Rymen *et al.*, 2019). However, since this wounding is artificial there may be differences in the observed histone modifications due to herbivore oral secretions and other herbivore associated molecular patterns. Furthermore in the Common Bean, *Phaseolus vulgaris* L, following biotrophic Rust, *Uromyces appendiculatus*, inoculation (Ayyappan *et al.*, 2015) lead to an increase of H3K9me2 and H4K12ac marks on chromosome 11 (Ayyappan *et al.*, 2015). This indicates the genes located here are important for the immune response. Such evidence indicates there is an important role for epigenetic mechanisms in the regulation of gene expression, with both key mechanisms appearing to have a role. This regulation may be evolutionarily favourable as expression can be switched on and off so valuable resources are channelled into immunity when there is a threat, increasing plant fitness.

Epigenetic adaptation has also been observed in non-model plant organisms (Thiebaut, Hemerly and Ferreira, 2019). For example, *Pinus pinea* has been shown to have low levels of genetic variation despite a high degree of phenotypic plasticity (Thiebaut, Hemerly and Ferreira, 2019), but has high variation in the reported levels of cytosine methylation between different populations (Sáez-Laguna *et al.*, 2014). Such observations indicate the possibility of epigenetic priming in important crop

plant species, providing a potential avenue of exploration to improve stress tolerance and, therefore, productivity.

Despite the evidence suggesting a role for DNA methylation in stress responses, it is important to consider that most studies, including those described here, are correlative and do not prove a link between stress and altered DNA methylation profiles. Currently, there is little evidence for a direct link between DNA methylation and stress tolerance, therefore it could be that alterations to the DNA methylation profile are a symptom of stress, rather than a stress tolerance mechanism. There is increasing evidence in methylation mutants for a direct role of DNA methylation in regulating bacterial infection responses (Dowen *et al.*, 2012), as well as cold and salt stress (Yang *et al.*, 2022), but may only mean that DNA methylation in required for "normal" plant activity. It is therefore important to be cautious assigning a direct effect of DNA methylation under stress conditions.

1.2.4.2. Interaction between Light and Epigenetics

The epigenetic effects of light have yet to be fully understood but are of increasing interest as with an ever-changing climate, improving crop productivity and stress tolerance are essential to feeding the growing global population. However, there are some key studies indicating the potential impacts of changing light on the epigenetic profile and plant physiology.

Dark stress has been demonstrated to have epigenetic effect. Under 3-days extended darkness, increased H3K4me3 was observed in many genes in *A. thaliana*, particularly those associated with autophagy and senescence (Yan *et al.*, 2019). Such evidence indicates that light, and a lack thereof, can induce epigenetic changes which affect the phenotypes of plants, demonstrating the potential

importance that understanding such changes may have. However, excess light stress has been shown to induce little stress-induced change to the methylome in *A. thaliana.* After applying excess light stress (1000 μmol m^{-2} s^{-1}) for 1 hour three times over a day for 7 days, a total of 6 differentially methylated regions were found compared to the control (Ganguly *et al.*, 2018), suggesting that acclimation to light stress may have little effect on the methylome.

Despite this, there has been further recent evidence for the interaction between light and epigenetic regulation. Histone variant H2A.Z was shown to be deposited in a light-dependent manner to regulate photomorphogenic growth through interactions with Nuclear Factor-Y through subunit NF-YC (Zhang *et al*, 2021), demonstrating the role of epigenetic regulation in plant growth. NF-YC modulates histone H4 acetylation by interacting with histone deacetylase HDAC15 in the light to modulate hypocotyl elongation (Tang *et al.*, 2017). Together, these data indicate that epigenetic regulation has a role to play in light regulated growth of plants. Furthermore, DNA methylation has been implicated in the repression of light signalling, with MET1 deficient *Arabidopsis thaliana* mutants showing activation of elements associated with light signalling and responses, as well as hormone signalling, compared to wild type (Shim, Lee and Seo, 2021). This indicates that light could impact the epigenome to alter gene regulation and attenuate cellular signals depending on the light stimuli provided, ultimately effecting plant growth and morphology.

Epigenetic changes have also been noted to act in stomatal regulation. Photoperiod, i.e. a long-day plant versus a short day plant, is known to affect stomatal shape and responses, with long-day plants showing a significantly larger stomatal aperture than short-day plants in response to light, as well as having a greater maximal

conductance (Aoki *et al.*, 2019). In long-days plants, expression of genes including *SOC1*, a positive regulator of stomatal opening, was seen to be upregulated, attributed to an increase in trimethylation of H3K4 around the gene region (Aoki *et al.*, 2019). This suggests that epigenetic regulation has a role in stomatal responses, meaning dynamic fluctuations of light could induce such alterations for acclimation to light regime.

1.2.4.3. Plant Breeding

Intensive breeding of crops has resulted in a decrease in genetic diversity, although some phenotypic variability cannot be accounted for with by the base sequence of the genome, called missing heritability, which can potentially be explained by epigenetic change and inheritance (Gallusci et al., 2017). Due to the heritability of 5-methylcystosine across both meiosis and mitosis, favourable epigenetic modification can be propagated in both clonal and sexual reproduction (Gallusci et al., 2017), making such change potentially useful for improving crop traits. Furthermore, relating phenotype and epigenetic change at a specific locus could provide new targets for crop breeding which have not previously been considered. More examples of the benefits and potential role of epigenetics in crop improvement are coming to light, with cases seen in agriculturally significant crops including tomato, rice, and soybean rice (Quadrana et al., 2014; Zhang et al., 2015; Raju et al., 2018). For example in tomato, the vitamin E content of fruit, a trait with low heritability, has been linked to promoter methylation of the VTE3 gene with an inversely proportional relationship (Quadrana *et al.*, 2014). Furthermore, leaf angle and grain size is impacted by epigenetic mutation of RAV6, with hypomethylation in the promoter region associated with smaller grain size and larger leaf angle compared to the wildtype

hypermethylation (Zhang *et al.*, 2015). These examples demonstrate that improving understanding of how epigenetic mechanisms are deployed in plants can have agriculturally significant impacts.

Important to the potential applications of epigenetic change to plant breeding are epialleles. Epialleles have been investigated for use in plant breeding because of methylation on gene expression. Early proof of the heritability of epigenetic changes came from Fieldes (1994). Treatment of flax seed with 5-azacytidine, a chemical which removed cytosine methylation, resulted in 22% of the A0 generation exhibiting a short phenotype, a phenotype which was stably inherited into the A1 and A2 generation (Fieldes, 1994), indicating epiallele methylation state is heritable across multiple generations in agriculturally significant crops. This technique, sometimes termed epimutagenesis, has received some attention in recent years as an alternative to traditional mutagenesis or gene editing (Corbin, Bolt and Rodríguez López, 2020).

Although relatively few have been identified, epialleles have been noted to have range of effects across plant species, including agriculturally significant crops such as tomato, soybean, and rice (Quadrana et al., 2014; Zhang et al., 2015; Raju et al., 2018). In rice (Oryza sativa), a naturally occurring epiallele RAV6, exhibiting hypomethylation in the promoter region of a B3 DNA-binding protein, resulted in an increased leaf angle and reduced grain size, with grain weight 57% that of the wild type (Zhang et al., 2015). This was linked to brassinosteroid (BR) homeostasis, a phytohormone pathway associated with growth, development, stress adaptation and light signaling (Wang, Zhu and Sae-Seaw, 2013; Wei and Li, 2020), with increased induction of BR receptor gene BRI1 in plants expressing the RAV6 epiallele, indicating RAV6 is involved in BR signalling and biosynthesis (Zhang et al., 2015).

This demonstrates the potential impact of naturally occurring epialleles on crops and plant breeding, as identification of further epialleles could explain variation within genetically identical cultivars.

1.2.5. Whole Genome Bisulfite Sequencing

A key method for quantifying genome-wide changes to DNA methylation is Whole Genome Bisulfite Sequencing (WGBS). Treatment of DNA with sodium bisulfite was noted to sulfonate cytosine, uracil, and thymidine residues at position 6 of the pyrimidine rings (Hayatsu *et al.*, 1970). This model was later extended to 5-methylcytosine (Wang, Gehrke and Ehrlich, 1980) and it was proposed that this could be utilized to determine cytosine methylation, as the rate of sulfonation of cytosine to uracil is faster than that of methylated cytosine (Wang, Gehrke and Ehrlich, 1980; Frommer *et al.*, 1992). The first whole genome methylation, termed methylome, data was obtained from *Arabidopsis thaliana* in 2008, and combined sodium bisulfite treatment with ultra-high throughput DNA sequencing technology (Figure **1.9**), allowing for single base resolution of DNA methylation to be achieved for the first time (Cokus *et al.*, 2008). This method has since been widely adopted in the epigenetics field across mammalian species, including human (Lister *et al.*, 2009; Vidal *et al.*, 2017; Zhou *et al.*, 2019), mouse (Dahlet *et al.*, 2020; Ma *et al.*, 2022), and plant species, including *Arabidopsis* (Ganguly *et al.*, 2017; Zabet *et al.*, 2017),

and wheat (Ramírez-González *et al.*, 2018; M. Zhang *et al.*, 2021), contributing to our understanding of genome regulation by cytosine methylation.

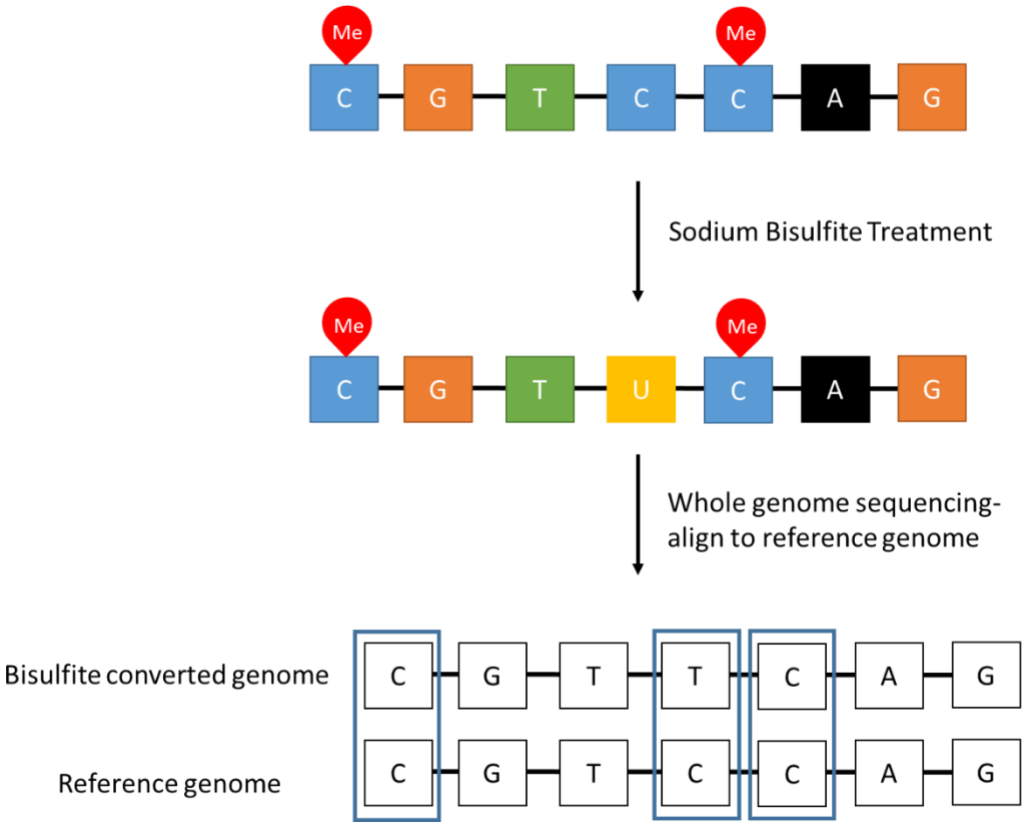

Figure 1.9: Schematic of whole genome bisulfite sequencing. DNA is treated with sodium bisulfite resulting in the conversion of un-methylated cytosine residues to uracil, while the methylated residues are protected from this process. The bisulfite converted genome undergoes whole genome sequencing and is then aligned to a known reference genome. Where a thymidine in the converted genome aligns to a cytosine in a reference, the cytosine is likely to be un-methylated, whereas a cytosine aligned to a cytosine indicates methylation

1.3. Impacts of Light on Plant Physiology

1.3.1. Effects of Light Acclimation

Light acclimation acts to balance the cost of increased photosynthetic capacity and of oxidation if excess excitation energy (EEE) is not sufficiently dissipated (Russell *et al.*, 1995; Karpinski *et al.*, 1999). Plants are known to acclimate to growth light intensity by altering physiology, molecular biology, and anatomy (Givnish, 1988; Walters and Horton, 1994), acting to improve their survival and tolerance of EEE. Distinct physiological and photosynthetic characteristics have been observed in plants grown under different light conditions. In *Arabidopsis thaliana,* high light intensities result in extensive cotyledon expansion and root growth, and thicker leaves, while low intensities have been reported to result in smaller leaves with long petioles and a failure to from well-ordered rosettes, as well as taking longer to reach maturity (Walters and Horton, 1994; Bailey *et al.*, 2001). Such responses indicate that light has important implications for growth of plants, potentially having implications for crop plants grown in greenhouse conditions, as different morphological and biochemical changes may be advantageous, in terms of yield, depending on which part of the plant is harvested. However, most studies into acclimation have investigated light intensity as opposed to light regimes or dynamic light that is delivered to plants in the field, meaning this understanding of acclimation may not be applicable to field plants.

1.3.1.1. Acclimation to Light Intensity

Acclimation under different light regimes has been noted to significantly affect photosynthesis. Karpinski et al (1999) provided early evidence for this response, demonstrating that, in low light (LL, 200 µmol m^{-2} s^{-1}) adapted *Arabidopsis thaliana* antioxidant gene expression is induced when exposed to excess light (2700 µmol m^{-2} $s^{-1)}$. This induction increases the capabilities of a plant to dissipate EEE, which is capable of generating Reactive Oxygen Species (ROS) (Karpinski *et al.*, 1999). Significantly, induction of antioxidant gene expression was induced in systemic tissues, i.e. tissues spatially distinct from that exposed to excess light (Karpinski *et al.*, 1999), meaning the rest of the plant becomes acclimated, improving its stress tolerance. Previously, Karpinski et al (1997) demonstrated acclimation to be reversible, with exposure of low light-adapted (LL, 200 µmol photons m^{-2} s^{-1})) *Arabidopsis thaliana* to excess light (EH, 2000 µmol photons m^{-2} s^{-1}) resulting in reversible photoinhibition (Karpinski *et al.*, 1997). The study demonstrates that PSII electron transport efficiency (F_q'/F_m') did not fully recover 24 hours after EL exposure, following a 2-fold increase in irradiance, indicating that this acclimation response was quickly inducible but slower to turn off, possibly due to oxidative stress caused by reaction oxygen species (ROS) generation under high light.

Changes in electron transport have been observed as an acclimation response to light intensity. Increases in the maximum rate of oxygen evolution (P_{max}) has been shown to increase with light intensity, reflecting an increase in the capacity for electron transport, requiring an increase in the availability of electrons (Walters and Horton, 1994; Bailey *et al.*, 2001). This can be attributed to an increase in Rubisco content, correlated to the increase in irradiance (Figure **1.10**). This increase in

Rubisco content following exposure to increased light intensities demonstrates the ability of plants to acclimate and alter their photosynthetic activity.

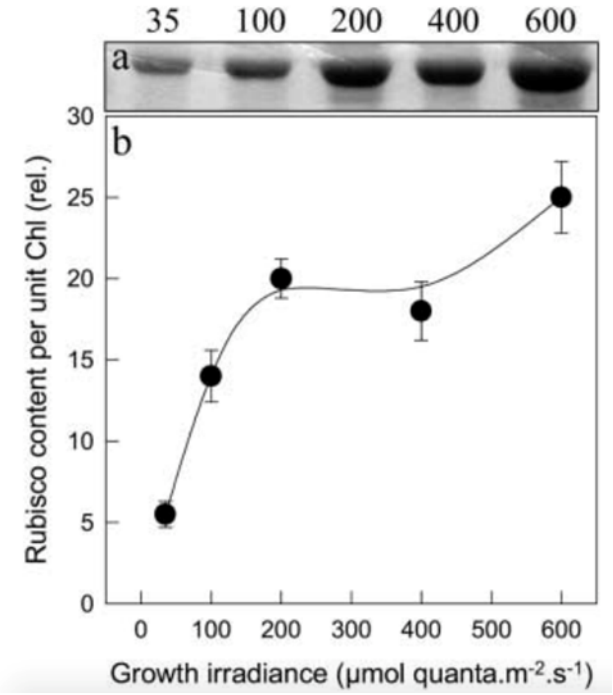

Figure 1.10: Demonstrated increase in the Rubisco content with increased irradiance in *Arabidopsis thaliana*. From Bailey *et al.*, 2001

Light harvesting complexes and the proportion of PSII has been shown to change under long-term acclimation. Kirchhoff *et al* (2007) found that a low light intensity of 30 µmol m^{-2} s^{-1} resulted in a 40-60% increase in antenna size of PSII, while the concentration of PSII and cytochrome b_6f complex was reduced by ~30% compared to plants grown at 300 µmol m^{-2} s^{-1}. This was not accompanied by a change in PSI content in the thylakoid membrane (Kirchhoff *et al.*, 2007), suggesting the acclamatory response to low light intensity is driven by light-dependent reactions via the upregulation of light-harvesting proteins. Similar was observed by Bailey *et al* (2001), who found only slight increases in PSI content between low light and high light-grown plants, while increased PSII content was observed. Furthermore, plants

acclimated to high light (800-1100 μmol m^{-2} s^{-1}) showed reduced levels of light harvesting complex proteins (LHCs) and a reduced antenna size compared to plants grown at low light intensities (Kouřil *et al.*, 2013). This indicates acclimation to light intensity is driven by PSII, providing a mechanism by which photosynthesis can be attenuated depending on light conditions.

Light intensity has been noted to alter anatomy, physiology, growth, and reproduction. In a meta-analysis by Poorter *et al.*, 2019, it was seen that the daily light integral (DLI) effects multiple traits across 760 plant species. They noted that anatomical leaf traits were positively affected by DLI, and that changes are strongest in low light, with an average 2.6-fold increase in leaf mass per area (LMA) driven by changes in leaf thickness and tissue density. Individual leaf area and internode length decrease with increased DLI between 2 and 50 mol m^{-2} d^{-1}, but also decrease when DLI drop below 2 mol m^{-2} d^{-1}, while specific root length decreases with DLI in a linear fashion (Poorter *et al.*, 2019). Furthermore, plants grown under high light increase biomass allocation to the roots, reducing the shoot to root ratio (Powelson and Lieffers, 1992; Poorter and Nagel, 2000), suggesting allocating resources to the roots is beneficial under high light.

1.3.1.2. Spectral Quality Acclimation

Spectral quality refers to the relative content of each wavelength within light. Plants are known to respond to distinct wavelengths of light in different ways, for example the red: far-red ratio is detected by phytochromes and signal that the plant is under shade, eliciting the shade response (Franklin and Whitelam, 2005).

Spectral quality has long been known to effect growth and morphology of plants (Hayes and Klein, 1974; Seibert, Wetherbee and Job, 1975; Drozdova *et al.*, 2001),

as well as the physiology and biochemistry (Murchie and Horton, 1997; Yu and Ong, 2003; Dickinson, Lalonde and McGinn, 2019). Under monochromatic radiation, *Acacia mangium* seedlings grown under blue light showed significantly higher PSII efficiency than those under red light, while displacing similar values to those grown under white light, with the total dry biomass of plants under monochromatic light being significantly lower than plants under white light (Yu and Ong, 2003). This is accompanied by a reduction in net photosynthesis which did not significantly differ between monochromatic grown plants (Yu and Ong, 2003), indicating that the wavelengths present in light have significant effects on productivity in plants. When shade-associated plants were grown in light with a low far-red content, chlorophyll *a/b* values decreased compared to when grown under high light, while high light increased mean dark respiration rates (Murchie and Horton, 1997), suggesting acclimation to spectral quality has multiple effects on physiology. Furthermore, acclimation to light enriched with far-red wavelengths, which are absorbed by PSI, results in an increase in PSII content relative to PSI when exposed to wavelengths absorbed by PSII (Kim, Click and Melis, 1993).

Morphology can be affected by spectral quality. This is well described under shade-avoidance in which a depletion of blue and red wavelengths leads to an enrichment of the far-red wavelengths (Walters, 2005). For example, in *Potentilla*, enrichment with far-red wavelengths results in significant biomass reductions compared to plants grown in full daylight despite exhibiting an average 28% increase in leaf area, accounted for by reduced leaf numbers (Stuefer and Huber, 1998). The shade-avoidance response is also well documented in *Arabidopsis*, with growth under a low red: far-red (R:FR) ratio resulting in a reduced leaf area due to a lower leaf cell number compared to growth under a high ratio (Carabelli *et al.*, 2007) alongside

rapid elongation of the stem and petioles (Franklin and Whitelam, 2005). This response acts to improve survival in shaded plants by allowing them to seek light with a greater R:FR ratio. Shade avoidance is also implicated in root system architecture. In spring barely, *Hordeum vulgare*, a lower R:FR ratio significantly increased total root surface area and root length (Klem *et al.*, 2019), suggesting that light has implications for plant growth beyond tissues directly exposed to light.

Spectral quality has also been demonstrated to affect the photosystems in the thylakoid membrane. Photosystem stoichiometry under a low red: far red ratio (1.20) showed an increase in photosystem II (PSII) per unit of chlorophyll compared to white light regimes in *Arabidopsis thaliana* (Walters and Horton, 1994). Furthermore photochemical quenching (qP), the value associated with oxidation of plastoquinone and the redox state of the acceptor side of PSII, demonstrated that under high white light content PSII was more oxidised than in plants under high far-red light (Walters and Horton, 1994). Measurements of non-photochemical quenching (NPQ) showed little difference between the two plant sets, suggesting that plants exposed to light with a high far-red content are capable of inducing energy-dissipating processes at lower irradiance (Walters and Horton, 1994). These studies provided early evidence for acclimation to spectral quality and suggest there may be advantages in terms of stress tolerance, with an improved ability to cope with EEE.

Blue light levels have been implicated in the acclimation response. When different blue light photon flux densities were applied to *Spinacia oleracea* L. there was a noted impact on photosynthesis and leaf nitrogen content. The light-saturated rate of photosynthesis increased with increased blue light content of the growth light up to 150 µmol m^{-2} s^{-1} , mirroring results seen under high irradiance, while leaf nitrogen content was also noted to be greater at higher blue light levels (Matsud*a et al*, 2007),

suggesting a higher blue light content could improve productivity. Blue light has also been associated with improved acclimation to high UV in pepper plants, with plants grown under 62% blue light had significantly higher F_v/F_m values than those acclimated to 30% blue light, while displaying similar NPQ values to control plants (Hoffmann, Noga and Hunsche, 2015). This evidence indicates that the spectral quality of light may have implications for further stress scenarios, indicating it could be important when considering how to create more stress-tolerant plants.

1.3.1.3. Anatomical Changes

Leaf thickness is effected by light intensity, with thicker leaves observed under high light conditions (Givnish, 1988; Schumann *et al.*, 2017; Vialet-Chabrand *et al.*, 2017; Hoshino, Yoshida and Tsukaya, 2019). Under low light (70 µmol m^{-2} s^{-1}) leaves had a single palisade layer of small, round cells (Figure **1.11**A), compared to high light (280 µmol m^{-2} s^{-1}) with multiple layers of elongated palisade cells (Figure **1.11**B) along the adaxial-abaxial axis in *Arabidopsis* (Hoshino, Yoshida and Tsukaya, 2019). These morphological differences could be noted in the leaf primordia as early as 4 days after sowing, indicating that developmental acclimation is fast acting under differing light intensities. When comparing square light and fluctuating light regimes, increased thickness of the spongy mesophyll layer was observed in square light-grown plants, with a higher number of cells that were more circular in shape compared to plants grown under fluctuating light (Vialet-Chabrand *et al.*, 2017), suggesting fluctuating light results in a phenotype similar to that of plants grown under low light intensities.

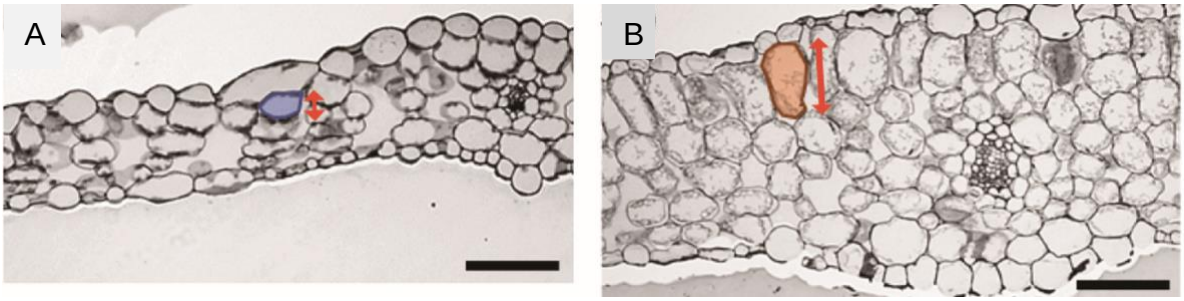

Figure 1.11: Leaf cross sections demonstrating the effect of low (A) and high (B) light on leaf morphology in wild type *Arabidopsis thaliana*, with a typical cell outlined and cell height indicated. Low light results in a thinner leaf, with high light plants having more palisade layers of a greater cell length. Adapted from Hoshino, Yoshida and Tsukaya (2019)

Tissue not directly light-exposed can also be affected by light intensity. In *Nicotiana tabacum* seedlings, root growth reacted rapidly to transition from 60 µmol m^{-2} s^{-1} to 300 µmol m^{-2} s^{-1}, increasing by a factor of 4 within 4 days (Nagel, Schurr and Walter, 2006). Similar has been observed in Arabidopsis, with transition from 38 to 150 µmol m^{-2} s^{-1} resulting in a two-times increase in lateral root number (Kumari *et al.*, 2019), suggesting that root development is stimulated by high light. This response has been attributed to translocation of a component of the light signal transduction pathway from the shoots to the roots, with genes involved in circadian regulation thought to play a role (Kumari *et al.*, 2019).

Plastid development, particularly of the chloroplasts, can acclimate to light intensity. A reduced number of chloroplasts has been observed under very low light intensity (20 µmol m^{-2} s^{-1}), as well as high intensity (400 µmol m^{-2} s^{-1}) in *Anthurium andraeanum* (Y. Wang *et al.*, 2018), while increases in chloroplast number were seen in soybean with light intensity between 100-400 µmol m^{-2} s^{-1} (Feng *et al.*, 2019). However, in *Sinapis alba* both high (~276 µmol m^{-2} s^{-1}) and low light (~27.6 µmol m^{-2} s^{-1}) chloroplast numbers increased, with little difference in the number of

chloroplasts per guard cell (Wild and Wolf, 1980). These contrasting results could be due to the different species utilised, the difference in light intensities, or due to improved technology allowing for improved measurements in the study of Wang et al (2018) compared to Wild and Wolf (1980). Within chloroplasts, the accumulation of chlorophyll was seen to be delayed under high (500 μmol m^{-2} s^{-1}) light, while an increase in the plastid NADPH/NADP+ ratio appeared to block the import of plastid associated proteins including components of electron transport chain, as well as chlorophyll synthase G4 (Zhang *et al.*, 2016). Chloroplast ultrastructure is also influenced by light, with increased thylakoid to chloroplast ratios under high light intensities, plus a higher cross-sectional area (Feng *et al.*, 2019), while acclimation to low light increased grana size (Chow *et al.*, 1988). Such acclamatory responses demonstrate that light intensity experienced during development can significantly alter phenotype, with both low and high light intensities having distinct impacts on plant physiology.

1.3.1.4. The Effects of Light on Stomata

Stomatal anatomy and responses are dependent on both light intensity and spectral quality, and the coordination of light signals and light-energy conversion ultimately result in stomatal pore opening (Shimazaki *et al.*, 2007). Blue and red light, alongside low carbon dioxide concentrations, induce stomatal opening (Hiyama *et al.*, 2017), so the spectral quality of light may have a significant impact on the stomatal responses to changing light quality. Differences in stomatal density in response to light intensity is well documented, with high light resulting in increased stomatal density per mm^2, particularly on the adaxial leaf surface (Pazourek, 1970; Gay and Hurd, 1975; Wild and Wolf, 1980), as well as on the abaxial surface in

some species (Schlüter *et al.*, 2003; Poorter *et al.*, 2019). This indicates that light acts as positive regulator of stomatal development, with cryptochromes and phytochromes, the blue light and red/far-red photoreceptors respectively, play a role in the signalling pathway to promote stomatal development (Casson *et al.*, 2009; Kang *et al.*, 2009). In *Arabidopsis*, increased stomatal density by overexpressing STOMAGEN, a positive regulator of stomatal development, has been shown to enhance light-saturated carbon assimilation by 30% and increase stomatal conductance at ambient carbon dioxide compared to wild type, correlated with an increase in intercellular carbon dioxide concentration (Tanaka *et al.*, 2013). This indicates that stomatal density can have a significant impact on physiological processes and provide explanation for phenotypic changes observed under different light conditions.

Stomatal opening is also affected by light. Blue light is known to stimulate stomatal opening in a guard cell-specific response (Zeiger and Zhu, 1998; Briggs and Christie, 2002), while red-light stimulated opening occurs as a photosynthetic response (Sharkey and Raschke, 1981a, 1981b) indicating that spectral quality effects stomatal opening to a greater degree than light intensity. Illumination, or increasing the light available at the leaf surface results in an increase in photosynthesis which is limited by stomata, as their aperture, i.e. how open or closed they are, limits the uptake of carbon dioxide (Lawson, von Caemmerer and Baroli, 2010). There is known to be a lag between the observed increase in photosynthesis and increases in stomatal aperture in response to increasing light and sun flecks (Pearcy, 1990; Lawson, von Caemmerer and Baroli, 2010).

1.3.2. Photoinhibition

Photoinhibition has been defined as a light-induced decrease in carbon assimilation, but is often used to refer to light-induced damage to the PSII reaction centre or the downregulation of PSII photochemistry (Baker, 1996; Kapri-Pardes, Naveh and Adam, 2007). It occurs as a result of the loss of electron transfer through the photosystems, with both PSI and PSII implicated, leading to the production of reactive oxygen species (ROS) that can damage cellular membrane, but also act as signalling components (Foyer, Ruban and Noctor, 2017; Wang *et al*, 2018). Photoinhibition can be characterised by decreases in the F_v/F_m and maximal P700 oxidation in PSI (F. Wang *et al.*, 2018), ultimately resulting in a reduced photosynthetic performance, as well as reduced growth and productivity, making the process particularly relevant when considering crops.

When a photon in absorbed by P680, the reaction centre of PSII, excitation leads to electron transfer between electron acceptors, ultimately resulting in production of NADPH and ATP. High light results in the generation of reactive oxygen species (ROS) as photoproducts (Mishra and Ghanotakis, 1994), which result in damage to PSII as the rate of damage exceeds the rate of repair (Figure **1.12**). This is as a result of excess energy absorption by chlorophyll in PSII antennae which cannot be utilised, leading to formation of the triplet chlorophyll which transfers its energy to O_2, forming an oxygen singlet $^1O_2$ (Pospíšil, 2016). An oxygen radical can also be generated when the plastoquinone pool is completely reduced. Such highly reducing conditions can result is double reduction and protonation of Q_A to Q_AH_2, which could be released from its binding site in PSII, so the electron is instead released to form the superoxide anion $\bullet O_2^-$ (Pospíšil, 2016). Furthermore, limited electron transport on the donor side can result in the formation of a hydroxyl radical, •OH, resulting from

incomplete oxidation of water. This incomplete oxidation results in the formation of hydrogen peroxide, H_2O_2, forming •OH when H_2O_2 remove is not fully catalysed by catalase (Pospíšil, 2016). The subsequent activities of ROS are thought to inhibit the repair of the PSII reaction centre rather than cause direct damage (Murata, Allakhverdiev and Nishiyama, 2012), so resulting in the observed decreases in chlorophyll fluorescence associated with photoinhibition.

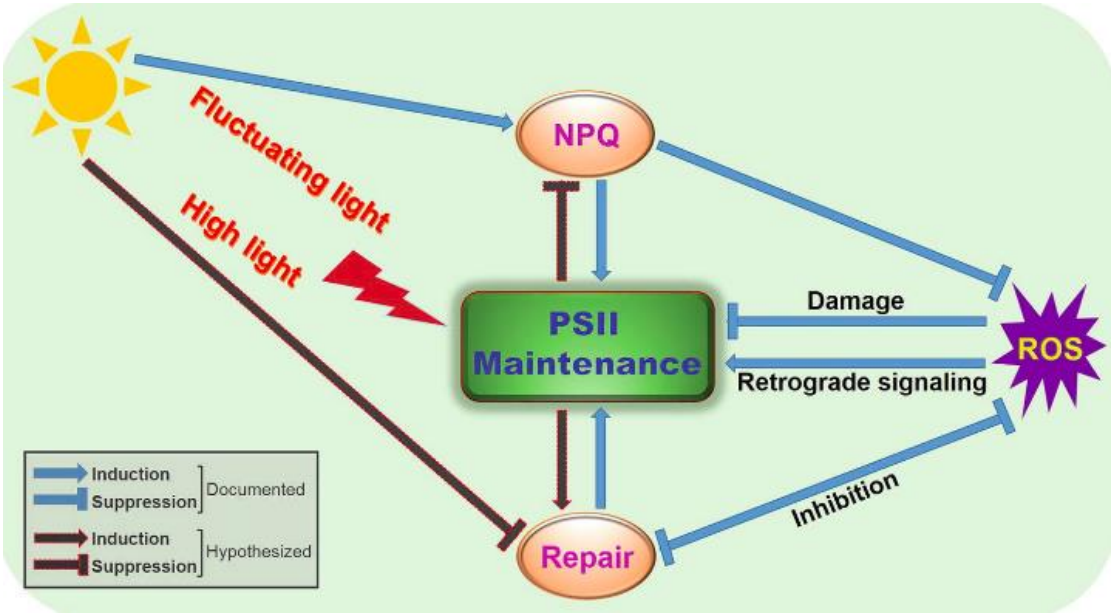

Figure 1.12: Simple proposed model of the inhibition and damage caused by ROS on PSII, and the counter activity of Non-Photochemical Quenching (NPQ) under high light. Taken from Liu *et al.*, 2019

Two reaction centre proteins of PSII, D1 and D2, have been linked to the photo-inhibitory response. *Cucurbita pepo* L. leaves acclimation to 80 μmol m^{-2} s^{-1} were noted to be more susceptible to photoinhibition than leaves acclimated to 1000 μmol m^{-2} s^{-1}, and had slower degradation of damaged D1 protein accompanied by a reduced repair cycle constant for PSII (Rintamäk*i et al*, 1995), indicating the D1 protein may be important in the signalling leading to repair of PSII. This can be related to the decreased rate of degradation of D1 noted in low light adapted leaves exposed to steps in high light (400, 1600, 2800 μmol m^{-2} s^{-1}), with lincomycin

treatment, an inhibitor of chloroplast protein synthesis, enhancing the rate photoinhibition in both high and low light adapted plants (Aro, Mccaffery and Anderson, 1993). Together, this evidence indicates that the rate of repair, in terms of protein synthesis, is a limiting step in recovery from photoinhibition, with acclimation to different light regimes altering the ability to cope with demand under high light stress. The D proteins are also subject to direct oxidative damage by ROS. Kale *et al.* (2017) found that multiple amino acid residues are oxidised in D1 and D2 during photoinhibition, many of which are associated with coordination of the electron transport chain. This demonstrates that multiple mechanisms may result in photoinhibition and are likely to influence each other and lead to reduced photosynthetic efficiency.

Photosystem I has also been implicated in photoinhibition, occurring when all the capacity of PSII to accept electrons is exceeded (Tikkanen and Grebe, 2018), but is more resistant to photoinhibition than PSII due to highly effective protection measures regulating electron flow to the donor side, such as non-photochemical quenching (Tikkanen and Aro, 2014; Lima-Melo *et al.*, 2019). It has been suggested that PSI photoinhibition is a protective mechanism to prevent ROS production. When pH-dependent control of electron transport is inactivated in *Arabidopsis*, high light induces rapid PSI photoinhibition in plants grown at 125 μmol m^{-2} s^{-1} despite no difference in ROS accumulation between mutant and WT plants, with a 40% reduction in assimilation compared to WT (Lima-Melo *et al.*, 2019). However an increase in ROS scavenging enzymes was noted in mutant plants, and were upregulated in all plants under a high light treatment (Lima-Melo *et al.*, 2019), suggesting that although ROS have a role in PSI photoinhibition, the pH controls are essential for regulation.

1.3.3. Fluctuating Light

Fluctuating light has been demonstrated to have important implications for plant physiology and morphology. Dynamic light has been noted to effect photosynthesis, with its efficiency theoretically dependent on the speed at which non photochemical quenching (NPQ) can be reduced in shade conditions (Kaiser, Galvis and Armbruster, 2019), as the transfer from high to low light can result in carbon assimilation losses due to the slow response of PSII (Zhu *et al.*, 2004). Photo-protective mechanisms, such as thermal dissipation, decrease F_v/F_m values and CO_2 assimilation, with modelling demonstrated a decreased maximum efficiency of photosynthesis in high light results in a delayed reversal of thermal energy dissipation once the leaf is shaded (Zhu *et al.*, 2004), demonstrating that dynamic light can have a significant impact on crop productivity.

One issue with many studies investigating the effects of fluctuating light on photosynthesis is the way “fluctuating” light is administered. Many studies apply fluctuating light in square waves of high – low- high lighting regimes (Yin and Johnson, 2000; Thormählen et al, 2017; Kaiser, Walther and Armbruster, 2020) rather than having a truly fluctuating light regime in which photosynthetic photon flux density (PPFD) fluctuates in a natural rhythm (see Figure **1.13**). This means that observed effects might not be reflective what occurs in natural environments, as light fluctuations in the natural environment do not occur over a square wave PPFD. Such issue was observed by Kono and Terashima (2014), who noted that many studies investigating acclimation of photosynthesis did not account for dynamic fluctuation of light, suggesting this is an important quality of light experienced in the field as plants must cope with changes in irradiance on a daily basis. Thus, it is important to

account for such dynamics in research focusing on the effects of light on photosynthesis.

Previously, work using naturally fluctuating light patterns has been performed on *Arabidopsis thaliana,* and resulted in distinct phenotypic changes (Vialet-Chabrand *et al.*, 2017). This study utilised four diurnal light regimes (Figure **1.13**), with two square light regimes, in which the light increases to a set intensity of 230 µmol m^{-2} s^{-1} and 460 µmol m^{-2} s^{-1} for the square low light regime (SQL) and square high light regime (SQH) respectively. To simulate true fluctuating light, a light sensor was used to measure the PPFD over an average day, with the high intensity regime (FLH) and low intensity regime (FLL) having the same integrated PPFD as their square regime counterpart. These regimes represent the differences in light environment plants experience depending on whether they are grown in a laboratory setting or in the field. The square wave regimes represent the laboratory or a hydroponic setting, where the light turns on and off at set times. This contrasts to the fluctuating regimes, where light gradually increases at dawn, followed by a general increase in light availability until the middle of the day, which is accompanied by dramatic fluctuations in the light intensity available. The light then decreases in the afternoon, with a gradual decrease in light intensity over the last 4 hours of the day until night.

Under these regimes, it was demonstrated that plants grown under the high square light (SQH) regime had a significantly higher photosynthetic capacity, than plants under fluctuating regimes. Supporting the observations of Vialet-Chabrand et al (2017), Matthews et al (2018) observed an increase in *A* in plants grown under SQH compared to high fluctuating light (FLH) but observed no significant difference between plants under low light conditions, indicating high light may be driving the observed physiological differences. The same authors also reported a significantly

higher stomatal density under high light regimes, with no observed change in density between growth treatments of the same light intensity, which resulted in high maximum stomatal conductance.

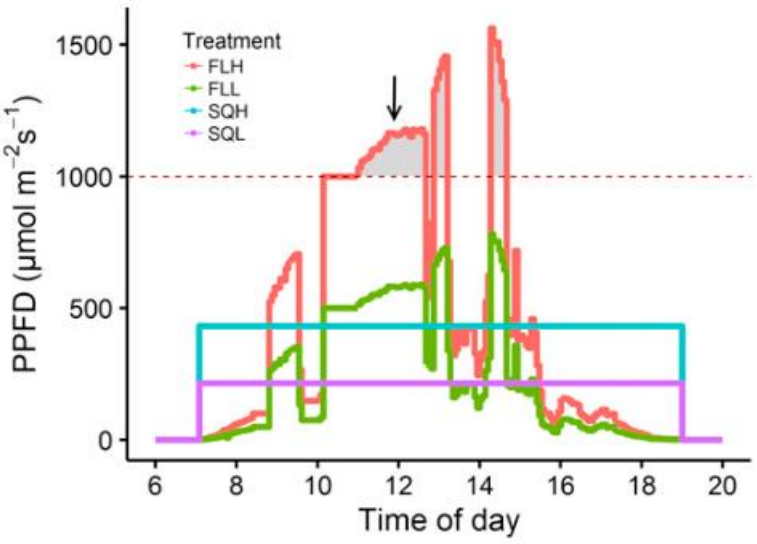

Figure 1.13: Diurnal light regimes utilised by Vialet-Chabrand *et al*. (2017). The area of the curves demonstrates the same average amount of light energy over a 12-hour period. FLH=fluctuating light high, FLL= fluctuating light low, SQH= square light high, SQL= square light low (copied from Vialet-Chabrand et al, 2017)

1.4. Aims and Objectives

Understanding how plants acclimate to dynamic light environments is a key step in improving crop productivity and protecting our food networks under a changing climate and increasing population. Plant breeding has bought light capture and grain biomass near to their theoretical maximums, with the final factor, the efficiency of conversion of capture light to biomass, still having the potential to be improved (Long *et al.*, 2006).

The aim of this work is to determine the physiological and epigenetic impacts of fluctuating light in *Arabidopsis thaliana.* This could provide the first hints that DNA methylation plays a role in regulating light acclimation, give potential evidence for new gene targets to improve light conversion, and contribute to our understanding of how light acclimation is controlled. Therefore, the key objects of this work are:

- Determine the physiological phenotype that occur as a result of real world fluctuating light acclimation, compared to square light as is commonly used in the laboratory
- Determine the effects of fluctuating light on DNA methylation, and whether this could be correlated with the physiological phenotype
- Investigate if DNA methylation resulting from light acclimation impacts gene expression
- Investigate the wider impact of fluctuating light acclimation on photosynthesis and energy conversion, utilizing CP12 triple knockout mutants

Chapter 2: General Materials and Methods

2.1. Plant Materials

Arabidopsis thaliana ecotype Columbia-0 (Col-0) was utilized throughout this study, with all mutant plants also having a Col-0 background. The previously described *cp12-1/2/3* lines 3.1 and 3.3 (López-Calcagn*o et al*, 2017) were kindly donated by Dr Patricia E. Lopez-Calcagno, University of Newcastle.

2.2. Arabidopsis Growth Conditions

2.2.1. Germination Conditions

Arabidopsis thaliana ecotype Col-0 were germinated in 5 cm^2 pots on a peat-based compost (Levingtons F2S, Everris, Ipswich, UK), and placed in a controlled growth environment at 22°C, 65% relative humidity, 8/16h light/dark cycle, CO_2 concentration 400 µmol mol^{-1}. At 14-days, the seedlings were transplanted to individual 5cm^3 pots containing the same soil as above and returned to the controlled environment.

2.2.2. Fluctuating Light Acclimation

A.thaliana (Col-0) at the 4-leaf stage were removed from the controlled environment and placed under Heliospectra LED light source (Heliospectra, Göteborg, Sweden) programmed to each light regime (Figure **2.1**) in a dark room maintained at 21°C/16°C Day/night, 50% relative humidity. Average light intensity for high light conditions was 460 µmol m^{-2} s^{-1} and 230 µmol m^{-2} s^{-1} for low light conditions on a 12h/12h day/night cycle. Plants were kept in well-watered conditions, with their position under the light source randomised every 3 days to remove any potential heterogeneity in spectral quantity and quality.

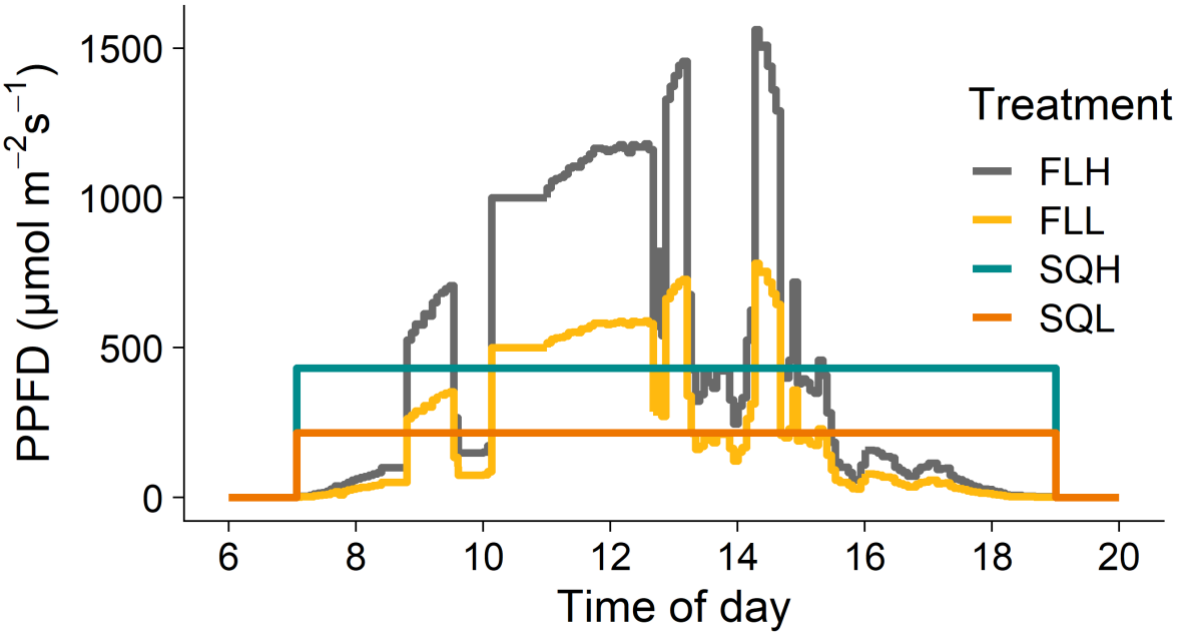

Figure 2.1: Diurnal light regimes utilised in this study. Area of the curves are equal, demonstrating the same average amount of light energy over a 12-hour period in low (square wave, SQL; fluctuating wave, FLL) and high light conditions(square wave, SQH; fluctuating wave, FLH).

2.3. Physiological Measurements

2.3.1. Chlorophyll Fluorescence Imaging

Images of chlorophyll *a* fluorescence were obtained using a CFImaging system (Technologica Ltd, Colchester, UK). For time series fluorescence, plants were subjected to imaging every day from the 4-leaf stage (day 0) to day 21 of exposure to the light regimes.

Four plants, one from each regime, were tested at a time, between the 8am and 3pm. Plants were dark adapted for at least 20 minutes prior to minimal fluorescence (F_o) being measured with a weak pulse. The maximal fluorescence (F_m) was then measured with an 800 ms exposure to a saturating pulse (6231 µmol m^{-2} s^{-1}). Plants were then exposed to an actinic light at 300 µmol m^{-2} s^{-1} for 30 minutes, and steady-

state *F'* continuously monitored while F_m' (maximum fluorescence in the light) was measured at 3 minute intervals by applying a saturating pulse, with and F_o' (minimum fluorescence in the light) measured after switching this off. This was followed by a light response curve, starting at PPFD value of 1500 µmol m^{-2} s^{-1} for 5 seconds, decreasing to 1250, 1000, 500, 250,150, and finally 50 µmol m^{-2} s^{-1}. *F'* was constantly monitored, with F_m' taken after 5 seconds at each light level by applying a saturating pulse, followed by F_o'. These parameters were used to calculate F_v/F_m, F_q'/F_m', F_v'/F_m', F_q'/F_v', and NPQ according to Table **2.1**.

Table 2.1: Calculations of chlorophyll fluorescence parameters obtained from imaging. Adapted from Murchie and Lawson (2013)

Parameter	Formula
F_v/F_m	$(F_m-F_o)/F_m$
F_v'/F_m'	$(F_m'-F_o')/F_m'$
F_q'/F_m'	$(F_m'-F')/F_m'$
F_q'/F_v'	$(F_m'-F')/(F_m'-F_o')$
NPQ	$(F_m-F_m')/F_m'$

2.3.2. Leaf Gas Exchange

For all gas exchange measurements, a Li-Cor 6800 portable gas exchange system (Li-Cor, Lincoln, Nebraska, USA) was utilised. A constant flow rate of 500 µmol s^{-1} was used, with constant cuvette conditions of 400 µmol mol^{-1} [CO_2], vapour pressure deficit of 1 .2 (±0.2) kPa and leaf temperature of 23°C unless otherwise stated. All measurements were taken between 8 am and 3 pm on the youngest fully expanded leaf on days 16-20 of exposure to light regimes. Differences in leaf area within the chamber were accounted for by determining the coverage of the chamber by photographing the leaf position in the chamber and analysed using open source image analysis software ImageJ version 1.52a (Schneider, Rasband and Eliceiri, 2012).

2.3.2.1. A/C_i Response Curves

Assimilation rate (*A*) measured as a function of intercellular [CO_2] (C_i) known as A/C_i curves were measured at 1500 µmol m^{-2} s^{-1} Photosynthetic Photon Flux Density (PPFD). Leaves were first stabilised in the chamber at ambient [CO_2] of 400 µmol mol^{-1}, and once stable, a measurement was taken, after which, [CO_2] was decreased to 300, 200, 100, 80, and 50 µmol m^{-2} s^{-1} before returning to ambient [CO_2]. This was followed by an increase in [CO_2] to 550, 700, 900, 1100, 1300, and 1500 µmol $^{-1}$. Measurements were taken at each new [CO_2] when *A* had stabilised which was usually within 30-120 seconds.

2.3.2.2. Light Response (A/Q) Curves

The response of *A* to changes in light intensity, was measured under the same conditions as A/C_i above. Leaves were stabilised at 1800 µmol m^{-2} s^{-1} to reduce stomatal limitation and a measurement recorded, and then PPFD was decreased to 1500, 1300, 1100, 900, 700, 550, 400, 250, 150,100, 50, and finally 0 µmol m^{-2} s^{-1}, with a measurement taken at each step when *A* was stable and before g_s responded to the new light level.

2.4. DNA Methylation Analysis

2.4.1. DNA extraction- CTAB method

A modified version of the CTAB extraction protocol described by Porebski, Bailey and Baum (1997) was utilized. Tissue was harvested between midday and 1pm on day 18-21 of exposure to light regimes.100 mg of leaf tissue from a single plant (fresh weight) was ground in liquid nitrogen, to which 1ml CTAB buffer warmed to 55°C was added. This was then incubated at 55°C for 15 minutes. 1 volume of chloroform was added, and samples were incubated on ice for 10 minutes. These

were vortexed for 1 minute then spun at 14000 r.p.m. for 5 minutes, and the supernatant recovered, at which point 5ul RNAse A (10mg/ml) was added and incubated at 37°C for 15 minutes. 1 volume chloroform was added, mixed by inversion for 5 minutes, centrifuged at 14000 r.p.m. for 10 minutes, and the supernatant recovered. To this 2.5 volumes 70% ethanol and 0.1 volumes 3M Sodium Acetate were added, and samples incubated at -20°C for 1 hour. Samples were then spun at 14000 r.p.m. for 5 minutes, the supernatant discarded and resulting pellet washed with 70% ethanol. Once dried, the pellet was resuspended in pure water. DNA integrity and purity was assessed using NanoDrop ND-1000 UV-Vis spectrophotometer was used along with the NanoDrop V3.1 software (Labtech International Limited, UK).

2.4.2. Whole Genome Bisulfite Sequencing

5µl genomic DNA from multiple samples per regime (n=6 plants/regime) were pooled together (total volume 30ul) to form a single sample. Previous work has shown for identifying differential methylation, 1 single replicate consisting of multiple individuals was sufficient (Catoni *et al.*, 2018). Library preparation and sequencing were carried out by Novogene. Genomic DNA was fragmented into 200-400bps using a S220 focussed-ultrasonicator (Covaris, Massachusetts, USA) and Bisulfite treated with EZ DNA Methylation Gold Kit (Zymo Research, California, USA). Library concentration was quantified by Qubit 2.0 Fluorometer (Invitrogen, ThermoFisher Scientific, Massachusetts, USA), diluted to 1ng/µl and insert size checked on Agilent 2100 before further quantification by qPCR. Libraries were then pooled and fed into NovaSeq 6000 (Illumina, California, USA), utilizing a paired end 150bp read length and 30x coverage sequencing depth, with 8Gb raw data generated per sample.

2.4.3. Computational Analysis

2.4.3.1. Preprocessing

Raw data was first processed through Trimmomatic -0.39 (Bolger, Lohse and Usadel, 2014) to remove adapter specific sequences, remove low quality reads, and reads below a minimum length. The resulting files were run through Bismark (Krueger and Andrews, 2011) and Bowtie2 (Langmead and Salzberg, 2012), acting to map the bisulfite data onto the Arabidopsis thaliana (Col-0) reference genome build TAIR10 (Howe *et al.*, 2020). This was converted from bam to sam format with SAMtools (Li *et al.*, 2009; Danecek *et al.*, 2021), with the Bismark deduplication capabilities (Krueger and Andrews, 2011) utilized to remove duplicated sequences ensuring removal of PCR amplification artefacts. Finally, cytosine methylation reads were extracted with the bismark_methylation_extractor function, resulting in a text file (called CX report) used in further processing.

2.4.3.2. Computation of Differentially Methylated Regions

2.4.3.2.1. DNA methylation data

CX report files were further analysed using R (version3.6) and package DMRcaller (Catoni *et al.*, 2018). Each file was read into an individual object, then files from the same light treatment pooled together into a single object with poolMethylationDatasets. Low resolution profiles, data coverage, and correlation were plotted to assess data quality. Differentially methylated regions were then computed using the bins method, with a bin size of 150 base pairs as done previously (Hansen, Langmead and Irizarry, 2012; Catoni *et al.*, 2017). A p-value threshold of 0.01 for all contexts was used, alongside a minimum cytosine count of 4,

minimum proportion difference of 0.2 for CG and CHG, and 0.1 for CHH, and minimum reads per cytosine of 4, allowing bins with few cytosine bases to be avoided (Stroud et al., 2013).

2.4.3.2.2. Genomic Annotation

Functional annotation utilized TAIR10 (Howe *et al.*, 2020) annotation. Several genomic functional annotations were utilized; introns, exons, 5'UTR, 3'UTR, transposable elements, promoters, and "other" regions encompassing regions outside of these annotations. Promoter regions calculated as sites with 1000 bp of the transcription start site of regions assigned the "gene" annotation.

2.5. RNA Sequencing Analysis (RNAseq)

2.5.1. RNA extraction

The RNA from 3 independent replicates (100mg/replicate) per regime were extracted using the Macherey-Nagel Mini kit for RNA purification (Macherey-Nagel, Allentown, PA). Sample purity was assessed using the NanoDrop ND-1000 Spectrophotometer (NanoDrop, ThermoFischer, Wilmington, DE).

2.5.2. RNA sequencing

Library preparation and sequencing were carried out by Novogene (Beijing, China). Messenger RNA was purified from total RNA with poly-T oligo-attached magnetic beads and fragmented. First strand cDNA was synthesized using random hexamer primers, followed by synthesis of the second strand. The library then underwent end repair, A-tailing, adapter ligation, size selection, amplification, and purification. Sequencing was performed on Illumina NovaSeq 6000 (Illumina, California, USA), utilizing a paired end 150bp read length, with 6Gb raw data generated per sample.

2.5.3. Computational Analysis

2.5.3.1. Preprocessing

Raw data files were first aligned with the Arabidopsis thaliana reference genome TAIR10 release (The Arabidopsis Information Resource, 2019) utilizing HISAT2 (Kim *et al.*, 2019). Resulting sam files were converted to bam and sorted with SAMtools (H *et al.*, 2009; Danecek *et al.*, 2021). Alignment metrics, insert size metrics, and RNASeq metrics were assessed with Picard tools package (Broad Institute, 2019), and built and indexed with HISAT2 (Kim et al., 2019). Finally, featureCounts was performed on each file pair to generate a tab file (Liao, Smyth and Shi, 2014).

2.5.3.2. Computation of Differentially Expressed Genes

The tab files from HISAT2 processing were loading into R (version 3.6) and analyzed using package DESeq2 (Love, Huber and Anders, 2014). Differentially expressed gene were filtered using a p-adjusted value ≤ 0.05, and a log2-fold change of 0.5.

2.6. Quantitative Reverse Transcriptase PCR (RT-qPCR)

2.6.1. RNA Extraction

9mm leaf discs were taken from the two newest fully expanded leaves of each plant, frozen in liquid nitrogen and stored at -80°c until used (total 6 leaf discs). 3 leaf discs were grounded to fine powder on dry ice, and RNA extracted using Trizol reagent (ThermoFisher Scientific, Massachusetts, USA) according to the manufacturer user guide. RNA integrity and purity was assessed using NanoDrop ND-1000 UV-Vis

spectrophotometer was used along with the NanoDrop V3.1 software (Labtech International Limited, UK).

2.6.2. RT-qPCR

cDNA was synthesised using RevertAid Reverse Transcriptase (ThermoFisher Scientific), with a total RNA content of 1µg in the reaction, otherwise following the manufacturer's protocol. Thermal cycling was performed according to the manufacturer's guide using a Bio-Rad T100 Thermal Cycler (Bio-Rad, California, USA). For qPCR, a minimum of 4 biological replicates were analysed, and each measured in triplicate using the ICycler iQ thermocycler (Bio-Rad, California, USA) and SyGreen Mix Lo-ROX (PCR Biosystems, UK).

2.7. Statistical Analysis

Statistical analysis was performed using open-source software R (R Core Team, Vienna Austria 2019, version 3.6.0 for Windows), utilising R Studio (version 1.2.5033). A two-way ANOVA was used to test for two factor differences, and Tukey post-hoc testing was performed where significant differences were observed.

Chapter 3: Characterising the photosynthetic phenotype of Arabidopsis thaliana grown under fluctuating light

3.1. Introduction

Plants experience constant dynamic changes in the surrounding environment due to their sessile nature and must adapt and acclimate to overcome these fluctuations to survive. The definition of acclimation used here, as seen above, is not the only definition for acclimation. It can be defined more broadly as the capacity to adapt to environmental changes within the lifetime of an individual, allowing for plants to survive the continuous variation to which they are exposed (Kleine *et al.*, 2021). However, the definition of acclimation can vary depending on the stress applied or research field. For example, thermal acclimation is defined as the capacity to adjust the temperature response of leaf-scale net photosynthesis following temporal changes in ambient temperature (Kumarathunge *et al.*, 2019). Chilling acclimation is also defined slightly differently, with a transitional low temperature acting to aid in low temperature tolerance, referred to as priming, required for a plant to acclimate(Hughes and Dunn, 1996). Despite these differences in definition, all agree that changes to the plants' biochemistry and physiology play a role.

The process of acclimation is key in ensuring survival and occurs under multiple scenarios including fluctuating light. Light is essential for plant processes, however too much or too little light can cause stress to the plant (Demmig-Adams and Adams, 1992; Kalaji *et al.*, 2012). In the field environment fluctuating light occurs naturally due to changes in cloud cover, season, and time of day. Although fluctuating light intensity is experienced by all plants grown in the field, little research has been conducted investigating the effect of naturally dynamic light on physiological processes. Several studies have simulating fluctuating light as a series of square waves (Yin and Johnson, 2000; Thormählen *et al.*, 2017; Kaiser, Walther and Armbruster, 2020) however, few have used regimes with true peaks and troughs

such as thought found in the field (Lawson, von Caemmerer and Baroli, 2010; Matthews, Vialet-Chabrand and Lawson, 2018). A handful of field studies have demonstrated that dynamic light impacts upon crop performance in wheat and soybean (Taylor and Long, 2017; Wang *et al.*, 2020), demonstrating the importance of understanding the impacts of fluctuating light on plant physiology

Measurements of chlorophyll fluorescence parameters can allow for the assessment of both photosynthesis and provide an non-destructive measure of plant stress (Maxwell and Johnson, 2000). Photosynthetic efficiency is determined by both photochemical processes as well as those associated with dissipation of excitation energy termed non-photochemical quenching. In order to measure or determine the different components that make up photosynthetic efficiency, chlorophyll fluorescence signals are required from both dark and light adapted samples when the photosynthetic machinery is in defined states (Lawson *et al.*, 2002). In dark-adapted material, NPQ should be fully relaxed and the plastoquinone pool in the electron transport chain fully oxidized. In this state the PSII reactions centres are considered open. In these conditions a small measuring beam (<1 µmol m^{-2} s^{-1}) is used to determine the minimum fluorescence (F_o,), while F_m, the maximum value of fluorescence is determined immediately after a short pulse (0.8 s) of high light (>6000 µmol m^{-2} s^{-1}), which transiently shuts all the reaction centres and fully reduces the PQ pool (Lawson *et al.*, 2002). The difference between F_m and F_o is variable fluorescence (F_v) and enable the calculation of the maximum quantum efficiency of PSII photochemistry (F_v/F_m). In light-adapted tissue, steady state *F'* is measured using the modulate beam and F_m' following a saturating pulse identical to that described above providing maximum fluorescence in the light (F_m'). F_m' – *F'* is

F_q' and enables the determination of one of the most useful fluorescence parameters F_q'/F_m' - operating efficiency of PSII photochemistry. Minimum fluorescence in the light F_o' can be calculated using the equation of Oxbrough and Baker 1997 to allow various quenching parameters to be determined, with differences between F_o' and F_m' termed F_v' (Baker, 2008). Combinations of these parameters can be used to determine different aspects of photosynthetic efficiency (Maxwell and Johnson, 2000). Combining these parameters into mathematical equations provides estimates of many elements of PSII function and photochemistry (summarised in Table ***3.1***). F_v'/F_m' is calculated as $(F_m'-F_o')/F_m'$, while F_q'/F_v' is $(F_m'-F')/(F_m'-F_o')$, and combining these equations gives $(F_m'-F')/F_m'$, the calculation for F_q'/F_m' (Murchie and Lawson, 2013), demonstrating the relationship between these parameters.

One of these parameters, NPQ, can be broken down further into qE, qT, qI, and qZ (Zaks *et al.*, 2013). Energy-dependent quenching (qE) is thought to be a major contributor to NPQ, requiring a low pH in the thylakoid lumen and ultimately resulting in the synthesis of protective molecules, particularly zeaxanthin, and relaxes in minutes when a leaf is in darkness (Maxwell and Johnson, 2000). PsbS, a pigment-binding PSII subunit, is central to qE. Chlorophyll fluorescence video imaging measuring NPQ induction and relaxation found that knockout of the PsbS resulted in complete loss of qE, (L*i et al*, 2000), demonstrating its central role in NPQ. This was attributed to a lack of pH and zeaxanthin-dependent conformational changes in the thylakoid membrane (Li *et al.*, 2000). It was also noted that this knockout had little to no effect on light harvesting and photosynthesis (Li *et al.*, 2000), suggesting PsbS is specifically involved in energy dissipation.

Redistribution of energy between PSI and PSII also contributes to NPQ, termed the state transition or qT, can also relax within minutes in the dark, and acts to balance the energy absorption at low light, but is thought to have minimal contribution in higher plants (Ware, Belgio and Ruban, 2015; Guidi, Lo Piccolo and Landi, 2019). A more slowly reversible component of NPQ is photoinhibition, qI, as it represents potential damage to PSII light (Ware, Belgio and Ruban, 2015; Guidi, Lo Piccolo and Landi, 2019), therefore requiring a longer recovery time. More recently, the contribution of zeaxanthins to NPQ, qZ, has been investigated as qE and qI do not always fully account for NPQ (Nilkens *et al.*, 2010). This parameter does not require PsbS presence or low lumen pH (Nilkens et al., 2010), while zeaxanthins function as a regulator or photoprotective molecule following light stress to indirectly impact qZ (Kress and Jahns, 2017). The relaxation of qZ was found to be closely correlated with zeaxanthin epoxidation, which has been shown to reverse NPQ at PSII (Gilmore, Mohanty and Yamamoto, 1994). This supports the theory of some link between the qZ component of NPQ and zeaxanthins.

Table 3.1: Parameters of chlorophyll fluorescence imaging and their description (adapted from Murchie and Lawson, 2013)

Parameter	Formula	Description
F_v/F_m	$(F_m-F_o)/F_m$	Maximum quantum efficiency of photosystem II photochemistry
F_v'/F_m'	$(F_m'-F_o')/F_m'$	Maximum efficiency of PSII photochemistry in the light if all reaction centres open
F_q'/F_m'	$(F_m'-F')/F_m'$	PSII operating efficiency
F_q'/F_v'	$(F_m'-F')/(F_m'-F_o')$	Photochemical quenching
NPQ	$(F_m-F_m')/F_m'$	Non photochemical quenching, an estimate of the heat loss rate constant at PSII
qL	$(F_q'/F_v')/(F_o'/F')$	Estimates the fraction of open PSII reaction centres
qE	Component of NPQ	High energy state quenching, involves light-induced formation of zeaxanthin (Maxwell and Johnson, 2000)
qI	Component of NPQ	Photoinhibition, referring to protective processes and damage to PSII reaction centres in fluorescence analysis(Maxwell and Johnson, 2000)
qT	Component of NPQ	State transition-involves reversible phosphorylation of light harvesting proteins, thought to be important in balancing energy distribution between PSI and PSII in low light (Maxwell and Johnson, 2000)
qZ	Component of NPQ	Zeaxanthin-dependent quenching (Nilkens *et al.*, 2010)

Light acclimation acts to balance the cost of increasing photosynthetic capacity with oxidative stress from excess excitation energy (EEE) if not sufficiently dissipated

(Russell *et al.*, 1995; Karpinski *et al.*, 1999). EEE is dissipated via non photochemical quenching (NPQ) as heat, returning excited electrons to ground state and preventing the formation of radicals which can damage biological membranes. Mechanisms associated with NPQ including the binding of protons and xanthophylls to PSII components, including core protein PSBS and the antenna, inducing a conformational change in PSII that reduces chlorophyll lifetime (Müller, Li and Niyogi, 2001). Plants are known to acclimate to growth light intensity by altering physiology, molecular biology, and anatomy (Givnish, 1988; Walters and Horton, 1994), acting to improve their survival and tolerance of EEE.

Phenotypic changes also include a higher stomatal density (Gay and Hurd, 1975; Wild and Wolf, 1980), while higher irradiance results in an increased Rubisco content (Bailey *et al.*, 2001). However, as outlined above, the majority of these studies were conducted under square wave light conditions, so may not represent the typical acclimation of plants in the field due to the fluctuating nature of light (Lawson, von Caemmerer and Baroli, 2010).

Recently, true fluctuating light was recorded and replicated and applied at high and low intensities to *Arabidopsis thaliana* plants, which resulted in consistent and distinct phenotypes (Vialet-Chabrand *et al.*, 2017; Matthews, Vialet-Chabrand and Lawson, 2018) , suggesting fluctuating light has a distinct effect on the acclamatory response. Both studies utilised four diurnal light regimes, with two square light regimes, in which the light increases to a set intensity of 230 and 460 μmol m^{-2} s^{-1} for the square low light regime (SQL) and square high light regime (SQH) respectively. To replicate a true fluctuating light regime, a logging PPFD sensor was used to measure the PPFD over a typical summer's day in Essex (UK) and was used as the

high intensity regime (FLH) whilst values were halved to provide the low intensity regime (FLL) with square counterpart regime having the same photon dose but provided by a constant intensity over the 12 h period. This work demonstrated that fluctuating light resulted in distinct phenotypes from the plants grown under square light, including a reduced photosynthetic capacity, lowered rates of Rubisco carboxylation, and a reduced electron transport rate for RuBP on an area basis (Vialet-Chabrand *et al.*, 2017), while plants grown under high intensity fluctuating light showed faster stomatal response to changes in light (Matthews, Vialet-Chabrand and Lawson, 2018). The differences between plants under these light conditions indicates acclimation results in a distinct phenotype, which would be important to understand as many significant crops are subjected to field conditions and therefore exposed to fluctuating light. This could mean there are potential losses in yield due to reduced photosynthetic capacity.

In this chapter, the aim of the work was to demonstrate phenotypic consistency in relation to the work of Vialet-Chabrand et al. (2017), and to further characterise the physiology driving these differences in phenotype.

3.2. Materials and Methods

3.2.1. Plant Material and Growth Conditions

Arabidopsis thaliana ecotype Col-0 were grown according to Chapter 2 section 2.1 and 2.2.

3.2.2. Tracking Plant Growth

Photographs were taken every 3 to 5 days until occurrence of first inflorescence. Rosette area was calculated through open-source software ImageJ version 1.52a (Schneider, Rasband and Eliceiri, 2012). Images were processed individually and calibrated using a known length within each.

3.2.3. Stomatal Impressions

Leaf surface impressions were taken using Xantopren dental impression material and activator, following the methods of Weyers and Johansen (1985), and applied to the youngest fully expanded leaf on the adaxial and abaxial surface. The negative impression was allowed to dry for 30 min before carefully removing. After which the resulting mould was painted with clear nail polish and dried for a further 15 minutes before clear cellotape was applied and used to peel off the nail polish positive impression and placed on a microscope slide. Stomata were counted at 20x magnification in an area of $1mm^2$ using a Leica ATC 2000 microscope (Leica Microsystems, Milton Keynes, UK), with 9 repetitions taken per impression, following the method of Poole *et al*. (1996) (Figure **3.1**).

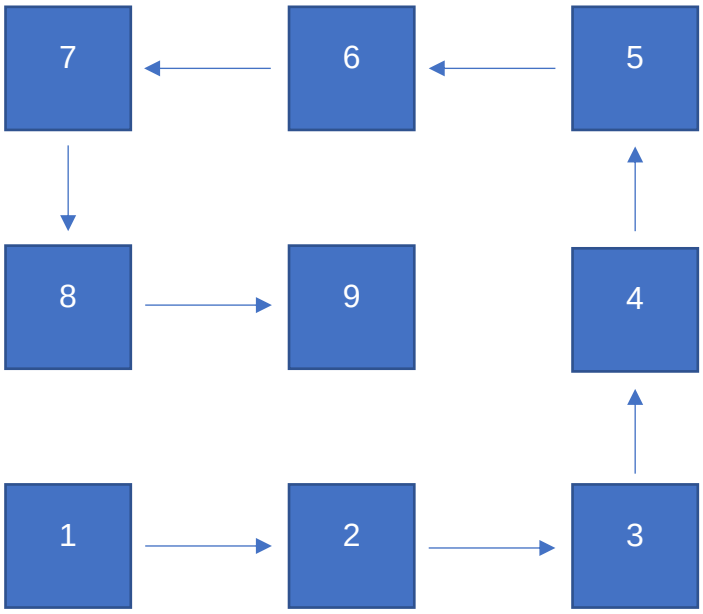

Figure 3.1: Schematic of the field of view (1mm^2) movement used to measure stomatal density

3.2.4. Leaf Gas Exchange

All leaf gas exchange was performed according to the methods in Chapter 2 section 2.3.2.

3.2.5. Chlorophyll Fluorescence Imaging

Chlorophyll Fluorescence Imaging was performed according to the protocol in Chapter 2 section 2.3.1. Imaging was performed before exposure to light regimes (day 0) and then every day for the following 9 days. After this, imaging was performed every 2-3 days.

3.3. Results

3.3.1. Impact of light regime on growth and stomatal density

To assess the impact of the 4 light regimes, high intensity square light (SQH); high intensity fluctuating light (FLH); low intensity square light (SQL); and low intensity fluctuating light (FLL), on plant phenotype, differences in the growth, in terms of visible leaf area, and stomatal density were assessed. There was a distinct growth phenotype seen (Figure **3.2**), with square light plants displaying larger leaves with smaller petioles than fluctuating light plants, as well as growing to a larger size at a greater rate. Prior to exposure to light regime, there was no significant difference in visible leaf area (p=1). Growth was initially delayed in plants in the fluctuating regime (Figure **3.3**), however these plants reached a significantly higher visible leaf area ($p<0.01$) than square light acclimated plants before bolting. SQH and SQL plants bolted first, at 20 and 25 days of light regime exposure respectively with a visible leaf area of 0.21 m^2 and 0.40 m^2 at this point. FLH and FLL plants bolted at day 43 and 46, with a visible leaf area of 0.69 m^2 and 0.70 m^2. Together, this indicated that light regime impacted the rate of development.

Figure 3.2: Growth phenotypes of *Arabidopsis thaliana* under square and fluctuating light regimes after 16 days if light exposure. There is a clear difference in growth, with fluctuating plants smaller than square wave plants, as well as differences in leaf morphology

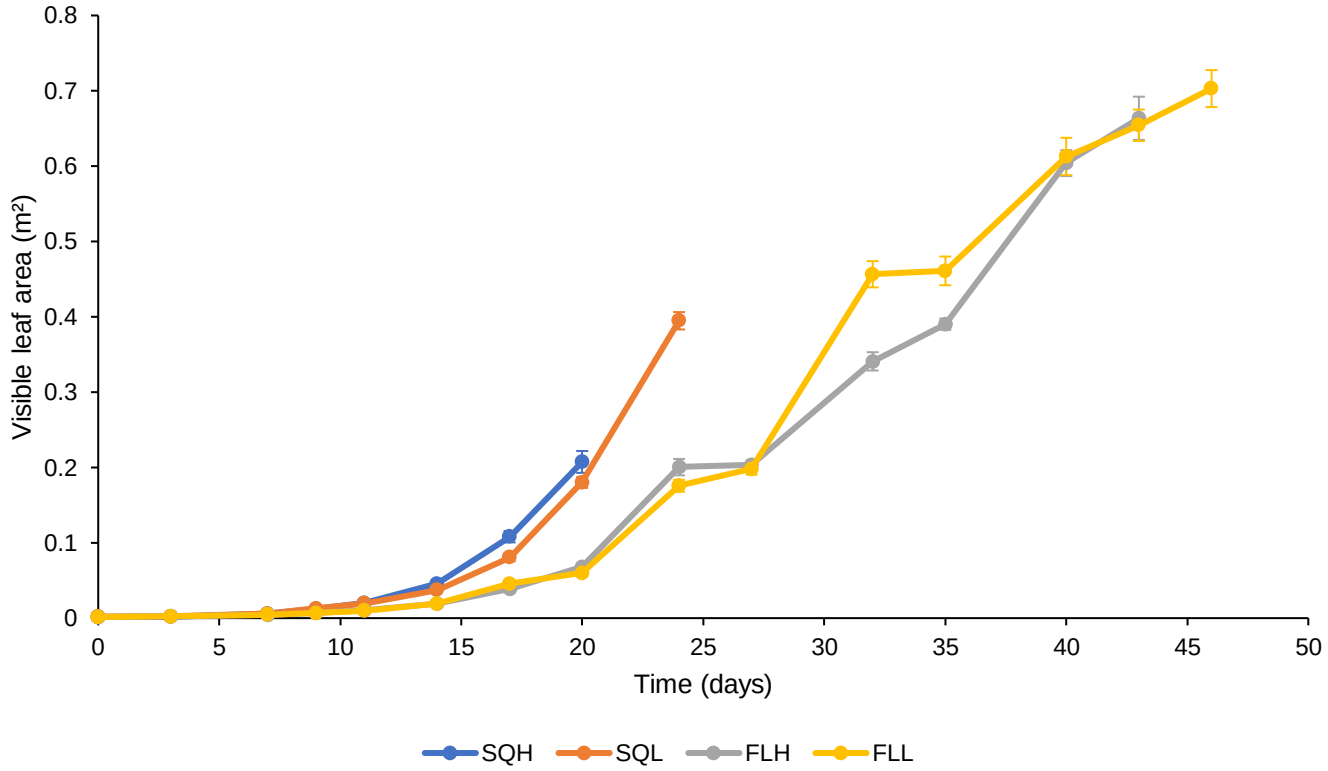

Figure 3.3: Growth of *Arabidopsis* exposed to each of the four light regimes in terms of visible leaf area of the whole rosette. Images were first taken prior to placing seedlings under the light regimes, and then taken every 3 to 5 days until the first inflorescence appeared. Growth was delayed in plants exposed to fluctuating regimes, with square light regimes resulting is earlier flowering, while low light regimes delayed flowering compared to their high light counterparts. Points show the mean ±SE (*n*=11 plants)

Stomatal density was significantly higher on both surfaces in SQH plants compared to all other regimes (Figure **3.4**) ($p<0.01$), and was more variable than plants under other regimes, while FLH plants have a significantly higher abaxial density than FLL ($p=0.03$) and SQL plants ($p=0.05$) despite no significant difference on the adaxial surface (FLH-FLL, $p=0.23$; FLH-SQL, $p=0.90$). SQL and FLL displayed no difference in stomatal density for either adaxial ($p=0.92$) or abaxial ($p=0.99$).

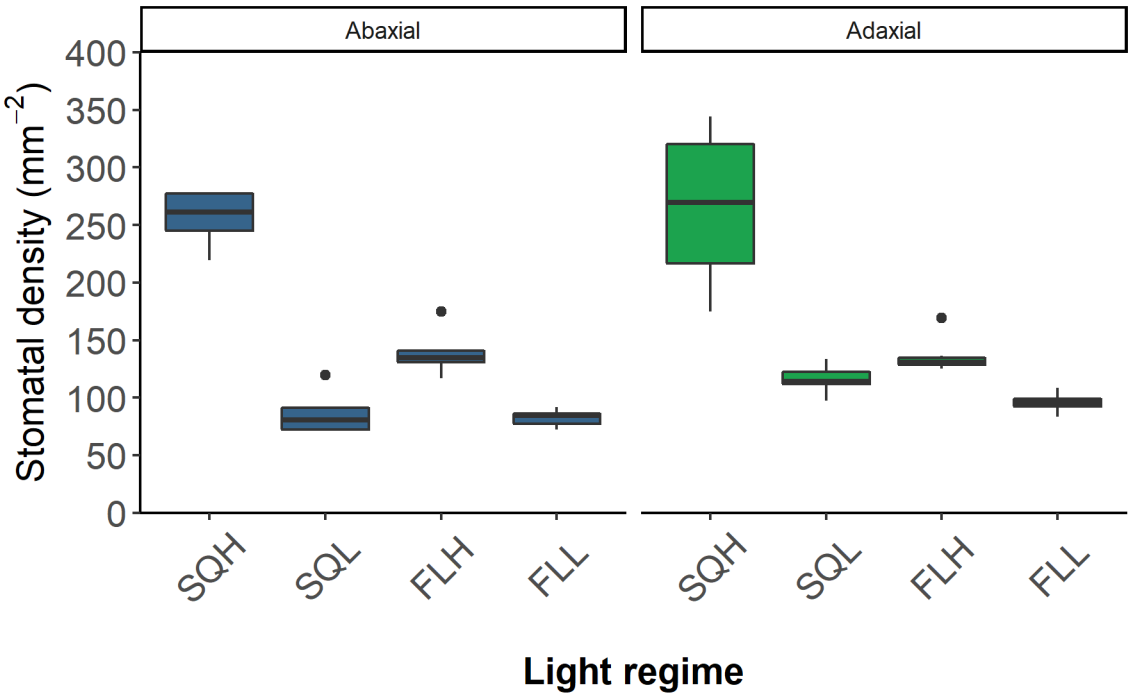

Figure 3.4: Variation (box and whiskers plot showing the distribution of replicates) of stomatal densities per mm^2 in plants grown under square wave light of high (SQH, 460 µmol m-2 s-1) and low (SQL, 230 µmol m-2 s-1) intensity, and fluctuating light of the same integrated intensity, FLH and FLL for high and low fluctuating intensities respectively. SQH plants displayed a significantly higher stomatal density than all over regimes, while low light intensities resulted in the lowest. Black dots represent outlying points within a data set. Bars represent the range (n=6)

3.3.2. Chlorophyll Fluorescence analysis revealed ongoing acclimation of photosynthesis

To assess the progress of photosynthetic acclimation to each light regime, a time series of chlorophyll fluorescence imaging was performed, utilising an induction-relaxation protocol, allowing for the maximum quantum efficiency of PSII (F_v/F_m) to be assessed in dark and the operating efficiency (F_q'/F_m') in the light (Figure **3.5**). This was followed by a light response curve, allowing for the effect of light acclimation on the maximum efficiency of PSII (F_v'/F_m'; Figure **3.6**A+B), PSII operating efficiency (F_q'/F_m'; Figure **3.6**C+D), and photochemical quenching (F_q'/F_v'; Figure **3.6**E+F). On day 0 (Figure **3.5**A, Figure **3.6**A, C, E) of the light regimes,

before plants were exposed to light, no significant difference (p=1) was observed between plants destined for each regime across assessed parameters. After 18 days, acclimation to light regime had distinct effects on all parameters (Figure **3.6**B, D, F). F_v'/F_m' (Figure **3.6**B) appears to be affected by light regime to a greater extent than light intensity, with no significant difference between SQH and SQL plants (p>0.9) or FLH and FLL plants (p>0.1), while a significant difference between SQL and FLL plants (p<0.005), as well as between SQH plants and fluctuating light plants (p<0.03). The F_q'/F_m' (Figure **3.6**D) was also affected by light acclimation with SQH plants having a significantly higher operating efficiency than the three other regimes across all PPFDs (p<0.009). The F_q'/F_m' (Figure **3.6**D) was also affected by light acclimation with SQH plants having a significantly higher operating efficiency than the three other regimes across all PPFDs (p<0.009). There was no significant difference between SQL and FLH plants (p>0.25), suggesting similar impacts of the regimes on PSII activity. FLH displayed a significantly higher F_q'/F_m' than FLL plants (p<0.009), demonstrating that high light acclimation, no matter the regime, resulted in increased PSII operating efficiency across this experiment. In contrast, the F_q'/F_v' (Figure **3.6**F) was only significantly higher in SQH plants compared to the other three regimes (p<0.03), with no significant difference between SQL, FLH, and FLL plants (p>0.1), suggesting this parameter is not driving the differences in F_q'/F_m', to which F_q'/F_v' is a contributor, between those three regimes.

Further differences were observed in the induction of photosynthesis (Figure **3.5**B). Square light regimes had a significantly higher maximum quantum efficiency of PSII (F_v/F_m) than plants grown under a fluctuating regime (p<0.001). Furthermore, there was a significant difference between SQL and fluctuating light plants (p<0.04) during induction, as well as a significant difference between FLH and FLL plants (p<0.02).

However, little difference was observed between regimes during relaxation (Figure **3.5**B), with FLL plants displaying a significantly lower values than plants under all other regimes ($p<0.03$), indicating little difference in the relaxation of NPQ.

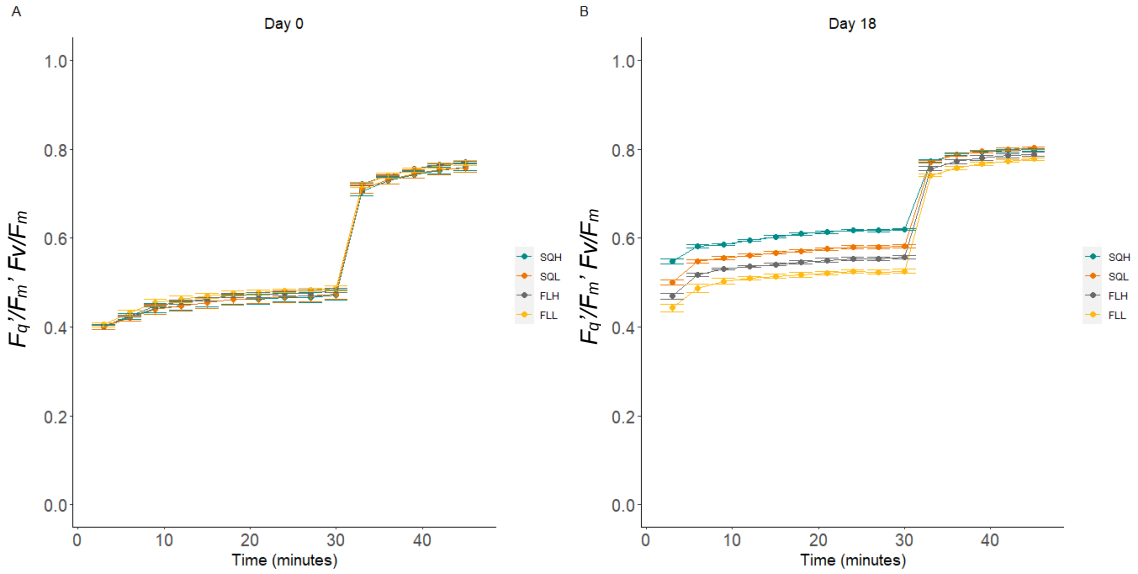

Figure 3.5: Chlorophyll fluorescence imaging of *A. thaliana* on day 0 and day 18 of light regime exposure. There was no significant difference ($p=1$) in induction (F_q'/F_m') or relaxation (F_v/F_m) on day 0 (**A**). By day 18 (**B**) the F_q'/F_m' had increased in under all regimes, with significant increases seen in SQH, SQL, and FLH plants. Data shows the mean ±SE (n=6)

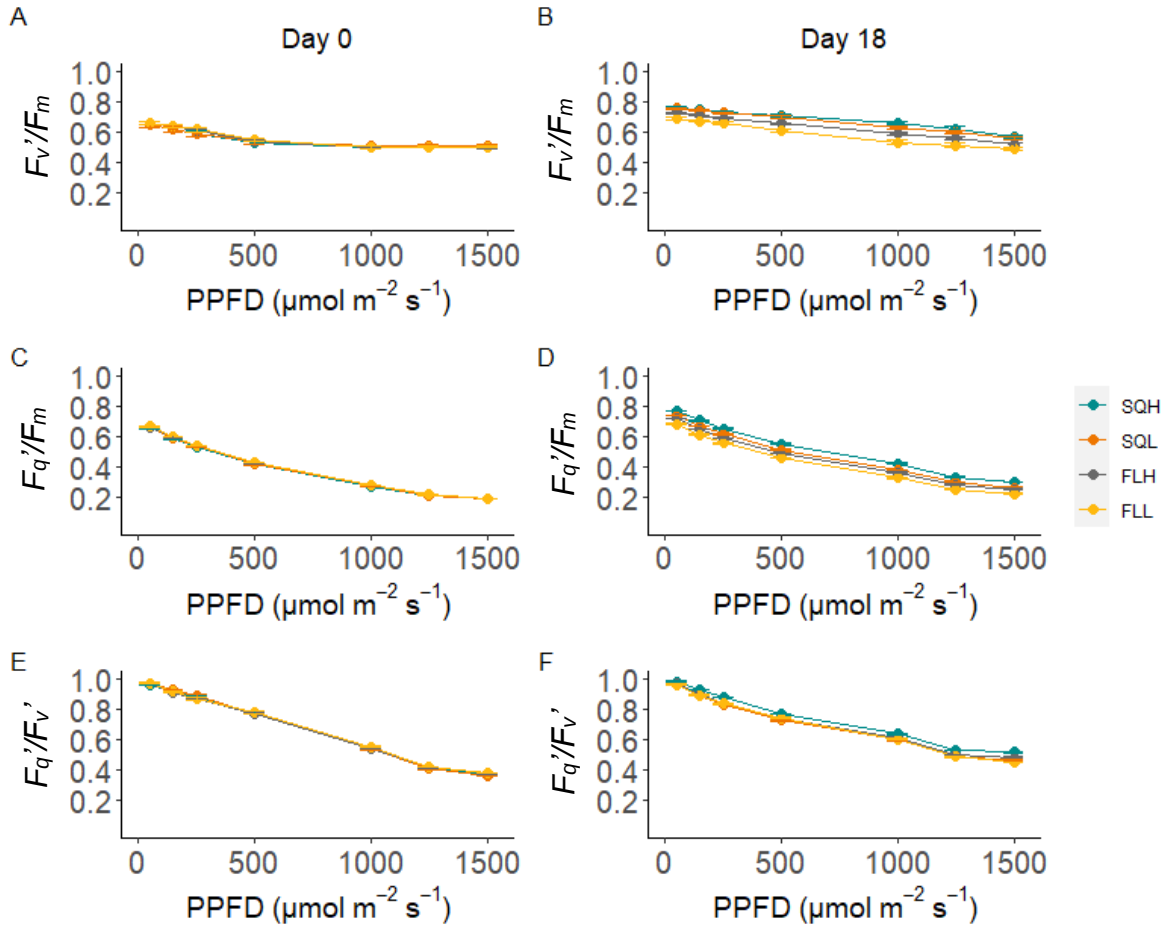

Figure 3.6: Chlorophyll fluorescence imaging on day 0 (A, C, E) and day 18 (B, D,F) of the time series indicates that light regime alters photosynthetic efficiency. Day 0 is displayed as it shows the efficiency before exposure to the different light regimes, while day 18 was selected as it was the final day on which the full rosettes were visible under the imager. No difference was seen across parameters at day 0, with significant changes noted by day 18. The F_v'/F_m' (B) demonstrates a greater maximum efficiency of PSII photochemistry in square light plants compared to fluctuating light plants with changing light, with high intensity plants having a higher efficiency than their low intensity counterparts. Similar is seen with the F_q'/F_m' (D) with a higher PSII operating efficiency in square light plants compared to fluctuating light plants. Higher photochemical quenching (F_q'/F_v', F) was seen in SQH plants compared to the other three regimes with no difference between SQL, FLH and FLL plants. Data shows the means ±SE (n=6)

Differences in the initial value for maximum PSII quantum efficiency (F_v/F_m) were also noted following dark adaptation (Figure **3.7**). A significant difference was found between SQL and both fluctuating regime plants (p<0.04), as well as between SQH and FLL plants (p<0.004).

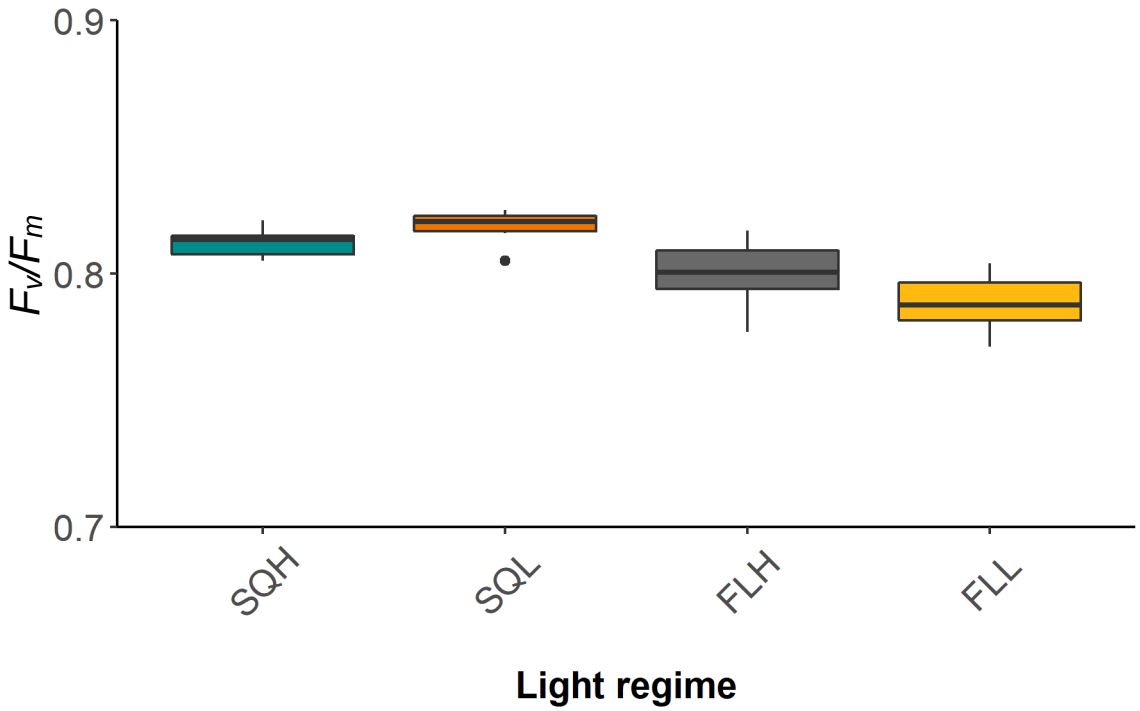

Figure 3.7: Variation (box and whiskers plot showing the variation of replicates) of the maximum quantum efficiency of PSII (F_v/F_m) after the first pulse in chlorophyll fluorescence imaging. There was no significant difference between plants grown under square wave regimes or those grown under fluctuating regime (p<0.2), while FLL plants had a significantly lower value than both square light regimes (p<0.004). Black dots show outlying data of the data set (n=6)

To investigate the acclimation of PSII to light regime, points at the PPFD and time point where the data plateaued were chosen; at 1000 µmol m^{-2} s^{-1} of the light response (Figure **3.8**A-C) and time=12 of the induction (Figure **3.8**D). From here, the name of the parameter followed by "$_{1000}$" or "$_{12}$" denotes that the parameter is related to the time series. A significant increase in the $F_v'/F_m'_{1000}$ (Figure **3.8**A) was observed between day 0 and day 21 in SQH, SQL, and FLH plants (p<0.0001). At day 21 no significant difference was observed in $F_v'/F_m'_{1000}$ between SQH and SQL plants (p>0.2) or FLH and SQL plants (p=1), however, a significant difference between FLH and SQH (p<0.05) and SQH and FLL plants (p<0.0001) was found. Acclimation of F_v'/F_m' resulted in an initial decrease in values between day 1 and 3, in SQH, SQL, and FLH plants after which these values increased. There was no significant change in this parameter until day 6 for SQH plants (p<0.02) and day 14 for SQL and FLH plants (p<0.001), with no significant difference between FLH and SQL plants at this point (p>0.99). FLL plants demonstrated no significant changes from day 0 across the $F_v'/F_m'_{1000}$ time series (p>0.6), indicating that FLL plants may take longer to acclimate. PSII operating efficiency, $F_q'/F_m'_{1000}$ also demonstrated an acclimation response the light regime (Figure **3.8**B), with all regimes resulting in a significant increase between day 0 and 21 (p<0.001). Changes in $F_q'/F_m'_{1000}$ occurred at different rates depending on regime, with square wave plants appearing to acclimate and increase in value more rapidly than those under fluctuating light. In SQH and SQL plants the value significant increase by day 3 and 4 respectively (p<0.007), while FLH plants only showed a significant increase by day 10 and finally FLL plants at day 16 (p<0.001). By day 21, $F_q'/F_m'_{1000}$ was significant difference between SQH plants and all other regimes (p<0.002), and between FLL and SQL grown plants (p<0.04). A similar trend was observed in the maximum quantum

efficiency of PSII photochemistry, $F_v/F_{m\ 12}$ (Figure **3.8**D), with significant increases in efficiency observed by day 3 for square light plants (p<0.04), day 10 for FLH plants (p<0.002), and day 16 for FLL plants (p<0.001). At day 21, there were significant differences between SQH plants and both fluctuating light regimes (p<0.001), and between SQL and FLL regimes (p<0.04). Contrasting to these parameters, photochemical quenching, $F_q'/F_v'_{1000}$ (Figure **3.8**C), demonstrated no significant difference (p>0.9) between all plants across time points. SQH and SQL plants showed a significant increase in photochemical quenching between day 0 and day 2 (p<0.004), and FLH plants at day 3 (p<0.05) with FLL plants showing no significant change (p<0.3). Overall, no significant change between day 0 and 21 was noted in FLH and FLL plants (p<0.6). In many cases, the values plateau following a peak

suggesting acclimation has occurred, resulting in stabilising of values, with no significant difference (p>0.3).

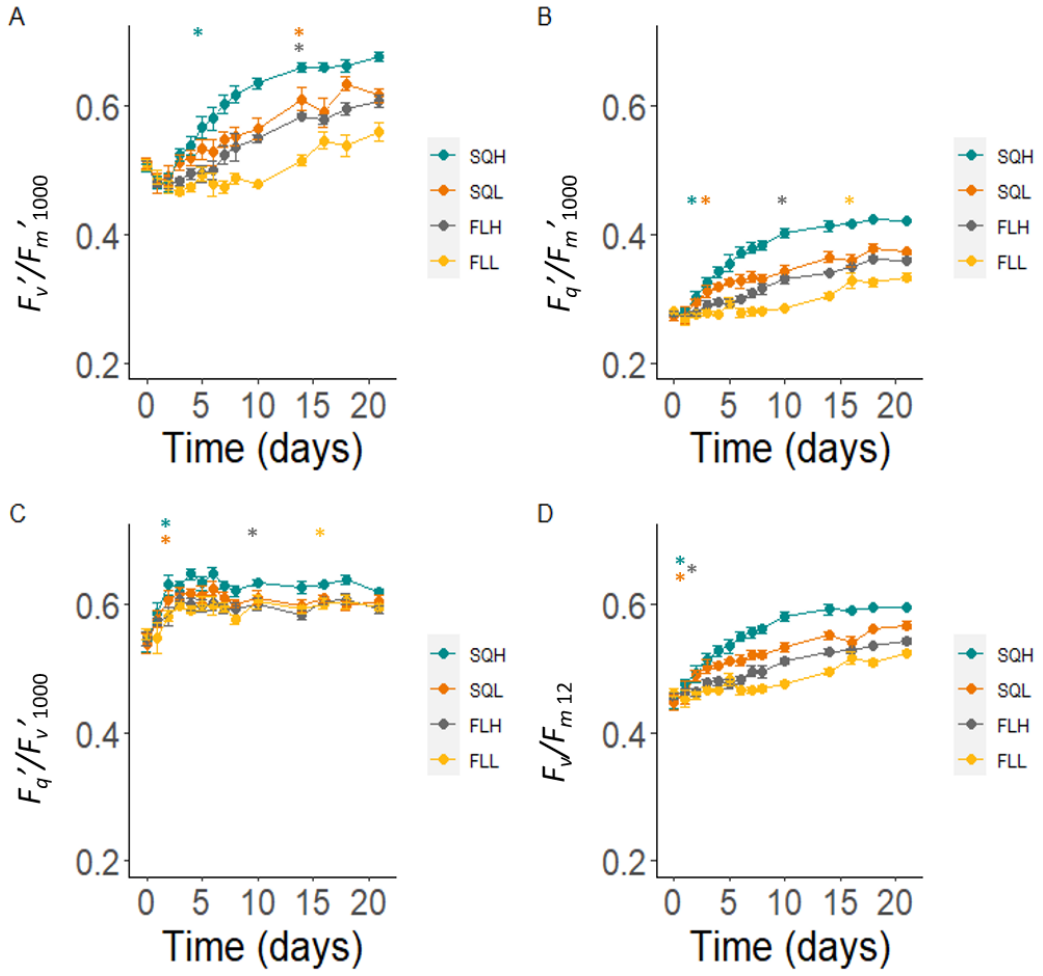

Figure 3.8: Time series of chlorophyll fluorescence over a 21-day period at PPFD=1000 µmol m^{-2} s^{-1} (**A-C**) and t=12 (**D**), selected as these were points of plateau in the data. At day 0 there was no significant difference in any parameter (p=0). An increase in maximum efficiency of PSII photochemistry (**A**) was seen in all regimes except FLL plants despite an initial decrease. The PSII operating efficiency (**B**) increased across all regimes, with fluctuating regime plants appearing to acclimate at a slower rate than square wave plants. Similarly, there was an increase in the photochemical quenching (F_q'/F_v', **C**) in plants under all light regimes, as did the maximum quantum efficiency of PSII photochemistry (F_v/F_m, **D**). Stars (*) indicate the day on which plants exposed to the indicated regime display a significant change in the given parameter compared to day 0 (p<0.05). No star means no significant change was observed. Data set shows the mean ±SE (n=6 plants).

3.3.3. Differences in photosynthetic capacity show impact of acclimation to fluctuating light

The impact of acclimation to fluctuating light was assessed by investigating carbon assimilation (*A*) as a function of internal CO_2 concentration (C_i) and using this to calculate the maximum rate of carboxylation of Rubisco (Vc_{max}) and maximum electron transport rate for RuBP regeneration (J_{max}). Differences in assimilation (Figure **3.9**A) between plants acclimated to square and fluctuating light became apparent above a C_i of 300 µmol m^{-2} s^{-1}. Significant differences (p<0.05) in Vc_{max} (Figure **3.9**B) were noted between all regimes, with SQH plants displaying the greatest values, followed by FLH, then SQL, and FLL. Further differences were found in the J_{max}, where SQH plants displayed significantly higher values than all others (p<0.05), suggesting a greater rate of RuBP regeneration. No significant difference was found between SQL plants both fluctuating groups (p>0.1), indicating little difference in RuBP regeneration. However, FLH displayed a significantly higher J_{max} than FLL plants (p<0.01), so suggesting that plants acclimated to higher light intensities have a greater rate of electron transport for regeneration of RuBP. Together, this demonstrates that fluctuations and low light intensities may be negatively impacting Rubisco activity and electron transport rate in the CBB cycle.

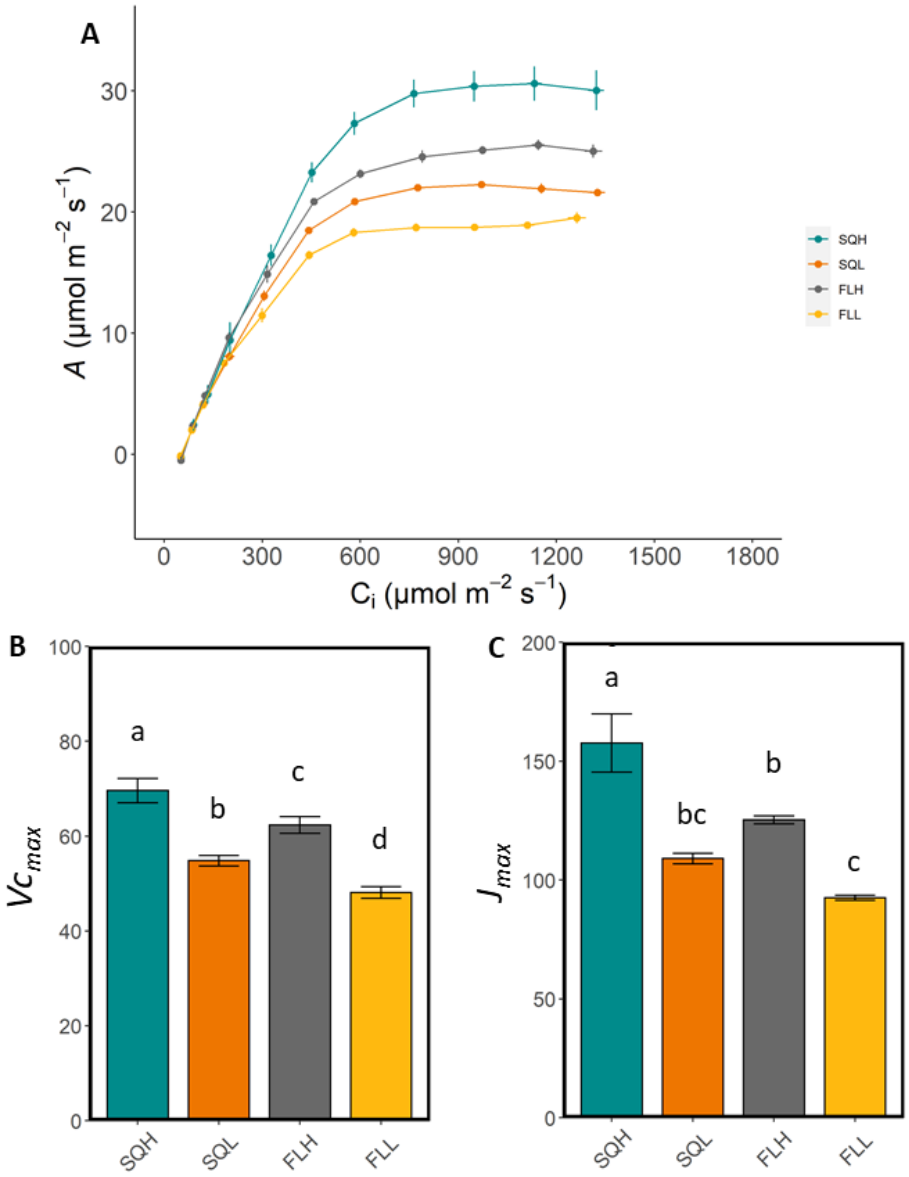

Figure 3.9: The effects of changing internal carbon dioxide concentration on photosynthesis in plants grown under four light treatments; SQH, SQL, FLH, FLL. **A** shows photosynthesis as a function of C_i, showing SQH plants perform best under changing CO_2 concentrations. Values for Vc_{max} (**B**) show a significant difference between SQL and FLL plants ($p<0.05$), as well as between high and low light acclimated plants ($p<0.05$). J_{max} values (**C**) demonstrate a significant decrease in RuBP regeneration in low light acclimated plants compared to high light plants ($p<0.05$). Letters on **B** and **C** indicate the results of Tukey post-hoc testing. Data shows the means ± SE (n=6 plants)

3.3.4. Light regime effects carbon assimilation under changing light

To determine the impact of growth light regime on carbon fixation under changing light *A* as a function of changing light (*Q*) was investigated (Figure **3.10**A). Between 0 and 100 µmol m^{-2} s^{-1} there was no significant difference in assimilation between all plants (p>0.4). At 150 µmol m^{-2} s^{-1}, FLH plants exhibited significantly higher assimilation than both SQH and SQL acclimated plants (p<0.04), suggesting some effect of square light vs fluctuating light acclimation. However, no significant difference was noted between SQH, SQL, and FLL plants (p>0.8). Above 250 µmol m^{-2} s^{-1}, FLH plants exhibited significantly higher assimilation than all other plants (p<0.01). Across light intensities, no significant difference was seen between SQL and FLL plants (p>0.9). Furthermore, only at intensities above 900 µmol m^{-2} s^{-1} was there a significant difference between SQH and SQL plants (p<0.02*)*, indicating that growth light intensity may only have an effect at higher light levels.

Stomatal conductance, a measure of how open the pores on the leaf surface are, is known to impact upon assimilation. There was no significant difference (p>0.1) in the stomatal conductance of water ($g_{sw;}$ Figure **3.10**B) between all regimes across light intensities. This indicates that stomatal conductance was unlikely to contribute to differences in assimilation under changing light. Instead, it may be linked to changes in light harvesting and the molecular machinery driving carbon fixation under changing light.

To understand the differences in physiology between plants under changing light, several parameters were calculated from the curve (Figure **3.10**C-E). The light intensity of *A* saturation (Figure **3.10**C) was significantly higher in plants acclimated to SQH light than all other regimes ($p<0.05$). This was not reflected in the electron

transport rate (Figure **3.10**D) with FLH plants instead exhibiting the greatest values but was only significantly higher than SQH (p<0.02). FLH plants also had the highest maximum g_{sw} ($g_{sw}max$) of all plants (Figure **3.10**E) but was only significantly higher than FLL plants (p<0.01).

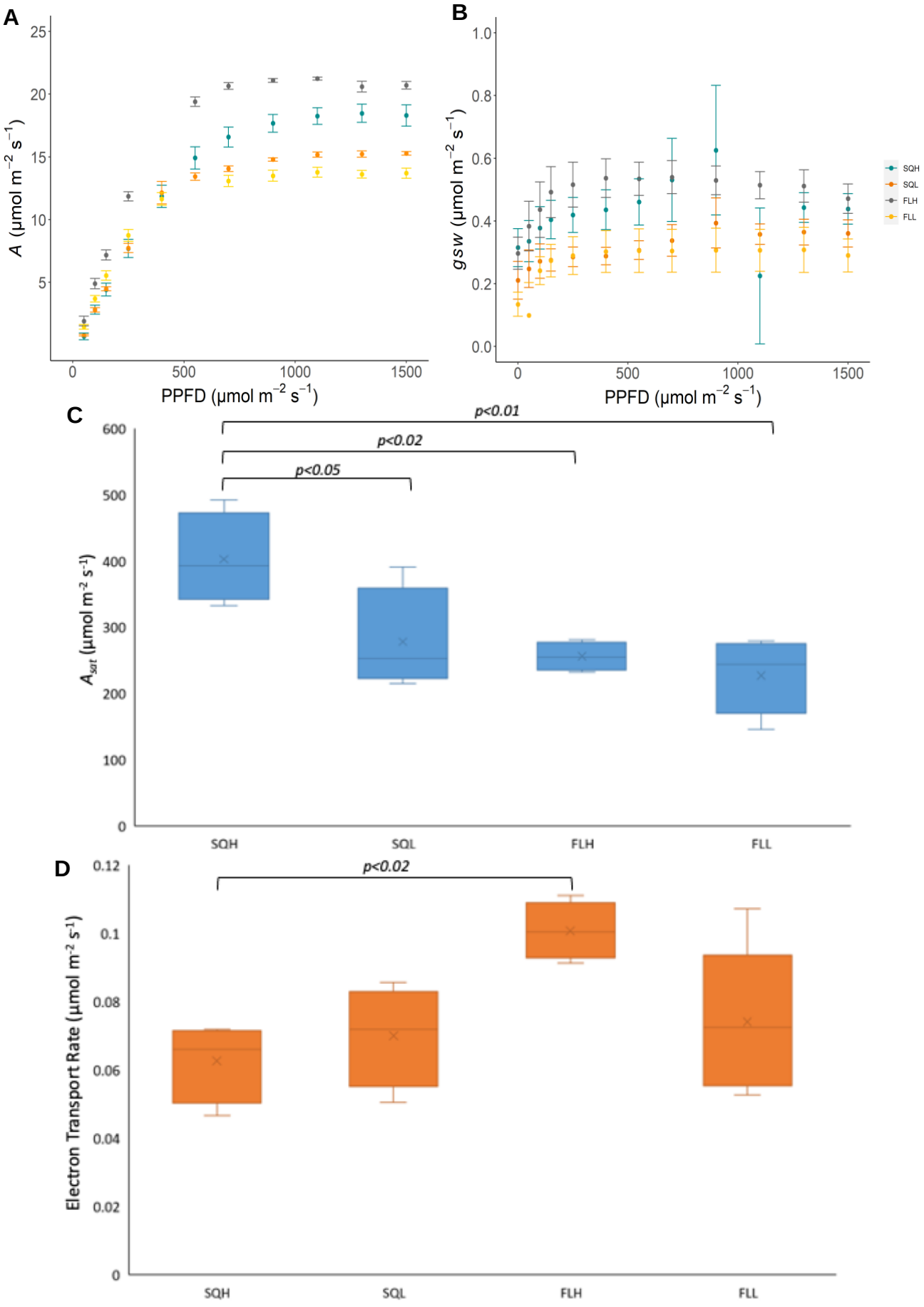
A
B
C
D
A (µmol m⁻² s⁻¹)
gsw (µmol m⁻² s⁻¹)
PPFD (µmol m⁻² s⁻¹)
SQH
SQL
FLH
FLL
p<0.01
p<0.02
p<0.05
Asat (µmol m⁻² s⁻¹)
Electron Transport Rate (µmol m⁻² s⁻¹)

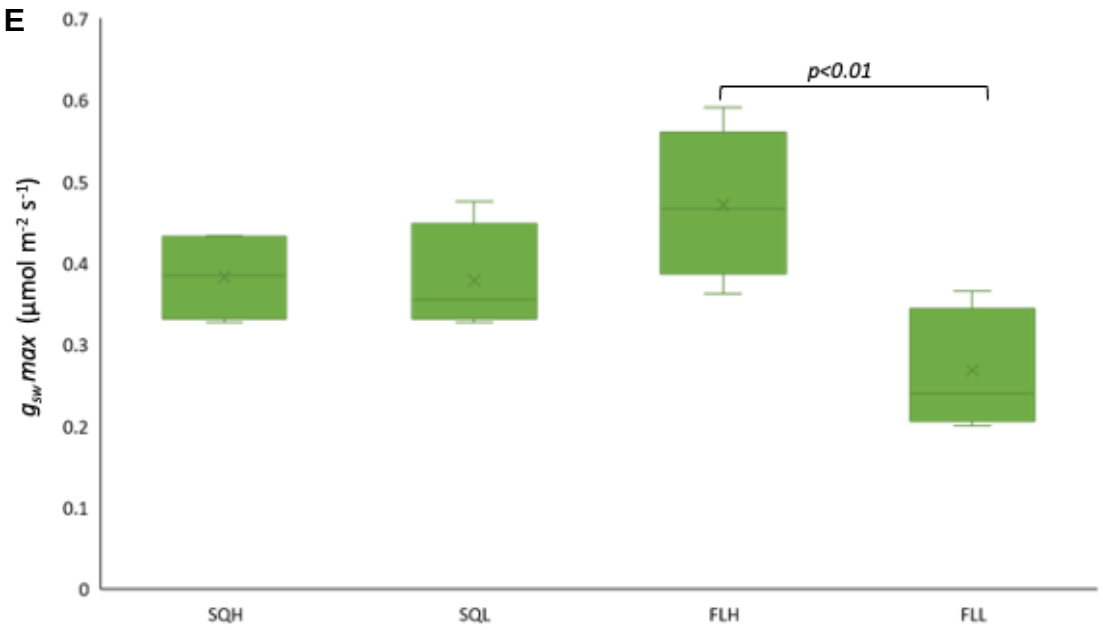

Figure 3.10: The effect of changing Photosynthetic Photon Flux Density (PPFD; µmol m^{-2} s^{-1}) on photosynthesis in plants grown under one of four light treatments; SQH, SQL, FLH, FLL. **A** shows photosynthesis (*A*) as a function of PPFD, demonstrating FLH plants to have a significantly higher assimilation rate than all other plants. Values for stomatal conductance to water (g_{sw}; **B**) show no significant difference between groups (p>0.1), indicating this is not driving the differences observed in *A*. Box and whiskers plot showing the variation of replicates for the saturating light intensity of *A* (**C**) show this was significantly higher in SQH plants than all others *(p<0.05*), while electron transport rate (ETR), calculated as the slope of the curve, was higher in FLH plants than all others, but only significantly so between SQH and FLH. The g_{sw} *max* (**D**), taken at 1500 µmol m^{-2} s^{-1}, was also highest in FLH plants, but only significantly higher than FLL. Points show the mean±SE, n=4-6 plants.

3.4. Discussion

Table 3.2: Summary of studied parameters in plants exposed to one of four light regimes. NSD indicated where there is no significant difference between the indicated lines. All descriptors are relative to the performance of plants under the other regimes.

Regime	Bolt	Stomatal Density	F_q'/F_m'	Vc_{max}	J_{max}	A_{sat}	ETR	$g_{sw}max$
SQH	Early	Up	High	High	High	Up	NSD	NSD
SQL	Early	NSD	Mid	Low	Mid	NSD	NSD	NSD
FLH	Late	NSD	Mid	Mid	Mid	NSD	Up	Up
FLL	Late	NSD	Low	Low	Low	NSD	NSD	NSD

Acclimation is an essential process in plant survival, and with an ever-changing climate and expanding global population there is a need to understand how acclimation can be used to our advantage. Most research into light acclimation has been under square wave regimes (Yin and Johnson, 2000; Thormählen *et al.*, 2017; Kaiser, Walther and Armbruster, 2020), with any data relating to fluctuating light being a series of square waves, which is not reflective of light conditions experienced by plants in the field (Lawson, Kramer and Raines, 2012). Recent research simulating true fluctuating light demonstrated that such light regimes result in a distinct phenotype, with fluctuating light resulting in thinner leaves and lower light absorption than plants grown under square light. Furthermore, plants grown under fluctuating regimes have a high photosynthetic efficiency per unit volume, driven by differences in the amount of proteins associated with various component of the ET chain, although little difference was found in carbon capture protein content between SQ and FL grown plants (Vialet-Chabran*d et al*, 2017; Matthews, Vialet-Chabrand and Lawson, 2018). Here, the aim was to demonstrate phenotypic consistency and further our understanding of the photosynthetic phenotype and acclimation to fluctuating light as experienced in nature by assessing photosystem II efficiency via chlorophyll fluorescence. Demonstration of this consistency was key to the

hypotheses of this thesis, as a consistent differential phenotype between a clonal population subjected to different light conditions would indicate epigenetic change.

The data presented here, summarised in Table **3.2**, is consistent with the findings of Vialet-Chabrand *et al* (2017) and Matthews, Vialet-Chabrand and Lawson (2018), who demonstrated changes in photosynthetic phenotype in plants grown under fluctuating light and changes in morphology depended on growth light regime. Supporting the previously observed phenotype, Matthews, Vialet-Chabrand and Lawson (2018) reported a higher stomatal density in plants grown under high light intensity compared to low light intensity, although no differences between plants grown under different growth patterns. Here high light regimes did result in higher stomatal densities on both leaf surfaces (Figure **3.4**), however was only significantly higher in the case of SQH plants. A higher stomatal density under high light is well documented (Gay and Hurd, 1975), however, research into fluctuating light is limited making it hard to determine whether the fluctuating regimes are effecting stomatal anatomy. This anatomical response is an integrated signal, with light known to activated transcription factor HY5, which directly binds to and stabilises STOMAGEN, a key signal in stomatal patterning (Wang *et al.*, 2021). Growth of HY5 knockouts resulted in signifcant reductions in stomatal denisties across three distinct intensites, 40, 80, and 160 $\mu mol\, m^{-2} s{-}^{1}$, in comparison to the wildtype (Wang *et al.*, 2021). This demonstrates that light intensity impacts upon the signalling cascade which controls stomatal patterning. Since this appears to be intensity depedent, the impact of a fluctuating regime, in which intensity is quickly changing, may have contrasting effects on stomatal patterning.

Differences in the efficiency of PSII indicate important differences in the photosynthetic performance between plants grown under different light regimes. In the dark adapted state, the maximum efficiency of PSII (F_v/F_m) of FLL and FLH plants exhibit a value much lower than 0.83 (Figure **3.7**), a value considered as an indicator of 'plant health' and suggests photoinhibition or downregulation of photosystem II (Murchie and Lawson, 2013). Previous studies have attributed long term acclimation to high light intensity to an increase in the PSII core protein CP43, and a reduction in antenna size compared to plants grown at 100 µmol m^{-2} s^{-1} (Kouřil *et al.*, 2013). Similar findings have been reported in a comparison of plants grown at 600 µmol m^{-2} s^{-1} and 200 µmol m^{-2} s^{-1} (Bielczynski, Schansker and Croce, 2016). However, the decrease in F_v/F_m observed here suggests increased level of photoinhibition in FLL rather than any change to photosystem II as noted in *Arabidopsis* grown at low light (Tian *et al.*, 2017). A decreased F_v/F_m is an established indicator of photoinhibition, but the exact mechanism for this can be complex (Baker, 2008). It may be that acclimation to fluctuating light regimes increased nonphotochemical quenching (NPQ), leading to photoinactivation of PSII reaction centres and ultimately oxidative damage, and loss, of reaction centres (Baker, 2008).

Differences in F_q'/F_m' could be driven by photochemical quenching, F_q'/F_v' (mathematically equivalent to qP), which relates PSII maximum efficiency to operating efficiency (Baker, 2008). A higher F_q'/F_m' was observed in square regimes compared to fluctuating regimes, with high intensity grown plants exhibiting higher values than their lower intensity counterparts, however, a higher F_q'/F_v' was only found in SQH plants indicating that a difference in NPQ and associated processes

may be driving the higher value found in SQL compared to FL plants. Kaiser, Walther and Armbruster (2020) noted that *Arabidopsis* accessions grown under fluctuating light displayed a significant reduction in F_q'/F_m' compared to plants grown under a uniform square light regime, while NPQ increased, supporting the differences in F_q'/F_m' as illustrated here. Furthermore F_v'/F_m' was not significantly higher in SQH plants compared to SQL plants, suggesting that another mechanism could be driving the increased F_q'/F_m' in SQH plants, as both F_v'/F_m' and F_q'/F_v' are mathematically related to F_q'/F_m'. The F_v'/F_m' is also an indicator of NPQ (Murchie and Lawson, 2013), with a decrease in this parameter reflecting an increase in NPQ, suggesting NPQ is occurring to a greater extent in plants under fluctuating light than square light. This could be related to differences in expression of carotenoid enzymes, particularly those functioning in photoprotection. Zeaxanthin (Zx), violaxanthin (Vx) and antheraxanthin are oxygenated Beta-carotenes which bind to antenna in PSII light-harvesting complexes and have been implicated in photoinhibition and photoprotection, with conversion of Vx to Zx in light harvesting complexes regulating photon harvesting and energy dissipation (Choudhury and Behera, 2001). These molecules function in non-photochemical quenching, particularly in pH-dependent energy dissipation (qE) (Müller, Li and Niyogi, 2001), and mutation effects on energy dissipation. For examples, *Arabidopsis* mutants lacking Zx show significantly lower chlorophyll fluorescence quenching and slower induction rates of NPQ when grown under low light compared to the WT (Z. Li *et al.*, 2009), suggesting that levels of carotenoids may be important when considering differences in photosynthetic efficiency.

Decreased photosynthetic capacity (Figure **3.9**B+C) and PSII efficiency (Figure **3.6**) was accompanied by an increased assimilation under changing light (Figure **3.10**) in

FLH plants compared to SQH plants. Decreased capacity and PSII efficiency would suggest a decreased assimilation, not reflected here, but is likely linked to leaf anatomy. Significantly thinner leaves were previously noted in plants grown under low light and fluctuating light compared to square light plants, related to the thickness of the mesophyll palisade layer (Vialet-Chabrand *et al.*, 2017). This was related to an increase in Rubisco content per cell in FLH plants (Vialet-Chabrand *et al.*, 2017), therefore accounting for this difference.

The differences in PSII efficiency demonstrated between light regimes could also be due to differences in thioredoxin (Trx) expression. In thioredoxin *m* knockout plants, high light treatment was noted to significantly decrease the F_v/F_m and F_q'/F_m' compared to the wildtype (Serrato *et al.*, 2021). Therefore, reduced expression of thioredoxins under fluctuating light could account for the decrease between SQ and FL light seen here (Figure **3.6**, Figure **3.7**) due to the high PPFD of peaks under fluctuating regimes. Thioredoxins are a group of proteins involved in a complex enzyme activation system believed to control chloroplast metabolic functions in a light-responsive manner (Thormählen *et al.*, 2017). Trxs are reduced by the ferredoxin: Trx reductase in a light dependent manner using electrons provided by photosystem I ferredoxin, resulting in the ability to cleave disulphide bonds in stromal target proteins and activate the target proteins (Thormählen *et al.*, 2017). Trxs are also able to act in signalling pathways to effect chloroplast gene expression (Q.-B. Yu *et al.*, 2014), meaning they could play an important role in the acclimation of photosynthesis to light. Photosystems are localised to the chloroplasts, so if signalling via Trxs plays a role in acclimation, there could be alterations to the photosystems in terms of protein content and therefore alter chlorophyll fluorescence parameters. Trxs are known to regulate chloroplast biogenesis via the pathway

which synthesises chlorophyll, while elevated Trx activity promotes vegetative growth (Nikkanen *et al.*, 2017). This system could be linked to the results seen in fluctuating light plants, with a decreased chlorophyll *a/b* ratio previously noted (Vialet-Chabrand *et al.*, 2017) while data shown here demonstrates prolonged vegetative growth and delayed flowering (Figure **3.3**) compared to square light grown lights, suggesting Trxs could be involved in light acclimation (Schippers, Foyer and van Dongen, 2016). *M*-type thioredoxins have also been noted to impact the CBB cycle. Deficiency in *m*-type trxs has been noted to decrease carbon assimilation rates upon transition from dark to light compared to the wildtype in *Arabidopsis* (Okegawa and Motohashi, 2015). The decrease in assimilation in SQH plants under changing light (Figure **3.10**A) could therefore be related to decreases in Trx-*m* expression.

Normalisation of assimilation parameters, such as those in Figure **3.10**A, has the potential to alter the conclusions drawn. Vialet-Chabrand et al. (2017) noted that normalising assimilation as a function of light to the leaf area mass (leaf dry weight per unit leaf area) resulted in FLL plants outperforming the SQ-acclimated plants. This suggests that differences in plant and leaf anatomy, weight, and cell density etc could account for the differences observed here. It may not necessarily be that the FLL plants are performing worse, just that there are cells and biomass in the measured areas to perform the same actions. Furthermore, the speed of stomatal opening and closure may impact upon assimilation. Diurnal measurements of g_s in plants acclimated to the same regimes utilised here revealed slower stomatal opening under fluctuating light acclimation accompanied by faster stomatal closing (Matthews, Vialet-Chabrand and Lawson, 2018) which could limit the diffusion of

CO_2 for assimilation (Barradas, Jones and Clark, 1998; McAusland *et al.*, 2016). This could explain the lower assimilation under changing CO_2 in FL-acclimated plants (Figure **3.9**) but does not account for the increased assimilation under changing light (Figure **3.10**).

Changes in physiological phenotype could also be related to changes in thylakoid membranes within the chloroplast. Comparative proteomics of the thylakoids in laboratory grown vs field grown *Arabidopsis* revealed that growth under a natural, fluctuating light regime results in plants that incorporate aspects of both high and low-light acclimation observed in laboratory grown plants (Flannery *et al.*, 2021). Field grown plants had 25% less PSI compared to lab grown plants, as well as a 30% decrease in the relative abundance of LHCII trimers (Flannery *et al.*, 2021). In relation to this study, this could partially explain the increased PSII efficiency in SQ plants (Figure **3.7**), as a decrease in light harvest trimers under fluctuating light may account for this. The same study also found that field grown plants showed an increase in protein associated with light harvesting regulation and electron transfer. For example KEA3, a K^+/H^+ antiporter which releases protons into the stroma as a response to sudden decreases in light intensity, was found to increase by 45% in field plants compared to laboratory grown plants (Flannery *et al.*, 2021). This suggests that acclimation to fluctuating light increase the ability of a plant to return LHCII to a light harvesting state, as KEA3 is known to impact upon this process. This could explain why FLH acclimated plants are better able to respond to changing light (Figure **3.10**).

The late flowering phenotype under long days in FL-acclimated plants was unexpected (Figure **3.3**). In *Arabidopsis thaliana*, flowering is known to be early under long days (Roden *et al.*, 2002), as observed with the SQ-acclimated plants. There are a range of possible reasons for this. It is possible that the light provided at dawn and dusk in the FL regimes is too low to be perceived by the plants, resulting in a shorter day length being perceived, and therefore flowering not triggered. However, it is widely considered that *Arabidopsis* plants are capable of perceiving extremely low light levels (Cho *et al.*, 2007; Shin-ichiro *et al.*, 2008), so this is unlikely to be the case. It is also unlikely be a stress response as stressed plants tend to flower earlier rather than later, and stressed plants that do display late flowering are noted to have slowed metabolism (Cho, Yoon and An, 2017). Instead, there may be alterations in the regulation of flowering time via changes in signalling or transcription factor regulation. Gibberellins (GAs) are known to promote flowering in long-day plants including *Arabidopsis* (Blázquez *et al.*, 1998), and are also thought to have a role in modulating photosynthesis by stimulating Rubisco activity (Yuan and Xu, 2001; Müller and Munné-Bosch, 2021). Lower expression of GAs in FL plants compared to SQ plants could explain both the delayed flowering time, and the reduced assimilation under changing CO_2 (Figure **3.9**). microRNAs can also impact flowering time. miR156 is a highly conserved microRNA in plants and targets a family of transcription factors called SQUAMOSA PROMOTER BINDING LIKEs (SPLs) (Wang, 2014). Mature miR156 is most highly expressed in seedlings and decreases over time, with overexpression resulting in delayed flowering (Cardon *et al.*, 1999). Therefore, the delay in flowering in FL-acclimated plants could be due to an increased expression or a delay in degradation of miR156. miR156 decline is partially regulated by photosynthetic sugars, with increased exogenous sugar rapidly

decreasing miR156 levels (Yang, Conway and Poethig, 2011). It could be that during early development FL plants have a lower concentration of sugars within the leaf, therefore delaying the degradation of miR156 and so accounting for the delay in flowering. To understand the exact cause of this late flowering phenotype, investigation into all these suggested possibilities could provide an answer.

This research is a step further towards investigating the true effects of naturally fluctuating light but does not account for the differences across the year and the possible effects that seasonal fluctuations in light may have. With rising interest in indoor farming, in which many aspects of the growth conditions can be controlled, research investigating the use of light regime is becoming increasingly relevant as the capabilities to control the light environment rise. The potential benefits and costs of light regime are important to understand to improve crop productivity and yield.

Chapter 4: The effects of fluctuating light acclimation on DNA methylation in *Arabidopsis thaliana*

4.1. Introduction

Epigenetics, defined as a layer of information that exists beyond the encoded DNA sequence (Greally, 2018), has long been studied in plants, providing early evidence for non-Mendelian inheritance, genomic imprinting, and epialleles (Soppe *et al.*, 2000; Arteaga-Vazquez and Chandler, 2010; Pikaard and Scheid, 2014). One of the key epigenetic mechanisms is DNA methylation, where DNA methyltransferases are directed to add a methyl group to cytosine bases in a DNA molecule (Law and Jacobsen, 2010). This acts as an additional layer to the regulation of gene expression and can ultimately result in changes to phenotype. The process of DNA methylation is highly dynamic, with both methyltransferases and demethylation active within the plant cell (Meyer, 2011). The dynamic nature of DNA methylation, and its potential to control gene expression, has previously been studied in plant stress responses and acclimation (Liu and He, 2020; Saeed *et al.*, 2022), as it represents a fast and changeable mechanism by which plants can respond to their environments.

There is currently limited evidence for the role of DNA methylation in light stress responses and acclimation. The application of excess light stress, whereby an hour long peak at 1000 μmol m^{-2} s^{-1} was applied three time daily over a week, resulted in *Arabidopsis thaliana* with no CpG DMRs and only 17 non-CpG DMRs when compared to untreated plants (Ganguly *et al.*, 2018). These plants displayed a photoprotective phenotype, including an increased photochemical capacity and fast NPQ relaxation (Ganguly *et al.*, 2018), suggesting DNA methylation does not contribute to light acclimation. However, DNA was harvested 1 day after the excess light priming stopped and plants were returned to 100-150μmol m^{-2} s^{-1} light

environment (Ganguly *et al.*, 2018), which could mean there is loss of some DMRs due to the dynamic nature of DNA methylation. Furthermore, under the same excess light stress, the physiology of *Arabidopsis* mutants with reduced abilities to establish, maintain, or remove DNA methylation was similar to that of the wild type (Ganguly *et al.*, 2018). Multiple physiological parameters, including the F_q'/F_m' and energy dissipation via NPQ, were not different between the wild type and methylation mutants (Ganguly *et al.*, 2018), suggesting that, despite the impacts on DNA methylation, they are capable of undergoing light acclimation. Together, these studies suggest a low likelihood of the involvement of DNA methylation in light acclimation. However, despite the excess light stress and large peaks and trough, the excess light regimes are not reflective of environmental light regimes, where the fluctuating frequency is much greater than simulated in these studies. From previous work, it is already known that the physiology of *Arabidopsis* is impacted by a naturally fluctuating light regime in a clonal population (Vialet-Chabrand *et al.*, 2017; Matthews, Vialet-Chabrand and Lawson, 2018), and the response is consistent, as seen in chapter 3, therefore it is possible that this excess light priming over a week, compared to over the life span of the plants, would result in a reduced number of DMRs.

In contrast to the above reports, there is evidence in *Arabidopsis* that high light induces changes to small RNA (sRNA) expression. sRNAs are capable of guiding DNA methylation via the RdDM pathway (Lewsey *et al.*, 2016). By studying the transcriptome following 3 hours, 6 hours, and 2 days of exposure to 450 μmol m^{-2} s^{-1}, they were able to identify a range of sRNAs, with an increase between 3 and 6 hours, but a decrease after 2 days (Tiwari *et al.*, 2021). These were predicted to target a range of genes known to have effects during light acclimation and was found

to affect their expression. For example, *Dark inducible 4* was downregulated, as was novel target *Hydroxysteroid dehydrogenase 3*, which impacts the sterol content of plant cell wall, the composition of which is known to be impacted by light stress (Tiwari *et al.*, 2021). Although this study did not investigate whether changes in methylation were correlated with sRNA presence, it does provide some suggestion that there could be some relationship between methylation and light acclimation.

Excess light stress or high light is known to induce the production of hydrogen peroxide (Baxendale and Wilson, 1957; Foyer and Noctor, 2016; Exposito-Rodriguez *et al.*, 2017), with this production associated to alterations to the methylome. In tobacco mutants which overproduce hydrogen peroxide (H_2O_2) hypomethylation was noted in comparison to the control plants (Villagómez-Aranda *et al.*, 2021), suggesting overproduction of H_2O_2 correlates with loss of methylation. More generally, reactive oxygen species (ROS), a group of oxidising agents that includes H_2O_2, have been related to epigenetic reprogramming. The MSH1 pathway present in sensory chloroplasts is capable of signalling to epigenetic machinery, including those involved in DNA methylation, providing a possible pathway to integrate ROS signalling under stress conditions into the epigenetic pathways (Virdi *et al.*, 2016; Foyer, 2018). Knockout of *MSH1* resulted in genome-wide reprogramming of DNA methylation (Virdi *et al.*, 2015), further suggesting a role for chloroplast signalling in epigenetic change. Combined with knowledge that high light stress results in ROS production (Edreva, 2005; Pospíšil, 2016), this indicates that under high light conditions, genome wide changes to the methylome is possible.

The aim of this chapter was to investigate the effects of a naturally fluctuating light regime on DNA methylation and how this may differ from plants grown under square wave light conditions, as is often used in a laboratory setting. It was also investigated

whether this could be correlated with gene expression and subsequently associated with the physiological responses reported in Chapter 3.

4.2. Materials and Methods

4.2.1. Plant Material

Arabidopsis thaliana (Col-0) were exposed to four light regimes and underwent physiological characterization (see Chapter 3). Six of the newest, fully expanded leaves were abscised and frozen in liquid nitrogen between midday and 1pm on day 20 of regime exposure, then stored at -80 C until required for use.

4.2.2. DNA methylation data analysis

DNA methylation data obtained according to the method in Chapter 2, section 2.4. Results of preprocessing can be seen in Table **4.1**.

Low resolution profiles (Figure 4.2), data coverage (Supplementary Figure S1), and correlation (Supplementary Figure S2) were plotted to assess data quality using DMRcaller prior to further analysis.

Table 4.1: Preprocessing data showing the raw read data, data removed by the trimming (Trimmomatic), mapping (Bismark –bowtie2), and deduplication (Deduplicate) of Whole Genome Bisulfite Sequencing data. Sample name relates to the pooled sample, with each sample sequenced in multiple lanes (L1 or L3) to achieve 30x coverage. Where no lane is stated, additional sequencing was conducted to obtain 30x coverage.

Sample	Raw Reads					Trimmomatic				Bismark --bowtie2				Deduplicate	
	Clean Reads	Containing N	Low quality	Adapter related	BS conversion rate (%)	Both surviving	Forward only surviving	Reverse only surviving	Dropped	Mapping efficiency (%)	% meC Cpg	% meC CHG	% meC CHH	Total number removed (bp)	Leftover sequences (bp)
FLHa_L1	11705716 (99.36)	0 (0.00)	4 (0.00)	72266 (0.61)	97	5944965 (99.28)	40986 (0.68)	1816 (0.03)	53 (0.00)	77.8	17.4	5.1	1.5	1815565 (39.26%)	2808909
FLH_L1	11909450 (99.45)	26 (0.00)	16 (0.00)	66148 (0.55)	97	5875977 (99.78)	11763 (0.2)	1223 (0.02)	30 (0.00)	77.5	17.3	5.1	1.5	1667642 (36.63%)	2884872
FLH_L3	48434696 (99.36)	0 (0.00)	56 (0.00)	313664 (0.64)	97.02	24300628 (99.7)	67602 (0.28)	5873 (0.02)	105 (0.00)	77.7	17.5	5.1	1.5	7494680 (39.68%)	11391986
FLLa_L1	10000806 (99.1)	18 (0.00)	20 (0.00)	90912 (0.90)	97.06	5003302 (99.16)	41036 (0.81)	1490 (0.03)	50 (0.00)	78.5	18.9	5.6	1.7	1388205 (35.34%)	2539925
FLL_L1	19201864 (98.95)	0 (0.00)	4 (0.00)	204206 (1.05)	97.02	9673288 (99.69)	27759 (0.29)	1904 (0.02)	185 (0.00)	78.2	18.8	5.6	1.7	2689568 (35.54%)	4877200
FLL_L3	43577448 (98.97)	0 (0.00)	42 (0.00)	452910 (1.03)	97.05	21918987 (99.56)	89239 (0.41)	6789 (0.03)	57 (0.00)	78.4	18.9	5.6	1.7	6226641 (36.23%)	10957599
SQHa_L1	8870284 (99.12)	30 (0.00)	14 (0.00)	78534 (0.88)	97.03	4441169 (99.26)	31846 (0.71)	1381 (0.03)	35 (0.00)	73	17.6	4.8	1.4	1216564 (37.52%)	2026017
SQH_L1	5801742 (99.1)	768 (0.01)	1040 (0.02)	50814 (0.87)	97.3	2348998 (80.25)	576721 (19.7)	1182 (0.04)	291 (0.01)	72.7	17.4	4.8	1.4	505399 (29.59%)	1202843
SQH4	21325906 (98.98)	0 (0.00)	0 (0.00)	220440 (1.02)	99.74	10559131 (98.01)	144016 (1.34)	65201 (0.61)	4825 (0.04)	72.5	17.3	4.7	1.4	4350624 (44.29%)	5473130
SQH_L3	40481564 (99.01)	0 (0.00)	38 (0.00)	404614 (0.99)	97.03	20368539 (99.64)	69604 (0.34)	4882 (0.02)	83 (0.00)	73	17.4	4.8	1.4	5866945 (39.46%)	9000665
SQL_L1	12218778 (99.4)	36 (0.00)	16 (0.00)	74000 (0.6)	97.06	6102750 (99.29)	41626 (0.68)	1982 (0.03)	57 (0.00)	75.8	17.9	4.8	1.3	1837572 (39.74%)	2786610
SQL4	26467178 (99.21)	2 (0.00)	0 (0.00)	210196 (0.79)	99.74	13069566 (97.98)	184400 (1.38)	79053 (0.59	5669 (0.04)	75.2	17.6	4.7	1.3	3292130 (43.00%)	4363622
SQL_L3	44878546 (99.32)	0 (0.00)	34 (0.00)	305670 (0.68)	97.04	22511912 (99.64)	74135 (0.33)	5976 (0.03)	102 (0.00)	75.7	18	4.9	1.3	6829947 (40.10%)	10200735

4.2.3. RNA analysis

RNA was extracted and sequenced according to methods in Chapter 2 Section 2.5.

The results of processing can be seen in Table ***4.2***.

Table 4.2: Processing data showing the alignment scores (hisat2), and the quality control (QC) and reference genome mapping (flagstat) for RNAseq data.

	hisat2						flagstat				
Sample	Paired (bp)	0 alignment (bp)	1 alignment (bp)	>1 alignment (bp)	Discordant alignment (bp)	Overall alignment rate (%)	QC-passed reads	QC-failed	Mapped to reference genome (%)	Properly paired (%)	Singletons (%)
SQH1	22563085	1176790	20848693	537602	160908	97.22	46563650	0	97.3	94.78	1.53
SQH2	23291022	1178654	21460102	652266	144952	97.25	48359764	0	97.35	94.94	1.52
SQH3	19684880	1067360	18000981	616539	131905	97.04	41037503	0	97.16	94.58	1.6
SQL1	22329483	1151122	20448219	730142	126577	97.22	46590771	0	97.33	94.84	1.62
SQL2	22188271	777478	20865605	545188	151087	98.24	45907822	0	98.3	96.5	0.91
SQL3	24218987	1260767	22306055	652165	149973	97.11	50199227	0	97.21	94.79	1.53
FLH1	21218109	1411548	19385072	421489	143173	95.82	43544021	0	95.92	93.35	1.62
FLH2	23066427	1117062	21219026	730339	142497	97.44	48048397	0	97.54	95.16	1.5
FLH3	19921925	1054883	18435457	431585	113216	97.03	40963203	0	97.11	94.7	1.59
FLL1	22153713	812393	20823873	517447	174778	98.17	45715544	0	98.22	96.33	0.84
FLL2	23657666	801228	22290835	565603	167061	98.34	48035204	0	98.37	96.61	0.85
FLL3	22189291	785082	20628366	775843	160741	98.23	45512065	0	98.3	96.46	0.83

4.3. Results

4.3.1. Acclimation to fluctuating light results in global changes to the methylome

To investigate whether light acclimation is linked to changes in DNA methylation, whole genome bisulfite sequencing of *Arabidopsis thaliana* acclimated to square and fluctuating light was carried out. These plants had not been exposed to the light regimes utilized here prior to this work (see Chapter 3). DMRcaller was used to identify Differentially Methylated Regions (DMRs) and the results revealed genome-wide differences in gene and transposable element methylation, potentially accounting for the phenotype seen in Chapter 3.

Low resolution plots (Figure 4.1) demonstrate that there is little change to the global methylation profiles, but there are some small differences in pericentromeric regions. This indicates that light acclimation is not resulting in changes to the epigenetic machinery, and instead may be impacting specific DNA regions,

To determine whether light acclimation altered DNA methylation at base pair resolution, the total number of DMRs, and their corresponding annotations and enrichment was investigated. Across treatments, significant effects on DNA methylation could be seen. In all regime comparisons except FLHvFLL, more regions lost methylation than gained (Figure **4.2**A) whereas the proportion of loss and gain in FLHvFLL was roughly the same.

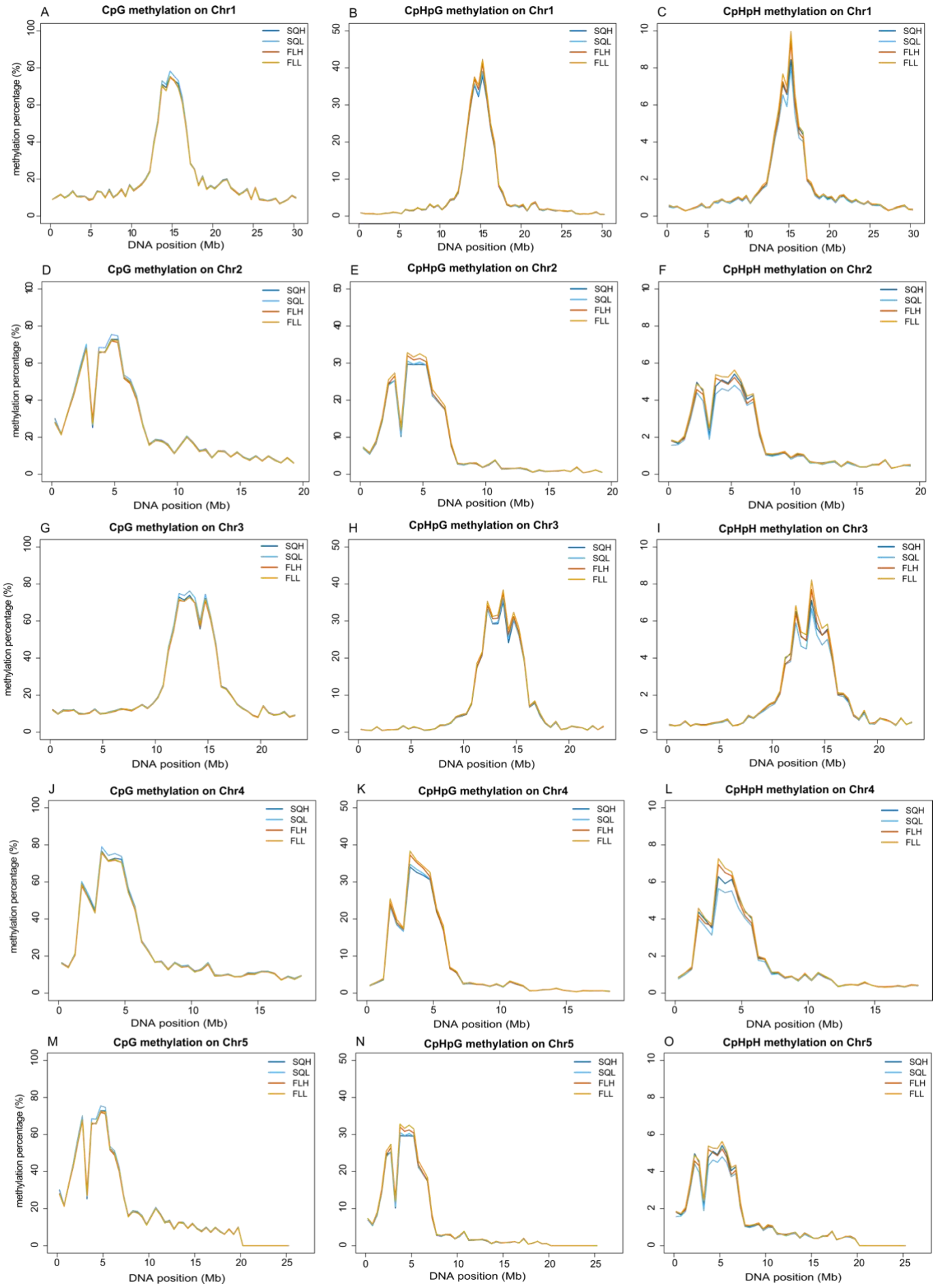

Figure 4.1: Low resolution profiles for *Arabidopsis thaliana* chromosome 1 (**A-C**), 2 (**D-F**) 3 (**G-I**), 4 (**J-L**), and 5 (**M-O**) in each sequence context- CpG, CpHpG, and CpHpH.

Functional annotation of these differentially methylated regions (Figure **4.2**B-D) indicated that acclimation could be linked to the function of sequences under differential methylation. Promoters were calculated as regions within 1kb of a gene. Methylation of introns and promoter regions, which included TEs found within promoter regions, varies across the regimes, suggesting splicing or transcriptional control could have a role in acclimation. Transposable elements genes accounted for most regions with a changed methylation state across contexts (Figure **4.2**B-D), indicating TE regulation an important mechanism during acclimation to all growth light regimes. Many exons also appear to undergo differential methylation, particularly in the CpG context (Figure **4.2**B), with SQLvFLL also showing a large number of differentially methylated CpHpG sites in comparison to the other three comparisons (Figure **4.2**C). This demonstrates differential effects of light regime on methylation.

Enrichment plots (Figure **4.2**E-G) demonstrated that TEs are enriched in the data across all three sequence contexts, suggesting potential for transposable element activation. All other functional annotations were seen to be depleated, particularly the 5'UTRs in both CpG (Figure **4.2**E) and CpHpG (Figure **4.2**F). In the CpHpH context (Fig.4.3G), exons, introns, 5'UTRs, and 3'UTRs were all noted to be depleated.

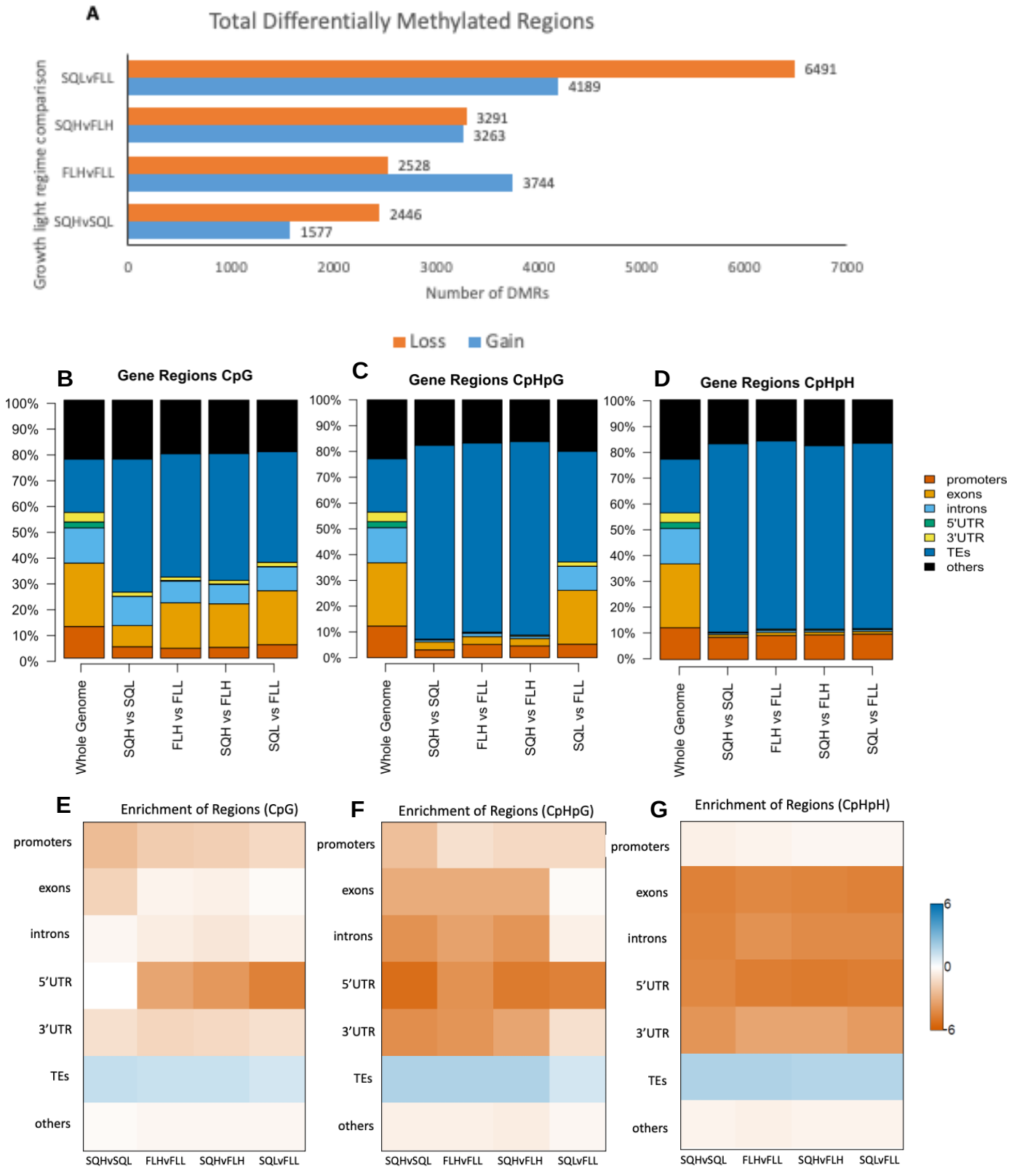

Figure 4.2: Results of differential methylation analysis using DMRcaller, demonstrating genome wide changes in methylation. **A**) Total number of differentially methylated regions (DMRs) when growth light regime is compared. Numbers on bars represent the number of regions. Functional annotation of the whole genome and DMRs in the CpG (**B**), CpHpG (**C**), and CpHpH (**D**) as a percentage of total DMRs in

each regime comparison. Transposable elements within the calculated promoter regions were counted as promoters and not TEs. The enrichment (log2[observed/expected]) of these functional annotations (**E-G**) reveals significantly higher enrichment of transposable elements across contexts. SQ= square light, FL=fluctuating light, H=high light intensity, L=low light intensity.

To determine whether genes showed differential methylation between regimes comparisons and show whether there was an effect of high vs low light acclimation compared to square vs fluctuating, a heatmap of loss and gain of methylation in the gene bodies, according to TAIR10, was plotted (Figure 4.3). Across contexts, it was notable that SQHvSQL had fewer differentially methylated genes than all other regimes, followed by FLHvFLL, indicating there was an effect of high versus low light compared to square versus fluctuating in terms of differential methylation of genes. In general, there were few gene clusters which were shared between regimes in the CG context (Figure 4.3A). Two clusters were identified; the first consisted of loss of methylation and was seen in all regimes bar SQHvSQL, indicating loss of methylation may be related to fluctuating light. The other showed downregulation in both square versus fluctuating conditions, with no differential methylation seen in SQHvSQL, while part of the cluster displays gain of methylation in FLHvFLL. This indicates that the cluster of genes may be upregulated in SQvFL conditions due to the loss of CpG methylation.

In the CpHpG context (Figure 4.3B), three clusters were identified. The first showed loss of methylation in high versus low comparisons, but gain in the SQvFL, suggesting these genes may have a role in fluctuating light acclimation. The second showed loss in FLHvFLL and SQLvFLL, while the third showed loss in SQvFL, gain in FLHvFLL, and no change in SQHvSQL.

The final context, CpHpH (Figure 4.3C) showed a great number of DMRs, resulting in identification of four clusters of interest. In the first, there was loss of methylation in both high versus low comparisons but gain in SQvFL, indicating this cluster may be responsive to both light intensity and light patterns. Similarly, the second cluster showed gain in SQvFL and loss in SQHvSQL, with no change in FLHvFLL. The third cluster demonstrated gain across all light regimes, suggesting these genes could be related to general light responses. Finally, the fourth cluster showed loss in SQvFL, while under high versus low light, some displayed gain while others displayed no change. This indicates that light had impacted upon methylation in all three contexts and could be resulting in differential regulation of gene expression.

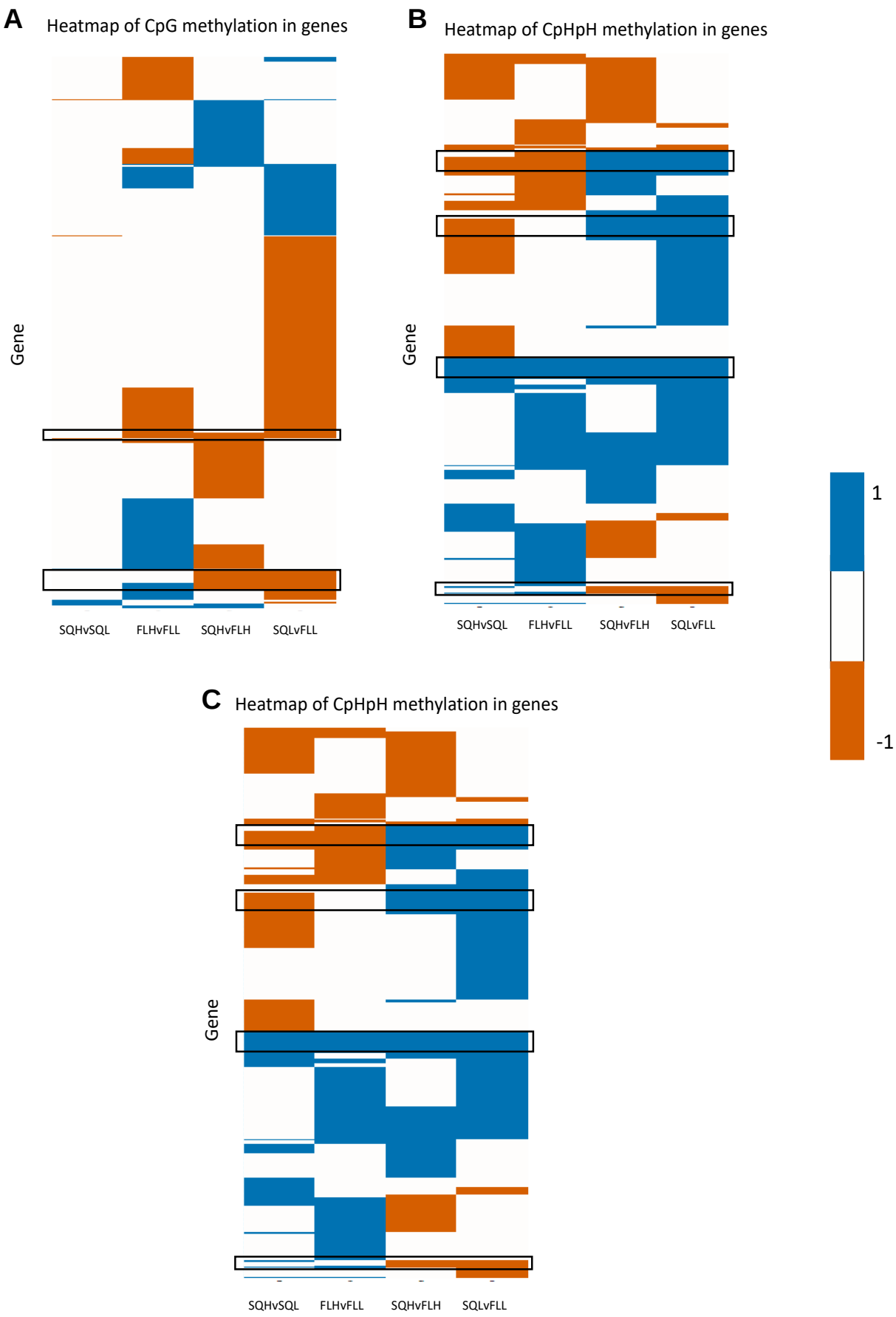

Figure 4.3: Heatmaps of differentially methylated genes in each regime comparison across CpG (A), CpHpG (B), and CpHpH (C) contexts. Black boxes show regions of interest, where there are differential changes in methylation between 2 or more comparisons. Blue represents 1, where methylation is gained at a DMR, orange represents -1, where methylation is lost, and white shows 0, where there is no differential methylation

To understand common changes in genes and TEs occurring between contexts, genes and TEs were grouped into a Venn diagram (Figure **4.4**). In all cases, most DMRs were unique to the context suggesting there is a distinct genetic change associated with acclimation to the growth light regimes. The highest number of unique DMRs were noted in SQLvFLL, suggesting a greater degree of regulation may be required under fluctuating low light conditions. A considerable number of DMRs overlap in FLHvFLL and the two squares versus fluctuating comparisons, both individually and combined, providing evidence that there may be a distinct set of genes related specifically to fluctuating light acclimation. Between both square vs fluctuating regimes, 170 differentially methylated genes and TEs were shared, while 57 were shared between the high vs low light comparisons. Furthermore, 122 genes and TEs were differentially methylated across regimes, indicating these may be key to in growth light acclimation, regardless of regime. Of these, the majority (90) were transposable element, meaning transposable element regulation could have a role in the acclimation response. Gene functions included Vacuolar H+ ATPase (AT3G58730), as well as proteins associated with signaling in the chloroplast (AT1G19090) and leaf senescence (AT1G54040). When the overrepresentation analysis of these groups was considered, no functional groups were found to be significantly enriched (FDR<0.05).

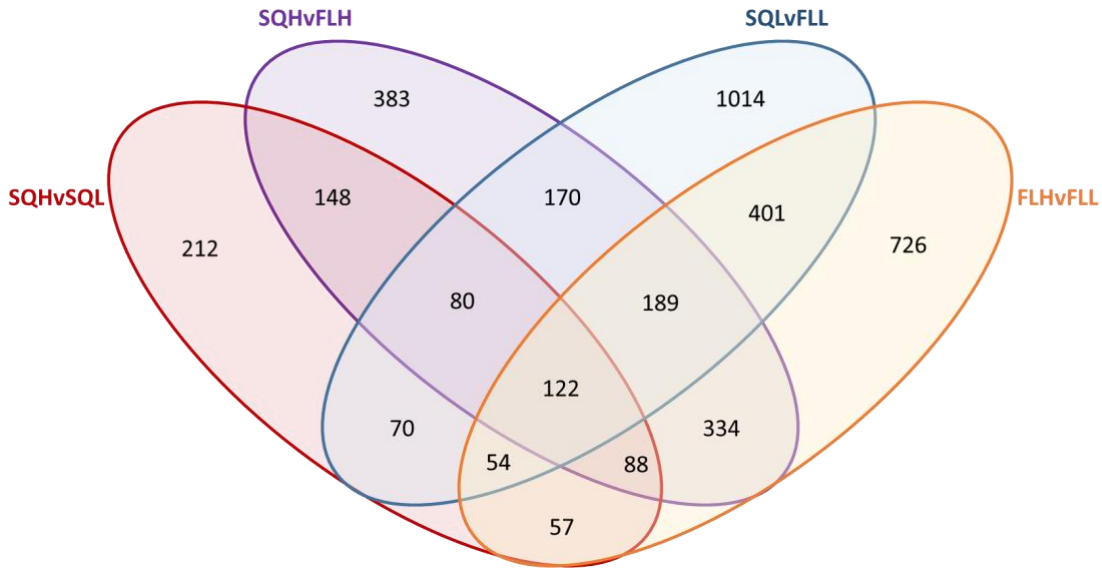

Figure 4.4: Venn diagram of all differentially methylated coding genes and transposable elements. Numbers indicate the total number of coding genes as found by comparing differentially methylated regions to their corresponding gene region according to TAIR10. Full lists of genes are available in Table S1

4.3.2. Transposable element methylation is affected by light acclimation

To investigate whether acclimation effects transposable element (TE) methylation and therefore activity, the different types of TEs which display differential methylation were classified. TEs can be separated, generally, into two classes; Class I, which transpose via an RNA intermediate with reverse transcription, often referred to as a 'copy and paste' mechanism, or Class II, which transpose by excision from the DNA, i.e., a 'cut and paste' mechanism. To better determine the amplitude of the change, the number of TEs was normalized to the current number of known TE copies, 32000, most of which are truncated and non-functional (Quesneville, 2020).Across regimes, there was a greater proportion of Class II TEs differentially methylated than Class I (Figure **4.5**), so could be acting as regulators for nearby genes or became active. SQHvFLH show the greatest number of differentially methylated TEs, with a far greater proportion than any other regime comparison.

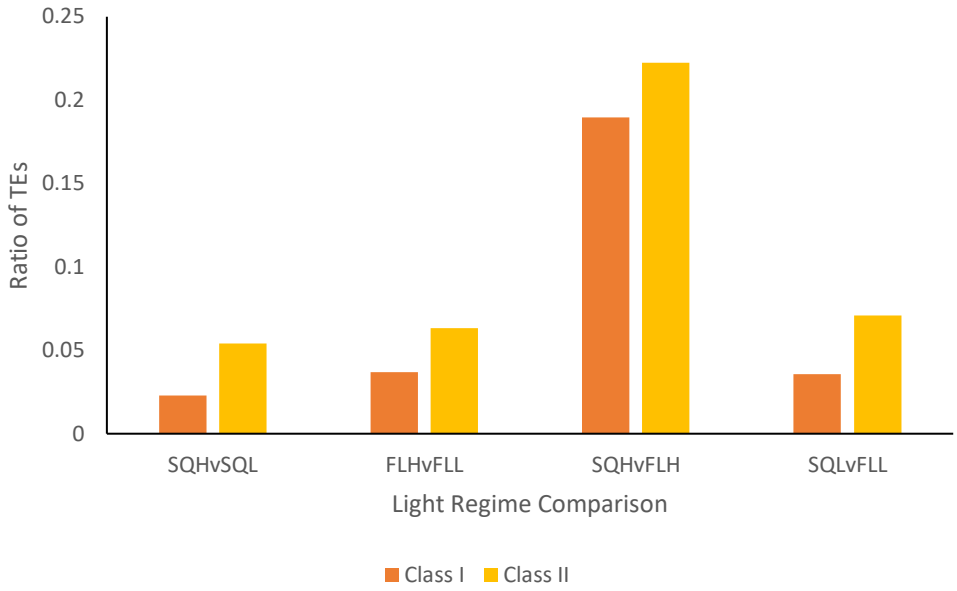

Figure 4.5: Proportion of transposable element genes differentially methylated, separated by Class. The ratio was normalized to the number of transposable element copies (32000) currently known to be annotated in the TAIR10 genome

To further understand changes in TE methylation resulting from light acclimation, differentially methylated TE genes were assigned to their functional family, defined by shared sequence structures. Class I TEs were broken down into Copia, Gypsy, LINE, SINE, and RathE families, and Class II into DNA/MuDR, Helitron, CACTA, En-Spm, Pogo, Harbinger, Mariner, hAT, and SADHU (Makałowski *et al.*, 2019), and those without a grouping defined as “Unassigned” (Figure **4.6**). Across regimes, Helitron, Gypsy, and DNA/MuDR were most abundant, suggesting these elements may be particularly responsive to light. SQHvSQL (Figure **4.6**A) lacked any SADHU transposable elements, indicating these could be impacted specifically by fluctuating light.

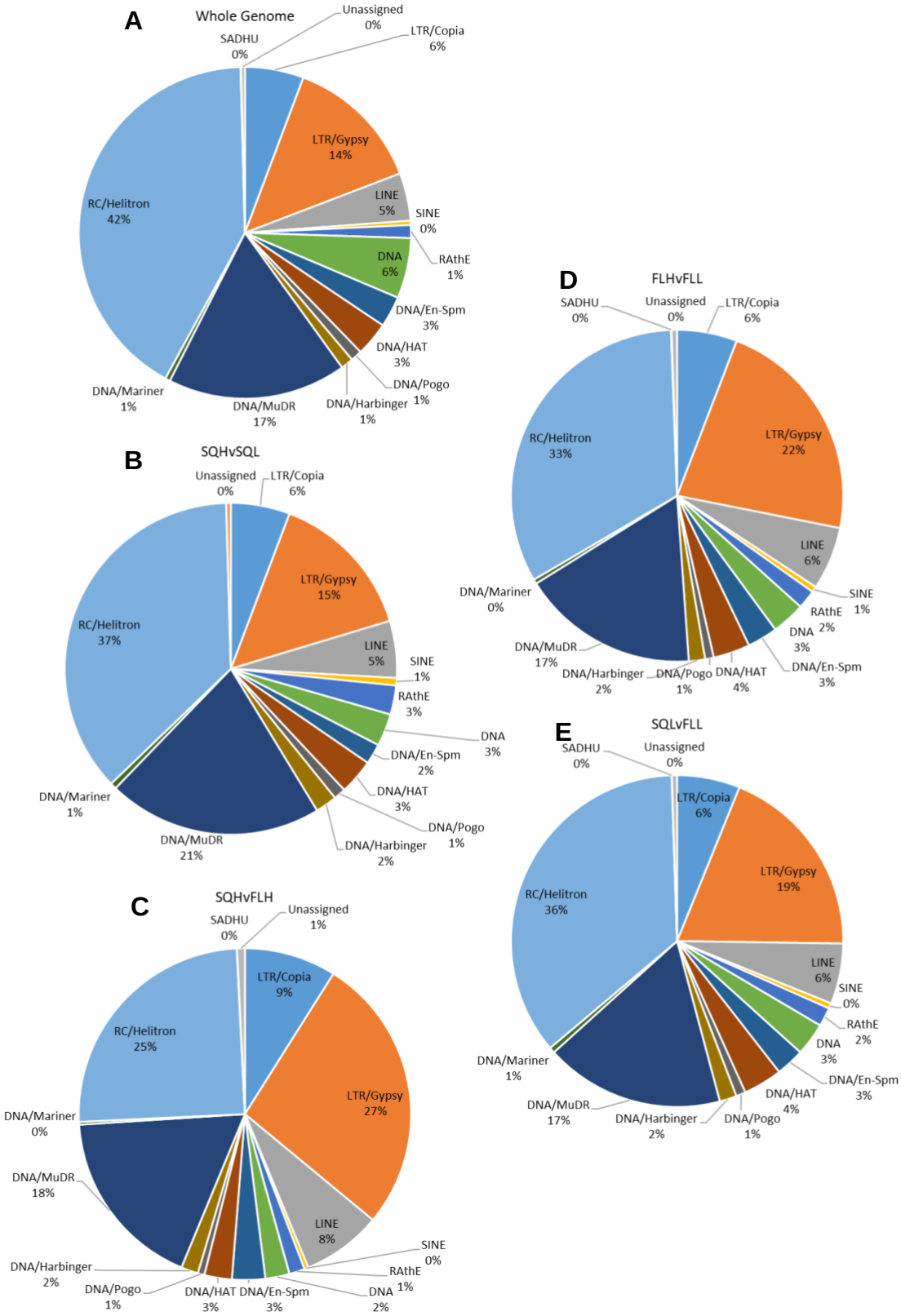

Figure 4.6: Pie charts of transposable element (TEs) which were differentially methylated under different light regimes grouped by family. The whole genome distribution of TEs (**A**) is provided for context of numbers. The distributions of differentially methylated TEs under SQHvSQL (**B**), FLHvFLL (**C**), SQHvFLH (**D**), and SQLvFLL (**E**) demonstrates the proportions methylated appeared to be growth light regime dependent

Enrichment analysis of differentially methylated TEs between regimes (Figure **4.7**) showed that some TEs are differentially methylated to a greater and lesser extent than would be expected. In general, it was seen that Class I TEs were enriched, while Class II were depleted, indicating Class I TEs may have a role in growth light acclimation. For example, SADHU TEs were found to be depleted in SQ vs FL conditions, while Helitrons were noted to be depleted across regimes, suggesting methylation could be under some form of light control. In contrast, LINE and Harbingers were enriched across regimes.

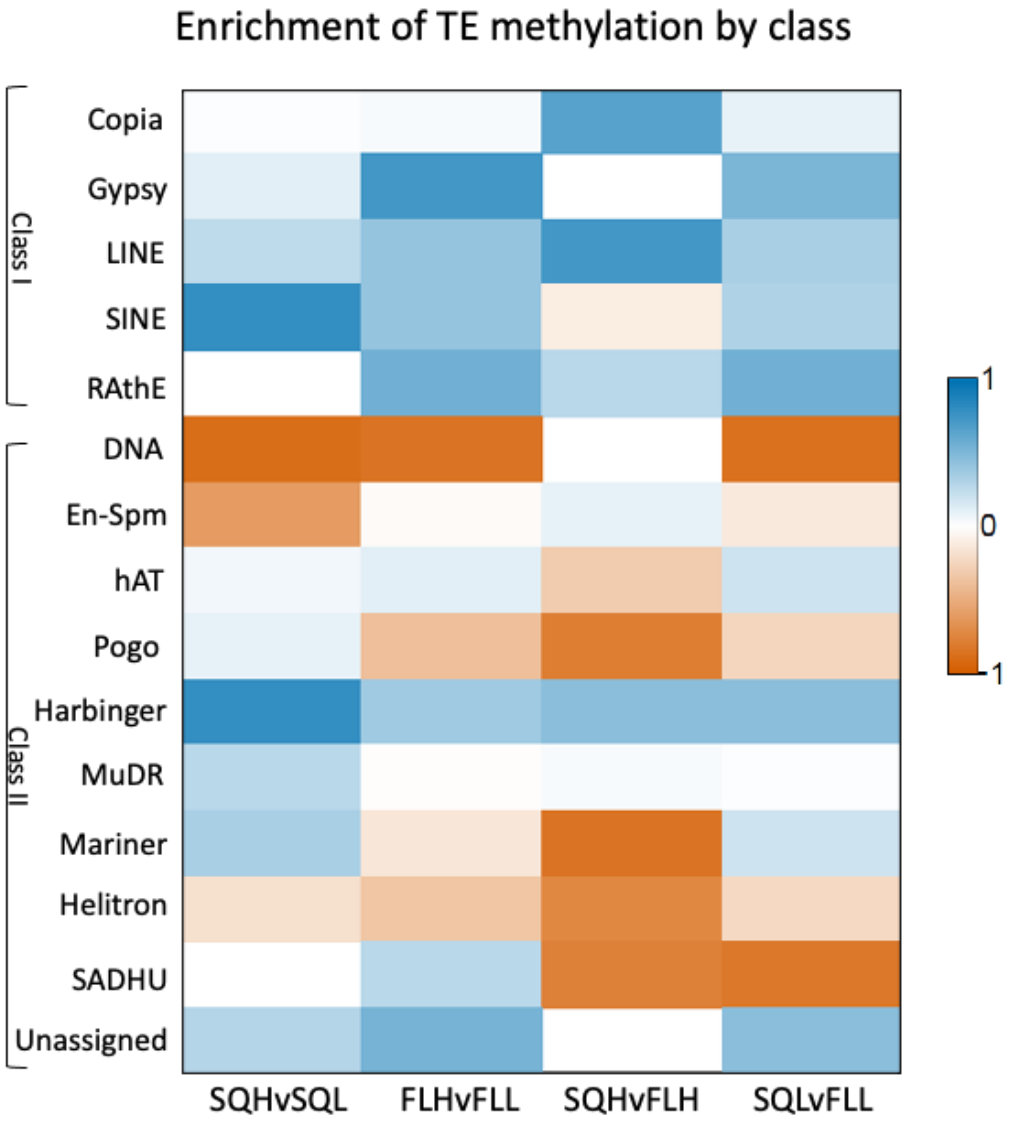

Figure 4.7: Enrichment analysis of each transposable element family subject to differential methylation under different growth light comparisons. Data shows the $\log_2$[observed/expected].

4.3.3. RNA sequencing reveals a role of DNA methylation in light acclimation

To determine whether DNA methylation is accompanied by change in the transcriptional profiles of plants acclimated to fluctuating light, RNA sequencing (RNAseq) was performed. PCA analysis (Figure 4.8) provided early evidence for transcriptional change. Generally, replicates from each regime are similar, particularly in the case of SQH and SQL. Data from the SQH and SQL plants were closer on the plot, suggesting a higher degree of similarity in gene expression than the fluctuating groups. Both FLH and FLL have one of three points away from the cluster of two points, indicating a greater degree of variability in gene expression under fluctuating light conditions. The groups of FLH and FLL clusters displayed a greater degree of spatial separation, indicating that gene expression differs depending on the intensity of fluctuating light to a greater extent than under square light regimes.

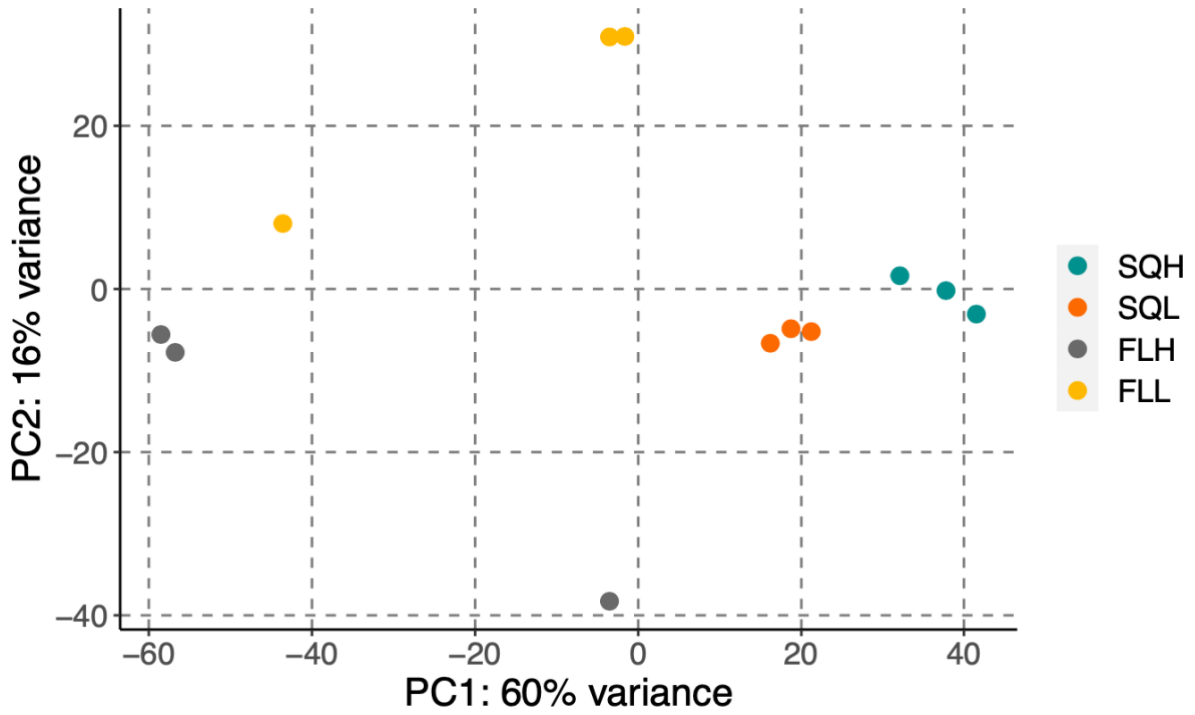

Figure 4.8: Principal component analysis (PCA) plot of RNAseq data demonstrating the similarity in transcription between replicates of plants exposure to each of the four light regimes. Each point is a single replicate. Clustering shows that all replicates under SQH and SQL light share similarity, while the groupings suggest some similarity in transcriptional profile. This was less clear in both fluctuating condtions, suggesting variability, while the grouping indicated transcription between fluctuating high and low light differed to a greater degree than under square light.

Supporting this, the heatmap of transcript per million (TPM;Figure **4.9**) further demonstrated the potential changes in transcription between light regimes. Differences in expression were noted between samples from square and fluctuating light environments, as well as between high and low, confirming there is an effect of both light intensity and regime. There was also within group variation, indicating there is some diversity in the response to a given light environment.

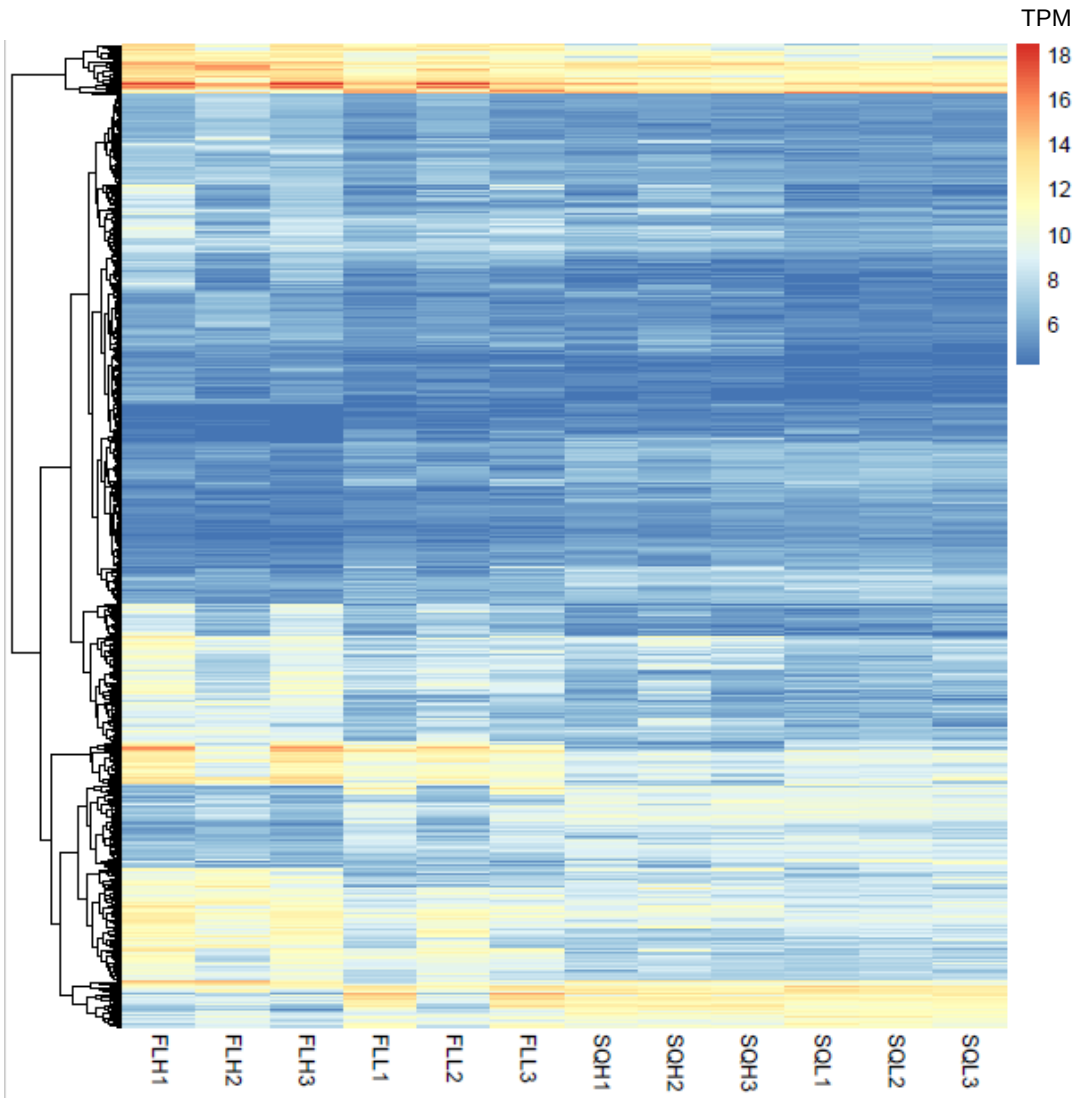

Figure 4.9: Heatmap of differentially expressed genes in transcripts per million (TPM) between samples of each light regime. Data is clustered by expression. Each sample is plotted, with three in total per regime. Included are genes that showed a Log_2 fold change of at least 0.5 and a *p-adj* of at most 0.05 in at least one regime comparison

To determine the significant of the differential expression observed in the heatmap (Figure **4.9**), volcano plots (Figure **4.10**) for the differential expression between regimes were plotted. A larger number of differentially expressed genes (DEGs) were found to be significantly differentially expressed (p<0.05) between regimes. Lower numbers of DEGs were noted under SQHvSQL (Figure **4.10**A) and FLHvFLL (Figure **4.10**B) compared to SQHvFLH (Figure **4.10**C) and SQLvFLL (Figure **4.10**D).

This indicates that acclimation to fluctuating light requires a greater magnitude of change than acclimation to light intensity.

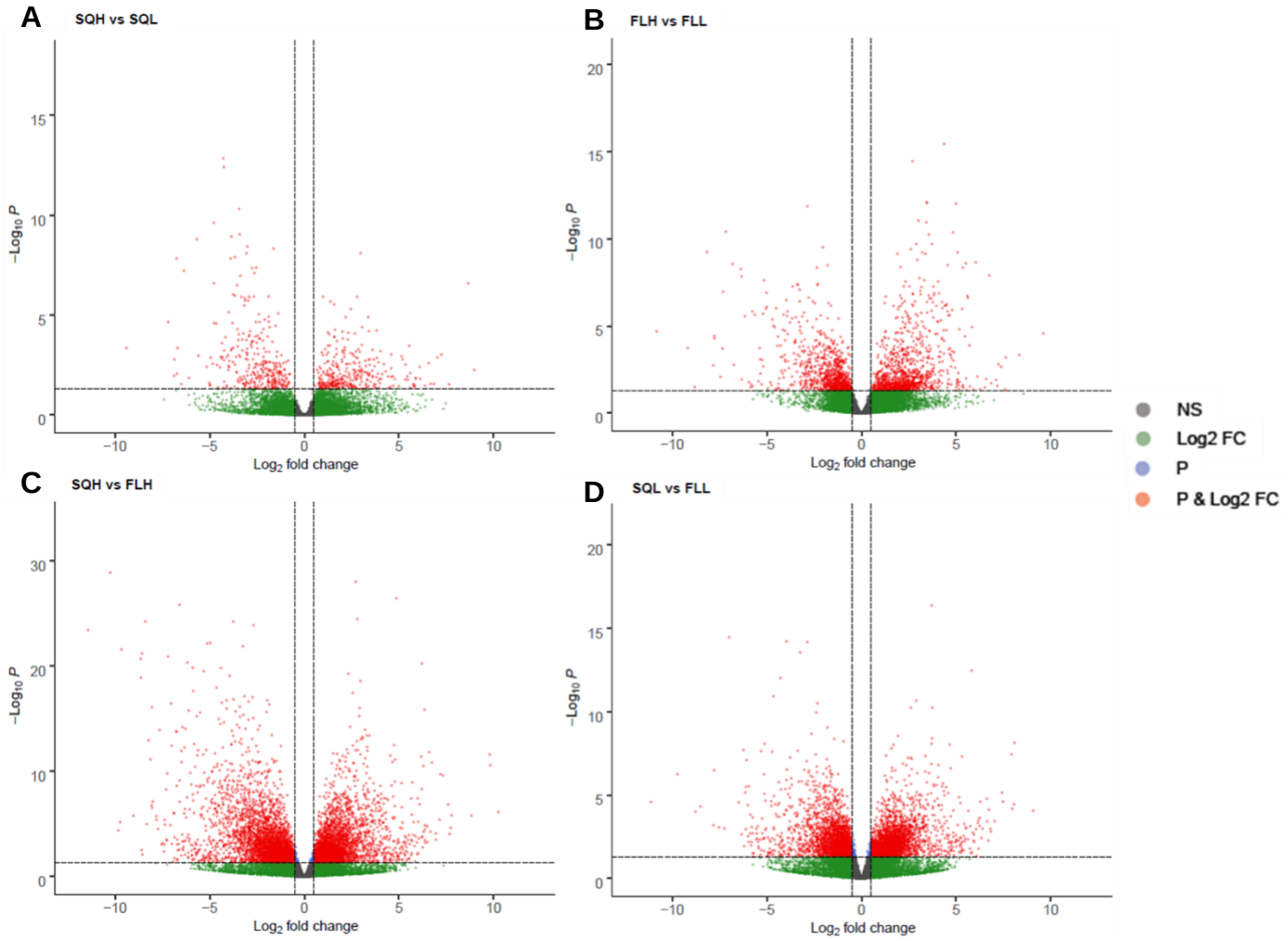

Figure 4.10:: Volcano plots of RNAseq data for each context comparison. Grey shows not significant points (NS). *p-adj*≤0.05, log2FC minimum=0.5, *n*=3

To assess whether a subset of these genes is shared across regimes, differentially expressed genes were grouped depending on regime (Figure **4.11**). 39 genes were found to be differentially expressed across all regime comparisons, indicating these genes may be key for light acclimation. A further 31 genes were shared between SQHvSQL and FLHvFLL, and 501 genes were differentially expressed between SQHvFLH and SQLvFLL.

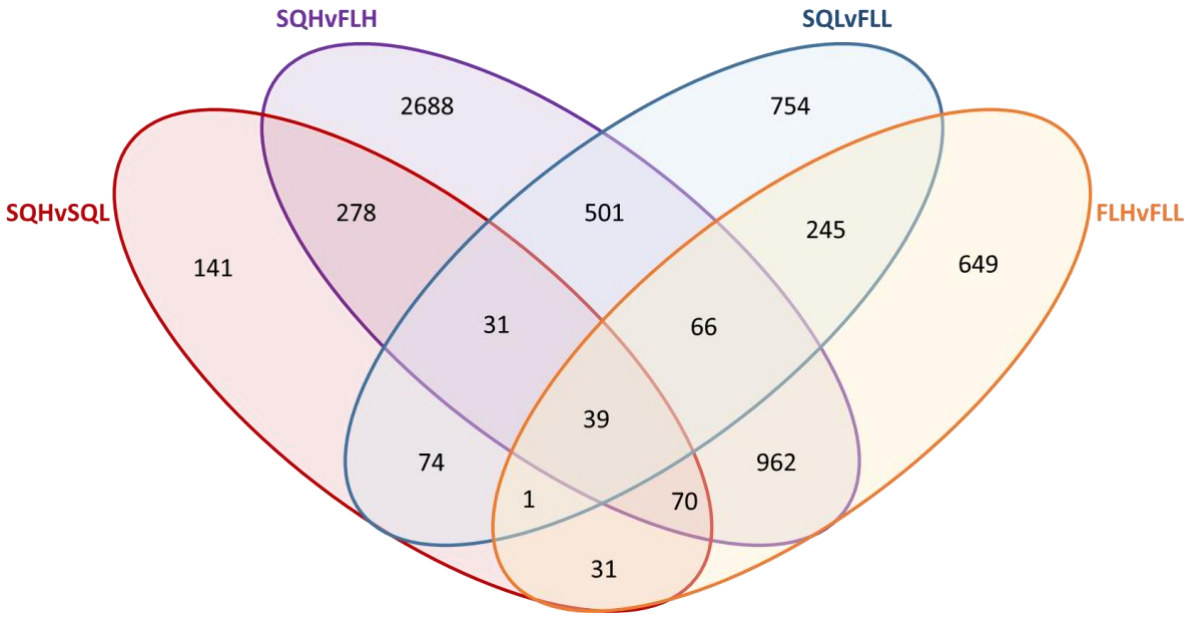

Figure 4.11: Venn diagram of differentially expressed genes according to RNAseq data. Numbers indicate the total number of genes according to the TAIR10 annotation. Full lists of genes are available in Table S2.

4.3.4. Differential methylation and gene expression resulting from growth light acclimation are correlated

The possible correlation between DNA methylation and transcription was investigated next. Some studies have found a correlation between changes in methylation and gene expression, but this is not always clear and may not translate into changes in gene expression (Lister *et al.*, 2008; de Mendoza *et al.*, 2022). The gene lists from WGBS and RNAseq were compared. The genes found to be differentially methylated in all regime comparisons (122), those associated with the high and low comparison (57), and those with square vs fluctuating light (170) were of specific interest (Figure **4.12**). Overlap between the genes differentially methylated and expressed was only noted in square vs fluctuating, with 2 shared genes. These were AT1G03090 (MCCA), a subunit MCCase, which is involved in leucine degradation in the mitochondria, and AT1G27880, a DEAD-box RNA helicase. The

otherwise lack of overlaps suggests these two genes could be central to acclimation to square vs fluctuating light, while indicating that acclimation at this level may be dependent on both regime and intensity.

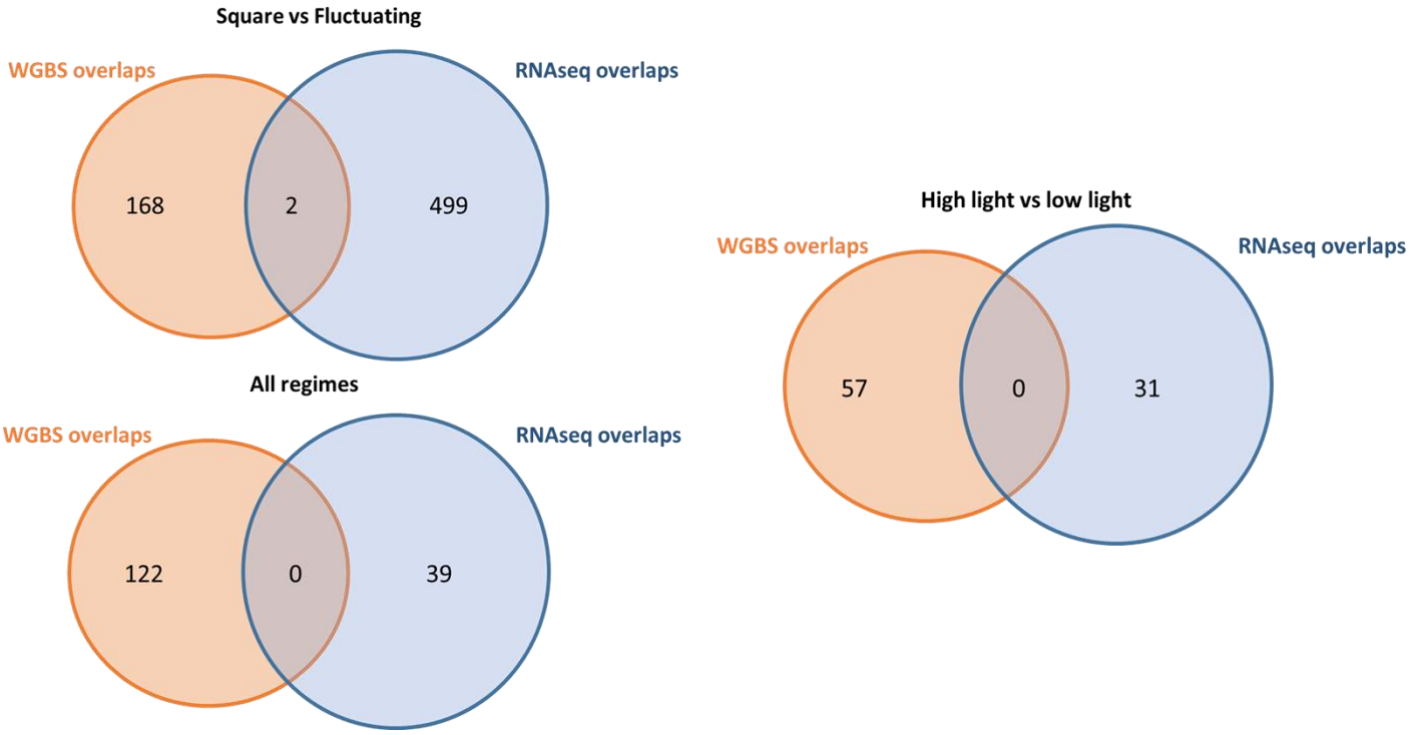

Figure 4.12: Venn diagrams of the overlaps between differentially methylated regions (DMRs) and differentially expressed genes (DEGs). Of the 170 genes differentially methylated and the 501 differentially expressed under square vs fluctuating light (**A**) of both high and low intensity, only 2 genes overlapped. The DMRs and DEGs which were found in all regimes (**B**) had no overlaps, as was the case under high vs low light (**C**).

Next it was investigated whether the specific regime comparisons, SQHvSQL, FLHvFLL, SQHvFLH, and SQLvFLL, had shared differentially methylated and expressed genes (Figure **4.13**). Overall, there was a greater number of overlaps between DMRs and DEGs under SQHvFLH (Figure **4.13**C) and SQLvFLL (Figure **4.13**D) than SQHvSQL (Figure **4.13**A) and FLHvFLL (Figure **4.13**B). However, none of these were found to be significantly over-represented (p>0.9).

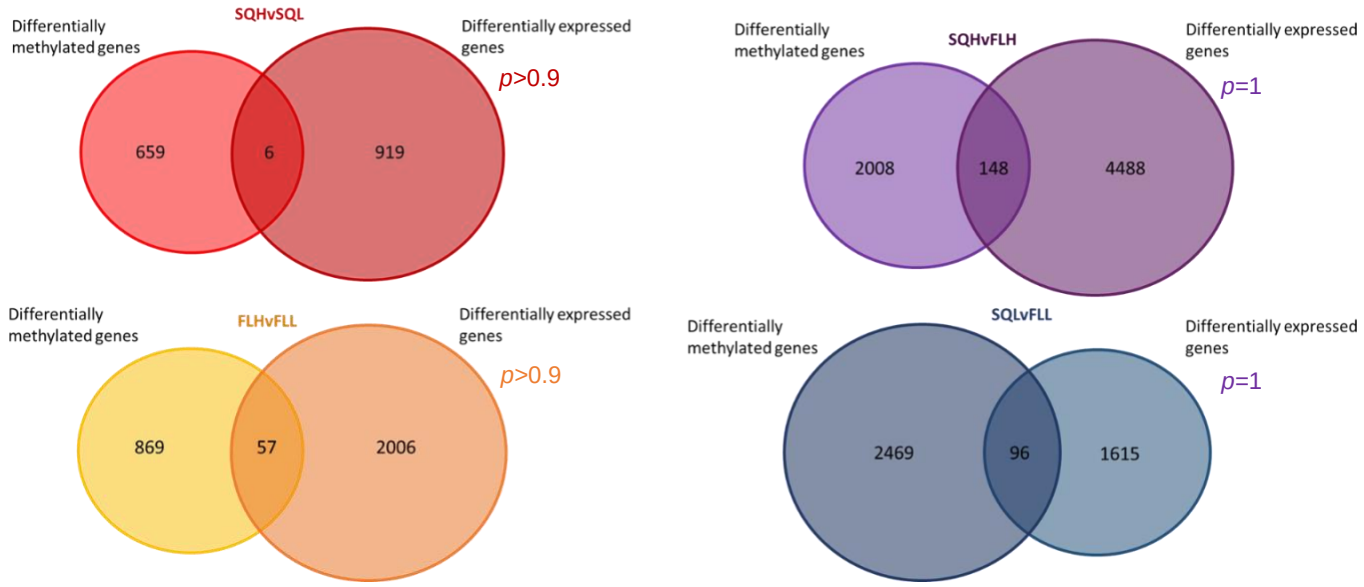

Figure 4.13: Venn diagrams of the differentially methylated and expressed genes between light regimes according to WGBS and RNAseq respectively. The least overlaps were seen in SQHvSQL (**A**) followed by FLHvFLL (**B**). This was followed by SQHvFLH (**C**), with the most seen under SQLvFLL (**D**). *p*-values indicate the results of hypergeometric distribution analysis, showing the probability of observing equal to or more overlaps than observed.

When the function of these overlaps was assessed, the results suggested (Table ***4.3***) that, under square light, there is little correlation between methylation and gene expression at a transcriptional level (6 genes). The number of overlaps increases when considering fluctuating light acclimated plants, with 57 noted overlaps. However, when these square light plants are compared to their fluctuating counterpart, a greater degree of overlap can be seen, with SQHvFLH showing 148 overlaps, and SQLvFLL showing 96. These genes under possible control by DNA methylation exhibit wide functionalities, demonstrating that light can have impacts on plant gene expression outside of photosynthesis.

Table 4.3: Reduced list of differentially methylated genes that are differentially expressed in RNA sequencing data. Data is grouped by growth light regime and shows the cytosine contexts where methylation is differential, whether methylation is lost or gained, the log_2fold change of RNAseq, and the associated gene function as described on TAIR. Coloured according to light regime comparison- Red= SQHvSQL, Orange= FLHvFLL, Purple= SQHvFLH, Blue= SQLvFLL. P-adj<0.05, n=3. Complete list available in Supplementary Information Table S3

Light Regime	Gene code	Context	Methylation	log_2FC	Gene	Function
SQHvSQL	AT1G62770	CpHpH	loss	3.03	PMEI9	PMEI9 pectin methylesterase inhibitor.
SQHvSQL	AT2G06255	CpHpH	loss	1.33	EFL3	DUF1313 domain containing protein, involved in photoperiodism
SQHvSQL	AT2G22710	CpG, CpHpG	gain	2.24		Transposable element (guard cell)
SQHvSQL	AT1G33950	CpHpH	loss	-4.97	IAN7	Avirulence induced gene (AIG1) family protein
SQHvSQL	AT2G18660	CpHpH	loss	-3.34	ATPNP-1	Encodes PNP-A (Plant Natriuretic Peptide A), exact role unknown but is stress responsive
SQHvSQL	AT4G00970	CpHpG	gain	-2.25	CRK41	Encodes a cysteine-rich receptor-like protein kinase.
FLHvFLL	AT1G11960	CpG	loss	2.89	OSCA1.3	Calcium channel that is phosphorylated by BIK1 in the presence of PAMPS and required for stomatal immunity.
FLHvFLL	AT1G29170	CpG	gain	-1.42	WAVE2	Encodes a member of the SCAR family. These proteins are part of a complex (WAVE) complex. The SCAR subunit activates the ARP2/3 complex which in turn act as a nucleator for actin filaments

FLHvFLL	AT1G64860	CpG	loss	-1.60	SIGA	Subunit of chloroplast RNA polymerase, confers the ability to recognize promoter sequences on the core enzyme
FLHvFLL	AT1G65070	CpG	gain	-1.60		DNA mismatch repair protein MutS, type 2
FLHvFLL	AT2G32950	CpG	loss	-1.00	COP1	Represses photomorphogenesis and induces skotomorphogenesis in the dark.
FLHvFLL	AT3G11670	CpG	gain	-1.09	DGD1	Responsible for the final assembly of galactolipids in photosynthetic membranes. Provides stability to the PS I core complex (e.g., subunits PsaD, PsaE).
FLHvFLL	AT3G17040	CpG	loss, gain	-1.09	HCF107	It is an RNA tetratricopeptide repeat-containing protein required for normal processing of transcripts from the polycistronic chloroplast psbB-psbT-psbH-petB-petD operon coding for proteins of the photosystem II and cytochrome b6/f complexes.
FLHvFLL	AT4G17610	CpG	gain	1.79	TRM3	tRNA/rRNA methyltransferase (SpoU) family protein
FLHvFLL	AT4G18520	CpG	loss	1.60	PDM1	Encodes a PPR (pentatricopeptide repeat) protein PDM1/SEL1. Involved in RNA editing and splicing of plastid genes
FLHvFLL	AT5G55760	CpG	loss	-0.75	SRT1	a member of the SIR2 (sirtuin) family HDAC (histone deacetylase)

SQHvFLH	AT1G03090	CpG	loss	-3.89	MCCA	MCCA is the biotinylated subunit of the dimer MCCase, which is involved in leucine degradation. Both subunits are nuclear coded, and the active enzyme is located in the mitochondrion
SQHvFLH	AT1G04400	CpG	loss	-2.14	CRY2	Blue light receptor mediating blue-light regulated cotyledon expansion and flowering time
SQHvFLH	AT1G32080	CpG	loss	1.62	LRGB	Encodes a plant LrgAB/CidAB protein localized to the chloroplast envelope that is involved in chloroplast development, carbon partitioning, ABA/drought response, and leaf senescence
SQHvFLH	AT1G62310	CpG	gain	-1.63	JMJ29	A probable H3K9me2 demethylase
SQHvFLH	AT1G75100	CpG	loss	1.86	JAC1	Required for the chloroplast accumulation response, but not for the avoidance response. No molecular function known. Influences the composition of photosynthetic pigments, the efficiency of photosynthesis, and the CO2 uptake rate
SQHvFLH	AT2G32410	CpG	loss	1.03	AXL1	Involved in chiasma distribution, affects expression of key DNA repair and meiotic genes, significant role in DNA repair
SQHvFLH	AT2G44900	CpG	loss	-0.80	ARABIDILLO-1	Promotes lateral root development

SQHvFLH	AT3G17185	CpHpH	gain	3.66	ATTAS3	Encodes a trans-acting siRNA (tasi-RNA) that regulates the expression of auxin response factor genes (ARF2, ARF4, ETT)
SQHvFLH	AT3G58730	CpG	loss	-0.59	VHA-D	Member of V-ATPase family. Vacuolar-type H + -ATPase (V-ATPase) is a multisubunit proton pump located on the endomembrane
SQHvFLH	AT5G17300	CpG	loss	3.58	RVE1	Myb-like transcription factor that regulates hypocotyl growth by regulating free auxin levels in a time-of-day specific manner
SQHvFLH	AT5G22920	CpG	loss	-6.75	ATRZPF34	Encodes a protein with sequence similarity to RING, zinc finger proteins. Loss of function mutations show reduced (15%) stomatal aperture under non stress conditions
SQHvFLH	AT5G28237	CpHpH	loss	-1.98	CMT2	Encodes a plant DNA methyltransferase that methylates mainly cytosines in CpHpH contexts
SQLvFLL	AT1G03090	CpG	gain	-2.48	MCCA	MCCA is the biotinylated subunit of the dimer MCCase, which is involved in leucine degradation. Both subunits are nuclear coded, and the active enzyme is located in the mitochondrion
SQLvFLL	AT1G20160	CpG	loss	-1.14	SBT5.2	Encodes two isoforms. One (SBT5.2(a)) is a secreted, cell wall localized subtilisin-like serine protease that is involved in regulation of stomatal development. The second isoform (SBT5.2(b) is localized to endosomes

SQLvFLL	AT1G53780	CpG	gain	-1.37		26S proteasome regulatory complex ATPase
SQLvFLL	AT2G15890	CpG	loss	-3.39	CBP1	a regulator of transcription initiation in central cell-mediated pollen tube guidance
SQLvFLL	AT3G01770	CpG	gain	-1.36	GTE11	Global transcription factor, Bromodomain protein that functions as a negative regulator of sugar and ABA signaling
SQLvFLL	AT3G18524	CpG	loss	0.96	ATMSH2	Encodes a DNA mismatch repair homolog of human MutS gene, MSH6. MSH2 is involved in maintaining genome stability and repressing recombination of mismatched heteroduplexes
SQLvFLL	AT3G20100	CpG	loss	-1.39	CYP705A19	Cytochrome P450 from family CYP705A
SQLvFLL	AT3G22300	CpG	loss	1.51	RPS10	Nuclear-encoded gene for mitochondrial ribosomal small subunit protein S10
SQLvFLL	AT3G57660	CpG	loss	2.54	NRPA1	Encodes a subunit of RNA polymerase I
SQLvFLL	AT4G30690	CpG	gain	-1.93	ATIF3-4	Ribosome disassembly in chloroplast, cytoplasm, cell wall, and plasma membrane
SQLvFLL	AT4G39280	CpG	loss	1.00		phenylalanyl-tRNA synthetase, putative / phenylalanine-tRNA ligase
SQLvFLL	AT5G02840	CpG	loss	-1.78	RVE4	a homolog of the circadian rhythm regulator RVE8, involved in heat shock response
SQLvFLL	AT5G11790	CpG	gain	2.07	NDL2	Plays a role in dehydration stress response

To determine whether differential methylation has impacted transposable element activity, overlaps between WGBS and RNAseq were extracted. A total of 23 transposable elements were differentially methylated and differentially expressed (Table **4.4**) across light regimes, indicating transposable element activation may have occurred. The most TEs with differential methylation and expression was noted under SQHvFLH (12) followed by SQLvFLL (7). Under SQHvFLH, 10 of 12 TEs showed a positive log_2FC, suggesting increased TE activation under SQH light than FLH light. In contrast, under SQLvFLL, 6 of the 7 TEs displayed a negative log_2FC. This indicates that under FLL light there was an increase in transcription of these TEs, demonstrating the possibility of TE activation under FLL acclimation. This is reflected in the data for FLHvFLL where all 3 TEs showed an increase in transcription in FLL plants compared to FLH plants. Both loss and gain of methylation was seen in different TEs, with no apparent relationship with increased or decreased transcription.

Table 4.4: List of differentially methylated and differentially expressed transposable elements. Data is grouped by growth light regime and shows the cytosine contexts where methylation is differential, whether methylation is lost or gained, the log2fold change of RNAseq, and the associated gene function as described on TAIR. Coloured according to light regime comparison- Red= SQHvSQL, Orange= FLHvFLL, Purple= SQHvFLH, Blue= SQLvFLL.

Light Regime	Gene code	Context	Methylation	log_2FC	TE Gene	Function
SQHvSQL	AT2G22710	CG, CHG	gain	2.24		Transposable element (guard cell)
FLHvFLL	AT3G17050	CG	loss	-1.42519		Transposable element, pseudogene
FLHvFLL	AT5G34800	CG	loss	-1.3646	VANDAL20	Transposable element
FLHvFLL	AT5G35495	CG, CHG	loss, gain/loss	-2.50617	ATLINE1_4	Transposable element, Class I
SQHvFLH	AT1G31570	CHH	loss, gain	2.17423	ATENSPM3	CACTA-like TE
SQHvFLH	AT2G05025	CG	loss	6.36154	ATIS112A	AT2TE08160, DNA/Harbinger TE
SQHvFLH	AT2G05040	CG	loss	2.454186	ATGP3	AT2TE08225, LTR/Gypsy TE
SQHvFLH	AT2G11780	CG	loss	-5.65736		TE, pseudogene
SQHvFLH	AT3G15310	CG	loss, gain	7.327073	ATSI112A	AT3E21700, DNA/Harbinger TE
SQHvFLH	AT3G28945	CHG	gain	-2.35488	TA11	AT3TE45620, LINE/L1
SQHvFLH	AT3G48523	CHG, CHH	gain	4.896449	ATCOPIA44	AT3TE72850, LTR/Copia
SQHvFLH	AT4G01490	CG, CHH	loss, gain	3.293343	ATLINE1_6	AT4TE03295, LINE/L1
SQHvFLH	AT4G01525	CHH	gain	3.423688	SADHU5-1	AT4TE03410, TE
SQHvFLH	AT4G06477	CG	loss	3.515067	ATLANTYS1	AT4TE14185, LTR/Gypsy
SQHvFLH	AT5G34790	CHG	gain	1.606699		CACTA-like TE
SQHvFLH	AT5G34800	CHG	loss	1.635572	VANDAL20	AT5TE46165, DNA/MuDR TE
SQLvFLL	AT1G25430	CG	loss	-1.4825		AT1TE28830, LINE TE
SQLvFLL	AT2G22710	CG	loss	-2.14592		Transposable element (guard cell)
SQLvFLL	AT3G17050	CG	loss	-1.83617		Pseudogene, TE
SQLvFLL	AT3G23085	CHH	gain	-3.89685		hAT-like transposase family, TE
SQLvFLL	AT3G28945	CG, CHH	gain	-2.36395	TA11	AT3TE45620, LINE/L1 TE
SQLvFLL	AT4G02960	CG	loss	4.852993	ATRE2	a copia-type retrotransposon element
SQLvFLL	AT4G10580	CHH	gain	-3.83937	ATGP1	AT4TE27915, LTR/Gypsy TE

To assess the possible impacts of changes transposable element methylation on nearby gene expression, expression of genes within 1kb of differentially methylated TEs was investigated. Across the regimes, a range of differentially expressed genes were noted within 1kb of a differentially methylated TE (Table ***4.5***). This appeared to correlate to a greater extent than when comparing differential methylation and expression of genes, with SQHvSQL showing a total of 29 differentially expressed genes within 1kb of a differentially methylated TE, while FLHvFLL had 110. In the square vs fluctuating comparisons, SQHvFLH displayed the greatest number of genes (258), while SQLvFLL yielded 97 genes, against the trend of SQLvFLL displaying the greatest magnitude of differences

Table 4.5: Subset of differentially expressed genes within 1kb of a differentially methylated transposable element (TE) Data is grouped by growth light regime and shows the cytosine contexts where methylation is differential, whether methylation is lost or gained, the log2fold change of RNAseq, and the associated gene function as described on TAIR. Coloured according to light regime comparison- Red= SQHvSQL, Orange= FLHvFLL, Purple= SQHvFLH, Blue= SQLvFLL. Full table available in supplementary Table S4

Regime	Differentially methylated TE	TE methylation		Gene within 1kb	log2FC	Gene Description
		Context	Region Type			
SQHvSQL	AT1TE25645	CHH, CHG	loss, gain	AT1G05680	5.13	Encodes a UDP-glucosyltransferase, UGT74E2, that acts on IBA (indole-3-butyric acid) and affects auxin homeostasis. induced by H2O2 and may allow integration of ROS (reactive oxygen species) and auxin signalling.
SQHvSQL	AT3TE94580	CHG, CHH	loss	AT1G22550	-1.85	Tonoplast localized pH dependent, low affinity nitrogen transporter.
SQHvSQL	AT1TE40120	CHH	loss	AT1G56600	3.88	GolS2 is a galactinol synthase that catalyzes the formation of galactinol from UDP-galactose and myo-inositol. GolS2 transcript levels rise in response to methyl viologen, an oxidative damage-inducing agent. Plants over-expressing GolS2 have increased tolerance to salt, chilling, and high-light stress.

SQHvSQL	AT2TE01120	CHH	loss	AT2G02990	1.99	Encodes a member of the ribonuclease T2 family that responds to inorganic phosphate starvation and inhibits production of anthocyanin.
SQHvSQL	AT1TE05585	CHH	gain	AT2G18470	6.09	Proline-rich extensin-like receptor kinase 4. Functions at an early stage of ABA signalling inhibiting primary root cell elongation by perturbing Ca2+ homeostasis.
SQHvSQL	AT4TE31060	CHH	loss	AT4G11890	-2.56	Encodes a receptor-like cytosolic kinase ARCK1. Negatively controls abscisic acid and osmotic stress signal transduction.
SQHvSQL	AT3TE61915	CHH	loss	AT5G50400	0.99	purple acid phosphatase 27
FLHvFLL	AT1TE08420	CHG, CHH	gain	AT1G08250	-1.93	Encodes a plastid-localized arogenate dehydratase involved in phenylalanine biosynthesis.
FLHvFLL	AT1TE10560	CHH	loss	AT1G09970	1.72	RLK7 belongs to a leucine-rich repeat class of receptor-like kinase (LRR-RLKs). It is involved in the control of germination speed and the tolerance to oxidant stress.
FLHvFLL	AT1TE31190	CG, CHH	loss, gain	AT1G27770	1.49	Encodes a chloroplast envelope Ca2+-ATPase with an N-terminal autoinhibitor.
FLHvFLL	AT1TE34300	CHH	loss, gain	AT1G30135	4.56	jasmonate-zim-domain protein 8
FLHvFLL	AT1TE41830	CHH	gain	AT1G35140	5.62	EXL1 is involved in the C-starvation response.

FLHvFLL	AT1TE55715	CG	gain	AT1G44350	1.83	encodes a protein similar to IAA amino acid conjugate hydrolase. NO-induced, involved in growth and disease resistance.
FLHvFLL	AT1TE56515	CHH	gain	AT1G45145	1.87	encodes a cytosolic thioredoxin that reduces disulfide bridges of target proteins by the reversible formation of a disulfide bridge between two neighbouring Cys residues present in the active site.
FLHvFLL	AT1TE74435	CHH	gain	AT1G61210	-1.28	DWA3 encodes a DWD (DDB1 binding WD40) protein. In vitro analyses suggest its involvement in the negative regulation of ABA responses.
FLHvFLL	AT1TE77880	CHH	gain	AT1G63750	1.30	miR825-5p target proposed as a phasiRNA producing locus.
FLHvFLL	AT2TE03875	CHH	gain	AT2G02990	2.14	Encodes a member of the ribonuclease T2 family that responds to inorganic phosphate starvation and inhibits production of anthocyanin.
FLHvFLL	AT2TE05800	CHH	gain	AT2G04030	2.66	Encodes a chloroplast-targeted 90-kDa heat shock protein located in the stroma involved in red-light mediated deetiolation response and crucial for protein import into the chloroplast stroma.
FLHvFLL	AT2TE28445	CHH	loss	AT2G16070	-1.14	An integral outer envelope membrane protein (its homolog in A thaliana PDV1), component of the plastid division machinery.

FLHvFLL	AT2TE29500	CHH	loss	AT2G16700	1.53	Encodes actin depolymerizing factor 5 (ADF5). Involved in actin cytoskeleton remodelling during a variety of processes including pollen tube growth and stomatal movement.
FLHvFLL	AT2TE37235	CHH	loss	AT2G20570	-0.84	Encodes GLK1, Golden2-like 1, one of a pair of partially redundant nuclear transcription factors that regulate chloroplast development
FLHvFLL	AT2TE64580	CHH	loss	AT2G34600	4.79	Key regulator in alternative splicing in the jasmonate signaling pathway, alone and in collaboration with other regulators.
FLHvFLL	AT3TE42600	CHH	loss	AT3G27690	-3.04	Encodes Lhcb2.4. Belongs to the Lhc super-gene family encodes the light-harvesting chlorophyll a/b-binding (LHC) proteins that constitute the antenna system of the photosynthetic apparatus.
FLHvFLL	AT4TE54340	CHH	gain	AT4G22200	-1.60	Encodes AKT2, a photosynthate- and light-dependent inward rectifying potassium channel with unique gating properties that are regulated by phosphorylation. Expressed in guard cell protoplasts and in the phloem and xylem of aerial portions of the plant.
FLHvFLL	AT4TE74390	CHH	gain	AT4G32295	-1.33	histone acetyltransferase

FLHvFLL	AT5TE36235	CG	loss	AT5G27930	1.34	EGR2 functions as a negative regulator of plant growth with prominent effect on plant growth during drought stress. EGR2 regulates microtubule organization and likely affects additional cytoskeleton and trafficking processes along the plasma membrane.
FLHvFLL	AT5TE70705	CG	loss	AT5G48490	-4.04	Encodes a protein with similarity to a lipid transfer protein that may contribute to systemic acquired resistance (SAR).
FLHvFLL	AT5TE72770	CHH	loss	AT5G49740	-2.09	Encodes a chloroplast ferric chelate reductase. Shows differential splicing and has three different mRNA products.
FLHvFLL	AT5TE94620	CHH	gain	AT5G65685	-0.51	SS5 is a chloroplast-localized protein that is related to the canonical starch synthases (most closely to SS4) but is catalytically inactive. *Arabidopsis* ss5 mutants have near-normal total transitory starch contents but produce fewer and larger starch granules in their chloroplast.
SQHvFLH	AT1TE03860	CHH	gain	AT1G04400	-2.14	Blue light receptor mediating blue-light regulated cotyledon expansion and flowering time.
SQHvFLH	AT1TE31190	CHH	loss, gain	AT1G27770	-1.76	Encodes a chloroplast envelope Ca2+-ATPase with an N-terminal autoinhibitor.

SQHvFLH	AT1TE41830	CG	gain	AT1G35140	-4.94	EXL1 is involved in the C-starvation response.
SQHvFLH	AT1TE56505	CHG	gain	AT1G45145	-1.70	encodes a cytosolic thioredoxin
SQHvFLH	AT1TE78765	CHH	loss	AT1G64440	0.61	Encodes a protein with UDP-D-glucose 4-epimerase activity.
SQHvFLH	AT2TE00535	CG	gain	AT2G01300	-4.43	mediator of RNA polymerase II transcription subunit
SQHvFLH	AT2TE37235	CHH	loss	AT2G20570	1.15	Encodes GLK1, Golden2-like 1, one of a pair of partially redundant nuclear transcription factors that regulate chloroplast development
SQHvFLH	AT2TE58505	CG	loss	AT2G31270	1.54	Encodes a cyclin-dependent protein kinase. Involved in nuclear DNA replication and plastid division.
SQHvFLH	AT3TE36105	CHH	loss	AT3G23840	1.54	Plant natriuretic peptide (PNP); participate in the regulation of ions and water homeostasis, required to induce plant stomatal aperture.
SQHvFLH	AT3TE36645	CG	loss	AT3G24190	2.07	ABC1-type kinase, located in chloroplast, involved in protein phosphorylation.
SQHvFLH	AT3TE41970	CHH	loss	AT3G27300	-1.34	Glucose-6-phosphate dehydrogenase.
SQHvFLH	AT3TE67815	CHH	gain	AT3G45590	-1.57	Encodes a catalytic subunit of tRNA splicing endonuclease.
SQHvFLH	AT3TE71530	CHH	gain	AT3G47860	1.17	Encodes a chloroplastic lipocalin AtCHL. Located in thylakoid lumen. Involved in the protection of thylakoidal membrane lipids against reactive oxygen species,

						especially singlet oxygen, produced upon excess light. LCNP is required for sustained photoprotective energy dissipation or NPQ (qH) to occur
SQHvFLH	AT3TE72645	CHH	gain	AT3G48420	-2.87	Phosphatase like protein, located in chloroplast, involved in response to H2O2.
SQHvFLH	AT4TE26180	CHG	gain	AT4G09820	5.06	TT8 is a regulation factor that acts in a concerted action with TT1, PAP1 and TTG1 on the regulation of flavonoid pathways, namely proanthocyanin and anthocyanin biosynthesis.
SQHvFLH	AT4TE31080	CHH	loss	AT4G11910	-2.96	Acts antagonistically with SGR1 to balance chlorophyll catabolism in chloroplasts with the dismantling and remobilizing of other cellular components in senescing leaf cells.
SQHvFLH	AT4TE33660	CHH	gain	AT4G13250	-1.40	Encodes a chlorophyll b reductase involved in the degradation of chlorophyll b and LHCII (light harvesting complex II).
SQHvFLH	AT4TE83950	CHH	gain	AT4G36910	1.13	Encodes a single cystathionine beta-synthase domain-containing protein. Modulates development by regulating the thioredoxin system.

SQHvFLH	AT5TE29530	CHH	gain	AT5G24120	3.54	Encodes a specialized sigma factor that functions in regulation of plastid genes and is responsible for the light-dependent transcription at the psbD LRP.
SQHvFLH	AT5TE65540	CHH	loss	AT5G45080	3.85	phloem protein 2-A6
SQHvFLH	AT5TE65540	CHH	loss	AT5G45090	-7.38	phloem protein 2-A7
SQHvFLH	AT5TE94620	CHH	gain	AT5G65685	0.76	SS5 is a chloroplast-localized protein that is related to the canonical starch synthases (most closely to SS4) but is catalytically inactive. *Arabidopsis* ss5 mutants have near-normal total transitory starch contents but produce fewer and larger starch granules in their chloroplast.
SQLvFLL	AT1TE41830	CHH	gain	AT1G35140	4.26	EXL1 is involved in the C-starvation response.
SQLvFLL	AT1TE52320	CHH	loss	AT1G42430	-1.71	Novel plant specific, chloroplast localized protein that is involved in regulation of starch degradation.
SQLvFLL	AT1TE70700	CHH	loss	AT1G57820	1.50	Encodes a 645-amino acid methylcytosine-binding protein. This protein functions as an E3 ubiquitin ligase in vitro. The protein has been shown to bind to methylated cytosines of CG, CNG and CNN motifs via its SRA domain It plays a role in the establishment/maintenance of chromatin structure during cell

						division and is localized in the nucleus.
SQLvFLL	AT1TE81305	CG	loss	AT1G66370	6.05	Encodes a member of the MYB family of transcription factors. Involved in regulation of anthocyanin biosynthesis. A
SQLvFLL	AT2TE27690	CHH	loss, gain	AT2G15570	-1.66	chloroplast protein similar to prokaryotic thioredoxin.
SQLvFLL	AT3TE39980	CHH	gain	AT3G26180	-1.29	putative cytochrome P450
SQLvFLL	AT3TE70960	CG	loss, gain	AT3G47520	1.49	Encodes a protein with NAD-dependent malate dehydrogenase activity, located in chloroplasts.
SQLvFLL	AT4TE01555	CHH	loss, gain	AT4G00720	-1.01	Encodes ASKtheta, a group III *Arabidopsis* GSK3/shaggy-like kinase. Functions in the brassinosteroid signalling pathway.
SQLvFLL	AT4TE31080	CHH	loss	AT4G11910	-3.36	Acts antagonistically with SGR1 to balance chlorophyll catabolism in chloroplasts with the dismantling and remobilizing of other cellular components in senescing leaf cells.
SQLvFLL	AT5TE34270	CHH	gain	AT5G26830	0.88	Encodes a dual-targeted threonyl-tRNA synthetase found in both the chloroplast and mitochondrion.
SQLvFLL	AT5TE67885	CHH	gain	AT5G46500	-2.02	protein VARIATION IN COMPOUND TRIGGERED ROOT growth protein

4.3.5. Differential transcription of photosynthetic genes was revealed in RNA sequencing data

The impact of growth light regime on the expression of photosynthetic genes was investigated (Figure **4.14**), and RNAseq data was mined for a range of photosynthetic genes. A list of genes was compiled from multiple sources [see Waters *et al.* (2009); López-Calcagno, Howard and Raines (2014); Yu *et al.* (2014); Wang, Hendron and Kelly (2017)]. Since few chloroplast and mitochondrial genes were found to be differentially transcribed between light regimes, nuclear encoded genes were targeted.

The most genes differentially transcribed were noted under SQHvFLH (45), followed by FLHvFLL (26). Of these, 17 genes are shared but have contrasting expression, demonstrating a possible difference in the mechanisms related to acclimation of square light compared to fluctuating light. Between SQHvFLH and SQLvFLL, there were 4 shared genes (ELF3, ELF4, RBCX1, G6PD2) which experienced the same change in transcript expression, suggesting these genes may be linked to photosynthetic acclimation to fluctuating light. Between SQHvSQL and FLHvFLL, there was a single shared gene (LTP), indicating potential involvement in acclimation to high light compared to low light. The otherwise lack of shared genes across comparisons could indicate separate mechanisms for acclimation depending on the intensity of growth light. This provided evidence that both light intensity and regime have different impacts on gene expression depending on how they are combined.

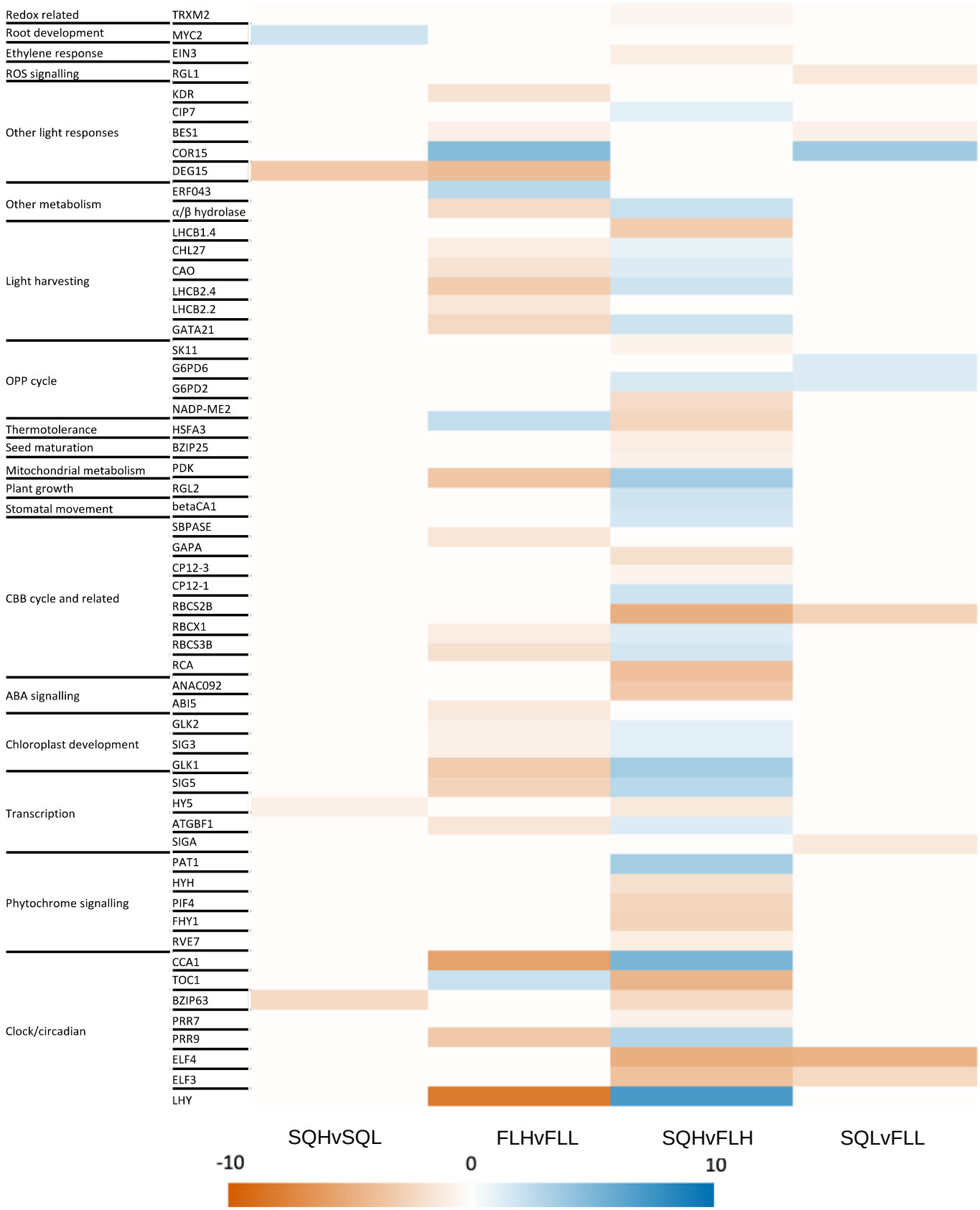

Figure 4.14: Heatmap of the log2-fold change in expression of photosynthetic genes according to RNA sequencing data under different growth light regimes. Colours indicate the log2 fold change in expression. Log2FC=0.5, *p-adj*<0.05, n=3. Table of data is available in Supplementary Material Table S5

4.4. Discussion

DNA methylation is highly dynamic and known to respond to environmental stimuli. There is limited evidence for the effects of long-term light stress and acclimation on the methylome, with these studies concluding there is little impact of light regime on DNA methylation (Ganguly *et al.*, 2018), finding few differentially methylated regions despite clear physiological phenotypes (Ganguly *et al.*, 2018). However, the impacts of natural light regimes and acclimation over the lifespan of *Arabidopsis* has not been conducted. This, combined with the known negative effects of fluctuating light on carbon assimilation in both tropical and crop plants (Chazdon and Pearcy, 1986b; Taylor and Long, 2017; Wang *et al.*, 2020), and the highly consistent phenotype exhibited under the regimes used here (Vialet-Chabrand *et al.*, 2017; Matthews, Vialet-Chabrand and Lawson, 2018), indicates some role of epigenetics. Data from previous chapters indicates a distinct photosynthetic phenotype in *Arabidopsis* acclimated to square and fluctuating light, so correlating these to possible changes in gene expression mediated by changes in DNA methylation is a potential way to identify new gene target to improve the acclimation response to dynamic light.

Multiple possible targets for improved light acclimation could be identified from this work. Analysis of differentially methylated regions indicated that V-type ATPase (AT3G58730), located on endomembranes, may have important role in acclimation since changes in methylation are seen across growth light regimes. The role of V-type ATPases (V-ATPase) in response to abiotic stress has previously been investigated in (Dietz *et al.*, 2001; Liu *et al.*, 2018). In cotton, virus induced silencing of the V-type ATPase resulted in decreased drought tolerance, alongside a 34%

decrease in chlorophyll content and significant decrease in superoxide dismutase and peroxide activity, while overexpression in tobacco improve tolerance to dehydration (Liu *et al.*, 2018). This indicates that changes to the expression of Vacuolar ATPase under light acclimation could alter sensitivity to drought, while also having some role in reactive oxygen species scavenging and signaling. Furthermore, abscisic acid (ABA) application in both barley and ice plants has been shown to increase V-ATPase activity, and its activity has also been implicated in response to acidification of the leaf, although this is poorly understood (Dietz *et al.*, 2001). Such evidence indicates that V-ATPase could play an important role in multiple stress responses. However, change in the expression on a transcriptional level of this V-type ATPase was only seen when comparing SQH and FLH light, with a log2-fold change of -0.59, suggesting high light peaks may be required for induction of expression.

FIB2 was also identified in both square versus fluctuating comparisons as differentially methylated and differentially expressed. FIB2 has previously been linked to the cold response (Gu*o et al*, 2021), as well as the cold response under low light (Prerostova *et al.*, 2021), where it was found to be overexpressed. FIB2 is an RNA methyltransferase which functions in processing rRNA and ribosome assembly (Barneche, Steinmetz and Echeverria, 2000). Its presence within this dataset indicates possible change to ribosome assembly and regulation could be important for acclimation to fluctuating light. In FLHvFLL, CpG methylation was lost within the gene, correlating to a log2 fold change of 4.73 in the RNAseq data, while CpG methylation was also lost in SQLvFLL, correlated with a log2 fold change of 4.37. This indicates that methylation of FIB2 is lost under fluctuating low light (FLL),

possibly contributing to an increased transcription, and a potential increase in regulation of ribosome assembly.

Two genes were noted to overlap under square versus fluctuating conditions in both differential methylation and expression: AT1G03090 (MCCA) and AT1G27880, a DEAD-box RNA helicase. Neither have previously been associated with light acclimation, with only MCCA being well characterised. MCCA codes the α subunit in 3-methylcrotonyl CoA carboxylase (MCCase) which is involved in leucine catabolism in the mitochondria (Anderson *et al.*, 1998). This indicates there may be some role for mitochondrial catabolism in acclimation to dynamic light, undergoing significant downregulation (log2FC; -3.9 SQHvFLH, -2.5 SQLvFLL) when square and fluctuating light plants are compared.

Despite these overlaps in methylation in changes in expression suggesting a possible correlation, it is important to note that there is currently little evidence linking gene body methylation (gbM) and altered gene expression. There is an increasing body of evidence, including the work here, that supports a correlation between gbM and altered gene expression (reviewed in Muyle *et al.* (2022)), but these have yet to establish whether there is a direct cause. This means that only correlative and not causative conclusions can be drawn from this data about the impacts of light regime induced methylation on gene expression.

Widespread changes in transposable element methylation across growth light regimes were also observed. Loss of methylation was seen across transposable element types and under different growth light regimes, suggesting the possibility of transposable element activation. Transposable element activation has been observed in *Arabidopsis thaliana* under heat stress, where *ONSEN* (ATCOPIA78)

became active under a repeated 6°C to 37°C heat stress treatment, producing both transcripts and extrachromosomal DNA (Ito *et al.*, 2011; Roquis *et al.*, 2021) with several novel insertions reported (Sanchez *et al.*, 2017; Roquis *et al.*, 2021). Progeny of these ONSEN insertion lines resulted in significantly smaller plants and conferred little improvement to heat tolerance (Roquis *et al.*, 2021), indicating that transposition is not causing any favourable transgenerational phenotypic change. Notably, insertion site were preferentially located in exon regions enriched in H2A.Z, which is known to be excluded by DNA methylation (Zilberman *et al.*, 2008), suggesting that loss of methylation at exons could be providing an increased number of insertion sites should any transposable elements be active in this study. In this study, differential methylation of VANDAL2 genes was noted, with FLHvFLL losing methylation at multiple gene sites, and SQHvFLH gaining methylation at one VANDAL2 site. VANDAL2 is known to be one of the most active TEs in the *Arabidopsis thaliana* genome (Quesneville, 2020), suggesting the possibility of increased VANDAL2 mobility under FLL light, potentially resulting in new insertions that could disrupt protein coding genes. Climatic variability is also known to activate several transposable element families found in this study, including ATGP2, ATCOPIA89, and ATENSPM2 (Quesneville, 2020), further suggesting potential for activation of TEs under different growth light conditions.

However, while activation of TEs is a possibility here, it is more likely that TEs could act to regulate up or downstream sequences. Here a range of genes within 1kb of a differentially methylated TE were noted in response to the light regimes. Increased methylation of TEs has previously been shown to impact neighbouring gene expression. For example, in *Arabidopsis,* silencing of a SINE TE neighbouring *FWA*, a locus associated with flowering, results in *FWA* silencing (Kinoshita *et al.*, 2007).

Furthermore, methylation has been noted to spread from TEs into neighbouring genes and the repressive chromatin state resulting from this has been proposed to also impact on nearby genes (Ahmed *et al.*, 2011). This could also mean that loss of methylation leads to increased expression of TE-neighbouring genes due to opening of the chromatin structure. Hypomethylation of TEs could reduce the expression of neighbouring genes due to the siRNA targeting systems to repress TEs. In *Arabidopsis thaliana* and *Arabidopsis lyrate*, such targeting of TEs has been shown to reduce the expression of neighbouring genes (Hollister *et al.*, 2011), so could account for the decrease in gene expression at some loci near TEs with loss of methylation. This supports the data presented here (Table ***4.5***), where a range of genes which are differentially expressed are found within 1kb of differentially methylated TEs, suggesting some role of TE methylation in the regulation of gene expression under fluctuating light.

Sun to shade transition has previously been associated with TE activation in *Solanum lycopersicum*, a TE rich tomato species (Deneweth, Van de Peer and Vermeirssen, 2022). Insertion of Harbinger TEs into the introns of stress-responsive genes was found, while both LINE and retrotransposon TE insertions were noted into introns and downstream of upregulated genes (Deneweth, Van de Peer and Vermeirssen, 2022). This demonstrates that TE activation may be positively correlated with, and possibly driving, acclimation to dynamic light conditions. TE insertions are known to have a role in changing gene expression. Previous studies looking at the epigenetic differences between two *Arabidopsis* ecotypes, Col-0 and Landsberg (Ler), found multiple different TE insertions, with some impacting gene expression (Vaughn *et al.*, 2007). For example, they predicted AT4G04330 (Rbcx1) would be reduced in expression in Ler compared to Col-0 due to a deletion but found

the opposite. This was attributed to insertion of a hAT transposon into the largest intron in Col-0 which was absent in Ler (Vaughn *et al.*, 2007), demonstrating the potential effects of transposon insertion. Interestingly, Rbcx1 was found to be differentially expressed in this study, so it could be possible that TE activation could have a role in this response, making this an interesting possibility for further investigation. There are also examples of TE insertions acting as enhancers for gene expression. In maize, insertion of retrotransposon *Hopscotch* into *teosinte branched1* (*tb1*) enhances gene expression and is partially responsible for increase apical dominance in the domestic crop (Studer *et al.*, 2011). Furthermore, in rapeseed, insertion of a CACTA TE into the upstream regulatory sequences of gene *BnaA9.CYP78A9* increases seed weight and silique length (Shi *et al.*, 2019). This insertion was positively correlated with increased expression of the gene, while increased auxin concentration was noted in the siliques (Shi *et al.*, 2019), demonstrating the physiological impact TE insertion can have.

Transposable element movement is known to have a range of effects on gene expression. TE insertions are capable of causing up- or down-regulation of neighbouring genes, interference with pre-mRNA processing, or integration into the coding sequence and transcribed as additional exons (reviewed in Gill *et al* [2021]). The activation and insertion of TEs has been noted in several stress studies in *Arabidopsis* (Sanchez *et al.*, 2017; Roquis *et al.*, 2021), but also in crops including rice (Naito *et al.*, 2009) and wild tomato (Bolger *et al.*, 2014). In both species, Class I TEs were noted to preferentially insert in the vicinity of stress responsive genes, often resulting in upregulation of transcription of these genes (Naito *et al.*, 2009; Bolger *et al.*, 2014). Here, transcription of TEs was upregulated under multiple growth light comparisons (Table **4.4**), e.g., FLL compared to SQL acclimation. It

could be that the insertion of these TEs is near stress-responsive elements and could contribute to some of the changes in transcription noted in the RNAseq data (section 4.3.3). To know whether this has occurred, whole genome sequencing would be required to find novel insertions and determine their potential effects.

RNA sequencing data revealed that there was differential expression of a range of photosynthesis-related genes under multiple light regime comparisons. The 4 genes shared by SQvFL (Figure **4.14**) have multiple known roles in light signaling and photosynthesis. Global changes to the transcriptome have previously been noted in *Arabidopsis* acclimated to light at 75 µmol m^{-2} s^{-1} with 20 second pulses at 1000 µmol m^{-2} s^{-1} every 5 minutes (Schneider *et al.*, 2019). They found that many clock-related genes were subject to differential expression, including ELF3 and ELF4 as seen here (Figure **4.14**), indicating some consistency in the response under a naturally fluctuating regime. Furthermore, they noted many genes involved in the CBB cycle were differentially expressed, including sedoheptulose-1,7-bisphosphatase (SBPase), as noted here under acclimation to SQHvFLH light, and multiple light harvesting proteins (Schneider *et al.*, 2019). This again demonstrates some consistency to the response to fluctuating light on a transcriptional level. However, multiple other differentially expressed genes were not noted in their work, suggesting some differences in regulation are due to natural fluctuations.

Relatively few differentially methylated genes were found to be differentially expressed (Table ***4.3***) in this work. This has been noted in previous studies into the effects of stress. For example, only 9 of 1562 differentially methylated genes were differentially expression under prolonged cold treatment in *Brassica rapa* (Liu *et al.*, 2017), while only 31 of over 5000 DMRs had differential expression under iron deficiency in rice (Sun *et al.*, 2021). Together, these studies demonstrate that the

magnitude of differential methylation between treatments is often larger than the resulting differential expression, suggesting differential methylation is not always controlling expression in the ways expected. Similar findings were noted here, with only a small subset of DMRs and DEGs overlapping (Figure **4.12**&Figure **4.13**).

It is possible there are indirect effects of DNA methylation at play here. Changes in methylation to one gene, leading to change of expression could then impact upon the genes it regulates. In maize mutants defective for part of the RdDM pathway, treatment with ABA revealed both a direct and indirect role of DNA methylation in the ABA response (Madzima *et al.*, 2021). In the short-term, DNA methylation was found to directly regulate genes for the early response to ABA (Madzima *et al.*, 2021). These methylated genes had downstream roles, impacting genes controlling mutliple plant ABA responses including growth (Madzima *et al.*, 2021), demonstrating an indirect effect of methylation. This could explain the lack of overlaps in DMRs and DEGs, as a differentially methylated gene with changes expression may be impacting upon the expression of genes to which it signals.

The peaks and troughs of the fluctuating light regimes are likely to act as cues for epigenetic change. For example, during the peaks of light in both FLH and FLL regimes, ROS are likely to be generated (Kono and Terashima, 2014). ROS generation has previously been associated with epigenetic change, and a recent has correlated increased ROS due to abiotic stress with hypomethylation (Jing *et al.*, 2022) . Troughs may act as a recovery period for the plants, where ROS production is reduced, and so could result in remethylation of the loci demethylated during high ROS. However, low light could also be considered as stressful for plants, prolonging vegetative growth (Xu, Hu and Scott Poethig, 2021) and reducing carbon assimilation capabilites (Vialet-Chabrand *et al.*, 2017), so itself could cause

hypomethylation. To better understand how the peaks and troughs in light may impact DNA methylation, simiplification of the fluctuating regimes could provide some insight, whereby the extent of variation in the regime is reduced. To determine whether the effects are due to extremely high light, a sinlge peak corresponding to the highest peak of FLH, for example, while the rest of the regime maintains a square wave quality, could determine whether the peak is respisnisble for the effects seen. Futhermore, sampling throughout the regime and comparing the differentially methylated regions could provide evidence for the dynamics of DNA mehtylation and help us understand whether it does indeed play a role in light responses.

Due to the unclear nature of the causality and correlation between DNA methylation and expression, it is difficult to conclude what the impact of light on methylation and gene expression truly are. It may be that methylation here acts as a priming event, so offspring from these plants are better able to cope with the parental light regime. Priming and transgenerational effects are well known to occur in plants as a response to multiple stresses, including cold stress and herbivory (López Sánchez *et al.*, 2016; Song *et al.*, 2020; Arora *et al.*, 2022). Therefore, transgenerational maintenance of DNA methylation may represent a competitive advantage for offspring under these light conditions.

There may also be short term effects of light on methylation, impacting plants earlier on in the regime than the analysed samples were taken. DNA methylation is known to be highly dynamic throughout plant development (Trap-Gentil *et al.*, 2011; Bartels *et al.*, 2018), so it follows that methylation could vary over the lifespan of a plant in response to recurring stress. Very few studies into temporal changes in DNA methylation in response to stress exist. Investigation into the impact of phosphate stress found that the number of DMRs between starved vs control plants increased

the longer plants were starved, and correlated with transcript levels (Secco *et al.*, 2015). Furthermore, resupplying of phosphate to starved plants resulted in a gradual shift in methylation back towards that of the non-starved plants, but even after >21 days of resupplying, the methylation profile was still closer to that of a starved plant than control (Secco *et al.*, 2015). This suggests that methylation may dynamically change over the stress period, and so there may be different effects over the lifespan of the plants, particularly those exposed to fluctuating light.

To establish whether the changes observed could impact upon crops in the field, repeating the experiment on an agriculturally significant crop would be of interest. For example repeating this experiment in wheat, which accounts for 15-20% of calorie and nutrient requirements worldwide (Wieser, Koehler and Scherf, 2020), could help to identify genes associated with improved light-use and improved yield. Another experiment of interest would be whether there is any transgenerational epigenetic inheritance (TGE) of DMRs. If there is inheritance of methylation, this could present an advantage for offspring as they may be pre-acclimated, or primed, for their light environment and improve their performance.

This work had demonstrated the importance of light regime, i.e., the pattern in which light changes, for plant growth and development. Comparisons of square light to fluctuating light resulted in a greater level of both epigenetic and transcriptomic change in genes and transposable elements, indicating substantial differences in the way plants respond to dynamic light environments than when high and low light are compared. This could have significant impacts on studies aimed at field crops grown under laboratory conditions, as this provides evidence as to how and why plants may react differently in laboratory and field studies.

Chapter 5: Acclimation of *Arabidopsis thaliana* mutant *cp12-1/2/3* to fluctuating light

5.1. Introduction

CP12 is a small protein localised to the chloroplast involved in thioredoxin-mediated regulation of the Calvin-Benson-Bassham (CBB) Cycle (López-Calcagno, Howard and Raines, 2014). The CP12 complex consists of two dimerised CP12 molecules, each loaded with a PRK dimer on its N terminal and a GADPH tetramer on the C terminal (Wedel, Soll and Paap, 1997) and is capable of forming a complex with phosphoribulokinase (PRK) and glyceraldehyde-3-phosphate dehydrogenase (GAPDH)(Wedel, Soll and Paap, 1997) which functions to regulate the CBB cycle (Figure **5.1**). In *Arabidopsis*, there are three nuclear-encoded CP12 genes; *CP12-1, CP12-2, and CP12-3*, with protein CP12-1 and CP12-2 being closely related, likely due to duplication (Singh, Kaloudas and Raines, 2008) and demonstrating functional redundancy (López-Calcagno *et al.*, 2017). Tissue-specific analysis of transcript levels demonstrated tissue-specific expression for each CP12 gene. Levels of *CP12-1* expression were similar across the leaves, stems, and flowers, but minimal in root tissue, while *CP12-2* expression was greatest in leaves, significantly lower in the stem and flowers and not detectable in roots (Singh, Kaloudas and Raines, 2008). Expression of *CP12-3* was greatest in stems and lower in leaves and roots (Singh, Kaloudas and Raines, 2008), suggesting the different isoforms have their own tissue-specific roles.

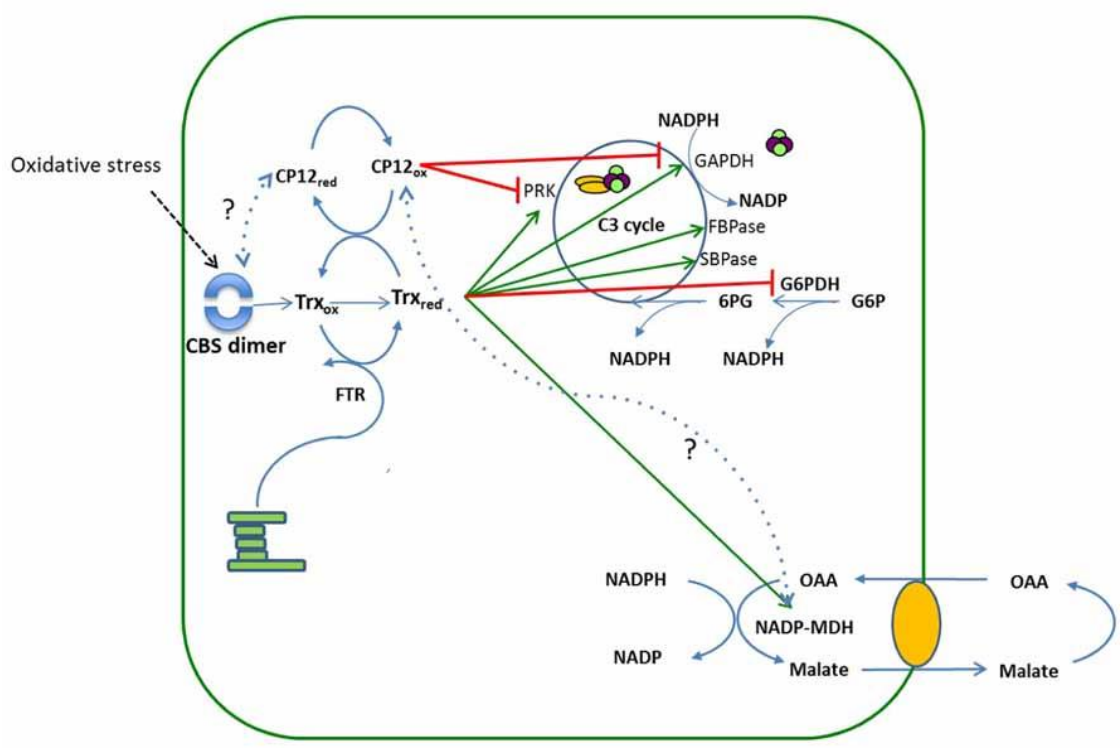

Figure 5.1: The role of CP12, PRK, and GAPDH in the Calvin-Benson Cycle. CP12/PRK/GAPDH complex formation inhibits PRK and GAPDH activity, reducing carbon fixation. Image taken from López-Calcagno, Howard and Raines (2014)

Severe reduction of all *CP12* genes by T-DNA gene disruption and RNAi (*cp12-1/2/*3) has been shown to reduce PRK protein levels by more than 85% of the wild type levels but with no decrease in transcript levels (López-Calcagno *et al*, 2017). This was accompanied by a significantly lower assimilation rate (*A*) under light- and CO_2-saturated conditions (A_{max}) (López-Calcagno *et al.*, 2017). The decrease in assimilation rate was accompanied by a significant decrease in the maximum PSII operating efficiency (F_q'/F_m') and the dark adapted maximum quantum efficiency of PSII photochemistry (F_v/F_m) (López-Calcagno *et al.*, 2017). These results suggest that severe reductions/ lack of all three *CP12* genes reduced photosynthetic efficiency which resulted in increased damage to the photosystems. Association of the GAPDH/PRK/CP12 complex is dependent on light intensity, with the activities of GAPDH and PRK varying in response to dynamic light (Howard *et al.*, 2008).

Illumination of dark-adapted peas for increasing periods of time resulted in sequential decreases in the concentration of the GAPDH/PRK/CP12 complex, alongside increases in the PRK dimer and GAPDH tetramer (Howard *et al.*, 2008). Re-association of the protein complex was triggered by dark-adapting illuminated plants, and 30 minutes of darkness was sufficient to reverse light-induced dissociation. A rapid decline in PRK and GAPDH activity correlated with formation of the complex (Howard *et al.*, 2008). This response to dark-light transition indicates that the formation of the complex most likely plays a central role in plant responses to fluctuating light intensity, such as those experienced by plants in the field.

Dissociation of GAPDH/PRK/CP12 under high light is mediated by thioredoxins (Trxs), with Trx *f* and *m* mediating breakdown of GAPDH/PRK/CP12 (López-Calcagno, Howard and Raines, 2014) by reducing cysteine pairs in the CP12 protein (Marri *et al.*, 2009). One of the CP12 proteins, CP12-2, has been shown to be upregulated under fluctuating light conditions in *Arabidopsis thaliana*, in which 5 min pulses of 1000 µmol m^{-2} s^{-1} light were applied over a 12 hours period, compared to plants grown under 75 µmol m^{-2} s^{-1} (Schneide*r et al*, 2019). This upregulation in response to short pulses of high light followed by troughs of low light indicates that CP12 expression may be important in acclimating to fluctuating growth light regimes.

Thioredoxins (Trxs) act to regulate the CBB cycle at via redox reactions linked to photosynthetic electron transport. Electrons are passed from photosystem I to ferredoxin (Shin, Tagawa and Arnon, 1963) and then thioredoxins via ferredoxin-thioredoxin reductase, oxidising and so activating the thioredoxin (Buchanan, 1980).

These oxidised Trxs reduce redox-active cysteine residues in targets including fructose bisphosphatase (FBPase) and sedoheptulose-bisphosphatase (SBPase), (both key enzymes within the generation of Ribulose 1,5-bisphosphate (RuBP) phase of the CBB cycle), and Rubisco activase, which is required for the removal of sugar phosphates prior to the carbamylation of Rubisco (Nikkanen *et al*, 2017). Pathways closely linked to the CBB cycle, such as NADP-malate dehydrogenase (Ruelland and Miginiac-Maslow, 1999), which functions to detoxify reaction oxygen species, including hydrogen peroxide, under high light conditions (Heyno *et al.*, 2014) are also influence by the activity of the ferredoxin-thioredoxin system. Furthermore, depletion of Trx *m* in cyanobacteria significantly reduced the rate of oxygen evolution and maximum efficiency in the light , as well as reducing the amount of oxidisable P700 (Mallen-Ponce *et al.*, 2021). The *in vivo* redox state of bifunctional FBPase/SBPase showed an increase in oxidation in the *trxm* cyanobacteria, which negatively impact CBB cycle enzyme activity (Mallen-Ponce *et al.*, 2021). This demonstrates the important role Trxs have in the CBB cycle, ensuring enzyme activity can continue keep enzymes in the active state.

Thioredoxins themselves have also been implicated in the functional responses to fluctuating light environments. Under a high light period of a fluctuating regime, double knockdowns for Trx *m*1 and Trx *m*2 (*trxm1trxm2)* displayed a significant decrease in PSII operating efficiency compared to the wild type, but in the low light periods PSII and PSI quantum efficiencies were significantly higher (Thormählen *et al.*, 2017), indicating thioredoxins impact on photosynthetic efficiency under light transitions, and so may have significant impacts in the field under a dynamic light environment. Redox regulation of NADP-malate dehydrogenase (MDH) has also

been implicated in the fluctuating light response. The impact of fluctuating light, where light was changed every 30 minutes between 60 µmol m^{-2} s^{-1} and 650 µmol m^{-2} s^{-1}, on *Arabidopsis* mutants for MDH was explored (Yokochi *et al.*, 2021) . A severe reduction in growth was noted under fluctuating light, accompanied by a significant reduction in the maximum quantum efficiency of PSII (F_v/F_m) compared to the wild type (Yokochi *et al.*, 2021), indicating the importance of redox regulation under fluctuating conditions.

Fluctuating light acclimation has previously been shown to reduce photosynthetic capacity and PSII operating efficiency in comparison to square light acclimated plants (Vialet-Chabrand *et al.*, 2017). Furthermore, data in Chapter 3 showed significant reductions in F_v/F_m under fluctuating light (Figure **3.7**), as well as a reduced growth rate (Figure **3.3**), compared to plants grown in square wave light regimes. Combined with the evidence above, this provides an argument that thioredoxins and redox regulation may have a role in acclimation to fluctuating light.

The aim of this chapter was to investigate the possible impacts of thioredoxins on photosynthetic acclimation to dynamic light regimes. In order to achieve this *cp12-1/2/3* mutants, described by López-Calcagno *et al* (2017), were utilised. CP12 has been shown to regulate activation and deactivation of CBB enzymes in response to changing light, and itself is reduced by Trxs in light, allowing for the impact of light on plant redox state to be studied. The *cp12-1/2/3* mutants were subjected to growth under square and fluctuating light regimes (SQL and FLL), with photosynthetic efficiency and assimilation measured to better understand the regulation of photosynthesis under fluctuating light.

5.2. Materials and Methods

5.2.1. Plant Material and Growth Conditions

Arabidopsis thaliana cp12-1/2/3 mutants, *RNAi3.1* and *RNAi3.3*, alongside their wild type, (López-Calcagn*o et al*, 2017; Kindly gifted by Dr Patricia E López-Calcagno) were germinated in 5 cm^2 pots on a peat-based compost (Levingtons F2S, Everris, Ipswich, UK), and placed in a controlled growth environment at 22°C, 65% relative humidity, 8/16h light/dark cycle, light at 220 µmol m^{-2} s^{-1}, CO_2 concentration 400 µmol mol^{-1}. At 14-days, the seedlings were transplanted to individual 5cm^3 pots containing the same soil as above and returned to the controlled environment.

5.2.2. Fluctuating Light Plant Material and Growth

A. thaliana at the 8-leaf stage were removed from the controlled environment and placed under Heliospectra LED light source (Heliospectra, Göteborg, Sweden) programmed to each light regime (Figure **5.2**) in a dark room maintained at 21°C/16°C Day/night, 50% relative humidity. Average light intensity for light conditions was 230 µmol m^{-2} s^{-1} (see methods chapter for full details) on a 12h/12h day/night cycle. Plants were kept in well-watered conditions, with their position under the light source randomised every 3 days to remove any potential heterogeneity in spectral quantity and quality.

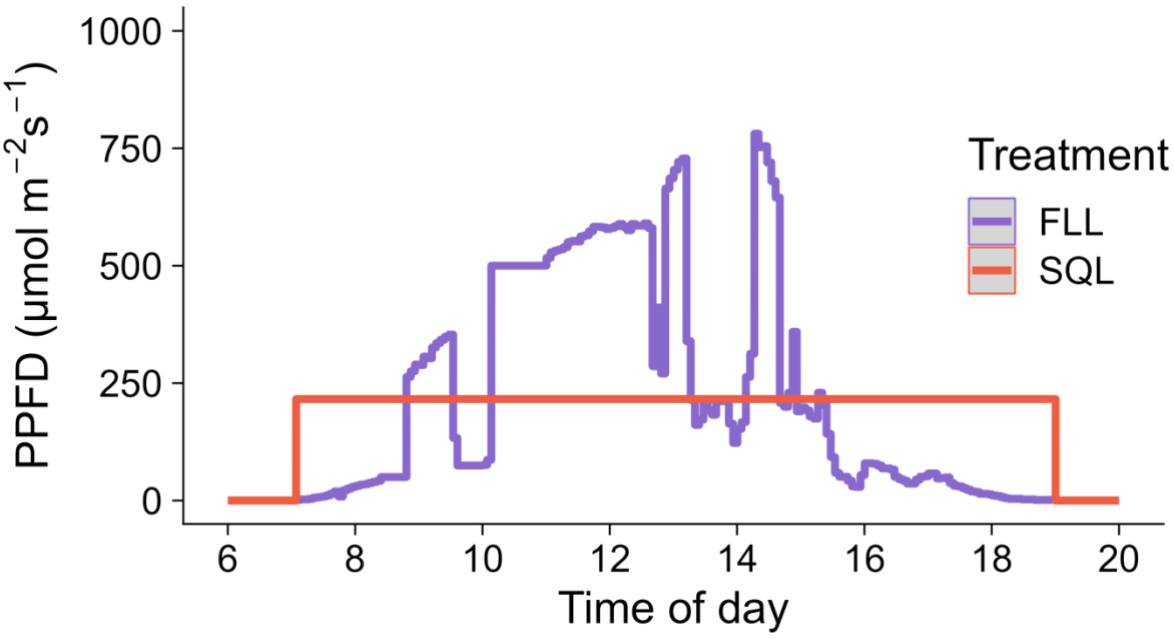

Figure 5.2: Diurnal light regimes utilised in this study. Area of the curves are equal, demonstrating the same average amount of light energy over a 12-hour period. Square light (SQL) represents a light intensity of 230 µmol m^{-2} s^{-1}, with FLL resulting in the same amount of light applied over the diurnal period.

5.2.3. Leaf Gas Exchange

All leaf gas exchange was carried out according to the methods described in Chapter 2, Section 2.3.2.

5.2.4. Chlorophyll fluorescence imaging

Four plants, including at least one wild type, were measured at a time (between 8am and 4pm). Protocols for induction-relaxation and light responses were conducted as described in Chapter 2 Section 2.3.1

For NPQ induction-relaxation, plants were first dark adapted for 30 minutes prior to minimal fluorescence (F_o) being measured with a weak pulse. The maximal fluorescence (F_m) was then measured with an 800 ms exposure to a saturating pulse

(6231 µmol m^{-2} s^{-1}). Plants were then exposed to an actinic light of 800 µmol m^{-2} s^{-1}, and F_q'/F_m' measured at 10 min intervals by applying a saturating pulse. The actinic light was then reduced to 1 µmol m^{-2} s^{-1}, and a saturating pulse applied every minute for 30 minutes to obtain PSII relaxation kinetics.

Plants were allowed to recover for 24 hours, and then subjected to a fluctuating light protocol, where 5 cycles of high light-low light were applied. Plants were first dark adapted for 30 minutes prior to imaging, with F_o and F_m obtained as above. The full protocol is described in Table ***5.1***.

Table 5.1: Protocol for chlorophyll fluorescence imaging with successive step changes. In orange is the section repeated where the light intensity goes up and down, green shows a final relaxation step.

delay	step	repeat	PPFD	
5"	change actinic		0	
20"	Pulse	1		
5"	change actinic		1500	Repeat 5 times
1'	Pulse	3		
5"	change actinic		200	
1'	Pulse	3		
5"	change actinic		0	
1'	Pulse	10		

5.2.5. cp12-1/2/3 RNA extraction and qPCR

The extraction of RNA and subsequent quantification were performed according to the methods in Chapter 2, Section 2.6. For qPCR primer sequences see Table ***5.2***. Cyclophilin, Elongation Factor, and Actin2 were used as internal standards.

Table 5.2: Forward and reverse primer sequences utilised in qPCR of CP12

Gene	**Forward primer**	**Reverse Primer**
CP12-1	GAAGCGGATGGTTGTGGTT	CTCTTCTCCACCTTCTCCGATA
CP12-2	TTCACAGGCTGCCGTGTACC	GACGAAGACACGCTGGGTTG
CP12-3	AGCCTGATGATGGTGACGAAGG	TCGCAAACCTCCTGTCGCTTCC
Cyclophilin	TCTTCCTCTTCGGAGCCATA	AAGCTGGGAATGATTCGATG
Elongation Factor	AGATCAACGAGCCCAAGA	CCGTTCCAATACCACCAAT
Actin2	ACCTTGCTGGACGGACCTTACTGAT	GTTGTCTCGTGGATTCCAGCAGCTT
PRK	CATCGTGATCGGGACTAGCTG	TGAGCCTCCGCATAAAGGTA
GAP-A	GAAGGTGCAGGGAAACACAT	TTTGCCTGGAGCAGTAATGA
GAP-B	TCGAGGGAACAGGAGTGTT	CTCCGGCTTGGATATGCTT
Trx *f*1	ATCTGGTTGCAGCGATTGA	AGACATGAGAGACTGGTTCATCC
Trx *m*1	TGTGAAGCTCAGGACACTGC	GCCCAAAAGTCGACAAACAC
Trx *m*2	GCTCCGAGACCAGAATCGTA	GAACATCCGCCGAGAAGAG

5.2.6. Statistics

Statistical analysis was performed using open-source software R (R Core Team, Vienna Austria 2019, version 3.6.0 for Windows), utilising R Studio (version 1.2.5033). A two-way ANOVA was used to test for two factor differences, and Tukey post-hoc testing was performed where significant differences were observed.

5.3. Results

5.3.1. RT-qPCR confirms knockout or severe knockdown of all three CP12 genes

To confirm reduced expression in all three CP12 genes in all the growth light regimes RT-qPCR was performed with primers for each of the three genes (see Table ***5.2***). Both *cp12-1/2/*3 lines were confirmed to have significantly (*p*<0.005*)* reduced expression of all CP12 proteins in all light regimes (Figure 5.3A+B) relative to their respective wild type.

To determine whether *cp12-1/2/3* has affected the expression of interacting proteins, qPCR was also performed on the two subunits (GAPA, GAPB) of GAPDH and PRK, two photosynthetic enzymes known to interact in complex with CP12 (Wedel, Soll and Paap, 1997), alongside three thioredoxins, Trx *f*1, Trx *m*1, and Trx *m*2, which are known to activate PRK (Marr*i et al*, 2009). Relative to the wild type, no signifcant changes in expression of GAPA, GAPB, or PRK were noted in SQL samples (Figure 5.3A; p>0.1). Significant upregulation of Trx f1 was observed in SQL-3.1 (p<0.05) but not SQL-3.3 (p>0.1). There was no signficant changes in Trx m1 or m2 (p>0.1),. Under fluctuating conditions (Figure 5.3B), FLL-3.1 shows a signficant decrease in GAPA and GAPB expression (p<0.05) However, no decreases were observed in FLL-3.3 (*p>0.1*). The expression of all three thioredoxin genes were significantly downregulated in FLL-3.1 (*p<0.05),* but not in FLL-3.3 (*p>0.05*). In summary, the lines selected have the expected reductions in expression of the CP12 genes.

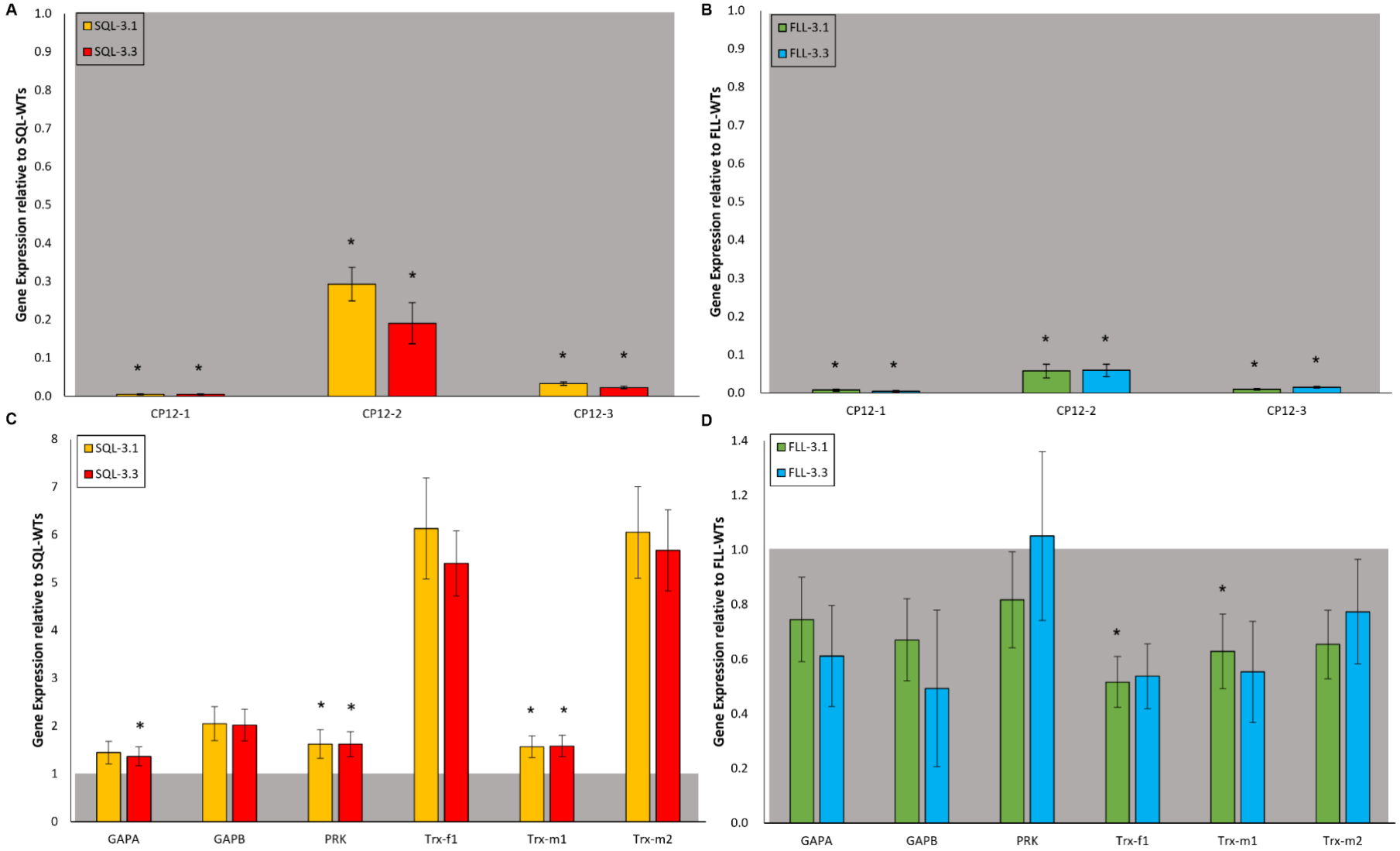

Figure 5.3: qRT-PCR analysis of cp12-1/2/3 lines and associated genes to determine knockdown status and the effect of light regime relative to the respective wild type. **A**) shows significant decrease in the expression of all three CP12 genes in plants acclimated to square light ($p<0.005$), while there were no significant changes to GAPA, GAPB, and PRK ($p>0.1$). SQH-3.1 showed a significant increase in Trx f1 ($p<0.05$) which is not seen in SQL-3.3 ($p>0.1$). Similar is seen under fluctuating conditions (**B**), with significant decrease in all CP12 genes ($P<0.0005$), while line FLL-3.1 shows significant decreases in the expression of GAPA, GAPB, and all three Trx genes ($p<0.05$), which is not reflected in FLL-3.3 ($p>0.05$). Grey boxes show wild type expression level. Bars shows the mean±SE (n=3-4). Actin2, the elongation factor gene (EF), and Cyclophilin were used as internal standards.

5.3.2. Chlorophyll fluorescence imaging suggest lack of CP12 affects acclimation to fluctuating light

To assess the impact of reduced expression of *cp12-1/2/3* on photosynthetic acclimation to square and fluctuating light regimes two independent knockdown lines, *RNAi3.1* and *RNAi3.3*, were grown under square (SQ) and fluctuating (FL) light of equal photon dose, along with wild type lines (WTs). These lines are hereby referred to as SQL-3.1 and FLL-3.1 for line *RNAi3.1* exposed to square and fluctuating light respectively, and SQL-3.3 and FLL-3.3 for line *RNAi3.3*.

The impact on photosynthetic efficiency throughout the acclimation period was investigated utilising chlorophyll fluorescence imaging of the maximum PSII efficiency (*F_v'/F_m';* Figure 5.5A-C*)*, PSII operating efficiency (*F_q'/F_m';* Figure 5.6A-C*)* and photochemical quenching (*F_q'/F_v';* Figure 5.6D-F).

Induction and relaxation of photosynthesis revealed significant effects of CP12 knockdown. During light induction (Figure 5.4), *F_q'/F_m'* was significantly lower in *cp12-1/2/3* plants compared with wild types (*$p<0.05$*),while a signficantly higher value was observed between SQL-WTs and FLL-WTs ($p<0.05$). However, relaxation of NPQ (measured as *F_v/F_m)* resulted in no significant differences between the *cp12-1/2/3* linesregardless of regime *($p>0.05$),* and wild types again exhibited a signifcantly higher *F_v/F_m* than all *cp12-1/2/3* lines($p<0.05$).

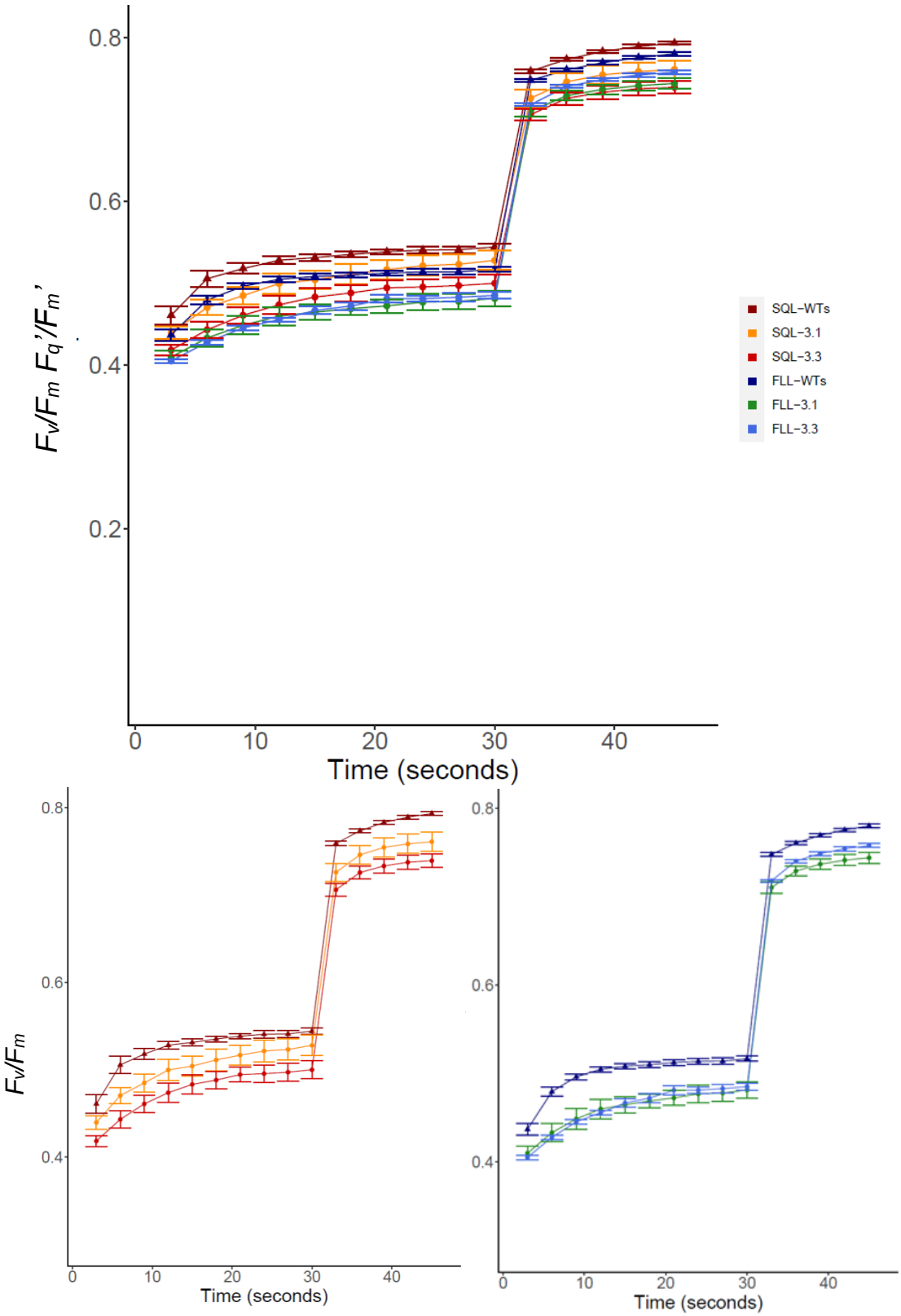

Figure 5.4: Chlorophyll fluorescence imaging of photosynthetic induction (*F_q'/F_m'*) and relaxation (*Fv/Fm)* in CP12 *RNAi* knockdown *A. thaliana*. **A** shows all lines, demonstrating the WT lines (SQL-WTs, FLL-WTs) have significantly higher values at induction (*F_q'/F_m'*) and relaxation (*F_v/F_m*) compared to their *RNAi* counterparts. Data for the square regime (SQL; **B**) shows the wild type lines to be significantly higher than both *RNAi* lines, while a difference is also seen between the SQL-3.1 and SQL-3.3 lines, suggesting one line may have a more severe phenotype. However, fluctuating data, **C**, shows no significant difference between *RNAi* lines, with the wild type exhibiting significantly higher PSII efficiency (*$p<0.05$*). Data shows the mean ±SE (*n=4-6*)

The efficiency of photosystem II (PSII) was affected by both regime and *cp12-1/2/3* under changing light. The overall efficiency of photosystem II (F_q'/F_m', Figure 5.5A-C) was signifcantly different between SQL and FLL grown wild types as expected, with the SQL-WT plants exhibiting a significantly higher efficiency at all light levels ($p<0.04$) except 1500 µmol m^{-2} s^{-1}. Both CP12 knockdown mutant 3.1 and 3.3 had reduced efficiency under both SQL and FLL conditions. (Figure 5.5A). FLL-3.1 showing significant decreases (Figure 5.5C) compared to FLL-WT ($p<0.04$) across all light intensities , while FLL-3.3 displayed significant decrease only at 1250 µmol m^{-2} s^{-1} and 1000 µmol m^{-2} s^{-1} ($p<0.01$), indicating FLL-3.1 may have the more severe phenotype. Under SQL conditions (Figure 5.5B), signficant decreases were only seen at 1000 µmol m^{-2} s^{-1} for SQL-3.1 ($p<0.002$) compared to the wild type. However, a signficant decrease in F_q'/F_m' in SQL-3.3 compared with wild type was noted at all light levels ($p<0.003$), again suggesting differing effects of *cp12-1/2/3* in the two lines.

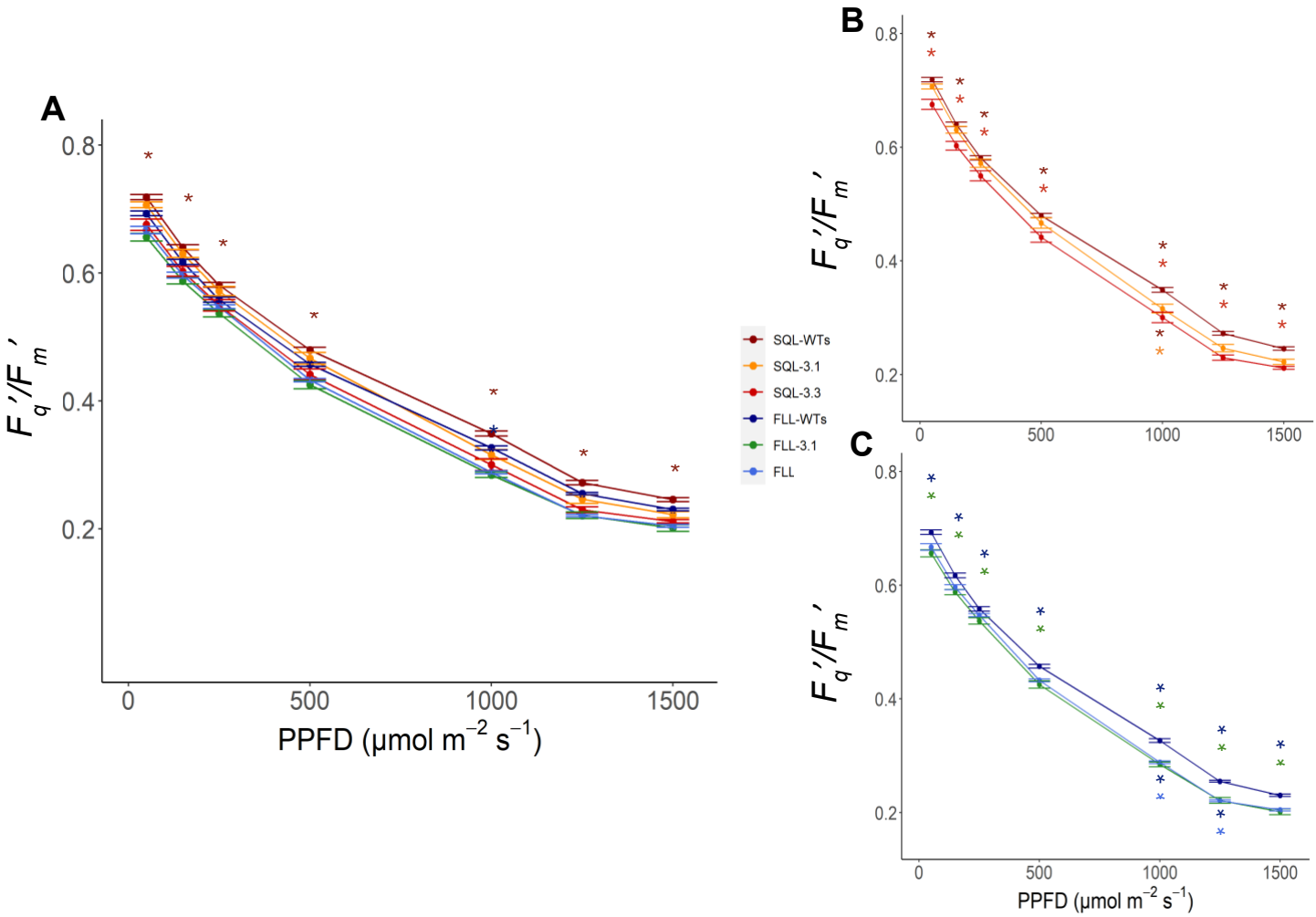

Figure 5.5: Chlorophyll fluorescence imaging of light response curve at day 7 of exposure to square (SQL) or fluctuating (FLL) light in cp12-1/2/3 knockdown lines RNAi3.1 (SQL-3.1 and FLL-3.1) and RNAi3.3 (SQL-3.3 and FLL3.3), and the wild type line (SQL-WTs and FLL-WTs). There were significant differences between plants exposed to SQL and FLL light, with the wild types having significantly higher F_q'/F_m' (**A-C**) than their cp12-1/2/3 counterparts ($p<0.05$) between light levels of 250 and 1250 µmol m^{-2} s^{-1}. There was no significant difference between cp12-1/2/3 lines within each treatment ($p>0.1$). Groups of stars show where there is a significant difference between the indicated lines. Data points show the mean ±SE (n=4-6)

When F_q'/F_m' was broken down into the maximum PSII efficiency (F_v'/F_m', Figure 5.6A-C) and photochemical quenching (F_q'/F_v'; Figure 5.6D-F), the consequences of dynamic light and CP12 knockdown can be further explored. A signficant reduction in F_v'/F_m' cmpared with wild type was observed for all knockdown lines and light treatments between 150 µmol m^{-2} s^{-1} and 1250 µmol m^{-2} s^{-1} ($p<0.01$) except SQL-3.1 which showned no signficant difference at 150 µmol m^{-2} s^{-1}($p<0.01$). Interestingly, there was a signficant increase in F_q'/F_v' in all *cp12-1/2/3* lines ($p<0.02$), at a single light intensity, 500 µmol m^{-2} s^{-1}, compared with wild type.

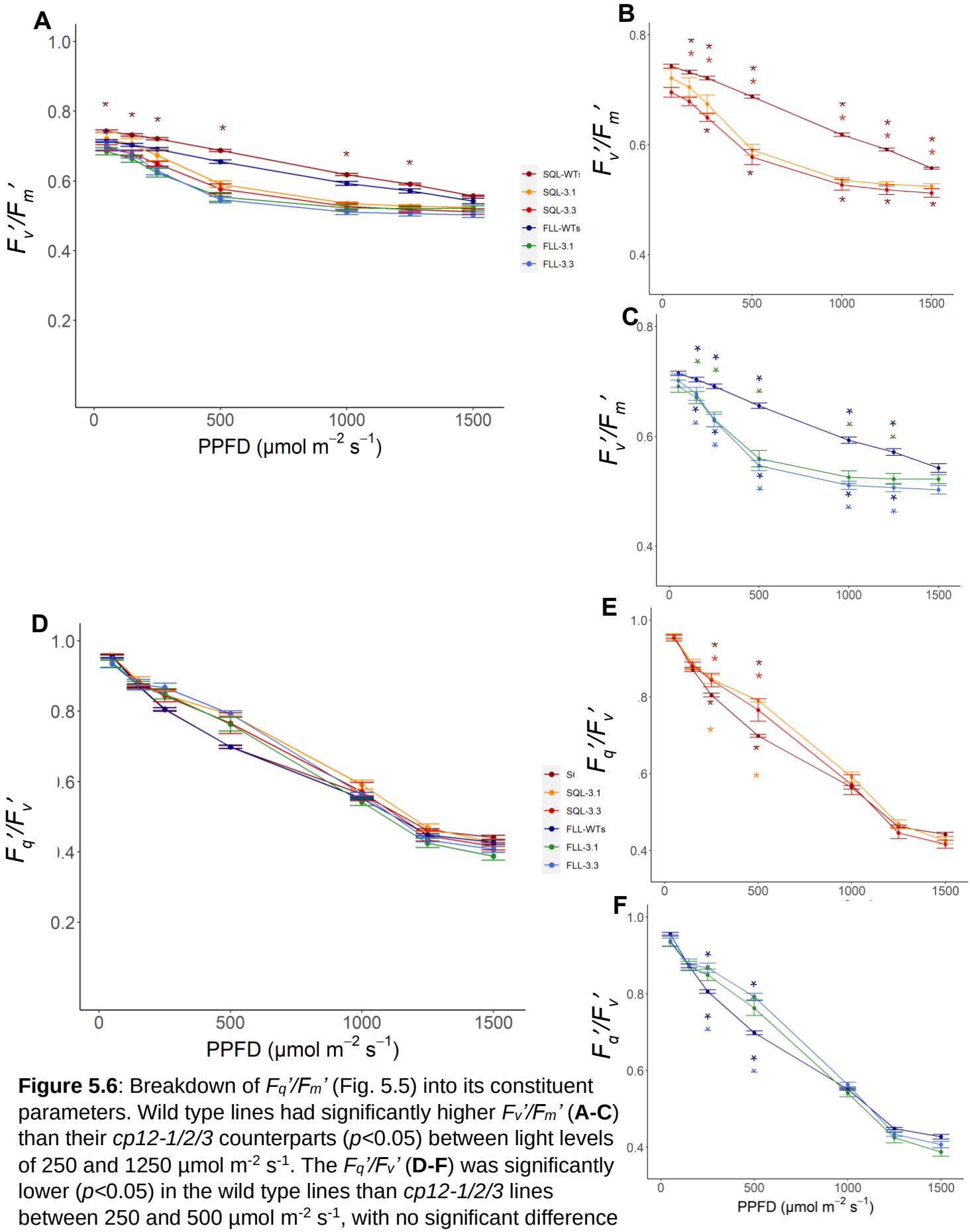

Figure 5.6: Breakdown of F_q'/F_m' (Fig. 5.5) into its constituent parameters. Wild type lines had significantly higher F_v'/F_m' (**A-C**) than their *cp12-1/2/3* counterparts (p<0.05) between light levels of 250 and 1250 µmol m^{-2} s^{-1}. The F_q'/F_v' (**D-F**) was significantly lower (p<0.05) in the wild type lines than *cp12-1/2/3* lines between 250 and 500 µmol m^{-2} s^{-1}, with no significant difference across other points. There was no significant difference between *cp12-1/2/3* lines within each treatment (p>0.1). Groups of stars show where there is a significant (p<0.05) difference between the indicated lines. Data points show the mean ±SE (n=4-6)

5.3.3. CP12 knockdown results in high levels of energy dissipation via NPQ

To determine whether the differences seen in photosystem II efficiency were due to non-photochemical quenching (NPQ), further chlorophyll fluorescence imaging was performed. Induction and relaxation of NPQ (Figure 5.7) shows that reduced expression of CP12-1, 2 and 3 resulted in an increase in the accumulation of NPQ. Under both square (Figure 5.7B) and fluctuating (Figure 5.7C), the magnitude build-up of NPQ was significantly higher in CP12 knockdown plants than in the wild type after 3 minutes under FLL ($p<0.01$) and 4 minutes under SQL ($p<0.001$), with no significant difference between lines 3.1 and 3.3 ($p>0.5$). Comparison between square and fluctuating light acclimated plants (Figure 5.7A) revealed there was no significant difference between the wild types during the induction or relaxation ($p=1$), indicating regime is not significantly impacting NPQ. There was also no significant difference (p=1) between the *cp12-1/2/3* lines independent of light regime.

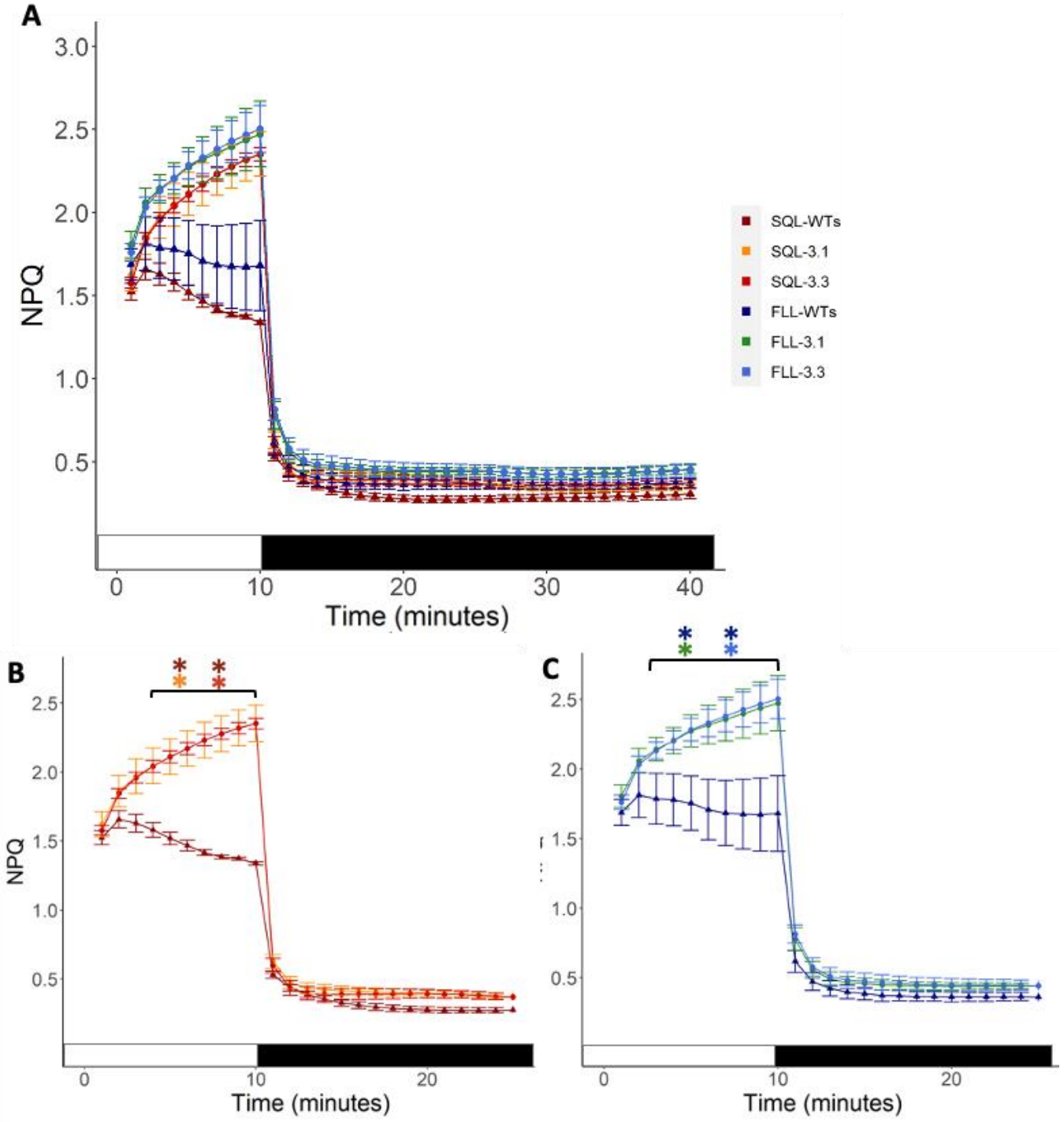

Figure 5.7: Induction and relaxation of non-photochemical quenching (NPQ) in *cp12-1/2/3* mutant lines 3.1 and 3.3, and the wild type after exposure to square (SQL) and fluctuating (FL) light. After 2 minutes, NPQ was significantly lower (*p<0.04)* in the wild types compared to mutant lines (A) regardless of growth light regime, indicating CP12 knockdown is affecting the shuttling of light energy to photochemistry, resulting in the build-up of NPQ. During the relaxation, NPQ remained higher in CP12 mutant plants than their wild type, indicating a higher base level of NPQ, although not significant (*p=1*). Acclimation of CP12 knockdowns to fluctuating light (FLL-3.1, FLL-3.3; C) resulted in higher levels of NPQ that those acclimated to square light (SQL-3.1, SQL-3.3; B), suggesting CP12 may have a role under fluctuating light conditions upon increasing light *(p<0.04*).). Bars at the bottom represent when the plant is exposed to light (white; 800 µmol m^{-2} s^{-1}) or darkness (black). Groups of stars show where there is a significant (*p<0.05*) difference between the indicated lines. Data shows the mean±SE (*n=4-6*)

To determine the effect of changing light on NPQ, chlorophyll fluorescence imaging was performed with quick light changes between 1000 µmol m^{-2} s^{-1} and 200 µmol m^{-2} s^{-1} (Figure 5.8). These repeat cycles of high and low light allowed for the build-up and relaxation of NPQ to be observed under fluctuating light. Wild type plants showed significantly lower levels of NPQ ($p<0.01$) than CP12 knockdown lines (Figure 5.8B & C). Interestingly, FLL-WTs showed a significantly higher level ($p<0.01$) of NPQ than SQL-WTs (Figure 5.8A), suggesting that, despite acclimation to changing light, this does not equate to an increased ability to cope with excess light energy via NPQ (Figure 5.7 & Figure 5.8). Under the lower light intensity (200 µmol m^{-2} s^{-1}; Figure 5.8), levels of NPQ in FLL-WTs were not significantly different ($p=1$) from that of SQL-3.1 and SQL-3.3. Under fluctuating light, both CP12 knockdown lines show a significantly higher level of NPQ ($p<0.03$) than all other lines (Figure 5.8C), suggesting CP12 plays an important role in energy dissipation for plants acclimated to fluctuating light. However, the magnitude of difference between the SQL-WTs and the SQL CP12 mutants (Figure 5.8B), and FLL-WTs and the FLL CP12 mutants (Figure 5.8C) is similar, suggesting it is the growth light regime responsible for differences in NPQ.

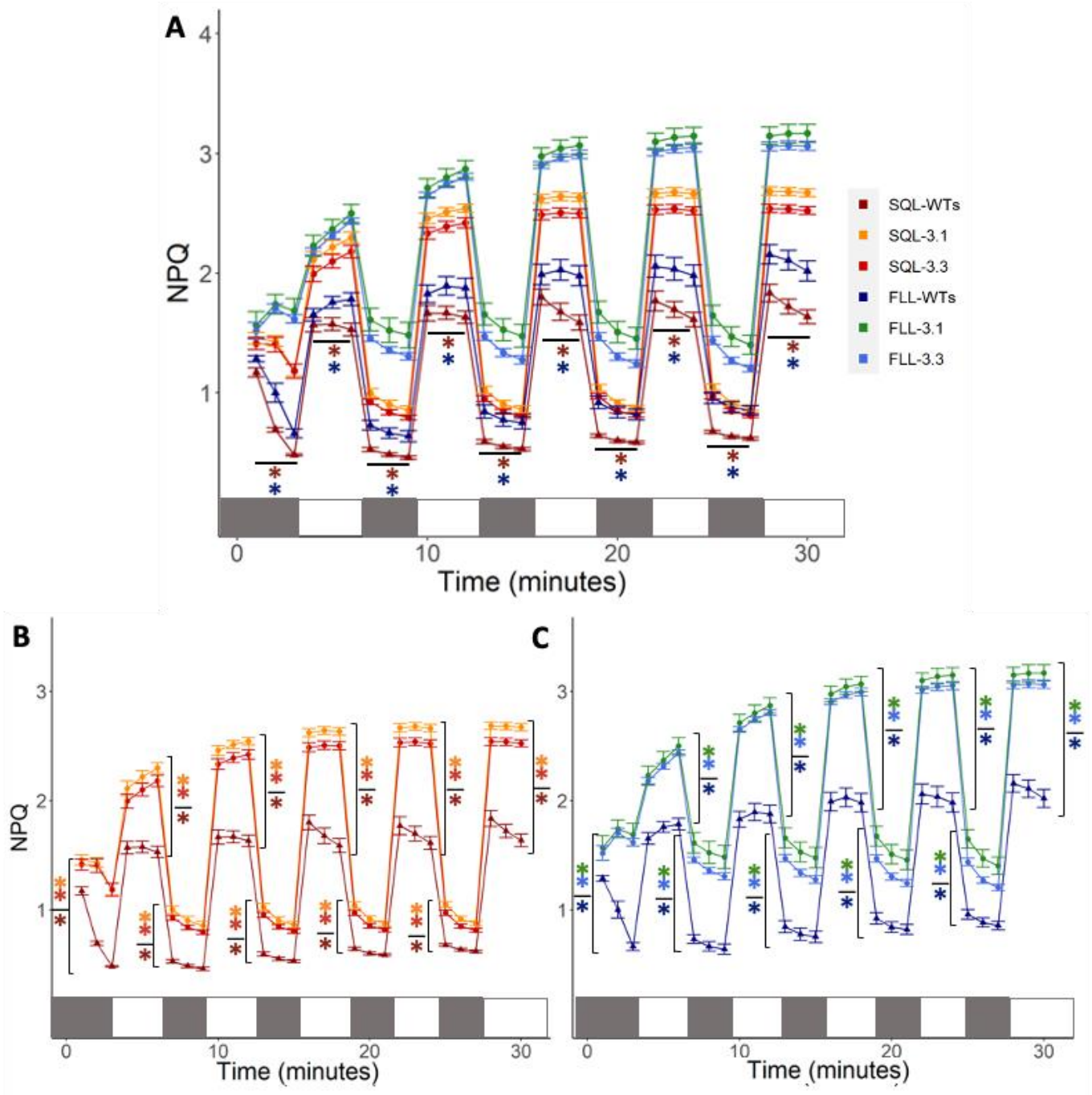

Figure 5.8: The effect of fluctuations in light from 200 µmol m^{-2} $s^{-1}$to 1000 µmol m^{-2} s^{-1} on NPQ of *cp12-1/2/3* knockdown and wild type lines acclimated to square (SQL-3.1, SQL-3.3, SQL-WTs) and fluctuating (FLL-3.1, FLL-3.3, FLL-WTs) light. Under fluctuating light, CP12 knockdown significantly (*p<0.03*) increased NPQ compared to all other lines (A), while FLL-WTs showed no significant difference from the SQL knockdown lines under lower light conditions (*p=1)*. Under both light regimes, the wild type lines showed significantly lower (*p<0.01)* NPQ than that of the *cp12-1/2/3* (**B**; SQL, **C**; FLL), indicating that CP12 knockdown is resulting in increased NPQ regardless of growth light regime. Bars represent when the plants are exposed to low light (grey; 200 µmol m^{-2} s^{-1}) or high light (white; 1000 µmol m^{-2} s^{-1}). Stars show where there is a significant difference (*p<0.*05), groups divided by a line demonstrate a significant difference between the groups. Data shows the mean±SE (*n=4-6*)

5.3.4. Infrared gas exchange shows significant differences in carbon assimilation in CP12 knockdowns and those acclimated to fluctuating light

The impact of CP12 knockdown on photosynthetic capacity in plants acclimated to square and fluctuating light was assessed using A/C_i analysis (Figure **5.9**). FLL-WTs showed a reduction in assimilation compared to SQL-WTs, reflecting previous work in Chapter 3. Both *RNAi3.1* and *RNAi3.3* lines have a lower A_{max} than the wild type lines (Figure **5.9**A). Within the *RNAi* lines, those acclimated to FL show the lowest A_{max} values, with FLL-3.1 displaying the lowest of all plants, and this was exacerbated by acclimation to fluctuating light. Assessment of the maximum rate of carboxylation of Rubisco (Vc_{max}; Figure **5.9**B) showed that reduced expression of all CP12 proteins significantly reduced the rate of carboxylation ($p<0.05$) compared to their wild type controls, while FL-exposed CP12 plants had lower values than those exposed to SQ light. Similarly, the maximum electron transport rate for RuBP regeneration (J_{max}; Figure **5.9**C) was lower for all CP12 lines compared to the wild types, with FLL-3.1 showing the lowest rates.

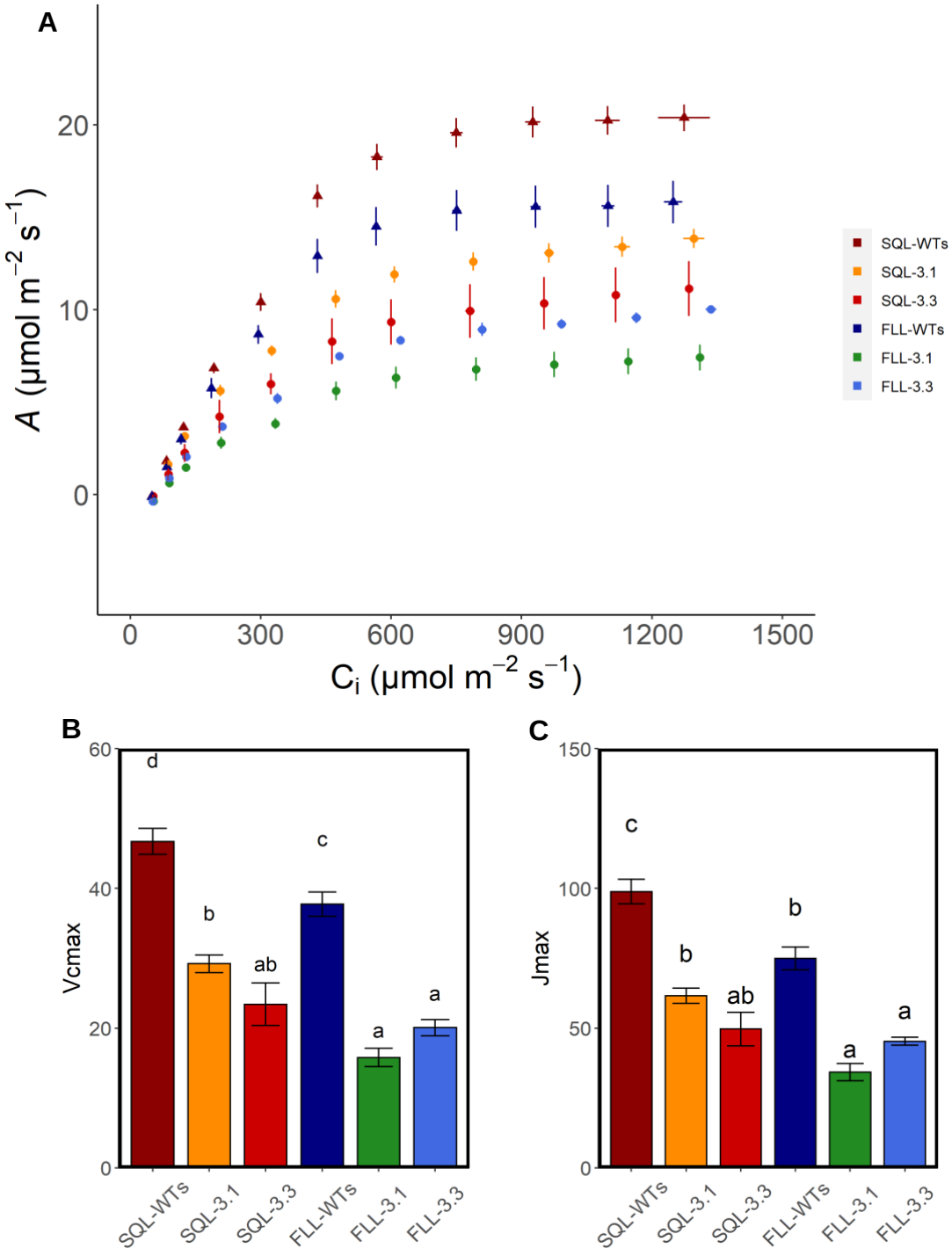

Figure 5.9: Photosynthesis as a function of internal CO_2 concentration (C_i) of wild type and *cp12-1/2/3* RNAi mutants acclimated to square (SQL) and fluctuating light (FLL). The A/C_i curves (**A**) reveal lower assimilation rates in RNAi lines than their corresponding wild type, with those acclimated to FLL displaying a lower assimilation than SQL acclimated plants. Photosynthetic parameters V_{Cmax} (**B**) and J_{max} (**C**) were estimated from **A**, with significant difference between the azygous lines ($p<0.05$), while significantly lower values for *RNAi* lines were noted compared to their corresponding wild type ($p<0.05$). Data shows the mean±SE ($n=5$), letters above bars show results of posthoc Tukey testing.

To assess the impact of CP12 knockdown on assimilation in plants acclimated to different light regimes, light response curves (*A/Q*; Figure 5.10A-C) were utilised. Wild type lines show a significantly higher assimilation rate than all RNAi lines (*p<0.02*), bar SQL-3.1 (*p>0.9*), between 700 and 1500 µmol m^{-2} s^{-1} demonstrating the lower assimilation rates resulting from both RNAi knockdown and their acclimation to fluctuating light. At higher PPFD values, SQL-3.3, FLL-3.1, and FLL-3.3 lines have a signficantly lower assimilation rates than both wild type lines (*p<0.05*), with SQL *cp12-1/2/3* lines having a signifcantly higher assimilation rate than the FLL *cp12-1/2/3* lines (*p<0.05*). At lower PPFDs, there was no signifcant difference between any lines (*p<0.1*), suggesting the effects of CP12 knockdown and light acclimation have a greater impact at higher light levels.

Stomatal coductance (*gs;* Figure 5.10D-F) was also measured as part of the light response curves and revealed that under SQL (Figure 5.10E), line 3.1 showed no signficant difference from the wild type (*p>0.9*), while line 3.3 showed a signifcantly lower conductance. However, under FLL, stomatal conductance in both *cp12-1/2/3* lines was signifcantly lower than the wild type (*p<0.05*), with no significant difference between 3.1 and 3.3 (*p>0.8*).

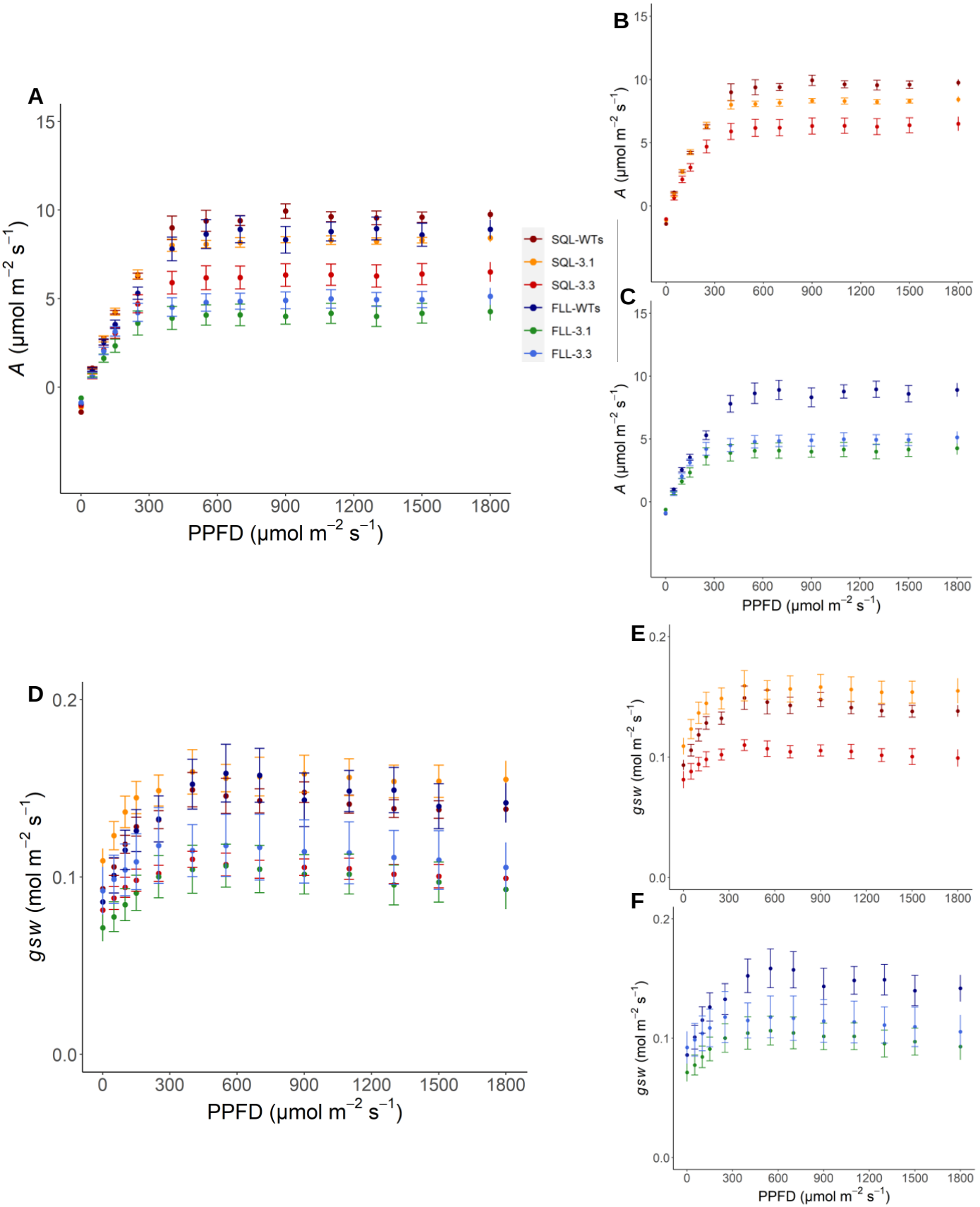

Figure 5.10: Photosynthesis as a function of light (PPFD) of azygous and *cp12-1/2/3* mutants acclimated to square and fluctuating light. The *A/Q* curves (**A**) reveal lower assimilation rates in acclimated to fluctuating light, and RNAi lines exhibiting lower values than their wild type. There was no significant difference between the wild type lines *(p>0.1*). The stomatal conductance (*gsw,* **D-F**) revealed that SQL-3.1 had a similar conductance to the wild type (**E**), which could account for the higher assimilation rate observed. Generally, *RNAi* lines had a lower stomatal conductance than their wild type. Data shows the mean±SE (*n=5*)

Under fluctuating light, the light saturated rate of photosynthesis ($A_{sat;}$ Figure 5.11A) was signficantly higher ($p<0.05$) in the wild type than in both FLL-3.1 and FLL-3.3, with no signficant difference between the two *cp12-1/2/3* lines. Under SQL, there was no signifcant difference across lines ($p>0.06$). There was no signficant difference between the SQL-WTs and FLL-WTs ($p>0.4$) and no signficant difference between the *cp12-1/2/3* lines acclimated to SQL and FLL ($p>0.9$). No signficant differences ($p>0.1$) were observed in any comparisons of electron transport rate (Figure 5.11B), although in all *cp12-1/2/3* lines the data displays a wide spread demonstrating heterogeneity in responses. Similarly, the compensation point (Figure 5.11C) , which shows the light intensity where photosynthesis is equal to photorespiration, was not signficantly different ($p>0.1$) within, or between, the light intensity groups.

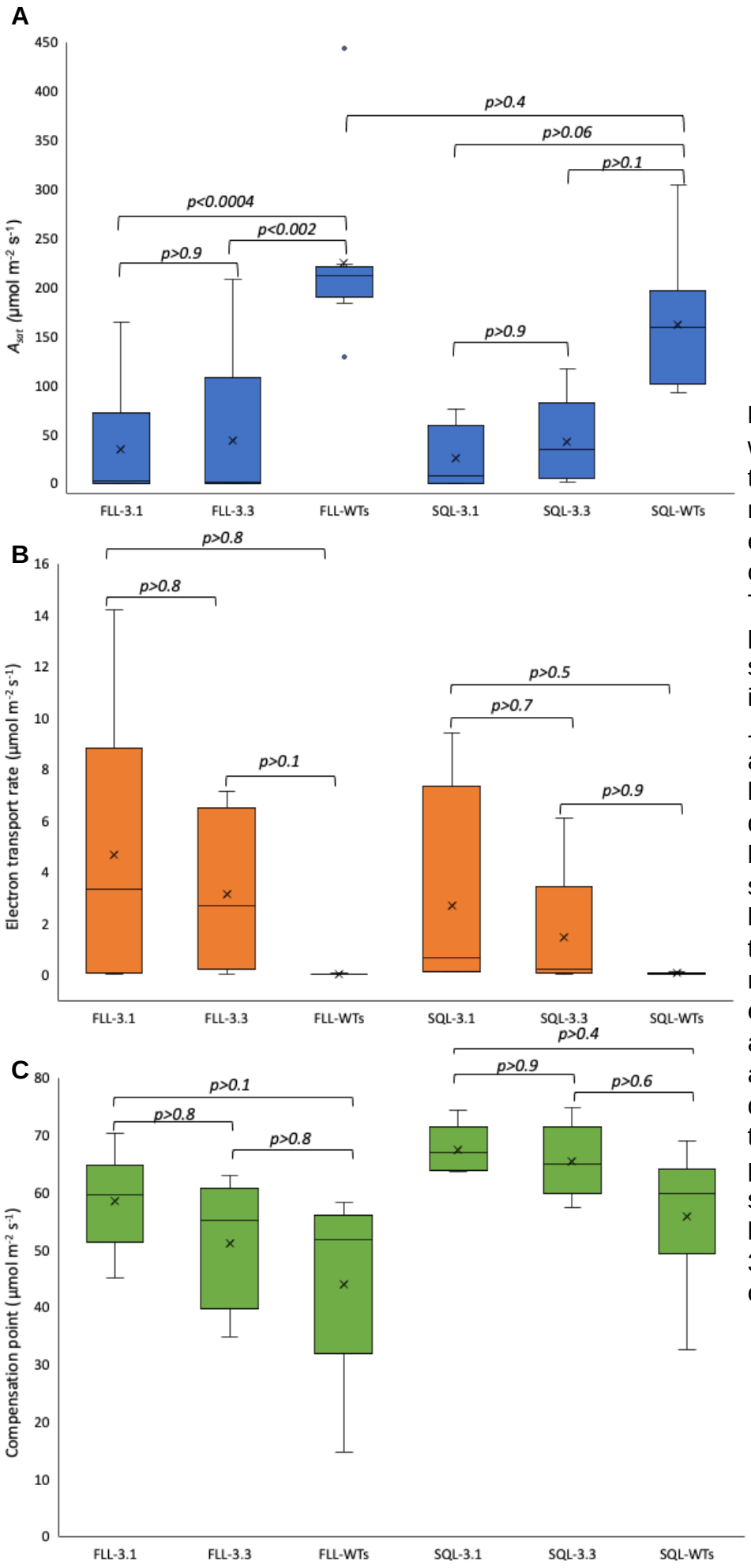

Figure 5.11: Box and whisker plots of showing the variation across replicates of parameters extracted from the *A/Q* curves seen in Figure 5.9. The light saturated rate of photosynthesis (A_{sat}, **A**) is significantly higher (*p<0.05*) in FLL-WTs than both *cp12-1/2/3* lines, 3.1 and 3.3 acclimated to fluctuating light, with no significant difference between the two lines (*p>0.9*). There was no significant difference between all lines acclimated to SQL (*p<0.06*). There was no significant difference in electron transport rate (**B**) across all lines (*p>0.1*), but all *cp12-1/2/3* lines displayed a large spread in the data. The compensation point (**C**) was also not significantly different between the WTs and lines 3.1 and 3.3. Dots show outlying data (*n=4-6).*

5.4. Discussion

Lines with severe knockdown or knockout of all 3 CP12 genes were used to evaluate how thioredoxin regulation of the CBB cycle could be impacted by fluctuating light. Previous work has demonstrated that acclimation to fluctuating light significantly reduced carbon assimilation as well as displaying increased levels of NPQ, compared to their square light counterparts (Vialet-Chabran*d et al*, 2017; Matthews, Vialet-Chabrand and Lawson, 2018). This, combined with knowledge that CP12 is both regulated by thioredoxins and has a role in regulating dark-light transition, led to the exploration of photosynthetic performance using of independent knockdown lines of CP12 acclimated to square and fluctuating light regimes. The results here suggest a role for CP12 in the acclimation to fluctuating light, with *cp12-1/2/3* knockouts negatively affected across all physiological parameters assessed.

Measurements of photosystem II efficiency presented here (Figure 5.4 & Figure 5.5) support the findings of López-Calcagn*o et al* (2017), who noted significant decreases in maximum PSII operating efficiency (F_q'/F_m') and the dark-adapted maximum quantum efficiency of PSII photochemistry (F_v/F_m) in *cp12-1/2/3* plants compared to the wild type. The data here are similar, with all knockdown lines showing a decreased F_v/F_m and F_q'/F_m' compared to the wild type lines after acclimation.

The reduced photosynthetic capacity in all *cp12-1/2/3* lines (Figure **5.9**B&C) could be due to the inability to regulate formation of the CP12/PRK/GAPDH complex. In plant model species *Nicotiana tabacum*, antisense repression CP12 reduced the activity of PRK and GAPDH, however, there was no significant effect on carbon fixation (Howard *et al.*, 2011). This suggests the effect of CP12 knockdown may differ between species and so may have different roles in CBB cycle regulation. It is

difficult to know the exact effect of CP12 knockdown on the CP12/PRK/GAPDH formation in *Arabidopsis*, as the complex has yet to be detected *in vivo* in both wild type and transgenic lines (Howard, Lloyd and Raines, 2011; López-Calcagno *et al.*, 2017). Due to this, it could be that the complex does not form in *Arabidopsis* as in other higher species and so CP12 could be playing other roles, e.g., in signalling.

Reduced carbon assimilation may also be linked to reduced levels of PRK. López-Calcagn*o et al* (2017) found that *cp12-1/2/3* knockdown *Arabidopsis*, the same as utilised here, had significantly reduced levels of PRK protein levels. Large reductions in PRK have previously been linked to decreases in CO_2 assimilation (Pau*l et al*, 1995; Habash *et al*, 1996). Tobacco plants with reduced PRK activity have downregulation of PSII activity and electron transport, with reduced PSII electron transport efficiency, increased energy dissipation in PSII antennae, and reductions in the rate of electron transport (Habash *et al.*, 1996). This is reflected in the data here, with reduced electron transport rate for RuBP regeneration (Figure **5.9**C) and increased NPQ (Figure 5.7, Figure 5.8) in *cp12-1/2/3* plants compared to their wild type, which is further decreased by acclimation to fluctuating light. If plants acclimated to fluctuating light experience further downregulation of PRK, this could account for both the reduced carbon assimilation and reduced PSII efficiency since this could be linked to reduced ROS scavenging. The formation of the CP12/GAPDH/PRK complex has been shown to provide protection to PRK and GAPDH (Marri *et al.*, 2014) which can be inhibited by oxidation (Marri *et al.*, 2009). With increased oxidants and reduced complex formation in *cp12-1/2/3*, an increase in the oxidation, and therefore inhibition, of GAPDH and PRK could be resulting in reduced CBB cycle activity.

The effect of fluctuating light acclimation and CP12 knockdown on NPQ could be linked to the thioredoxins. Thioredoxins *f* and *m* are known to interact with CP12 (Marri *et al.*, 2009), with increased levels of their oxidation related to increased CP12 oxidation and CP12/GAPDH/PRK formation (López-Calcagno, Howard and Raines, 2014). This interaction is reduced in the *cp12-1/2/3* mutants, so the possible increase in thioredoxin oxidation under fluctuating light compared to square light may increase the energy lost via NPQ processes (Figure 5.7, Figure 5.8). CP12 also interacts with NADP-malate dehydrogenase (MDH) (Gütle *et al.*, 2017) which produces malate from NADPH, and zeaxanthin epoxidase (ZE) in the xanthophyll cycle to regulate NPQ (Da *et al.*, 2018), both of which are key in regulating reducing power within the chloroplast (Gütle *et al.*, 2017; Da *et al.*, 2018). With reduced levels of CP12 in the knockdowns used in this study, the number of substrates for Trx *f* and *m* is reduced, with only so many available NADP-MDH and ZE. This could result in an electron build-up in the electron transport chain, as availability of Trxs to act as sinks is not increasing, demonstrated in the qPCR data (Figure **5.2**). This could potentially result in increased NPQ, to dissipate the additional energy, and reactive oxygen species production, due to over reduction of the photosynthetic electron transport chain. This is supported by the NPQ data (Figure 5.7 & Figure 5.8), which demonstrated increased NPQ across knockdowns in comparison to wild type controls, where CP12 functionality could be more important due to the peaks and troughs in growth light, compared to those acclimated to square light.

Significant build-up of NPQ in fluctuating light acclimated plants compared to square light acclimated plants was found in induction (Figure 5.7) and fluctuating light (Figure 5.8). Changes in NPQ are known to lag behind changes in irradiance (Pérez-

Bueno *et al.*, 2008), so repeated peaks and troughs in light, as experienced in the FLL regime here, could result in a build-up of NPQ that does not relax during the lower light periods due to insufficient time. This is reflected in the data (Figure 5.8) where NPQ can been seen to increase across light cycles in FLL-acclimated plants, suggesting ineffective NPQ dissipation. This is not reflected in the SQL-WTs, but interestingly was observed in the SQL *cp12-1/2/3* lines, indicating CP12 and its interactions may be affecting NPQ dissipation. This response could be due to the high rate of fluctuations FLL-acclimated plants are exposed to over the light period. Previous work has noted that long acclimation to short sun flecks (SSF; 20 seconds of 650 or 1250 every 6 minutes) significantly increased NPQ compared to those acclimated to longer sun flecks (one 40 mins peak of 650) upon induction with 1000 (Alter *et al.*, 2012). This was accompanied by an increased NPQ following relaxation of NPQ following 14 minutes of darkness in SSF plants compared to those acclimated to longer a sun fleck or constant light (Alter *et al.*, 2012). Similar patterns are noted in the NPQ of FLL-acclimated plants compared to SQL-acclimated plants (Figure 5.7& Figure 5.8). This indicates that the frequency of fluctuations has a role to play in the NPQ dynamics, resulting in higher NPQ capabilities including during relaxation. Intensity of sun flecks has also been noted to impact NPQ in shade tolerant plant *Panax notoginseng*. Increased sun fleck intensity increased NPQ during both induction and relaxation (J. Y. Zhang *et al.*, 2021), suggesting that the results seen here may depend on both the intensity and frequency of fluctuations.

The activity of thioredoxins to regulate CP12 could also explain the differences in assimilation between fluctuating light-acclimated wild types and *cp12-1/2/3.* In wild type peas, CP12/PRK/GAPDH complex dissociates under high light and reforms in under 1 minute (Howard *et al.*, 2008), providing a quick switch to regulate the Calvin-Benson cycle in a changing light environment. The reductions in assimilation under both light conditions (Figure 5.10A) could be attributed to the increased reduction of Glucose-6-Phosphate Dehydrogenase (G6PDH), a known substrate of Trx *f* (Née *et al.*, 2009), leading to its inactivation, and so a decrease in carbon assimilation due to slowing of the Calvin-Benson cycle in knockdown plants.

A key limitation of this study is that *cp12-1/2/3* did not completely abolish CP12 expression. The seed lines utilised here were originally characterised by López-Calcagn*o et al* (2017), and maintain around a 10% expression of CP12-2, while CP12-1 and CP12-3 were completely knocked out, as demonstrated in the qPCR data (Figure 5.3). Since CP12-2 shares a high level of homology with CP12-1 and is highly expressed in the leaves (Singh, Kaloudas and Raines, 2008), there could be a degree of interaction between the remaining CP12 and complex components GAPDH and PRK.

In chapter 3 it has been theorised that thioredoxin regulation could account for the differences in photosynthetic efficiency between square and fluctuating light adapted plants. Here it has been shown that knockout expression of CP12-1 and CP12-3 and reduced expression of CP12 results in decreases in both photosynthetic efficiency and assimilation, indicating there is a role for this protein in the acclimation response.

Chapter 6: General Discussion

Approximately 1.6 billion hectares of land is used to grow the world's crops (FAOSTAT, 2020). These crops are subject to highly dynamic light conditions, meaning it is important to understand how plants can acclimate and respond to such conditions on both a physiological and molecular level. With increasing pressure on global food supplies due to climate change and an increase population, it is important to improve how crops utilise the resources available. It was already known that crop productivity is negatively impacted by dynamic light (Taylor and Long, 2017), and that, in *Arabidopsis thaliana*, acclimation to fluctuating light resulted in a distinctly different phenotype to plants grown under square light (Vialet-Chabrand et al., 2017; Matthews, Vialet-Chabrand and Lawson, 2018). The work presented here (summarized in Table ***6.1***) shows a potential role for DNA methylation in acclimation to fluctuating light, while providing further evidence as to how fluctuating light impacts physiology and the molecular consequences of this.

Table 6.1: Summary of key results across the chapters in both square versus fluctuating light comparisons

Regime	Flowering	PSII efficiency	A_{sat}	DEGs			CP12 NPQ
				Total	With DMRs	In 1kb of TE	
SQH v FLH	Early	Higher ($p<0.05$)	Higher ($p<0.05$)	4636	148 (*p=1*)	258	.
SQL v FLL	Early	Higher ($p<0.05$)	Higher ($p>0.1$)	1711	96 (*p=1*)	97	Lower ($p<0.05$), exacerbated by CP12 knockdown

A range of genes with known physiological functions and which could help explain the physiological phenotypes were found to be differentially methylated or within 1kb of a differentially methylated TE. A further subset of these were found to be differentially expressed, suggesting a correlation between methylation and gene expression which may aid light acclimation.

It is not well understood if there is a link between DNA methylation and effects on physiology. Previous work has investigated whether DNA methylation was linked to transcriptional changes in plants exposed to recurring excess light (Ganguly et al., 2019). It was proposed that the physiological effects of excess light were independent of DNA methylation, and that any transcriptional changes were a consequence, not cause, of the physiology seen (Ganguly et al., 2019). However, due to the magnitude of change in methylation, as well as the number of differentially methylated regions (DMRs) and differentially expressed genes (DEGs) overlapping in some comparisons (Table ***4.3***) it is likely that there is some causative effect of DNA methylation on physiology. There have been few studies looking at long-term acclimation to light, and particularly fluctuating light, so it could be that methylation has an important role in long-term acclimation.

Here, multiple genes with potential impacts on physiology were noted to have differential methylation and expression. For example, under SQHvFLH light, LRGB and JAC1 lost methylation at CpG sites and gained in expression (Table ***4.3***). LRGB, also known as PLGG1, is a key transporter of photorespiratory carbon skeletons in the chloroplasts (Pick et al, 2013; Walker, South and Ort, 2016). It allows for exhange of glycolate, produced by oxidation by Rubisco, for glycerate produced in the peroxisome, key in the process of photorespiration (Pick et al, 2013). Knockouts for plgg1 were reported to have signficantly reduced photosynthetic capacity under

changing internal CO_2, demonstrated by significant reductions in Vc_{max}, J_{max}, and F_v/F_m. These findings are in agreement with data described in Chapter 3, where SQ plants displayed higher values than their FL counterparts across Vc_{max}, J_{max}, and F_v/F_m (Figure **3.4**;Figure **3.9**). Furthermore, LRGB knockout have been shown to have reduced thylakoid membranes in the chloroplast (Yang et al., 2012), demonstrating the importance of the gene in chloroplast development, which could also be linked to the observed differences seen in physiology. Overall, this evidence indicates some role for LRGB/PLGG1 in acclimation to fluctuating light and that photorespiration may be a key process in the acclimation process.

JAC1 was also differentially expressed and methylated in SQHvFLH. It is known to function in chloroplast photorecolation, acting to impact actin filament appearance and disappearance (Suetsugu, Kagawa and Wada, 2005; Ichikawa et al., 2011). It is known to impact upon photosynthetic efficiency and assimilation, with jac1 knockouts having increased F_v/F_m and F_q'/F_m', as well as increase CO_2 uptake under changing light in comparison to wildtype plants (Czarnocka et al., 2020). Here, JAC1 was noted to increase in expression between SQH and FLH plants, suggesting it could impact upon the physiology seen, with SQH plants having signficantly higher F_v/F_m and F_q'/F_m' (Figure **3.6**D; Figure **3.7**) than FLH plants.

Under square versus fluctuating light of both high and low intensity, the MCCA subunit (AT1G03090) of 3-Methylcrotonyl-coenzyme A carboxylase (MCCase) was differentially methylated and expressed (Table ***4.3***), being upregulated under fluctuating light. It has previously been noted that the expression of MCCase is inhibited by exogenous sugars, in particular sucrose (Che, Wurtele and Nikolau, 2002). Expression was also seen to be affected by light, with increasing light intensity associated with decreasing expression of both MCCA and MCCB (Che,

Wurtele and Nikolau, 2002). Due to the impact of light on MCCase expression, it follows that fluctuating light could affect expression of one or both subunits and indicates that the expression of MCCase could have a role in acclimation to regime and so impact on the physiology. Increased expression of MCCase acts as a starvation response (Aubert et al., 1996), which could explain the significantly smaller rosette size in fluctuating light-acclimated plants compared to their square light counterparts (Figure **3.2**; Figure **3.3**).

Upregulation of MCCB (AT4G34030) transcripts was also noted between SQH and FLH acclimated plants (log_2FC= -1.53), but not SQLvFLL. This indicates both subunits may require upregulation under high light but not low light, however, the effects are likely to be similar, as there may be less of the assembled enzyme available under both scenarios. This could also account for some of the differences seen in the physiology (see Chapter **Error! Reference source not found.**), as SQH acclimated plants may not experience the starvation response. Under FLH light, there are dramatic decreases in the light available throughout the photoperiod, meaning it is possible the plants experience starvation due to low light availability. At the time of writing, there have been no physiological studies into the effects of MCCase or MCCase overexpression, so it is difficult to know the impacts that differential expression may have on plant physiology.

A range of genes related to photosynthesis were found to be differentially expressed (Figure **4.14**), which could be related to the physiological differences noted in Chapter 3. For example, Rubisco Activase (RCA) was found to be upregulated in FLH compared to FLL plants and downregulated in SQH plants compared to FLH plants. Downregulation of RCA in FLL-acclimated plants vs FLH activated plants could account for the differences in assimilation under changing CO_2, particularly the

Vc_{max} (Figure **3.9**B). Vc_{max} relates to the maximum activity of Rubisco carboxylase (Farquhar, von Caemmerer and Berry, 1980), therefore an increase in the activation, if enough Rubisco is available to activate, will likely increase this parameter. This is supported by data in Chapter 3 which showed FLH acclimated plants to have a significantly higher Vc_{max} than FLL plants (Figure **3.9**), possibly related to increased Rubisco activation. Changes in RCA concentration have been found to strongly effect dynamic photosynthesis (Kaiser et al., 2016). Reductions of Rubisco concentration to 22% that of the wildtype resulted in significantly slower times to reach 90% maximum photosynthesis under changing light, e.g. the transition from 130 to 600 took 29.8±1.7 minutes in the RCA knockdown line compared to 9±2.2 minutes in the wildtype (Kaiser et al, 2016). This could explain the differences in assimilation under changing light between SQH and FLH plants (Figure **3.10**A), as if RCA is downregulated in SQH plants compared to FLH plants, the response to changing light could be less effective.

Only 4 of photosynthesis-related genes investigated were found to be significantly differentially expressed in both square vs fluctuating comparisons (Figure **4.14**); ELF3, ELF4, RBCX1, and G6PD2. ELF3 and ELF4 are circadian clock genes which act to integrate light and temperature stimuli from phytochromes (reviewed in Zhao et al., 2021). They have diverse targets with functions including regulating flowering time, and hypocotyl elongation (Zhao et al., 2021). ELF3 and 4 interact with the transcription factor PHYTOCLOCK1 to form the evening complex (Zhao et al., 2021), ultimately acting to repress flowering. The downregulation of ELF3 and 4 in fluctuating plants compared to square plants could account for the delayed development noted in fluctuating light acclimated plants (Figure **3.2**; Figure **3.3**). The interaction of ELF3, ELF4, and LUX are known to be required for expression of the

growth promoting transcription factors PIF4 and PIF5, with knockouts of ELF3 associated with an increased hypocotyl elongation compared to the wildtype (Nusinow et al., 2011). Here, elongated leaf anatomy was observed under fluctuating light (Figure **3.2**), suggesting this decrease in expression of ELF 3 and 4 impacted upon plant growth. However, due to the circadian nature of these genes, it is difficult to know with a single time point how time-of-day is impacting dynamics.

RBCX1 and G6PD2 arguably have more obvious applications to photosynthetic acclimation. RBCX1 is a molecular chaperone in the chloroplast thylakoid which aids the folding of Rubisco, and is a distinct homologue of the cyanobacterial protein RbcX (Kolesinski et al., 2013). It is one of two isoforms found in *A.thaliana* which have similar architecture, and binds to the large subunits of Rubisco, RbcL (Liu et al., 2010; Kolesinski et al., 2013). Overexpression of RbcX increased the amount of soluble RbcL measured (Cai et al., 2014), indicating its expression is important for proper protein folding and therefore activity. Here, an increase in transcripts between square and fluctuating plants (Figure **4.14**) could indicate an increased need for regulation of Rubisco assembly in fluctuating light plants which could be related to increased protein turnover, or a need to downregulate Rubisco under square light. Previous work has directly associated RbcL with the expression of acetyl-coA carboxylase (accD), key in fatty acid biosynthesis in the chloroplast (He, Mu and Chi, 2015). Inefficient transcription of RbcL resulted in accumulation of accD protein during chloroplast development (He, Mu and Chi, 2015). In tobacco, overexpression of accD resulted in extended leaf longevity (Madoka et al., 2002), which could account for the increased lifespan under fluctuating light compared to square light (Figure **3.3**). In contrast, knockdown resulted in impaired chloroplast division in *Arabidopsis* (He, Mu and Chi, 2015), and reduced leaf lamina and resulting in pale

green sections in tobacco (Caroca et al., 2021). In the pale green sections, there was no clear palisade layer, which requires functional plastids to develop, demonstrating the importance of accD in normal leaf development (Caroca et al., 2021). Here, there may be a reduction in properly folded RbcL, due to reduced RbcX expression in square plants, which could reduce accD accumulation, impairing leaf and chloroplast development and reducing leaf longevity. This could account for the shorter lifespan in square light plants, and a reduced number of chloroplasts could also account for decreased assimilation (Figure **3.10**). However, this would not account for the significantly higher CO_2 assimilation kinetics seen here (Figure **3.9**B+C), or the increased content of chloroplast proteins in SQH plants previously noted, including Rieske FeS and Lhca1 (Vialet-Chabrand et al., 2017), as a reduction in the number of chloroplasts would be expected to decrease these parameters.

In contrast, G6PD2 is downregulated in fluctuating light plants compared to square light plants. G6PD2 is a plastid isoform of glucose-6-phosphate dehydrogenase (Wakao and Benning, 2005) which is a key enzyme in the oxidative pentose phosphate (OPP) pathway, converting Glucose-6-phospahte (G6P) to 6-phosphoglucanate. Changes in the OPP pathway, specifically G6PD, have been noted under salt stress in rice (Hou et al., 2007), while salt stress in *Arabidopsis* activates glycogen synthase kinase 3 which is able to phosphorylate cytosolic G6PD (Dal Santo et al., 2012). This demonstrates the potential role of G6PD under stress conditions. Plastid G6PDs are known to be regulated by light, with the activity of multiple G6PDs strongly inhibited by NAPDH (Preiser et al., 2019), suggesting their activity could be differentially impacted by square and fluctuating light regimes. An increase in transcripts under square light could indicate upregulation of the OPP

pathway in plants acclimated to square light. The activity of G6PDs are thought to initiate the G6P shunt around the CBB cycle, where G6P is oxidized and decarboxylated to ribulose-5-phosphate in a futile cycle proposed to stabiles photosynthesis (Preiser et al., 2019). This shunt has been proposed to induce cyclic electron flow, which could act to protect photosystem I by dissipating excess energy which could otherwise cause photosystem damage (Sharkey and Weise, 2016). With reduced expression of G6PD2 under fluctuating light, there could be reduced cyclic electron flow and so increased photosystem damage. This could account for the decreases in F_q'/F_m' noted in fluctuating light plants compared to square light (Figure **3.6**; Figure 5.5) plants due to possible PSII damage.

Trx m2 was found to be downregulated between SQH and FLH acclimated plants (Figure **4.14**), indicating reduced expression under SQH light, and therefore a role in acclimation to FLH light. Knockout of trxm2 has been noted to have multiple effects on plant physiology in *Arabidopsis thaliana*. Knockouts were noted to have significantly reduced assimilation as a function of light and a significant increase in stomatal density compared to wildtype (Sahrawy et al., 2022). This could account for some of the differences in physiology seen here, with SQH plants showing reduced assimilation compared to FLH plants (Figure **3.10**), alongside an increased stomatal density (Figure **3.4**). Trx-m2 is highly expressed in the roots alongside CBB cycle enzyme fructose-1,6-bisphospahte (Sahrawy et al., 2022), indicating there could be a contrasting root phenotype in SQH and FLH which may partially account for physiological differences. Knockout of trx-m2 also resulted in upregulation of multiple CBB cycle and photosynthesis related enzymes, including RCA, ATP synthase subunit beta, and chlorophyll a-b binding protein (Fernández-Trijueque, Serrato and Sahrawy, 2019). These studies demonstrate the possible impact reduced thioredoxin

expression could have on regulation and activity of photosynthesis and the CBB cycle, providing evidence for the molecular mechanism underlying changes in physiology.

Trx-m2 is also known to regulate several differentially expressed genes seen here. For example, CP12 proteins are known to be regulated by thioredoxins, including Trx-m2 (López-Calcagno, Howard and Raines, 2014). CP12-2 and CP12-3 were found to be upregulated in FLH plants compared to SQH plants (Figure **4.14**), indicating a role for CP12 and thioredoxin regulation of the Calvin Cycle under high intensity dynamic light. Under low light this differential expression was not found or may be present but did not meet the log_2FC or *p*-adjusted value requirements. This contrast suggests that regulation of CP12 expression may be light intensity and regime dependent. CP12-1 and CP12-2 are closely related and display functional redundancy (Singh, Kaloudas and Raines, 2008; López-Calcagno et al., 2017), meaning upregulation of either CP12-1 and CP12-2 would likely have similar effects, with both displaying high levels of expression in the leaves (Singh, Kaloudas and Raines, 2008). This increase in expression of CP12-2 under FLH acclimation suggests an increase in the regulation of the CBB cycle by CP12 and thioredoxin mediation.

Increased expression of CP12-2 under fluctuating light has previously been seen (Schneider et al., 2019), indicating there is some consistency in this response under high-low light transitions. In *Stylosanthes guianensis*, which possess one CP12 gene, overexpression of CP12 resulted in significant increases in net photosynthetic rate, and was accompanied by significant increases in GAPDH and PRK enzymatic activity (Li et al., 2018). This suggests that increased expression of CP12 could improve photosynthesis, supporting the improvements in assimilation observed

under changing light (Figure **3.10**). Decreases in expression of all three CP12 genes (*cp12-1/2/3*) supports this role for CP12, with data here demonstrating decreased photosynthetic efficiency (Figure 5.5), suppressed electron flow, reduced assimilation (Figure 5.10) and increased NPQ (Figure 5.7; Figure 5.8). Knockout of CP12 in cyanobacteria suggested that CP12 has a role in separating the oxidative and reductive pentose phosphate pathways (Tamoi et al., 2005), where the first step in higher plants is catalysed by glucose-6-phosphate dehydrogenase (G6PD) (Kruger and Von Schaewen, 2003). Under SQLvFLL, downregulation of G6PD2 and G6PD6 was noted (Figure **4.14**), both of which are potential targets for thioredoxins (Wenderoth, Scheibe and Von Schaewen, 1997). However, in tobacco this need for CP12 to separate the two pathways was not noted (Howard et al., 2011), indicating that CP12 regulation may not explain the differences in physiology seen. However, there are distinct differences between *Arabidopsis* and tobacco, so the potential role of CP12 proteins may differ and not yet fully understood.

Considerations on the results and future work

There are several key limitations to this study. Primarily, a single fluctuating regime has been applied which is not representative of long-term fluctuations that would naturally occur in the field over the lifetime of a plant. This means that the responses seen on a physiological and epigenetic level were the result of acclimation to the single regime, and therefore may not be applicable to the field. Furthermore, samples for methylation and transcriptomic analysis were taken at a single time point, meaning it is possible that early differential methylation in the acclimation response, as well as the transcriptome, may not have been noted in the study. This may also mean that key genes early in the acclimation process may be missed. It is also known that DNA methylation is a signal for the recruitment of other epigenetic

factors such as histones and chromatin-remodelling proteins (Geiman and Robertson, 2002), so early methylation marks may have been lost in subsequent cell-divisions, but their effects maintained due to this mechanism. Therefore, it would be of interest to carry out time-course sampling throughout the acclimation process to look at how the methylome may change throughout the process of acclimation, and the plant's lifespan.

As the current effects of gene body methylation on gene expression are currently unclear (Muyle *et al.*, 2022), further investigation of the genes differentially methylated within their gene bodies, and how methylation impacts their expression, would be of interest. Such investigation could provide evidence for both the effect of gene body methylation and whether these genes do have some impact during light acclimation. New technologies are being developed with allow for the addition or removal of methylation within a target sequence, most of which are based on CRISPR (Vojta *et al.*, 2016; Ghoshal *et al.*, 2021). This technology has started to be applied to investigate how DNA methylation can impact both biotic and abiotic stress tolerance (Niu *et al.*, 2022; Veley *et al.*, 2023), so could provide insight as to whether differentially methylated genes are impacting the physiology of plants acclimated to fluctuating light.

Investigation of potential inheritance of DNA methylation would be of interest, as plants could experience a priming response. In plants, DNA methylation can be inherited along the germline (Rendina González et al, 2018), so there is potential for the progeny of the plants utilized in chapter **Error! Reference source not found.** and **Error! Reference source not found.** to inherit some of this epigenetic information. This could impact upon the response to growth light regime, potentially conferring a growth advantage and impacted upon the physiology. In rice, heavy

metal treatment resulted in widespread changes in DNA methylation, and the progeny of these treated plants were noted to have inherited some of the altered methylation patterns and more tolerant of heavy metals (Ou et al., 2012). This demonstrates the possibility of inheritance which could confer an advantage under naturally fluctuating light.

Over a 24 hour period, dynamic light drives temporal and spatial differences in carbon assimilation and water use (Vialet-Chabrand et al, 2017; Matthews, Vialet-Chabrand and Lawson, 2018), while over a season, the light environment, and therefore these dynamics, vary massively (reviewed in Morales and Kaiser, 2020). The findings in this study emphasise the physiological effects of dynamic light, while demonstrating that both the methylome and transcriptome are significantly impacted by growth light regime, with DNA methylation appearing to have some effect on differential gene expression.

While the diurnal effects of dynamic light acclimation have been investigated in *A.thaliana* (Vialet-Chabrand et al, 2017; Matthews, Vialet-Chabrand and Lawson, 2018), the effects of seasonal acclimation are slightly harder to understand. Field studies have previously been carried out using *Arabidopsis* accessions (Mishra et al., 2012), but it is difficult to attribute the effects of seasonal light acclimation when there are multiple possible stressors impacting upon physiology. Therefore, repeating this experiment with seasonal regimes, e.g., recorded over spring and autumn growth periods, could show whether acclimation does occur despite each 24-hour period being different. WGBS and RNAseq on such acclimated plants could also provide further evidence for how plants acclimate to their light environments when subjects to different daily conditions.

The effects of fluctuating light on key crops, e.g., wheat and rice, would be an important progression for this work. Understanding the effects of dynamic light acclimation in these crops, and the impacts this may have on yield and quality, would demonstrate the real-world application of this work. It is already known that the sun-shade transitions impact carbon assimilation in field-grown wheat (Taylor and Long, 2017), but the impacts this has upon the seed and therefore food is not clear. Furthermore, WGBS and RNAseq in these species could provide further clues as to gene targets which could improve plant responses to dynamic light.

The distinct effects of dynamic light on physiology, methylation and gene expression emphasizes that greenhouse studies are often unable to reflect the effects of field conditions. It is well documented that field studies are often not reflective of the results obtained under greenhouse conditions, whether positive or negative (Zeller et al., 2010; López-Calcagno et al., 2019, 2020). Work in Chapter **Error! Reference source not found.** demonstrates significant molecular effects of dynamic light acclimation compared to the square light often used in greenhouse and growth cabinet experiments. This provides evidence that light regime should be considered when investigating crop plants in a laboratory setting, as the impact of light regime on the transcriptome (Chapter 4, section **Error! Reference source not found.**.) likely could result in significant changes in gene regulation.

The findings here emphasize that acclimation to naturally dynamic light has distinctly different consequences for physiology, methylation, and gene expression. Acclimation to fluctuating light impacts many key plant processes, including carbon

assimilation and photosystem II efficiency and is accompanied by genome-wide differences in methylation and global changes in transcription, allowing for identification of genes that may be key in the process. The work here is a step in improving our understanding of plant light responses and how these are regulated at an epigenetic level, while demonstrating the importance of consider growth light regime in plant productivity studies.

Chapter 7: Bibliography

Abcam (no date) *Histone modifications | Abcam*. Available at: https://www.abcam.com/epigenetics/histone-modifications (Accessed: 24 August 2022).

Ahlert, D., Stegemann, S., Kahlau, S., Ruf, S. and Bock, R. (2009) 'Insensitivity of chloroplast gene expression to DNA methylation', *Molecular Genetics and Genomics*, 282(1), pp. 17–24. Available at: https://doi.org/10.1007/s00438-009-0440-z.

Ahmed, I., Sarazin, A., Bowler, C., Colot, V. and Quesneville, H. (2011a) 'Genome-wide evidence for local DNA methylation spreading from small RNA-targeted sequences in Arabidopsis', *Nucleic Acids Research*, 39(16), p. 6919. Available at: https://doi.org/10.1093/NAR/GKR324.

Ahmed, I., Sarazin, A., Bowler, C., Colot, V. and Quesneville, H. (2011b) 'Genome-wide evidence for local DNA methylation spreading from small RNA-targeted sequences in Arabidopsis', *Nucleic Acids Research*, 39(16), pp. 6919–6931. Available at: https://doi.org/10.1093/NAR/GKR324.

Alter, P., Dreissen, A., Luo, F.L. and Matsubara, S. (2012) 'Acclimatory responses of Arabidopsis to fluctuating light environment: Comparison of different sunfleck regimes and accessions', in *Photosynthesis Research*. Photosynth Res, pp. 221–237. Available at: https://doi.org/10.1007/s11120-012-9757-2.

Anderson, M.D., Che, P., Song, J., Nikolau, B.J. and Wurtele, E.S. (1998) '3-Methylcrotonyl-Coenzyme A Carboxylase Is a Component of the Mitochondrial Leucine Catabolic Pathway in Plants', *Plant Physiology*, 118(4), p. 1127. Available at: https://doi.org/10.1104/PP.118.4.1127.

Aoki, S., Toh, S., Nakamichi, N., Hayashi, Y., Wang, Y., Suzuki, T., Tsuji, H. and Kinoshita, T. (2019) 'Regulation of stomatal opening and histone modification by photoperiod in Arabidopsis thaliana', *Scientific Reports*, 9(1). Available at: https://doi.org/10.1038/s41598-019-46440-0.

Aro, E.-M., Mccaffery, S. and Anderson, J.M. (1993) *Photoinhibition and D 1 Protein Degradation in Peas Acclimated to Different Growth Irradiances'*, *Plant Physiol*.

Arora, H., Singh, R.K., Sharma, S., Sharma, N., Panchal, A., Das, T., Prasad, A. and Prasad, M. (2022) 'DNA methylation dynamics in response to abiotic and pathogen stress in plants', *Plant Cell Reports*, 41(10), pp. 1931–1944. Available at: https://doi.org/10.1007/S00299-022-02901-X/FIGURES/2.

Arteaga-Vazquez, M.A. and Chandler, V.L. (2010) 'Paramutation in maize: RNA mediated trans-generational gene silencing', *Current opinion in genetics & development*, 20(2), p. 156. Available at: https://doi.org/10.1016/J.GDE.2010.01.008.

Athanasiou, K., Dyson, B.C., Webster, R.E. and Johnson, G.N. (2010) 'Dynamic acclimation of photosynthesis increases plant fitness in changing environments', *Plant Physiology*, 152(1), pp. 366–373. Available at: https://doi.org/10.1104/pp.109.149351.

van Attikum, H. and Gasser, S.M. (2009) 'Crosstalk between histone modifications during the DNA damage response', *Trends in Cell Biology*, pp. 207–217. Available at: https://doi.org/10.1016/j.tcb.2009.03.001.

Aubert, S., Alban, C., Bligny, R. and Douce, R. (1996) 'Induction of β-methylcrotonyl-coenzyme A carboxylase in higher plant cells during carbohydrate starvation: evidence for a role of MCCase in leucine catabolism', *FEBS Letters*, 383(3), pp. 175–180. Available at: https://doi.org/https://doi.org/10.1016/0014-5793(96)00244-X.

Ayyappan, V., Kalavacharla, V., Thimmapuram, J., Bhide, K.P., Sripathi, V.R., Smolinski, T.G., Manoharan, M., Thurston, Y., Todd, A., Kingham, B. and Mantovani, R. (2015) 'Genome-wide profiling of histone modifications (H3K9 me2 and H4K12 ac) and gene expression in rust (uromyces appendiculatus) inoculated common bean (Phaseolus vulgaris L)', *PLoS ONE*, 10(7). Available at: https://doi.org/10.1371/journal.pone.0132176.

Bai, F. and Settles, A.M. (2015) 'Imprinting in plants as a mechanism to generate seed phenotypic diversity', *Frontiers in Plant Science*, 5(JAN), pp. 1–10. Available at: https://doi.org/10.3389/FPLS.2014.00780/XML/NLM.

Bailey-Serres, J., Leroy, P., Jones, S.S., Wahleithner, J.A. and Wolstenholme, D.R. (1987) 'Size distributions of circular molecules in plant mitochondrial DNAs', *Current Genetics*, 12(1), pp. 49–53. Available at: https://doi.org/10.1007/BF00420727/METRICS.

Bailey, S., Walters, R.G., Jansson, S. and Horton, P. (2001) 'Acclimation of Arabidopsis thaliana to the light environment: The existence of separate low light and high light responses', *Planta*, 213(5), pp. 794–801. Available at: https://doi.org/10.1007/s004250100556.

Baker, N.R. (1996) 'Photoinhibition of Photosynthesis', in *Light as an Energy Source and Information Carrier in Plant Physiology*. Springer US, pp. 89–97. Available at: https://doi.org/10.1007/978-1-4613-0409-8_7.

Baker, N.R. (2008) 'Chlorophyll Fluorescence: A Probe of Photosynthesis In Vivo', *Annual Review of Plant Biology*, 59(1), pp. 89–113. Available at: https://doi.org/10.1146/annurev.arplant.59.032607.092759.

Barneche, F., Steinmetz, F. and Echeverria, M. (2000) 'Fibrillarin genes encode both a conserved nucleolar protein and a novel small nucleolar RNA involved in ribosomal RNA methylation in Arabidopsis thaliana', *The Journal of biological chemistry*, 275(35), pp. 27212–27220. Available at: https://doi.org/10.1074/JBC.M002996200.

Barradas, V.L., Jones, H.G. and Clark, J.A. (1998) 'Sunfleck dynamics and canopy structure in a Phaseolus vulgaris L. canopy', *International Journal of Biometeorology*, 42(1), pp. 34–43. Available at: https://doi.org/10.1007/S004840050081/METRICS.

Bartels, A., Han, Q., Nair, P., Stacey, L., Gaynier, H., Mosley, M., Huang, Q.Q., Pearson, J.K., Hsieh, T.F., An, Y.Q.C. and Xiao, W. (2018) 'Dynamic DNA Methylation in Plant Growth and Development', *International Journal of Molecular Sciences*, 19(7). Available at: https://doi.org/10.3390/IJMS19072144.

Baubec, T., Pecinka, A., Rozhon, W. and Mittelsten Scheid, O. (2009) 'Effective, homogeneous and transient interference with cytosine methylation in plant genomic DNA by zebularine', *The Plant Journal*, 57(3), pp. 542–554. Available at: https://doi.org/10.1111/J.1365-313X.2008.03699.X.

Baxendale, J.H. and Wilson, J.A. (1957) 'The photolysis of hydrogen peroxide at high light intensities', *Transactions of the Faraday Society*, 53(0), pp. 344–356.

Available at: https://doi.org/10.1039/TF9575300344.

Bayat, L., Arab, M., Aliniaeifard, S., Seif, M., Lastochkina, O. and Li, T. (2018) 'Effects of growth under different light spectra on the subsequent high light tolerance in rose plants', *AoB Plants*, 10(ply052). Available at: https://doi.org/10.1093/aobpla/ply052.

Benhamed, M., Bertrand, C., Servet, C. and Zhou, D.X. (2006) 'Arabidopsis GCN5, HD1, and TAF1/HAF2 interact to regulate histone acetylation required for liqht-responsive gene expression', *Plant Cell*, 18(11), pp. 2893–2903. Available at: https://doi.org/10.1105/tpc.106.043489.

Berger, S.L., Kouzarides, T., Shiekhattar, R. and Shilatifard, A. (2009) 'An operational definition of epigenetics', *Genes and Development*, 23(7), pp. 781–783. Available at: https://doi.org/10.1101/gad.1787609.

Berry, Z.C. and Smith, W.K. (2012) 'Cloud pattern and water relations in Picea rubens and Abies fraseri, southern Appalachian Mountains, USA', *Agricultural and Forest Meteorology*, 162–163, pp. 27–34. Available at: https://doi.org/10.1016/J.AGRFORMET.2012.04.005.

Bewick, A.J., Ji, L., Niederhuth, C.E., Willing, E.M., Hofmeister, B.T., Shi, X., Wang, L., Lu, Z., Rohr, N.A., Hartwig, B., Kiefer, C., Deal, R.B., Schmutz, J., Grimwood, J., Stroud, H., Jacobsen, S.E., Schneeberger, K., Zhang, X. and Schmitza, R.J. (2016) 'On the origin and evolutionary consequences of gene body DNA methylation', *Proceedings of the National Academy of Sciences of the United States of America*, 113(32), pp. 9111–9116. Available at: https://doi.org/10.1073/PNAS.1604666113/-/DCSUPPLEMENTAL.

Bhandary, S.K., Dhakal, R., Sanghavi, V. and Verkicharlai, P.K. (2021) 'Ambient light level varies with different locations and environmental conditions: Potential to impact myopia', *PLoS ONE*, 16(7). Available at: https://doi.org/10.1371/JOURNAL.PONE.0254027.

Bielczynski, L.W., Schansker, G. and Croce, R. (2016) 'Effect of Light Acclimation on the Organization of Photosystem II Super- and Sub-Complexes in Arabidopsis thaliana', *Frontiers in Plant Science*, 7(FEB2016), p. 105. Available at: https://doi.org/10.3389/fpls.2016.00105.

Blázquez, M.A., Green, R., Nilsson, O., Sussman, M.R. and Weigel, D. (1998) 'Gibberellins Promote Flowering of Arabidopsis by Activating the LEAFY Promoter', *The Plant Cell*, 10(5), pp. 791–800. Available at: https://doi.org/10.1105/tpc.10.5.791.

Bolger, A., Scossa, F., Bolger, M.E., Lanz, C., Maumus, F., Tohge, T., Quesneville, H., Alseekh, S., Sørensen, I., Lichtenstein, G., Fich, E.A., Conte, M., Keller, H., Schneeberger, K., Schwacke, R., Ofner, I., Vrebalov, J., Xu, Y., Osorio, S., Aflitos, S.A., Schijlen, E., Jiménez-Goméz, J.M., Ryngajllo, M., Kimura, S., Kumar, R., Koenig, D., Headland, L.R., Maloof, J.N., Sinha, N., Van Ham, R.C.H.J., Lankhorst, R.K., Mao, L., Vogel, A., Arsova, B., Panstruga, R., Fei, Z., Rose, J.K.C., Zamir, D., Carrari, F., Giovannoni, J.J., Weigel, D., Usadel, B. and Fernie, A.R. (2014) 'The genome of the stress-tolerant wild tomato species Solanum pennellii', *Nature genetics*, 46(9), pp. 1034–1038. Available at: https://doi.org/10.1038/NG.3046.

Bolger, A.M., Lohse, M. and Usadel, B. (2014) 'Trimmomatic: a flexible trimmer for

Illumina sequence data', *Bioinformatics*, 30(15), p. 2114. Available at: https://doi.org/10.1093/BIOINFORMATICS/BTU170.

Botta, A., Viovy, N., Ciais, P., Friedlingstein, P. and Monfray, P. (2000) 'A global prognostic scheme of leaf onset using satellite data', *Global Change Biology*, 6(7), pp. 709–725. Available at: https://doi.org/10.1046/J.1365-2486.2000.00362.X.

Bowman, G.D. and Poirier, M.G. (2015a) 'Post-translational modifications of histones that influence nucleosome dynamics', *Chemical Reviews*. American Chemical Society, pp. 2274–2295. Available at: https://doi.org/10.1021/cr500350x.

Bowman, G.D. and Poirier, M.G. (2015b) 'Post-translational modifications of histones that influence nucleosome dynamics', *Chemical Reviews*. American Chemical Society, pp. 2274–2295. Available at: https://doi.org/10.1021/cr500350x.

Boycheva, I., Vassileva, V. and Iantcheva, A. (2014) 'Histone Acetyltransferases in Plant Development and Plasticity', *Current Genomics*, 15(1), pp. 28–37. Available at: https://doi.org/10.2174/1389202915011403061127 42.

Boyko, A. and Kovalchuk, I. (2008) 'Epigenetic control of plant stress response', *Environmental and Molecular Mutagenesis*, pp. 61–72. Available at: https://doi.org/10.1002/em.20347.

Briggs, W.R. and Christie, J.M. (2002) 'Phototropins 1 and 2: Versatile plant blue-light receptors', *Trends in Plant Science*. Elsevier Current Trends, pp. 204–210. Available at: https://doi.org/10.1016/S1360-1385(02)02245-8.

Broad Institute (2019) *GitHub - broadinstitute/picard: A set of command line tools (in Java) for manipulating high-throughput sequencing (HTS) data and formats such as SAM/BAM/CRAM and VCF.*, *GitHub Repository*. Available at: https://github.com/broadinstitute/picard (Accessed: 8 April 2022).

Buchanan, B.B. (1980) *ROLE OF LIGHT IN THE REGULATION OF CHLOROPLAST ENZYMESl*, *Ann. Rev. Plant Physio*. Available at: www.annualreviews.org (Accessed: 2 June 2021).

Cai, Z., Liu, G., Zhang, J. and Li, Y. (2014) 'Development of an activity-directed selection system enabled significant improvement of the carboxylation efficiency of Rubisco', *Protein and Cell*, 5(7), pp. 552–562. Available at: https://doi.org/10.1007/S13238-014-0072-X/FIGURES/6.

Calarco, J.P., Borges, F., Donoghue, M.T.A., Van Ex, F., Jullien, P.E., Lopes, T., Gardner, R., Berger, F., Feijó, J.A., Becker, J.D. and Martienssen, R.A. (2012) 'Reprogramming of DNA methylation in pollen guides epigenetic inheritance via small RNA', *Cell*, 151(1), pp. 194–205. Available at: https://doi.org/10.1016/j.cell.2012.09.001.

Caputi, F.F., Candeletti, S. and Romualdi, P. (2017) 'Epigenetic Approaches in Neuroblastoma Disease Pathogenesis', in *Neuroblastoma - Current State and Recent Updates*. InTech. Available at: https://doi.org/10.5772/intechopen.69566.

Carabelli, M., Possenti, M., Sessa, G., Ciolfi, A., Sassi, M., Morelli, G. and Ruberti, I. (2007) 'Canopy shade causes a rapid and transient arrest in leaf development through auxin-induced cytokinin oxidase activity', *Genes and Development*, 21(15), pp. 1863–1868. Available at: https://doi.org/10.1101/gad.432607.

Cardon, G., Höhmann, S., Klein, J., Nettesheim, K., Saedler, H. and Huijser, P. (1999) 'Molecular characterisation of the Arabidopsis SBP-box genes', *Gene*, 237(1), pp. 91–104. Available at: https://doi.org/10.1016/S0378-1119(99)00308-X.

Caroca, R., Howell, K.A., Malinova, I., Burgos, A., Tiller, N., Pellizzer, T., Annunziata, M.G., Hasse, C., Ruf, S., Karcher, D. and Bock, R. (2021) 'Knockdown of the plastid-encoded acetyl-CoA carboxylase gene uncovers functions in metabolism and development', *Plant Physiology*, 185(3), p. 1091. Available at: https://doi.org/10.1093/PLPHYS/KIAA106.

Carrozza, M.J., Utley, R.T., Workman, J.L. and Côté, J. (2003a) 'The diverse functions of histone acetyltransferase complexes', *Trends in Genetics*. Elsevier Ltd, pp. 321–329. Available at: https://doi.org/10.1016/S0168-9525(03)00115-X.

Carrozza, M.J., Utley, R.T., Workman, J.L. and Côté, J. (2003b) 'The diverse functions of histone acetyltransferase complexes', *Trends in Genetics*. Elsevier Ltd, pp. 321–329. Available at: https://doi.org/10.1016/S0168-9525(03)00115-X.

Casson, S.A., Franklin, K.A., Gray, J.E., Grierson, C.S., Whitelam, G.C. and Hetherington, A.M. (2009) 'phytochrome B and PIF4 Regulate Stomatal Development in Response to Light Quantity', *Current Biology*, 19(3), pp. 229–234. Available at: https://doi.org/10.1016/j.cub.2008.12.046.

Catoni, M., Griffiths, J., Becker, C., Zabet, N.R., Bayon, C., Dapp, M., Lieberman-Lazarovich, M., Weigel, D. and Paszkowski, J. (2017) ' DNA sequence properties that predict susceptibility to epiallelic switching ', *The EMBO Journal*, 36(5), pp. 617–628. Available at: https://doi.org/10.15252/embj.201695602.

Catoni, M., Tsang, J.M., Greco, A.P. and Zabet, N.R. (2018) 'DMRcaller: a versatile R/Bioconductor package for detection and visualization of differentially methylated regions in CpG and non-CpG contexts', *Nucleic Acids Research*, 46(19), pp. e114–e114. Available at: https://doi.org/10.1093/NAR/GKY602.

Catoni, M. and Zabet, N.R. (2021) 'Analysis of Plant DNA Methylation Profiles Using R', *Methods in Molecular Biology*, 2250, pp. 219–238. Available at: https://doi.org/10.1007/978-1-0716-1134-0_21/FIGURES/5.

Cavrak, V. V., Lettner, N., Jamge, S., Kosarewicz, A., Bayer, L.M. and Mittelsten Scheid, O. (2014) 'How a Retrotransposon Exploits the Plant's Heat Stress Response for Its Activation', *PLOS Genetics*, 10(1), p. e1004115. Available at: https://doi.org/10.1371/JOURNAL.PGEN.1004115.

Chazdon, R.L. and Pearcy, R.W. (1986a) 'Photosynthetic responses to light variation in rainforest species : I. Induction under constant and fluctuating light conditions', *Oecologia*, 69(4), pp. 517–523. Available at: https://doi.org/10.1007/BF00410357.

Chazdon, R.L. and Pearcy, R.W. (1986b) 'Photosynthetic responses to light variation in rainforest species : II. Carbon gain and photosynthetic efficiency during lightflecks', *Oecologia*, 69(4), pp. 524–531. Available at: https://doi.org/10.1007/BF00410358.

Che, P., Wurtele, E.S. and Nikolau, B.J. (2002) 'Metabolic and Environmental Regulation of 3-Methylcrotonyl-Coenzyme A Carboxylase Expression in Arabidopsis', *Plant Physiology*, 129(2), pp. 625–637. Available at: http://www.jstor.org/stable/4280493.

Cheung, P. and Lau, P. (2005) ‘Epigenetic Regulation by Histone Methylation and Histone Variants’, *Molecular Endocrinology*, 19(3), pp. 563–573. Available at: https://doi.org/10.1210/me.2004-0496.

Cho, H.-Y., Tseng, T.-S., Kaiserli, E., Sullivan, S., Christie, J.M. and Briggs, W.R. (2007) ‘Physiological Roles of the Light, Oxygen, or Voltage Domains of Phototropin 1 and Phototropin 2 in Arabidopsis’, *Plant Physiology*, 143(1), pp. 517–529. Available at: https://doi.org/10.1104/pp.106.089839.

Cho, L.-H., Yoon, J. and An, G. (2017) ‘The control of flowering time by environmental factors’, *The Plant Journal*, 90(4), pp. 708–719. Available at: https://doi.org/https://doi.org/10.1111/tpj.13461.

Choudhury, N.K. and Behera, R.K. (2001) ‘Photoinhibition of photosynthesis: Role of carotenoids in photoprotection of chloroplast constituents’, *Photosynthetica*. Springer, pp. 481–488. Available at: https://doi.org/10.1023/A:1015647708360.

Chow, W., Qian, L., Goodchild, D. and Anderson, J. (1988) ‘Photosynthetic Acclimation of Alocasia macrorrhiza (L.) G. Don’, *Functional Plant Biology*, 15(2), p. 107. Available at: https://doi.org/10.1071/pp9880107.

Cokus, S.J., Feng, S., Zhang, X., Chen, Z., Merriman, B., Haudenschild, C.D., Pradhan, S., Nelson, S.F., Pellegrini, M. and Jacobsen, S.E. (2008) ‘Shotgun bisulphite sequencing of the Arabidopsis genome reveals DNA methylation patterning’, *Nature*, 452(7184), pp. 215–219. Available at: https://doi.org/10.1038/nature06745.

Crisp, P.A., Ganguly, D., Eichten, S.R., Borevitz, J.O. and Pogson, B.J. (2016) ‘Reconsidering plant memory: Intersections between stress recovery, RNA turnover, and epigenetics’, *Science Advances*. American Association for the Advancement of Science. Available at: https://doi.org/10.1126/sciadv.1501340.

Cubas, P., Vincent, C. and Coen, E. (1999) ‘An epigenetic mutation responsible for natural variation in floral symmetry’, *Nature*, 401(6749), pp. 157–161. Available at: https://doi.org/10.1038/43657.

Czarnocka, W., Rusaczonek, A., Willems, P., Sujkowska-Rybkowska, M., Van Breusegem, F. and Karpiński, S. (2020) ‘Novel Role of JAC1 in Influencing Photosynthesis, Stomatal Conductance, and Photooxidative Stress Signalling Pathway in Arabidopsis thaliana’, *Frontiers in Plant Science*, 11, p. 1124. Available at: https://doi.org/10.3389/FPLS.2020.01124/BIBTEX.

Da, Q., Ting Sun, ·, Wang, M., Jin, H., Li, M., Feng, D., Wang, J., Wang, H.-B. and Liu, B. (2018) ‘M-type thioredoxins are involved in the xanthophyll cycle and proton motive force to alter NPQ under low-light conditions in Arabidopsis’, *Plant Cell Reports*, 37, pp. 279–291. Available at: https://doi.org/10.1007/s00299-017-2229-6.

Dahlet, T., Argüeso Lleida, A., Al Adhami, H., Dumas, M., Bender, A., Ngondo, R.P., Tanguy, M., Vallet, J., Auclair, G., Bardet, A.F. and Weber, M. (2020) ‘Genome-wide analysis in the mouse embryo reveals the importance of DNA methylation for transcription integrity’, *Nature Communications 2020 11:1*, 11(1), pp. 1–14. Available at: https://doi.org/10.1038/s41467-020-16919-w.

Dal Santo, S., Stampfl, H., Krasensky, J., Kempa, S., Gibon, Y., Petutschnig, E., Rozhon, W., Heuck, A., Clausen, T. and Jonaka, C. (2012) ‘Stress-induced GSK3

regulates the redox stress response by phosphorylating glucose-6-phosphate dehydrogenase in Arabidopsis', *The Plant cell*, 24(8), pp. 3380–3392. Available at: https://doi.org/10.1105/TPC.112.101279.

Danecek, P., Bonfield, J., Liddle, J., Marshall, J., Ohan, V., Pollard, M., Whitwham, A., Keane, T., McCarthy, S., Davies, R. and Li, H. (2021) 'Twelve years of SAMtools and BCFtools', *GigaScience*, 10(2). Available at: https://doi.org/10.1093/GIGASCIENCE/GIAB008.

Deal, R.B. and Henikoff, S. (2011) 'Histone variants and modifications in plant gene regulation', *Current Opinion in Plant Biology*, pp. 116–122. Available at: https://doi.org/10.1016/j.pbi.2010.11.005.

DEFRA (2023) *Agricultural facts: East of England Region - GOV.UK*. Available at: https://www.gov.uk/government/statistics/agricultural-facts-england-regional-profiles/agricultural-facts-east-of-england-region (Accessed: 19 February 2023).

Demmig-Adams, B. and Adams, W.W. (1992) 'Photoprotection and Other Responses of Plants to High Light Stress', *Annual Review of Plant Physiology and Plant Molecular Biology*, 43(1), pp. 599–626. Available at: https://doi.org/10.1146/annurev.pp.43.060192.003123.

Deneweth, J., Van de Peer, Y. and Vermeirssen, V. (2022) 'Nearby transposable elements impact plant stress gene regulatory networks: a meta-analysis in A. thaliana and S. lycopersicum', *BMC Genomics*, 23(1), pp. 1–19. Available at: https://doi.org/10.1186/S12864-021-08215-8/FIGURES/3.

Dickinson, K.E., Lalonde, C.G. and McGinn, P.J. (2019) 'Effects of spectral light quality and carbon dioxide on the physiology of Micractinium inermum: growth, photosynthesis, and biochemical composition', *Journal of Applied Phycology*, 31(6), pp. 3385–3396. Available at: https://doi.org/10.1007/s10811-019-01880-z.

Dietz, K.J., Tavakoli, N., Kluge, C., Mimura, T., Sharma, S.S., Harris, G.C., Chardonnens, A.N. and Golldack, D. (2001) 'Significance of the V-type ATPase for the adaptation to stressful growth conditions and its regulation on the molecular and biochemical level', *Journal of Experimental Botany*, 52(363), pp. 1969–1980. Available at: https://doi.org/10.1093/JEXBOT/52.363.1969.

Dowen, R.H., Pelizzola, M., Schmitz, R.J., Lister, R., Dowen, J.M., Nery, J.R., Dixon, J.E. and Ecker, J.R. (2012) 'Widespread dynamic DNA methylation in response to biotic stress', *Proceedings of the National Academy of Sciences of the United States of America*, 109(32). Available at: https://doi.org/10.1073/pnas.1209329109.

Drozdova, I.S., Bondar, V. V., Bukhov, N.G., Kotov, A.A., Kotova, L.M., Maevskaya, S.N. and Mokronosov, A.T. (2001) 'Effects of light spectral quality on morphogenesis and source-sink relations in radish plants', *Russian Journal of Plant Physiology*, 48(4), pp. 415–420. Available at: https://doi.org/10.1023/A:1016725207990.

Du, J., Johnson, L.M., Groth, M., Feng, S., Hale, C.J., Li, S., Vashisht, A.A., Gallego-Bartolome, J., Wohlschlegel, J.A., Patel, D.J. and Jacobsen, S.E. (2014) 'Mechanism of DNA methylation-directed histone methylation by KRYPTONITE', *Molecular Cell*, 55(3), pp. 495–504. Available at: https://doi.org/10.1016/j.molcel.2014.06.009.

Du, J., Zhong, X., Bernatavichute, Y. V., Stroud, H., Feng, S., Caro, E., Vashisht, A.A., Terragni, J., Chin, H.G., Tu, A., Hetzel, J., Wohlschlegel, J.A., Pradhan, S.,

Patel, D.J. and Jacobsen, S.E. (2012) ‘Dual binding of chromomethylase domains to H3K9me2-containing nucleosomes directs DNA methylation in plants’, *Cell*, 151(1), pp. 167–180. Available at: https://doi.org/10.1016/j.cell.2012.07.034.

Edreva, A. (2005) ‘Generation and scavenging of reactive oxygen species in chloroplasts: a submolecular approach’, *Agriculture, Ecosystems & Environment*, 106(2–3), pp. 119–133. Available at: https://doi.org/10.1016/J.AGEE.2004.10.022.

Eichten, S.R., Ellis, N.A., Makarevitch, I., Yeh, C.T., Gent, J.I., Guo, L., McGinnis, K.M., Zhang, X., Schnable, P.S., Vaughn, M.W., Dawe, R.K. and Springer, N.M. (2012) ‘Spreading of Heterochromatin Is Limited to Specific Families of Maize Retrotransposons’, *PLOS Genetics*, 8(12), p. e1003127. Available at: https://doi.org/10.1371/JOURNAL.PGEN.1003127.

Eichten, S.R., Schmitz, R.J. and Springer, N.M. (2014) ‘Epigenetics: Beyond chromatin modifications and complex genetic regulation’, *Plant Physiology*, 165(3), pp. 933–947. Available at: https://doi.org/10.1104/pp.113.234211.

Exposito-Rodriguez, M., Laissue, P.P., Yvon-Durocher, G., Smirnoff, N. and Mullineaux, P.M. (2017) ‘Photosynthesis-dependent H2O2 transfer from chloroplasts to nuclei provides a high-light signalling mechanism’, *Nature Communications 2017 8:1*, 8(1), pp. 1–11. Available at: https://doi.org/10.1038/s41467-017-00074-w.

FAOSTAT (2020) ‘Land statistics and indicators Global, regional and country trends, 2000-2020’, *FAOSTAT ANALYTICAL BRIEF 48* [Preprint]. Available at: http://www.fao.org/faostat/en/#data/RL (Accessed: 15 September 2022).

Farquhar, G.D., von Caemmerer, S. and Berry, J.A. (1980) ‘A biochemical model of photosynthetic CO2 assimilation in leaves of C 3 species’, *Planta*, 149(1), pp. 78–90. Available at: https://doi.org/10.1007/BF00386231.

Fedoroff, N. V. (2012) ‘Transposable elements, epigenetics, and genome evolution’, *Science*, 338(6108), pp. 758–767. Available at: https://doi.org/10.1126/SCIENCE.338.6108.758/ASSET/4D4639DF-CF55-418E-9680-EFB443D9A854/ASSETS/GRAPHIC/338_758_F9.JPEG.

Feng, L., Raza, M.A., Li, Z., Chen, Y., Khalid, M.H. Bin, Du, J., Liu, W., Wu, X., Song, C., Yu, L., Zhang, Z., Yuan, S., Yang, W. and Yang, F. (2019) ‘The influence of light intensity and leaf movement on photosynthesis characteristics and carbon balance of Soybean’, *Frontiers in Plant Science*, 9, p. 1952. Available at: https://doi.org/10.3389/fpls.2018.01952.

Feng, S., Jacobsen, S.E. and Reik, W. (2010) ‘Epigenetic reprogramming in plant and animal development’, *Science*, pp. 622–627. Available at: https://doi.org/10.1126/science.1190614.

Fenley, A.T., Anandakrishnan, R., Kidane, Y.H. and Onufriev, A. V. (2018) ‘Modulation of nucleosomal DNA accessibility via charge-altering post-translational modifications in histone core’, *Epigenetics and Chromatin*, 11(1). Available at: https://doi.org/10.1186/s13072-018-0181-5.

Fernández-Trijueque, J., Serrato, A.-J. and Sahrawy, M. (2019) ‘Proteomic Analyses of Thioredoxins f and m Arabidopsis thaliana Mutants Indicate Specific Functions for These Proteins in Plants’, *Antioxidants*, 8(3). Available at: https://doi.org/10.3390/antiox8030054.

Flannery, S.E., Pastorelli, F., Wood, W.H.J., Hunter, C.N., Dickman, M.J., Jackson, P.J. and Johnson, M.P. (2021) 'Comparative proteomics of thylakoids from Arabidopsis grown in laboratory and field conditions', *Plant Direct*, 5(10), p. e355. Available at: https://doi.org/10.1002/PLD3.355.

Foyer, C.H. (2018) 'Reactive oxygen species, oxidative signaling and the regulation of photosynthesis', *Environmental and Experimental Botany*, 154, pp. 134–142. Available at: https://doi.org/10.1016/J.ENVEXPBOT.2018.05.003.

Foyer, C.H. and Noctor, G. (2016) 'Stress-triggered redox signalling: what's in pROSpect?', *Plant, Cell & Environment*, 39(5), pp. 951–964. Available at: https://doi.org/10.1111/PCE.12621.

Foyer, C.H., Ruban, A. V. and Noctor, G. (2017) 'Viewing oxidative stress through the lens of oxidative signalling rather than damage', *Biochemical Journal*. Portland Press Ltd, pp. 877–883. Available at: https://doi.org/10.1042/BCJ20160814.

Franklin, K.. and Whitelam, G.. (2005) 'Phytochromes and Shade-avoidance Responses in Plants', *Annals of Botany*, 96, pp. 169–175. Available at: https://doi.org/10.1093/aob/mci165.

Frommer, M., McDonald, L.E., Millar, D.S., Collis, C.M., Watt, F., Grigg, G.W., Molloy, P.L. and Paul, C.L. (1992) 'A genomic sequencing protocol that yields a positive display of 5-methylcytosine residues in individual DNA strands.', *Proceedings of the National Academy of Sciences of the United States of America*, 89(5), pp. 1827–1831. Available at: https://doi.org/10.1073/pnas.89.5.1827.

Ganguly, D.R., Crisp, P.A., Eichten, S.R. and Pogson, B.J. (2017) 'The Arabidopsis DNA Methylome Is Stable under Transgenerational Drought Stress', *Plant Physiology*, 175(4), p. 1893. Available at: https://doi.org/10.1104/PP.17.00744.

Ganguly, D.R., Crisp, P.A., Eichten, S.R. and Pogson, B.J. (2018) 'Maintenance of pre-existing DNA methylation states through recurring excess-light stress', *Plant, Cell & Environment*, 41(7), pp. 1657–1672. Available at: https://doi.org/10.1111/pce.13324.

Ganguly, D.R., Stone, B.A.B., Bowerman, A.F., Eichten, S.R. and Pogson, B.J. (2019) 'Excess Light Priming in Arabidopsis thaliana Genotypes with Altered DNA Methylomes', *G3: Genes|Genomes|Genetics*, 9(11), p. 3611. Available at: https://doi.org/10.1534/G3.119.400659.

Gay, A.P. and Hurd, R.G. (1975) 'THE INFLUENCE OF LIGHT ON STOMATAL DENSITY IN THE TOMATO', *New Phytologist*, 75(1), pp. 37–46. Available at: https://doi.org/10.1111/j.1469-8137.1975.tb01368.x.

Gebert, D. and Rosenkranz, D. (2015) 'RNA-based regulation of transposon expression', *Wiley Interdisciplinary Reviews: RNA*, 6(6), pp. 687–708. Available at: https://doi.org/10.1002/wrna.1310.

Gehring, M., Bubb, K.L. and Henikoff, S. (2009) 'Extensive demethylation of repetitive elements during seed development underlies gene imprinting', *Science*, 324(5933), pp. 1447–1451. Available at: https://doi.org/10.1126/science.1171609.

Geiman, T.M. and Robertson, K.D. (2002) 'Chromatin remodeling, histone modifications, and DNA methylation - How does it all fit together?', *Journal of*

Cellular Biochemistry, 87(2), pp. 117–125. Available at: https://doi.org/10.1002/JCB.10286.

Ghoshal, B., Picard, C.L., Vong, B., Feng, S. and Jacobsen, S.E. (2021) 'CRISPR-based targeting of DNA methylation in Arabidopsis thaliana by a bacterial CG-specific DNA methyltransferase', *Proceedings of the National Academy of Sciences of the United States of America*, 118(23), p. 2125016118. Available at: https://doi.org/10.1073/PNAS.2125016118/-/DCSUPPLEMENTAL.

Gill, R.A., Scossa, F., King, G.J., Golicz, A., Tong, C., Snowdon, R.J., Fernie, A.R. and Liu, S. (2021) 'On the Role of Transposable Elements in the Regulation of Gene Expression and Subgenomic Interactions in Crop Genomes', *https://doi.org/10.1080/07352689.2021.1920731*, 40(2), pp. 157–189. Available at: https://doi.org/10.1080/07352689.2021.1920731.

Gilmore, A.M., Mohanty, N. and Yamamoto, H.Y. (1994) 'Epoxidation of zeaxanthin and antheraxanthin reverses non-photochemical quenching of photosystem II chlorophyll a fluorescence in the presence of trans-thylakoid delta pH.', *FEBS letters*, 350(2–3), pp. 271–274. Available at: https://doi.org/10.1016/0014-5793(94)00784-5.

Givnish, T.J. (1988) 'Adaptation to sun and shade: a whole-plant perspective', *Australian Journal of Plant Physiology*, 15(1–2), pp. 63–92. Available at: https://doi.org/10.1071/pp9880063.

Godwin, J. and Farrona, S. (2020) 'Plant Epigenetic Stress Memory Induced by Drought: A Physiological and Molecular Perspective', *Methods in Molecular Biology*, 2093, pp. 243–259. Available at: https://doi.org/10.1007/978-1-0716-0179-2_17/TABLES/1.

Grativol, C., Hemerly, A.S. and Ferreira, P.C.G. (2012) 'Genetic and epigenetic regulation of stress responses in natural plant populations', *Biochimica et Biophysica Acta (BBA) - Gene Regulatory Mechanisms*, 1819(2), pp. 176–185. Available at: https://doi.org/10.1016/J.BBAGRM.2011.08.010.

Greally, J.M. (2018) 'A user's guide to the ambiguous word "epigenetics"', *Nature Reviews Molecular Cell Biology 2018 19:4*, 19(4), pp. 207–208. Available at: https://doi.org/10.1038/nrm.2017.135.

Grewal, S.I.S. and Rice, J.C. (2004) 'Regulation of heterochromatin by histone methylation and small RNAs', *Current Opinion in Cell Biology*. Elsevier Current Trends, pp. 230–238. Available at: https://doi.org/10.1016/j.ceb.2004.04.002.

Guidi, L., Lo Piccolo, E. and Landi, M. (2019) 'Chlorophyll fluorescence, photoinhibition and abiotic stress: Does it make any difference the fact to be a C3 or C4 species?', *Frontiers in Plant Science*. Frontiers Media S.A., p. 174. Available at: https://doi.org/10.3389/fpls.2019.00174.

Guo, M., Liu, X., Jiang, Y., Yu, J. and Meng, T. (2021) 'Identification Of Arabidopsis genes associated with cold tolerance based on integrated bioinformatics analysis', *Journal of Plant Interactions*, 16(1), pp. 344–353. Available at: https://doi.org/10.1080/17429145.2021.1955164.

Gütle, D.D., Roret, T., Hecker, A., Reski, R. and Jacquot, J.P. (2017) 'Dithiol disulphide exchange in redox regulation of chloroplast enzymes in response to evolutionary and structural constraints', *Plant Science*, 255, pp. 1–11. Available at:

https://doi.org/10.1016/J.PLANTSCI.2016.11.003.

Haag, J.R. and Pikaard, C.S. (2011) ‘Multisubunit RNA polymerases IV and V: Purveyors of non-coding RNA for plant gene silencing’, *Nature Reviews Molecular Cell Biology*, pp. 483–492. Available at: https://doi.org/10.1038/nrm3152.

Habash, D.Z., Parry, M.A.J., Parmar, S., Paul, M.J., Driscoll, S., Knight, J., Gray, J.C. and Lawlor, D.W. (1996) ‘The regulation of component processes of photosynthesis in transgenic tobacco with decreased phosphoribulokinase activity’, *Photosynthesis Research*, 49(2), pp. 159–167. Available at: https://doi.org/10.1007/BF00117666.

Hansen, K.D., Langmead, B. and Irizarry, R.A. (2012) ‘BSmooth: from whole genome bisulfite sequencing reads to differentially methylated regions’, *Genome Biology*, 13(10), pp. 1–10. Available at: https://doi.org/10.1186/GB-2012-13-10-R83/FIGURES/4.

Hauser, M.-T., Aufsatz, W., Jonak, C. and Luschnig, C. (2011) ‘Transgenerational epigenetic inheritance in plants☆’. Available at: https://doi.org/10.1016/j.bbagrm.2011.03.007.

Hayatsu, H., Wataya, Y., Kai, K. and Iida, S. (1970) ‘Reaction of sodium bisulfite with uracil, cytosine, and their derivatives’, *Biochemistry*, 9(14), pp. 2858–2865. Available at: https://doi.org/10.1021/bi00816a016.

Hayes, R.G. and Klein, W.H. (1974) ‘Spectral quality influence of light during development of Arabidopsis thaliana plants in regulating seed germination’, *Plant and Cell Physiology*, 15(4), pp. 643–653. Available at: https://doi.org/10.1093/oxfordjournals.pcp.a075049.

He, B., Mu, Y. and Chi, W. (2015) ‘Effects of inefficient transcription termination of rbcL on the expression of accD in plastids of Arabidopsis thaliana’, *Photosynthesis Research*, 126(2–3), pp. 323–330. Available at: https://doi.org/10.1007/S11120-015-0159-0/FIGURES/4.

Herman, J.J. and Sultan, S.E. (2016) ‘DNA methylation mediates genetic variation for adaptive transgenerational plasticity’, *Proceedings of the Royal Society B: Biological Sciences*, 283(1838), p. 20160988. Available at: https://doi.org/10.1098/rspb.2016.0988.

Heyno, E., Innocenti, G., Lemaire, S.D., Issakidis-Bourguet, E. and Krieger-Liszkay, A. (2014) ‘Putative role of the malate valve enzyme NADP-malate dehydrogenase in H2O2 signalling in Arabidopsis’, *Philosophical Transactions of the Royal Society B: Biological Sciences*, 369(1640). Available at: https://doi.org/10.1098/rstb.2013.0228.

Hilker, M. and Schmülling, T. (2019) ‘Stress priming, memory, and signalling in plants’, *Plant, Cell & Environment*, 42(3), pp. 753–761. Available at: https://doi.org/10.1111/PCE.13526.

Hiyama, A., Takemiya, A., Munemasa, S., Okuma, E., Sugiyama, N., Tada, Y., Murata, Y. and Shimazaki, K.I. (2017) ‘Blue light and CO2 signals converge to regulate light-induced stomatal opening’, *Nature Communications*, 8(1). Available at: https://doi.org/10.1038/s41467-017-01237-5.

Hoffmann, A.M., Noga, G. and Hunsche, M. (2015) ‘High blue light improves

acclimation and photosynthetic recovery of pepper plants exposed to UV stress', *Environmental and Experimental Botany*, 109, pp. 254–263. Available at: https://doi.org/10.1016/j.envexpbot.2014.06.017.

Hollister, J.D. and Gaut, B.S. (2009) 'Epigenetic silencing of transposable elements: A trade-off between reduced transposition and deleterious effects on neighboring gene expression', *Genome Research*, 19(8), pp. 1419–1428. Available at: https://doi.org/10.1101/GR.091678.109.

Hollister, J.D., Smith, L.M., Guo, Y.L., Ott, F., Weigel, D. and Gaut, B.S. (2011) 'Transposable elements and small RNAs contribute to gene expression divergence between Arabidopsis thaliana and Arabidopsis lyrata', *Proceedings of the National Academy of Sciences of the United States of America*, 108(6), pp. 2322–2327. Available at: https://doi.org/10.1073/PNAS.1018222108/SUPPL_FILE/PNAS.201018222SI.PDF.

Hoshino, R., Yoshida, Y. and Tsukaya, H. (2019) 'Multiple steps of leaf thickening during sun-leaf formation in Arabidopsis', *The Plant Journal*, 100(4), pp. 738–753. Available at: https://doi.org/10.1111/tpj.14467.

Hou, F.Y., Huang, J., Yu, S.L. and Zhang, H.S. (2007) 'The 6-phosphogluconate Dehydrogenase Genes Are Responsive to Abiotic Stresses in Rice', *Journal of Integrative Plant Biology*, 49(5), pp. 655–663. Available at: https://doi.org/10.1111/J.1744-7909.2007.00460.X.

Howard, T.P., Fryer, M.J., Singh, P., Metodiev, M., Lytovchenko, A., Obata, T., Fernie, A.R., Kruger, N.J., Quick, W.P., Lloyd, J.C. and Raines, C.A. (2011) 'Antisense suppression of the small chloroplast protein cp12 in tobacco alters carbon partitioning and severely restricts growth', *Plant Physiology*, 157(2), pp. 620–631. Available at: https://doi.org/10.1104/pp.111.183806.

Howard, T.P., Lloyd, J.C. and Raines, C.A. (2011) 'Inter-species variation in the oligomeric states of the higher plant Calvin cycle enzymes glyceraldehyde-3-phosphate dehydrogenase and phosphoribulokinase', *Journal of Experimental Botany*, 62(11), pp. 3799–3805. Available at: https://doi.org/10.1093/jxb/err057.

Howard, T.P., Metodiev, M., Lloyd, J.C. and Raines, C.A. (2008) 'Thioredoxin-mediated reversible dissociation of a stromal multiprotein complex in response to changes in light availability', *Proceedings of the National Academy of Sciences of the United States of America*, 105(10), pp. 4056–4061. Available at: https://doi.org/10.1073/pnas.0710518105.

Howe, K.L., Contreras-Moreira, B., De Silva, N., Maslen, G., Akanni, W., Allen, J., Alvarez-Jarreta, J., Barba, M., Bolser, D.M., Cambell, L., Carbajo, M., Chakiachvili, M., Christensen, M., Cummins, C., Cuzick, A., Davis, P., Fexova, S., Gall, A., George, N., Gil, L., Gupta, P., Hammond-Kosack, K.E., Haskell, E., Hunt, S.E., Jaiswal, P., Janacek, S.H., Kersey, P.J., Langridge, N., Maheswari, U., Maurel, T., McDowall, M.D., Moore, B., Muffato, M., Naamati, G., Naithani, S., Olson, A., Papatheodorou, I., Patricio, M., Paulini, M., Pedro, H., Perry, E., Preece, J., Rosello, M., Russell, M., Sitnik, V., Staines, D.M., Stein, J., Tello-Ruiz, M.K., Trevanion, S.J., Urban, M., Wei, S., Ware, D., Williams, G., Yates, A.D. and Flicek, P. (2020) 'Ensembl Genomes 2020—enabling non-vertebrate genomic research', *Nucleic Acids Research*, 48(D1), pp. D689–D695. Available at:

https://doi.org/10.1093/NAR/GKZ890.

Hsieh, T.F., Ibarra, C.A., Silva, P., Zemach, A., Eshed-Williams, L., Fischer, R.L. and Zilberman, D. (2009) 'Genome-wide demethylation of Arabidopsis endosperm', *Science*, 324(5933), pp. 1451–1454. Available at: https://doi.org/10.1126/science.1172417.

Huang, L.C., Hsiao, L.J., Pu, S.Y., Kuo, C.I., Huang, B.L., Tseng, T.C., Huang, H.J. and Chen, Y.T. (2012) 'DNA methylation and genome rearrangement characteristics of phase change in cultured shoots of Sequoia sempervirens', *Physiologia Plantarum*, 145(2), pp. 360–368. Available at: https://doi.org/10.1111/J.1399-3054.2012.01606.X.

Hughes, M.A. and Dunn, M.A. (1996) 'The molecular biology of plant acclimation to low temperature', *Journal of Experimental Botany*, 47(3), pp. 291–305. Available at: https://doi.org/10.1093/JXB/47.3.291.

Hughes, T.R. and Lambert, S.A. (2017) 'Transcription factors read epigenetics', *Science*. American Association for the Advancement of Science, pp. 489–490. Available at: https://doi.org/10.1126/science.aan2927.

Iacobazzi, V., Castegna, A., Infantino, V. and Andria, G. (2013) 'Mitochondrial DNA methylation as a next-generation biomarker and diagnostic tool', *Molecular Genetics and Metabolism*, 110(1–2), pp. 25–34. Available at: https://doi.org/10.1016/J.YMGME.2013.07.012.

Ibarra, C.A., Feng, X., Schoft, V.K., Hsieh, T.F., Uzawa, R., Rodrigues, J.A., Zemach, A., Chumak, N., Machlicova, A., Nishimura, T., Rojas, D., Fischer, R.L., Tamaru, H. and Zilberman, D. (2012) 'Active DNA demethylation in plant companion cells reinforces transposon methylation in gametes', *Science*, 337(6100), pp. 1360–1364. Available at: https://doi.org/10.1126/science.1224839.

Ichikawa, S., Yamada, N., Suetsugu, N., Wada, M. and Kadota, A. (2011) 'Red light, Phot1 and JAC1 modulate Phot2-dependent reorganization of chloroplast actin filaments and chloroplast avoidance movement', *Plant & cell physiology*, 52(8), pp. 1422–1432. Available at: https://doi.org/10.1093/PCP/PCR087.

IPCC (2019) *IPCC Special Report on Climate Change, Desertification, Land Degradation, Sustainable Land Management, Food Security, and Greenhouse gas fluxes in Terrestrial Ecosystems*, *Summary for Policymakers Approved Draft*. Available at: https://doi.org/10.4337/9781784710644.

Ito, H., Gaubert, H., Bucher, E., Mirouze, M., Vaillant, I. and Paszkowski, J. (2011) 'An siRNA pathway prevents transgenerational retrotransposition in plants subjected to stress', *Nature 2011 472:7341*, 472(7341), pp. 115–119. Available at: https://doi.org/10.1038/nature09861.

Jackson, J.P., Lindroth, A.M., Cao, X. and Jacobsen, S.E. (2002) 'Control of CpNpG DNA methylation by the KRYPTONITE histone H3 methyltransferase', *Nature*, 416(6880), pp. 556–560. Available at: https://doi.org/10.1038/nature731.

Jing, M., Zhang, H., Wei, M., Tang, Y., Xia, Y., Chen, Y., Shen, Z. and Chen, C. (2022) 'Reactive Oxygen Species Partly Mediate DNA Methylation in Responses to Different Heavy Metals in Pokeweed', *Frontiers in Plant Science*, 13, p. 845108. Available at: https://doi.org/10.3389/FPLS.2022.845108/FULL.

Johannes, F., Porcher, E., Teixeira, F.K., Saliba-Colombani, V., Simon, M., Agier, N., Bulski, A., Albuisson, J., Heredia, F., Audigier, P., Bouchez, D., Dillmann, C., Guerche, P., Hospital, F. and Colot, V. (2009) 'Assessing the impact of transgenerational epigenetic variation on complex traits', *PLoS Genetics*, 5(6). Available at: https://doi.org/10.1371/journal.pgen.1000530.

Joosten, S.C., Smits, K.M., Aarts, M.J., Melotte, V., Koch, A., Tjan-Heijnen, V.C. and Van Engeland, M. (2018) 'Epigenetics in renal cell cancer: Mechanisms and clinical applications', *Nature Reviews Urology*. Nature Publishing Group, pp. 430–451. Available at: https://doi.org/10.1038/s41585-018-0023-z.

Kaiser, E., Galvis, V.C. and Armbruster, U. (2019) 'Efficient photosynthesis in dynamic light environments: A chloroplast's perspective', *Biochemical Journal*, 476(19), pp. 2725–2741. Available at: https://doi.org/10.1042/BCJ20190134.

Kaiser, E., Morales, A., Harbinson, J., Heuvelink, E., Prinzenberg, A.E. and Marcelis, L.F.M. (2016) 'Metabolic and diffusional limitations of photosynthesis in fluctuating irradiance in Arabidopsis thaliana', *Scientific Reports 2016 6:1*, 6(1), pp. 1–13. Available at: https://doi.org/10.1038/srep31252.

Kaiser, E., Walther, D. and Armbruster, U. (2020) 'Growth under Fluctuating Light Reveals Large Trait Variation in a Panel of Arabidopsis Accessions', *Plants*, 9(3), p. 316. Available at: https://doi.org/10.3390/plants9030316.

Kalaji, H.M., Carpentier, R., Allakhverdiev, S.I. and Bosa, K. (2012) 'Fluorescence parameters as early indicators of light stress in barley', *Journal of Photochemistry and Photobiology B: Biology*, 112, pp. 1–6. Available at: https://doi.org/10.1016/j.jphotobiol.2012.03.009.

Kaldis, A., Tsementzi, D., Tanriverdi, O. and Vlachonasios, K.E. (2011) 'Arabidopsis thaliana transcriptional co-activators ADA2b and SGF29a are implicated in salt stress responses', *Planta*, 233(4), pp. 749–762. Available at: https://doi.org/10.1007/s00425-010-1337-0.

Kale, R., Hebert, A.E., Frankel, L.K., Sallans, L., Bricker, T.M. and Pospíšil, P. (2017) 'Amino acid oxidation of the D1 and D2 proteins by oxygen radicals during photoinhibition of Photosystem II', *Proceedings of the National Academy of Sciences of the United States of America*, 114(11), pp. 2988–2993. Available at: https://doi.org/10.1073/pnas.1618922114.

Kami, C., Lorrain, S., Hornitschek, P. and Fankhauser, C. (2010) 'Light-regulated plant growth and development', in *Current Topics in Developmental Biology*. Academic Press Inc., pp. 29–66. Available at: https://doi.org/10.1016/S0070-2153(10)91002-8.

Kang, C.Y., Lian, H.L., Wang, F.F., Huang, J.R. and Yang, H.Q. (2009) 'Cryptochromes, phytochromes, and COP1 regulate light-controlled stomatal development in arabidopsis', *Plant Cell*, 21(9), pp. 2624–2641. Available at: https://doi.org/10.1105/tpc.109.069765.

Kankel, M.W., Ramsey, D.E., Stokes, T.L., Flowers, S.K., Haag, J.R., Jeddeloh, J.A., Riddle, N.C., Verbsky, M.L. and Richards, E.J. (2003) 'Arabidopsis MET1 cytosine methyltransferase mutants', *Genetics*, 163(3), pp. 1109–1122.

Kapri-Pardes, E., Naveh, L. and Adam, Z. (2007) 'The thylakoid lumen protease

Deg1 is involved in the repair of photosystem II from photoinhibition in Arabidopsis', *Plant Cell*, 19(3), pp. 1039–1047. Available at: https://doi.org/10.1105/tpc.106.046573.

Karan, R., DeLeon, T., Biradar, H. and Subudhi, P.K. (2012) 'Salt Stress Induced Variation in DNA Methylation Pattern and Its Influence on Gene Expression in Contrasting Rice Genotypes', *PLoS ONE*. Edited by K. Wu, 7(6), p. e40203. Available at: https://doi.org/10.1371/journal.pone.0040203.

Karpinski, S., Escobar, C., Karpinska, B., Creissen, G. and Mullineaux, P.M. (1997) 'Photosynthetic electron transport regulates the expression of cytosolic ascorbate peroxidase genes in arabidopsis during excess light stress', *Plant Cell*, 9(4), pp. 627–640. Available at: https://doi.org/10.1105/tpc.9.4.627.

Karpinski, S., Reynolds, H., Karpinska, B., Wingsle, G., Creissen, G. and Mullineaux, P. (1999) 'Systemic signaling and acclimation in response to excess excitation energy in Arabidopsis', *Science*, 284(5414), pp. 654–657. Available at: https://doi.org/10.1126/science.284.5414.654.

Kashkush, K., Feldman, M. and Levy, A.A. (2003) 'Transcriptional activation of retrotransposons alters the expression of adjacent genes in wheat', *Nature Genetics*, 33(1), pp. 102–106. Available at: https://doi.org/10.1038/ng1063.

Kaul, S., Koo, H.L., Jenkins, J., Rizzo, M., Rooney, T., Tallon, L.J., Feldblyum, T., Nierman, W., Benito, M.I., Lin, X., Town, C.D., Venter, J.C., Fraser, C.M., Tabata, S., Nakamura, Y., Kaneko, T., Sato, S., Asamizu, E., Kato, T., Kotani, H., Sasamoto, S., Ecker, J.R., Theologis, A., Federspiel, N.A., Palm, C.J., Osborne, B.I., Shinn, P., Dewar, K., Kim, C.J., Buehler, E., Dunn, P., Chao, Q., Chen, H., Theologis, A., Osborne, B.I., Vysotskaia, V.S., Lenz, C.A., Kim, C.J., Hansen, N.F., Liu, S.X., Buehler, E., Alta, H., Sakano, H., Dunn, P., Lam, B., Pham, P.K., Chao, Q., Nguyen, M., Yu, G., Chen, H., Southwick, A., Lee, J.M., Miranda, M., Toriumi, M.J., Davis, R.W., Federspiel, N.A., Palm, C.J., Conway, A.B., Conn, L., Hansen, N.F., Hootan, A., Lam, B., Wambutt, R., Murphy, G., Düsterhöft, A., Stiekema, W., Pohl, T., Entian, K.D., Terryn, N., Volckaert, G., Salanoubat, M., Choisne, N., Artiguenave, F., Weissenbach, J., Quetier, F., Rieger, M., Ansorge, W., Unseld, M., Fartmann, B., Valle, G., Wilson, R.K., Sekhon, M., Pepin, K., Murray, J., Johnson, D., Hillier, L., de la Bastide, M., Huang, E., Spiegel, L., Gnoj, L., Habermann, K., Dedhia, N., Parnell, L., Preston, R., Marra, M., McCombie, W.R., Chen, E., Martienssen, R., Mayer, K., Lemcke, K., Haas, B., Haase, D., Rudd, S., Schoof, H., Frishman, D., Morgenstern, B., Zaccaria, P., Mewes, H.W., White, O., Creasy, T.H., Bielke, C., Maiti, R., Peterson, J., Ermolaeva, M., Pertea, M., Quackenbush, J., Volfovsky, N., Wu, D., Salzberg, S.L., Bevan, M., Lowe, T.M., Rounsley, S., Bush, D., Subramaniam, S., Levin, I., Norris, S., Schmidt, R., Acarkan, A., Bancroft, I., Brennicke, A., Eisen, J.A., Bureau, T., Legault, B.A., Le, Q.H., Agrawal, N., Yu, Z., Copenhaver, G.P., Luo, S., Preuss, D., Pikaard, C.S., Paulsen, I.T., Sussman, M., Britt, A.B., Selinger, D.A., Pandey, R., Chandler, V.L., Jorgensen, R.A., Mount, D.W., Pikaard, C., Juergens, G., Meyerowitz, E.M., Dangl, J., Jones, J.D.G., Chen, M., Chory, J. and Somerville, C. (2000) 'Analysis of the genome sequence of the flowering plant Arabidopsis thaliana', *Nature*, 408(6814), pp. 796–815. Available at: https://doi.org/10.1038/35048692.

Kim, D., Paggi, J.M., Park, C., Bennett, C. and Salzberg, S.L. (2019) 'Graph-based genome alignment and genotyping with HISAT2 and HISAT-genotype', *Nature*

Biotechnology 2019 37:8, 37(8), pp. 907–915. Available at: https://doi.org/10.1038/s41587-019-0201-4.

Kim, J., Kim, J.H., Richards, E.J., Chung, K.M. and Woo, H.R. (2014) 'Arabidopsis VIM proteins regulate epigenetic silencing by modulating DNA methylation and histone modification in cooperation with MET1', *Molecular Plant*, 7(9), pp. 1470–1485. Available at: https://doi.org/10.1093/mp/ssu079.

Kim, J.H., Click, R.E. and Melis, A. (1993) *Dynamics of Photosystem Stoichiometry Adjustment by Light Quality in Chloroplasts'*, *Plant Physiol*. Available at: www.plantphysiol.org (Accessed: 29 May 2020).

Kinoshita, Y., Saze, H., Kinoshita, T., Miura, A., Soppe, W.J.J., Koornneef, M. and Kakutani, T. (2007) 'Control of FWA gene silencing in Arabidopsis thaliana by SINE-related direct repeats', *The Plant journal : for cell and molecular biology*, 49(1), pp. 38–45. Available at: https://doi.org/10.1111/J.1365-313X.2006.02936.X.

Kirchhoff, H., Haase, W., Wegner, S., Danielsson, R., Ackermann, R. and Albertsson, P.A. (2007) 'Low-Light-induced formation of semicrystalline photosystem II arrays in higher plant chloroplasts', *Biochemistry*, 46(39), pp. 11169–11176. Available at: https://doi.org/10.1021/bi700748y.

Kleine, T., Nägele, T., Neuhaus, H.E., Schmitz-Linneweber, C., Fernie, A.R., Geigenberger, P., Grimm, B., Kaufmann, K., Klipp, E., Meurer, J., Möhlmann, T., Mühlhaus, T., Naranjo, B., Nickelsen, J., Richter, A., Ruwe, H., Schroda, M., Schwenkert, S., Trentmann, O., Willmund, F., Zoschke, R. and Leister, D. (2021) 'Acclimation in plants – the Green Hub consortium', *The Plant Journal*, 106(1), pp. 23–40. Available at: https://doi.org/10.1111/TPJ.15144.

Klem, K., Gargallo-Garriga, A., Rattanapichai, W., Oravec, M., Holub, P., Veselá, B., Sardans, J., Peñuelas, J. and Urban, O. (2019) 'Distinct Morphological, Physiological, and Biochemical Responses to Light Quality in Barley Leaves and Roots', *Frontiers in Plant Science*, 10, p. 1026. Available at: https://doi.org/10.3389/fpls.2019.01026.

Kobayashi, S., Goto-Yamamoto, N. and Hirochika, H. (2004) 'Retrotransposon-Induced Mutations in Grape Skin Color', *Science*, 304(5673), p. 982. Available at: https://doi.org/10.1126/SCIENCE.1095011/SUPPL_FILE/KOBAYASHI.SOM.PDF.

Köhler, C. and Lafon-Placette, C. (2015) 'Evolution and function of epigenetic processes in the endosperm'. Available at: https://doi.org/10.3389/fpls.2015.00130.

Kolesinski, P., Golik, P., Grudnik, P., Piechota, J., Markiewicz, M., Tarnawski, M., Dubin, G. and Szczepaniak, A. (2013) 'Insights into eukaryotic Rubisco assembly — Crystal structures of RbcX chaperones from Arabidopsis thaliana', *Biochimica et Biophysica Acta (BBA) - General Subjects*, 1830(4), pp. 2899–2906. Available at: https://doi.org/10.1016/J.BBAGEN.2012.12.025.

Kono, M. and Terashima, I. (2014) 'Long-term and short-term responses of the photosynthetic electron transport to fluctuating light', *Journal of Photochemistry and Photobiology B: Biology*, 137, pp. 89–99. Available at: https://doi.org/10.1016/j.jphotobiol.2014.02.016.

Kooke, R., Johannes, F., Wardenaar, R., Becker, F., Etcheverry, M., Colot, V., Vreugdenhil, D. and Keurentjes, J.J.B. (2015) 'Epigenetic basis of morphological

variation and phenotypic plasticity in Arabidopsis thaliana', *Plant Cell*, 27(2), pp. 337–348. Available at: https://doi.org/10.1105/tpc.114.133025.

Kouřil, R., Wientjes, E., Bultema, J.B., Croce, R. and Boekema, E.J. (2013) 'High-light vs. low-light: Effect of light acclimation on photosystem II composition and organization in Arabidopsis thaliana', *Biochimica et Biophysica Acta - Bioenergetics*, 1827(3), pp. 411–419. Available at: https://doi.org/10.1016/j.bbabio.2012.12.003.

Kress, E. and Jahns, P. (2017) 'The Dynamics of Energy Dissipation and Xanthophyll Conversion in Arabidopsis Indicate an Indirect Photoprotective Role of Zeaxanthin in Slowly Inducible and Relaxing Components of Non-photochemical Quenching of Excitation Energy ', *Frontiers in Plant Science* . Available at: https://www.frontiersin.org/articles/10.3389/fpls.2017.02094.

Krueger, F. and Andrews, S.R. (2011) 'Bismark: a flexible aligner and methylation caller for Bisulfite-Seq applications', *Bioinformatics*, 27(11), p. 1571. Available at: https://doi.org/10.1093/BIOINFORMATICS/BTR167.

Kruger, N.J. and Von Schaewen, A. (2003) 'The oxidative pentose phosphate pathway: Structure and organisation', *Current Opinion in Plant Biology*, 6(3), pp. 236–246. Available at: https://doi.org/10.1016/S1369-5266(03)00039-6.

Kumarathunge, D.P., Medlyn, B.E., Drake, J.E., Tjoelker, M.G., Aspinwall, M.J., Battaglia, M., Cano, F.J., Carter, K.R., Cavaleri, M.A., Cernusak, L.A., Chambers, J.Q., Crous, K.Y., De Kauwe, M.G., Dillaway, D.N., Dreyer, E., Ellsworth, D.S., Ghannoum, O., Han, Q., Hikosaka, K., Jensen, A.M., Kelly, J.W.G., Kruger, E.L., Mercado, L.M., Onoda, Y., Reich, P.B., Rogers, A., Slot, M., Smith, N.G., Tarvainen, L., Tissue, D.T., Togashi, H.F., Tribuzy, E.S., Uddling, J., Vårhammar, A., Wallin, G., Warren, J.M. and Way, D.A. (2019) 'Acclimation and adaptation components of the temperature dependence of plant photosynthesis at the global scale', *New Phytologist*, 222(2), pp. 768–784. Available at: https://doi.org/10.1111/NPH.15668.

Kumari, S., Yadav, S., Patra, D., Singh, S., Sarkar, A.K. and Panigrahi, K.C.S. (2019) 'Uncovering the molecular signature underlying the light intensity-dependent root development in Arabidopsis thaliana', *BMC Genomics*, 20(1), p. 596. Available at: https://doi.org/10.1186/s12864-019-5933-5.

Langmead, B. and Salzberg, S.L. (2012) 'Fast gapped-read alignment with Bowtie 2', *Nature methods*, 9(4), p. 357. Available at: https://doi.org/10.1038/NMETH.1923.

Lauria, M., Rupe, M., Guo, M., Kranz, E., Pirona, R., Viotti, A. and Lund, G. (2004) 'Extensive Maternal DNA Hypomethylation in the Endosperm of Zea mays', *Plant Cell*, 16(2), pp. 510–522. Available at: https://doi.org/10.1105/tpc.017780.

Law, J.A. and Jacobsen, S.E. (2010) 'Establishing, maintaining and modifying DNA methylation patterns in plants and animals', *Nature Reviews Genetics*, pp. 204–220. Available at: https://doi.org/10.1038/nrg2719.

Lawson, T., von Caemmerer, S. and Baroli, I. (2010) 'Photosynthesis and Stomatal Behaviour', in. Springer, Berlin, Heidelberg, pp. 265–304. Available at: https://doi.org/10.1007/978-3-642-13145-5_11.

Lawson, T., Kramer, D.M. and Raines, C.A. (2012) 'Improving yield by exploiting mechanisms underlying natural variation of photosynthesis', *Current Opinion in Biotechnology*. Elsevier Current Trends, pp. 215–220. Available at:

https://doi.org/10.1016/j.copbio.2011.12.012.

Lawson, T., Oxborough, K., Morison, J.I.L. and Baker, N.R. (2002) 'Responses of photosynthetic electron transport in stomatal guard cells and mesophyll cells in intact leaves to light, CO2, and humidity', *Plant Physiology*, 128(1), pp. 52–62. Available at: https://doi.org/10.1104/pp.010317.

Lewsey, M.G., Hardcastle, T.J., Melnyk, C.W., Molnar, A., Valli, A., Urich, M.A., Nery, J.R., Baulcombe, D.C. and Ecker, J.R. (2016) 'Mobile small RNAs regulate genome-wide DNA methylation', *Proceedings of the National Academy of Sciences of the United States of America*, 113(6), pp. E801–E810. Available at: https://doi.org/10.1073/PNAS.1515072113/SUPPL_FILE/PNAS.1515072113.SD05.XLSX.

Li, H., Handsaker, B., Wysoker, A., Fennell, T., Ruan, J., Homer, N., Marth, G., Abecasis, G. and Durbin, R. (2009) 'The Sequence Alignment/Map format and SAMtools', *Bioinformatics*, 25(16), pp. 2078–2079. Available at: https://doi.org/10.1093/BIOINFORMATICS/BTP352.

Li, K., Qiu, H., Zhou, M., Lin, Y., Guo, Z. and Lu, S. (2018) 'Chloroplast protein 12 expression alters growth and chilling tolerance in tropical forage stylosanthes guianensis (aublet) sw', *Frontiers in Plant Science*, 9. Available at: https://doi.org/10.3389/FPLS.2018.01319/.

Li, W., Liu, H., Cheng, Z.J., Su, Y.H., Han, H.N., Zhang, Y. and Zhang, X.S. (2011) 'DNA Methylation and Histone Modifications Regulate De Novo Shoot Regeneration in Arabidopsis by Modulating WUSCHEL Expression and Auxin Signaling', *PLoS Genetics*. Edited by L.-J. Qu, 7(8), p. e1002243. Available at: https://doi.org/10.1371/journal.pgen.1002243.

Li, Z., Ahn, T.K., Avenson, T.J., Ballottari, M., Cruz, J.A., Kramer, D.M., Bassi, R., Fleming, G.R., Keasling, J.D. and Niyogi, K.K. (2009) 'Lutein accumulation in the absence of zeaxanthin restores nonphotochemical quenching in the arabidopsis thaliana npq1 mutant', *Plant Cell*, 21(6), pp. 1798–1812. Available at: https://doi.org/10.1105/tpc.109.066571.

Liao, Y., Smyth, G.K. and Shi, W. (2014) 'featureCounts: an efficient general purpose program for assigning sequence reads to genomic features', *Bioinformatics*, 30(7), pp. 923–930. Available at: https://doi.org/10.1093/BIOINFORMATICS/BTT656.

Lima-Melo, Y., Alencar, V.T.C.B., Lobo, A.K.M., Sousa, R.H. V., Tikkanen, M., Aro, E.-M., Silveira, J.A.G. and Gollan, P.J. (2019) 'Photoinhibition of Photosystem I Provides Oxidative Protection During Imbalanced Photosynthetic Electron Transport in Arabidopsis thaliana', *Frontiers in Plant Science*, 10, p. 916. Available at: https://doi.org/10.3389/fpls.2019.00916.

Lippman, Z., Gendrel, A.V., Black, M., Vaughn, M.W., Dedhia, N., McCombie, W.R., Lavine, K., Mittal, V., May, B., Kasschau, K.B., Carrington, J.C., Doerge, R.W., Colot, V. and Martienssen, R. (2004) 'Role of transposable elements in heterochromatin and epigenetic control', *Nature*, 430(6998), pp. 471–476. Available at: https://doi.org/10.1038/nature02651.

Lister, R., O'Malley, R.C., Tonti-Filippini, J., Gregory, B.D., Berry, C.C., Millar, A.H.

and Ecker, J.R. (2008) ‘Highly Integrated Single-Base Resolution Maps of the Epigenome in Arabidopsis’, *Cell*, 133(3), pp. 523–536. Available at: https://doi.org/10.1016/j.cell.2008.03.029.

Lister, R., Pelizzola, M., Dowen, R.H., Hawkins, R.D., Hon, G., Tonti-Filippini, J., Nery, J.R., Lee, L., Ye, Z., Ngo, Q.M., Edsall, L., Antosiewicz-Bourget, J., Stewart, R., Ruotti, V., Millar, A.H., Thomson, J.A., Ren, B. and Ecker, J.R. (2009) ‘Human DNA methylomes at base resolution show widespread epigenomic differences’, *Nature*, 462(7271), p. 315. Available at: https://doi.org/10.1038/NATURE08514.

Liu, C., Young, A.L., Starling-Windhof, A., Bracher, A., Saschenbrecker, S., Rao, B.V., Rao, K.V., Berninghausen, O., Mielke, T., Hartl, F.U., Beckmann, R. and Hayer-Hartl, M. (2010) ‘Coupled chaperone action in folding and assembly of hexadecameric Rubisco’, *Nature 2010 463:7278*, 463(7278), pp. 197–202. Available at: https://doi.org/10.1038/nature08651.

Liu, J., Feng, L., Li, J. and He, Z. (2015) ‘Genetic and epigenetic control of plant heat responses’, *Frontiers in Plant Science*, 6(APR), p. 267. Available at: https://doi.org/10.3389/FPLS.2015.00267/BIBTEX.

Liu, J. and He, Z. (2020) ‘Small DNA Methylation, Big Player in Plant Abiotic Stress Responses and Memory’, *Frontiers in Plant Science*, 11, p. 1977. Available at: https://doi.org/10.3389/FPLS.2020.595603/BIBTEX.

Liu, J., Lu, Y., Hua, W. and Last, R.L. (2019) ‘A New Light on Photosystem II Maintenance in Oxygenic Photosynthesis’, *Frontiers in Plant Science*. Frontiers Media S.A. Available at: https://doi.org/10.3389/fpls.2019.00975.

Liu, J., Zhao, Y., Sial, T.A., Liu, H., Wang, Y. and Zhang, J. (2022) ‘Photosynthetic Responses of Two Woody Halophyte Species to Saline Groundwater Irrigation in the Taklimakan Desert’, *Water*. Available at: https://doi.org/10.3390/w14091385.

Liu, N., Ni, Z., Zhang, H., Chen, Q., Gao, W., Cai, Y., Li, M., Sun, G. and Qu, Y.Y. (2018) ‘The gene encoding subunit a of the vacuolar h+-atpase from cotton plays an important role in conferring tolerance to water deficit’, *Frontiers in Plant Science*, 9, p. 758. Available at: https://doi.org/10.3389/FPLS.2018.00758/BIBTEX.

Liu, S., de Jonge, J., Trejo-Arellano, M.S., Santos-González, J., Köhler, C. and Hennig, L. (2021) ‘Role of H1 and DNA methylation in selective regulation of transposable elements during heat stress’, *New Phytologist*, 229(4), pp. 2238–2250. Available at: https://doi.org/10.1111/NPH.17018.

Liu, T., Li, Y., Huang, F. and Hou, X. (2017) ‘Cold acclimation alters DNA methylation patterns and confers tolerance to heat and increases growth rate in Brassica rapa’, *Journal of Experimental Botany*, 68(5), pp. 1213–1224.

Long, S.P., Zhu, X.-G., Naidu, S.L. and Ort, D.R. (2006) ‘Can improvement in photosynthesis increase crop yields?’, *Plant, Cell & Environment*, 29(3), pp. 315–330. Available at: https://doi.org/https://doi.org/10.1111/j.1365-3040.2005.01493.x.

López-Calcagno, P.E., Abuzaid, A.O., Lawson, T. and Raines, C.A. (2017) ‘Arabidopsis CP12 mutants have reduced levels of phosphoribulokinase and impaired function of the Calvin-Benson cycle’, *Journal of Experimental Botany*, 68(9), pp. 2285–2298. Available at: https://doi.org/10.1093/jxb/erx084.

López-Calcagno, P.E., Brown, K.L., Simkin, A.J., Fisk, S.J., Vialet-Chabrand, S., Lawson, T. and Raines, C.A. (2020) 'Stimulating photosynthetic processes increases productivity and water-use efficiency in the field', *Nature Plants*, 6(8), pp. 1054–1063. Available at: https://doi.org/10.1038/s41477-020-0740-1.

López-Calcagno, P.E., Fisk, S., Brown, K.L., Bull, S.E., South, P.F. and Raines, C.A. (2019) 'Overexpressing the H-protein of the glycine cleavage system increases biomass yield in glasshouse and field-grown transgenic tobacco plants', *Plant Biotechnology Journal*, 17(1), pp. 141–151. Available at: https://doi.org/https://doi.org/10.1111/pbi.12953.

López-Calcagno, P.E., Howard, T.P. and Raines, C.A. (2014) 'The CP12 protein family: A thioredoxin-mediated metabolic switch?', *Frontiers in Plant Science*. Frontiers Research Foundation, p. 9. Available at: https://doi.org/10.3389/fpls.2014.00009.

López Sánchez, A., Stassen, J.H.M., Furci, L., Smith, L.M. and Ton, J. (2016) 'The role of DNA (de)methylation in immune responsiveness of Arabidopsis', *The Plant Journal*, 88(3), pp. 361–374. Available at: https://doi.org/10.1111/TPJ.13252.

Love, M.I., Huber, W. and Anders, S. (2014) 'Moderated estimation of fold change and dispersion for RNA-seq data with DESeq2', *Genome Biology*, 15(12), pp. 1–21. Available at: https://doi.org/10.1186/S13059-014-0550-8/FIGURES/9.

Lu, L., Chen, X., Qian, S. and Zhong, X. (2018) 'The plant-specific histone residue Phe41 is important for genome-wide H3.1 distribution', *Nature Communications*, 9(1). Available at: https://doi.org/10.1038/s41467-018-02976-9.

Ma, Y., Long, C., Liu, G., Bai, H., Ma, L., Bai, T., Zuo, Y. and Li, S. (2022) 'WGBS combined with RNA-seq analysis revealed that Dnmt1 affects the methylation modification and gene expression changes during mouse oocyte vitrification', *Theriogenology*, 177, pp. 11–21. Available at: https://doi.org/10.1016/J.THERIOGENOLOGY.2021.09.032.

Madoka, Y., Tomizawa, K.I., Mizoi, J., Nishida, I., Nagano, Y. and Sasaki, Y. (2002) 'Chloroplast Transformation with Modified accD Operon Increases Acetyl-CoA Carboxylase and Causes Extension of Leaf Longevity and Increase in Seed Yield in Tobacco', *Plant and Cell Physiology*, 43(12), pp. 1518–1525. Available at: https://doi.org/10.1093/PCP/PCF172.

Madzima, T.F., Vendramin, S., Lynn, J.S., Lemert, P., Lu, K.C. and McGinnis, K.M. (2021) 'Direct and Indirect Transcriptional Effects of Abiotic Stress in Zea mays Plants Defective in RNA-Directed DNA Methylation', *Frontiers in Plant Science*, 12, p. 1645. Available at: https://doi.org/10.3389/FPLS.2021.694289/BIBTEX.

Makałowski, W., Gotea, V., Pande, A. and Makałowska, I. (2019) 'Transposable Elements: Classification, Identification, and Their Use As a Tool For Comparative Genomics', *Methods in Molecular Biology*, 1910, pp. 177–207. Available at: https://doi.org/10.1007/978-1-4939-9074-0_6.

Malagnac, F., Bartee, L. and Bender, J. (2002) 'An Arabidopsis SET domain protein required for maintenance but not establishment of DNA methylation', *EMBO Journal*, 21(24), pp. 6842–6852. Available at: https://doi.org/10.1093/emboj/cdf687.

Mallen-Ponce, M.J., Huertas, M.J., Sanchez-Riego, A.M. and Florencio, F.J. (2021)

‘Depletion of m-type thioredoxin impairs photosynthesis, carbon fixation, and oxidative stress in cyanobacteria’, *Plant Physiology*, 187(3), pp. 1325–1340. Available at: https://doi.org/10.1093/PLPHYS/KIAB321.

Marri, L., Thieulin-Pardo, G., Lebrun, R., Puppo, R., Zaffagnini, M., Trost, P., Gontero, B. and Sparla, F. (2014) ‘CP12-mediated protection of Calvin–Benson cycle enzymes from oxidative stress’, *Biochimie*, 97(1), pp. 228–237. Available at: https://doi.org/10.1016/J.BIOCHI.2013.10.018.

Marri, L., Zaffagnini, M., Collin, V., Issakidis-Bourguet, E., Lemaire, S.D., Pupillo, P., Sparla, F., Miginiac-Maslow, M. and Trost, P. (2009) ‘Prompt and easy activation by specific thioredoxins of calvin cycle enzymes of arabidopsis thaliana associated in the GAPDH/CP12/PRK supramolecular complex’, *Molecular Plant*, 2(2), pp. 259–269. Available at: https://doi.org/10.1093/mp/ssn061.

Masson, V., Le Moigne, P., Martin, E., Faroux, S., Alias, A., Alkama, R., Belamari, S., Barbu, A., Boone, A., Bouyssel, F., Brousseau, P., Brun, E., Calvet, J.C., Carrer, D., Decharme, B., Delire, C., Donier, S., Essaouini, K., Gibelin, A.L., Giordani, H., Habets, F., Jidane, M., Kerdraon, G., Kourzeneva, E., Lafaysse, M., Lafont, S., Lebeaupin Brossier, C., Lemonsu, A., Mahfouf, J.F., Marguinaud, P., Mokhtari, M., Morin, S., Pigeon, G., Salgado, R., Seity, Y., Taillefer, F., Tanguy, G., Tulet, P., Vincendon, B., Vionnet, V. and Voldoire, A. (2013) ‘The SURFEXv7.2 land and ocean surface platform for coupled or offline simulation of earth surface variables and fluxes’, *Geoscientific Model Development*, 6(4), pp. 929–960. Available at: https://doi.org/10.5194/GMD-6-929-2013.

Mathieu, O., Reinders, J., Čaikovski, M., Smathajitt, C. and Paszkowski, J. (2007) ‘Transgenerational Stability of the Arabidopsis Epigenome Is Coordinated by CG Methylation’, *Cell*, 130(5), pp. 851–862. Available at: https://doi.org/10.1016/j.cell.2007.07.007.

Matsuda, R., Ohashi-KANEKO, K., Fujiwara, K. and Kurata, K. (2007) ‘Analysis of the relationship between blue-light photon flux density and the photosynthetic properties of spinach (*Spinacia oleracea* L.) leaves with regard to the acclimation of photosynthesis to growth irradiance’, *Soil Science and Plant Nutrition*, 53(4), pp. 459–465. Available at: https://doi.org/10.1111/j.1747-0765.2007.00150.x.

Matthews, J.S.A., Vialet-Chabrand, S. and Lawson, T. (2018) ‘Acclimation to fluctuating light impacts the rapidity of response and diurnal rhythm of stomatal conductance’, *Plant Physiology*, 176(3), pp. 1939–1951. Available at: https://doi.org/10.1104/pp.17.01809.

Matzke, M.A. and Mosher, R.A. (2014) ‘RNA-directed DNA methylation: An epigenetic pathway of increasing complexity’, *Nature Reviews Genetics*. Nature Publishing Group, pp. 394–408. Available at: https://doi.org/10.1038/nrg3683.

Maxwell, K. and Johnson, G.N. (2000) ‘Chlorophyll fluorescence—a practical guide’, *Journal of Experimental Botany*, 51(345), pp. 659–668. Available at: https://doi.org/10.1093/jexbot/51.345.659.

McAusland, L., Vialet-Chabrand, S., Davey, P., Baker, N.R., Brendel, O. and Lawson, T. (2016) ‘Effects of kinetics of light-induced stomatal responses on photosynthesis and water-use efficiency’, *New Phytologist*, 211(4), pp. 1209–1220. Available at: https://doi.org/10.1111/nph.14000.

McClintock, B. (1950) ‘The Origin and Behavior of Mutable Loci in Maize’, *Proceedings of the National Academy of Sciences of the United States of America*, 36(6), p. 344. Available at: https://doi.org/10.1073/PNAS.36.6.344.

McClintock, B. (1953) ‘INDUCTION OF INSTABILITY AT SELECTED LOCI IN MAIZE’, *Genetics*, 38(6), pp. 579–599. Available at: https://doi.org/10.1093/GENETICS/38.6.579.

de Mendoza, A., Nguyen, T.V., Ford, E., Poppe, D., Buckberry, S., Pflueger, J., Grimmer, M.R., Stolzenburg, S., Bogdanovic, O., Oshlack, A., Farnham, P.J., Blancafort, P. and Lister, R. (2022) ‘Large-scale manipulation of promoter DNA methylation reveals context-specific transcriptional responses and stability’, *Genome Biology*, 23(1), pp. 1–31. Available at: https://doi.org/10.1186/S13059-022-02728-5/FIGURES/4.

Meyer, P. (2011) ‘DNA methylation systems and targets in plants’, *FEBS Letters*, 585(13), pp. 2008–2015. Available at: https://doi.org/10.1016/J.FEBSLET.2010.08.017.

Mishra, N.P. and Ghanotakis, D.F. (1994) ‘Exposure of a photosystem II complex to chemically generated singlet oxygen results in D1 fragments similar to the ones observed during aerobic photoinhibition’, *BBA - Bioenergetics*, 1187(3), pp. 296–300. Available at: https://doi.org/10.1016/0005-2728(94)90003-5.

Mishra, Y., Johansson Jänkänpää, H., Kiss, A.Z., Funk, C., Schröder, W.P. and Jansson, S. (2012) ‘Arabidopsis plants grown in the field and climate chambers significantly differ in leaf morphology and photosystem components’, *BMC Plant Biology*, 12(1), pp. 1–18. Available at: https://doi.org/10.1186/1471-2229-12-6/FIGURES/10.

Moore, L.D., Le, T. and Fan, G. (2013) ‘DNA methylation and its basic function’, *Neuropsychopharmacology*, pp. 23–38. Available at: https://doi.org/10.1038/npp.2012.112.

Morales, A. and Kaiser, E. (2020) ‘Photosynthetic Acclimation to Fluctuating Irradiance in Plants’, *Frontiers in Plant Science*, 11, p. 268. Available at: https://doi.org/10.3389/FPLS.2020.00268/BIBTEX.

Mousavi, S., Regni, L., Bocchini, M., Mariotti, R., Cultrera, N.G.M., Mancuso, S., Googlani, J., Chakerolhosseini, M.R., Guerrero, C., Albertini, E., Baldoni, L. and Proietti, P. (2019) ‘Physiological, epigenetic and genetic regulation in some olive cultivars under salt stress’, *Scientific Reports*, 9(1), pp. 1–17. Available at: https://doi.org/10.1038/s41598-018-37496-5.

Müller, M. and Munné-Bosch, S. (2021) ‘Hormonal impact on photosynthesis and photoprotection in plants’, *Plant Physiology*, 185(4), pp. 1500–1522. Available at: https://doi.org/10.1093/plphys/kiaa119.

Müller, P., Li, X.P. and Niyogi, K.K. (2001) ‘Non-photochemical quenching. A response to excess light energy’, *Plant Physiology*. American Society of Plant Biologists, pp. 1558–1566. Available at: https://doi.org/10.1104/pp.125.4.1558.

Muniandy, K., Tan, M.H., Shehnaz, S., Song, B.K., Ayub, Q. and Rahman, S. (2020) ‘Cytosine methylation of rice mitochondrial DNA from grain and leaf tissues’, *Planta*, 251(2), pp. 1–12. Available at: https://doi.org/10.1007/S00425-020-03349-

7/FIGURES/4.

Murata, N., Allakhverdiev, S.I. and Nishiyama, Y. (2012) ‘The mechanism of photoinhibition in vivo: Re-evaluation of the roles of catalase, α-tocopherol, non-photochemical quenching, and electron transport’, in *Biochimica et Biophysica Acta - Bioenergetics*. Elsevier, pp. 1127–1133. Available at: https://doi.org/10.1016/j.bbabio.2012.02.020.

Murchie, E.H. and Horton, P. (1997) ‘Acclimation of photosynthesis to irradiance and spectral quality in British plant species: Chlorophyll content, photosynthetic capacity and habitat preference’, *Plant, Cell and Environment*, 20(4), pp. 438–448. Available at: https://doi.org/10.1046/j.1365-3040.1997.d01-95.x.

Murchie, E.H., Hubbart, S., Peng, S. and Horton, P. (2005) ‘Acclimation of photosynthesis to high irradiance in rice: gene expression and interactions with leaf development’, *Journal of Experimental Botany*, 56(411), pp. 449–460. Available at: https://doi.org/10.1093/JXB/ERI100.

Murchie, E.H. and Lawson, T. (2013) ‘Chlorophyll fluorescence analysis: a guide to good practice and understanding some new applications’, *Journal of Experimental Botany*, 64(13), pp. 3983–3998. Available at: https://doi.org/10.1093/jxb/ert208.

Muyle, A.M., Seymour, D.K., Lv, Y., Huettel, B. and Gaut, B.S. (2022) ‘Gene Body Methylation in Plants: Mechanisms, Functions, and Important Implications for Understanding Evolutionary Processes’, *Genome Biology and Evolution*, 14(4). Available at: https://doi.org/10.1093/GBE/EVAC038.

Nagel, K.A., Schurr, U. and Walter, A. (2006) ‘Dynamics of root growth stimulation in Nicotiana tabacum in increasing light intensity’, *Plant, Cell and Environment*, 29(10), pp. 1936–1945. Available at: https://doi.org/10.1111/j.1365-3040.2006.01569.x.

Naito, K., Zhang, F., Tsukiyama, T., Saito, H., Hancock, C.N., Richardson, A.O., Okumoto, Y., Tanisaka, T. and Wessler, S.R. (2009) ‘Unexpected consequences of a sudden and massive transposon amplification on rice gene expression’, *Nature*, 461(7267), pp. 1130–1134. Available at: https://doi.org/10.1038/NATURE08479.

Naumann, K., Fischer, A., Hofmann, I., Krauss, V., Phalke, S., Irmler, K., Hause, G., Aurich, A.-C., Dorn, R., Jenuwein, T. and Reuter, G. (2005) ‘Pivotal role of AtSUVH2 in heterochromatic histone methylation and gene silencing in Arabidopsis’, *The EMBO Journal*, 24(7), pp. 1418–1429. Available at: https://doi.org/10.1038/sj.emboj.7600604.

Née, G., Zaffagnini, M., Trost, P. and Issakidis-Bourguet, E. (2009) ‘Redox regulation of chloroplastic glucose-6-phosphate dehydrogenase: A new role for f-type thioredoxin’, *FEBS Letters*, 583(17), pp. 2827–2832. Available at: https://doi.org/10.1016/J.FEBSLET.2009.07.035.

Nikkanen, L., Toivola, J., Diaz, M.G. and Rintamäki, E. (2017) ‘Chloroplast thioredoxin systems: Prospects for improving photosynthesis’, *Philosophical Transactions of the Royal Society B: Biological Sciences*, 372(1730). Available at: https://doi.org/10.1098/rstb.2016.0474.

Nilkens, M., Kress, E., Lambrev, P., Miloslavina, Y., Müller, M., Holzwarth, A.R. and Jahns, P. (2010) ‘Identification of a slowly inducible zeaxanthin-dependent component of non-photochemical quenching of chlorophyll fluorescence generated

under steady-state conditions in Arabidopsis', *Biochimica et Biophysica Acta - Bioenergetics*, 1797(4), pp. 466–475. Available at: https://doi.org/10.1016/j.bbabio.2010.01.001.

Niu, C., Jiang, L., Cao, F., Liu, C., Guo, J., Zhang, Z., Yue, Q., Hou, N., Liu, Z., Li, X., Tahir, M.M., He, J., Li, Z., Li, C., Ma, F. and Guan, Q. (2022) 'Methylation of a MITE insertion in the MdRFNR1-1 promoter is positively associated with its allelic expression in apple in response to drought stress', *The Plant cell*, 34(10), pp. 3983–4006. Available at: https://doi.org/10.1093/PLCELL/KOAC220.

Nusinow, D.A., Helfer, A., Hamilton, E.E., King, J.J., Imaizumi, T., Schultz, T.F., Farré, E.M. and Kay, S.A. (2011) 'The ELF4–ELF3–LUX complex links the circadian clock to diurnal control of hypocotyl growth', *Nature 2011 475:7356*, 475(7356), pp. 398–402. Available at: https://doi.org/10.1038/nature10182.

Okegawa, Y. and Motohashi, K. (2015) 'Chloroplastic thioredoxin m functions as a major regulator of Calvin cycle enzymes during photosynthesis in vivo', *The Plant Journal*, 84(5), pp. 900–913. Available at: https://doi.org/https://doi.org/10.1111/tpj.13049.

Onuchic, V., Lurie, E., Carrero, I., Pawliczek, P., Patel, R.Y., Rozowsky, J., Galeev, T., Huang, Z., Altshuler, R.C., Zhang, Z., Harris, R.A., Coarfa, C., Ashmore, L., Bertol, J.W., Fakhouri, W.D., Yu, F., Kellis, M., Gerstein, M. and Milosavljevic, A. (2018) 'Allele-specific epigenome maps reveal sequence-dependent stochastic switching at regulatory loci', *Science*, 361(6409). Available at: https://doi.org/10.1126/science.aar3146.

Ort, D.R., Merchant, S.S., Alric, J., Barkan, A., Blankenship, R.E., Bock, R., Croce, R., Hanson, M.R., Hibberd, J.M., Long, S.P., Moore, T.A., Moroney, J., Niyogi, K.K., Parry, M.A.J., Peralta-Yahya, P.P., Prince, R.C., Redding, K.E., Spalding, M.H., Van Wijk, K.J., Vermaas, W.F.J., Von Caemmerer, S., Weber, A.P.M., Yeates, T.O., Yuan, J.S. and Zhu, X.G. (2015) 'Redesigning photosynthesis to sustainably meet global food and bioenergy demand', *Proceedings of the National Academy of Sciences of the United States of America*. National Academy of Sciences, pp. 8529–8536. Available at: https://doi.org/10.1073/pnas.1424031112.

Ou, X., Zhang, Y., Xu, C., Lin, X., Zang, Q., Zhuang, T., Jiang, L., von Wettstein, D. and Liu, B. (2012) 'Transgenerational Inheritance of Modified DNA Methylation Patterns and Enhanced Tolerance Induced by Heavy Metal Stress in Rice (Oryza sativa L.)', *PLOS ONE*, 7(9), p. e41143. Available at: https://doi.org/10.1371/JOURNAL.PONE.0041143.

Park, P.J. (2009) 'ChIP-seq: Advantages and challenges of a maturing technology', *Nature Reviews Genetics*. Nature Publishing Group, pp. 669–680. Available at: https://doi.org/10.1038/nrg2641.

Paul, M.J., Knight, J.S., Habash, D., Parry, M.A.J., Lawlor, D.W., Barnes, S.A., Loynes, A. and Gray, J.C. (1995) 'Reduction in phosphoribulokinase activity by antisense RNA in transgenic tobacco: effect on CO2 assimilation and growth in low irradiance', *The Plant Journal*, 7(4), pp. 535–542. Available at: https://doi.org/10.1046/j.1365-313X.1995.7040535.x.

Pavlopoulou, A. and Kossida, S. (2007) 'Plant cytosine-5 DNA methyltransferases: Structure, function, and molecular evolution', *Genomics*, 90(4), pp. 530–541.

Available at: https://doi.org/10.1016/j.ygeno.2007.06.011.

Pazourek, J. (1970) ‘The effect of light intensity on stomatal frequency in leaves of Iris hollandica hort., var. wedgwood’, *Biologia Plantarum*, 12(2), pp. 208–215. Available at: https://doi.org/10.1007/BF02920869.

Pearcy, R.W. (1990) ‘Sunflecks and Photosynthesis in Plant Canopies’, *https://doi.org/10.1146/annurev.pp.41.060190.002225*, 41(1), pp. 421–453. Available at: https://doi.org/10.1146/ANNUREV.PP.41.060190.002225.

Pearcy, R.W., Chazdon, R.L. and Kirschbaum, M.U.F. (1987) ‘Photosynthetic Utilization of Lightflecks by Tropical Forest Plants’, *Progress in Photosynthesis Research*, pp. 257–260. Available at: https://doi.org/10.1007/978-94-017-0519-6_56.

Pearcy, R.W., Gross, L.J. and He, D. (1997) ‘An improved dynamic model of photosynthesis for estimation of carbon gain in sunfleck light regimes’, *Plant, Cell & Environment*, 20(4), pp. 411–424. Available at: https://doi.org/10.1046/J.1365-3040.1997.D01-88.X.

Pérez-Bueno, M.L., Johnson, M.P., Zia, A., Ruban, A. V. and Horton, P. (2008) ‘The Lhcb protein and xanthophyll composition of the light harvesting antenna controls the ΔpH-dependency of non-photochemical quenching in Arabidopsis thaliana’, *FEBS Letters*, 582(10), pp. 1477–1482. Available at: https://doi.org/10.1016/J.FEBSLET.2008.03.040.

Pick, T.R., Bräutigam, A., Schulz, M.A., Obata, T., Fernie, A.R. and Weber, A.P.M. (2013) ‘PLGG1, a plastidic glycolate glycerate transporter, is required for photorespiration and defines a unique class of metabolite transporters’, *Proceedings of the National Academy of Sciences of the United States of America*, 110(8), pp. 3185–3190. Available at: https://doi.org/10.1073/PNAS.1215142110/-/DCSUPPLEMENTAL.

Pikaard, C.S. and Scheid, O.M. (2014) ‘Epigenetic Regulation in Plants’, *Cold Spring Harbor Perspectives in Biology*, 6(12). Available at: https://doi.org/10.1101/CSHPERSPECT.A019315.

Pontvianne, F., Blevins, T. and Pikaard, C.S. (2010) ‘Arabidopsis Histone Lysine Methyltransferases’, in *Advances in botanical research*. NIH Public Access, pp. 1–22. Available at: https://doi.org/10.1016/s0065-2296(10)53001-5.

Poorter, H. and Nagel, O. (2000) ‘The role of biomass allocation in the growth response of plants to different levels of light, CO2, nutrients and water: A quantitative review’, *IMF Occasional Papers*, 27(189), pp. 595–607. Available at: https://doi.org/10.1071/pp99173_co.

Poorter, H., Niinemets, Ü., Ntagkas, N., Siebenkäs, A., Mäenpää, M., Matsubara, S. and Pons, T.L. (2019) ‘A meta-analysis of plant responses to light intensity for 70 traits ranging from molecules to whole plant performance’, *New Phytologist*. Blackwell Publishing Ltd, pp. 1073–1105. Available at: https://doi.org/10.1111/nph.15754.

Porebski, S., Bailey, L.G. and Baum, B.R. (1997) *Modification of a CTAB DNA Extraction Protocol for Plants Containing High Polysaccharide and Polyphenol Components*, *Plant Molecular Biology Reporter*.

Pospíšil, P. (2016) ‘Production of reactive oxygen species by photosystem II as a response to light and temperature stress’, *Frontiers in Plant Science*, 7(DECEMBER2016). Available at: https://doi.org/10.3389/fpls.2016.01950.

Powelson, R.A. and Lieffers, V.J. (1992) ‘Effect of Light and Nutrients on Biomass Allocation in Calamagrostis canadensis’, *Ecography*. WileyNordic Society Oikos, pp. 31–36. Available at: https://doi.org/10.2307/3682960.

Preiser, A.L., Fisher, N., Banerjee, A. and Sharkey, T.D. (2019) ‘Plastidic glucose-6-phosphate dehydrogenases are regulated to maintain activity in the light’, *The Biochemical journal*, 476(10), pp. 1539–1551. Available at: https://doi.org/10.1042/BCJ20190234.

Preite, V., Oplaat, C., Biere, A., Kirschner, J., van der Putten, W.H. and Verhoeven, K.J.F. (2018) ‘Increased transgenerational epigenetic variation, but not predictable epigenetic variants, after environmental exposure in two apomictic dandelion lineages’, *Ecology and Evolution*, 8(5), pp. 3047–3059. Available at: https://doi.org/10.1002/ece3.3871.

Prerostova, S., Černý, M., Dobrev, P.I., Motyka, V., Hluskova, L., Zupkova, B., Gaudinova, A., Knirsch, V., Janda, T., Brzobohatý, B. and Vankova, R. (2021) ‘Light Regulates the Cytokinin-Dependent Cold Stress Responses in Arabidopsis’, *Frontiers in Plant Science*, 11. Available at: https://doi.org/10.3389/fpls.2020.608711.

Qian, Y., Hu, W., Liao, J., Zhang, J. and Ren, Q. (2019) ‘The Dynamics of DNA methylation in the maize (Zea mays L.) inbred line B73 response to heat stress at the seedling stage’, *Biochemical and Biophysical Research Communications*, 512(4), pp. 742–749. Available at: https://doi.org/10.1016/J.BBRC.2019.03.150.

Quadrana, L., Almeida, J., Asís, R., Duffy, T., Dominguez, P.G., Bermúdez, L., Conti, G., Corrêa Da Silva, J. V., Peralta, I.E., Colot, V., Asurmendi, S., Fernie, A.R., Rossi, M. and Carrari, F. (2014) ‘Natural occurring epialleles determine vitamin e accumulation in tomato fruits’, *Nature Communications*, 5(1), pp. 1–11. Available at: https://doi.org/10.1038/ncomms5027.

Quadrana, L., Etcheverry, M., Gilly, A., Caillieux, E., Madoui, M.A., Guy, J., Bortolini Silveira, A., Engelen, S., Baillet, V., Wincker, P., Aury, J.M. and Colot, V. (2019) ‘Transposition favors the generation of large effect mutations that may facilitate rapid adaption’, *Nature Communications*, 10(1). Available at: https://doi.org/10.1038/S41467-019-11385-5.

Quesneville, H. (2020) ‘Twenty years of transposable element analysis in the Arabidopsis thaliana genome’, *Mobile DNA*, 11(1), pp. 1–13. Available at: https://doi.org/10.1186/S13100-020-00223-X/FIGURES/4.

Raha, D., Hong, M. and Snyder, M. (2010) ‘ChIP-Seq: A method for global identification of regulatory elements in the genome’, *Current Protocols in Molecular Biology*. Curr Protoc Mol Biol. Available at: https://doi.org/10.1002/0471142727.mb2119s91.

Ramírez-González, R.H., Borrill, P., Lang, D., Harrington, S.A., Brinton, J., Venturini, L., Davey, M., Jacobs, J., Van Ex, F., Pasha, A., Khedikar, Y., Robinson, S.J., Cory, A.T., Florio, T., Concia, L., Juery, C., Schoonbeek, H., Steuernagel, B., Xiang, D., Ridout, C.J., Chalhoub, B., Mayer, K.F.X., Benhamed, M., Latrasse, D.,

Bendahmane, A., Wulff, B.B.H., Appels, R., Tiwari, V., Datla, R., Choulet, F., Pozniak, C.J., Provart, N.J., Sharpe, A.G., Paux, E., Spannagl, M., Bräutigam, A. and Uauy, C. (2018) 'The transcriptional landscape of polyploid wheat', *Science*, 361(6403). Available at: https://doi.org/10.1126/SCIENCE.AAR6089/SUPPL_FILE/AAR6089_RAMIREZ-GONZALES_SM_TABLES.XLSX.

Razin, A. and Cedar, H. (1991) 'DNA methylation and gene expression.', *Microbiology and Molecular Biology Reviews*, 55(3), pp. 451–458.

Rendina González, A.P., Preite, V., Verhoeven, K.J.F. and Latzel, V. (2018) 'Transgenerational Effects and Epigenetic Memory in the Clonal Plant Trifolium repens', *Frontiers in Plant Science*, 9, p. 1677. Available at: https://doi.org/10.3389/fpls.2018.01677.

Rintamäki, E., Salo, R., Lehtonen, E. and Aro, E.M. (1995) 'Regulation of D1-protein degradation during photoinhibition of photosystem II in vivo: Phosphorylation of the D1 protein in various plant groups', *Planta*, 195(3), pp. 379–386. Available at: https://doi.org/10.1007/BF00202595.

Roden, L.C., Song, H.R., Jackson, S., Morris, K. and Carre, I.A. (2002) 'Floral responses to photoperiod are correlated with the timing of rhythmic expression relative to dawn and dusk in Arabidopsis', *Proceedings of the National Academy of Sciences of the United States of America*, 99(20), pp. 13313–13318. Available at: https://doi.org/10.1073/PNAS.192365599/SUPPL_FILE/3655FIG7NEW.PDF.

Roquis, D., Robertson, M., Yu, L., Thieme, M., Julkowska, M. and Bucher, E. (2021) 'Genomic impact of stress-induced transposable element mobility in Arabidopsis', *Nucleic Acids Research*, 49(18), pp. 10431–10447. Available at: https://doi.org/10.1093/NAR/GKAB828.

Roudier, F., Ahmed, I., Bérard, C., Sarazin, A., Mary-Huard, T., Cortijo, S., Bouyer, D., Caillieux, E., Duvernois-Berthet, E., Al-Shikhley, L., Giraut, L., Després, B., Drevensek, S., Barneche, F., Dèrozier, S., Brunaud, V., Aubourg, S., Schnittger, A., Bowler, C., Martin-Magniette, M.-L., Robin, S., Caboche, M. and Colot, V. (2011) 'Integrative epigenomic mapping defines four main chromatin states in Arabidopsis', *The EMBO Journal*, 30(10), pp. 1928–1938. Available at: https://doi.org/10.1038/emboj.2011.103.

Ruelland, E. and Miginiac-Maslow, M. (1999) 'Regulation of chloroplast enzyme activities by thioredoxins: Activation or relief from inhibition?', *Trends in Plant Science*. Trends Plant Sci, pp. 136–141. Available at: https://doi.org/10.1016/S1360-1385(99)01391-6.

Russell, A.W., Critchley, C., Robinson, S.A., Franklin, L.A., Seaton, C.C.R., Chow, S., Anderson, J.M. and Osmond, C.B. (1995) *Photosystem II Regulation and Dynamics of the Chloroplast D1 Protein in Arabidopsis Leaves during Photosynthesis and Photoinhibition'*, *Plant Physiol*. Available at: www.plantphysiol.org (Accessed: 25 March 2020).

Rymen, B., Kawamura, A., Lambolez, A., Inagaki, S., Takebayashi, A., Iwase, A., Sakamoto, Y., Sako, K., Favero, D.S., Ikeuchi, M., Suzuki, T., Seki, M., Kakutani, T., Roudier, F. and Sugimoto, K. (2019) 'Histone acetylation orchestrates wound-induced transcriptional activation and cellular reprogramming in Arabidopsis',

Communications Biology, 2(1). Available at: https://doi.org/10.1038/s42003-019-0646-5.

Saeed, F., Chaudhry, U.K., Bakhsh, A., Raza, A., Saeed, Y., Bohra, A. and Varshney, R.K. (2022) 'Moving Beyond DNA Sequence to Improve Plant Stress Responses', *Frontiers in Genetics*, 13, p. 929. Available at: https://doi.org/10.3389/FGENE.2022.874648/BIBTEX.

Sáez-Laguna, E., Guevara, M.-Á., Díaz, L.-M., Sánchez-Gómez, D., Collada, C., Aranda, I. and Cervera, M.-T. (2014) 'Epigenetic Variability in the Genetically Uniform Forest Tree Species Pinus pinea L', *PLoS ONE*. Edited by K. Kashkush, 9(8), p. e103145. Available at: https://doi.org/10.1371/journal.pone.0103145.

Sahrawy, M., Fernández-Trijueque, J., Vargas, P. and Serrato, A.J. (2022) 'Comprehensive Expression Analyses of Plastidial Thioredoxins of Arabidopsis thaliana Indicate a Main Role of Thioredoxin m2 in Roots', *Antioxidants*, 11(7). Available at: https://doi.org/10.3390/antiox11071365.

Sahu, P.P., Pandey, G., Sharma, N., Puranik, S., Muthamilarasan, M. and Prasad, M. (2013) 'Epigenetic mechanisms of plant stress responses and adaptation', *Plant Cell Reports*, 32(8), pp. 1151–1159. Available at: https://doi.org/10.1007/S00299-013-1462-X/TABLES/1.

Sanchez, D.H., Gaubert, H., Drost, H.G., Zabet, N.R. and Paszkowski, J. (2017) 'High-frequency recombination between members of an LTR retrotransposon family during transposition bursts', *Nature Communications*, 8(1). Available at: https://doi.org/10.1038/s41467-017-01374-x.

Schippers, J.H., Foyer, C.H. and van Dongen, J.T. (2016) 'Redox regulation in shoot growth, SAM maintenance and flowering.', *Current opinion in plant biology*, 29, pp. 121–128. Available at: https://doi.org/10.1016/j.pbi.2015.11.009.

Schlüter, U., Muschak, M., Berger, D. and Altmann, T. (2003) 'Photosynthetic performance of an Arabidopsis mutant with elevated stomatal density (sdd1-1) under different light regimes', *Journal of Experimental Botany*, 54(383), pp. 867–874. Available at: https://doi.org/10.1093/jxb/erg087.

Schmidt, D., Wilson, M.D., Spyrou, C., Brown, G.D., Hadfield, J. and Odom, D.T. (2009) 'ChIP-seq: Using high-throughput sequencing to discover protein-DNA interactions', *Methods*, 48(3), pp. 240–248. Available at: https://doi.org/10.1016/j.ymeth.2009.03.001.

Schneider, C.A., Rasband, W.S. and Eliceiri, K.W. (2012) 'NIH Image to ImageJ: 25 years of image analysis', *Nature Methods*. Nature Publishing Group, pp. 671–675. Available at: https://doi.org/10.1038/nmeth.2089.

Schneider, T., Bolger, A., Zeier, J., Preiskowski, S., Benes, V., Trenkamp, S., Usadel, B., Farré, E.M. and Matsubara, S. (2019) 'Fluctuating Light Interacts with Time of Day and Leaf Development Stage to Reprogram Gene Expression', *Plant Physiology*, 179(4), p. 1632. Available at: https://doi.org/10.1104/PP.18.01443.

Schumann, T., Paul, S., Melzer, M., Dörmann, P. and Jahns, P. (2017) 'Plant growth under natural light conditions provides highly flexible short-term acclimation properties toward high light stress', *Frontiers in Plant Science*, 8. Available at: https://doi.org/10.3389/fpls.2017.00681.

Secco, D., Wang, C., Shou, H., Schultz, M.D., Chiarenza, S., Nussaume, L., Ecker, J.R., Whelan, J. and Lister, R. (2015) 'Stress induced gene expression drives transient DNA methylation changes at adjacent repetitive elements', *eLife*, 4(JULY2015). Available at: https://doi.org/10.7554/eLife.09343.001.

Seibert, M., Wetherbee, P.J. and Job, D.D. (1975) *The Effects of Light Intensity and Spectral Quality on Growth and Shoot Initiation in Tobacco Callus*, *Plant Physiol*. Available at: www.plantphysiol.org (Accessed: 28 May 2020).

Serrato, A.J., Rojas-González, J.A., Torres-Romero, D., Vargas, P., Mérida, Á. and Sahrawy, M. (2021) 'Thioredoxins m are major players in the multifaceted light-adaptive response in Arabidopsis thaliana', *The Plant Journal*, 108(1), pp. 120–133. Available at: https://doi.org/https://doi.org/10.1111/tpj.15429.

Shan, X., Wang, X., Yang, G., Wu, Y., Su, S., Li, S., Liu, H. and Yuan, Y. (2013) 'Analysis of the DNA methylation of maize (Zea mays L.) in response to cold stress based on methylation-sensitive amplified polymorphisms', *Journal of Plant Biology*, 56(1), pp. 32–38. Available at: https://doi.org/10.1007/S12374-012-0251-3/METRICS.

Sharkey, T.D. and Raschke, K. (1981a) 'Effect of Light Quality on Stomatal Opening in Leaves of Xanthium strumarium L.', *Plant Physiology*. American Society of Plant Biologists (ASPB), pp. 1170–1174. Available at: https://doi.org/10.2307/4267066.

Sharkey, T.D. and Raschke, K. (1981b) 'Separation and Measurement of Direct and Indirect Effects of Light on Stomata', *Plant Physiology*, 68(1), pp. 33–40. Available at: https://doi.org/10.1104/pp.68.1.33.

Sharkey, T.D. and Weise, S.E. (2016) 'The glucose 6-phosphate shunt around the Calvin–Benson cycle', *Journal of Experimental Botany*, 67(14), pp. 4067–4077. Available at: https://doi.org/10.1093/JXB/ERV484.

Shi, L., Song, J., Guo, C., Wang, B., Guan, Z., Yang, P., Chen, X., Zhang, Q., King, G.J., Wang, J. and Liu, K. (2019) 'A CACTA-like transposable element in the upstream region of BnaA9.CYP78A9 acts as an enhancer to increase silique length and seed weight in rapeseed', *The Plant Journal*, 98(3), pp. 524–539. Available at: https://doi.org/10.1111/TPJ.14236.

Shim, S., Lee, H.G. and Seo, P.J. (2021) 'MET1-Dependent DNA Methylation Represses Light Signaling and Influences Plant Regeneration in Arabidopsis', *Molecules and Cells*, 44(10), p. 746. Available at: https://doi.org/10.14348/MOLCELLS.2021.0160.

Shimazaki, K., Doi, M., Assmann, S.M. and Kinoshita, T. (2007) 'Light Regulation of Stomatal Movement', *Annual Review of Plant Biology*, 58(1), pp. 219–247. Available at: https://doi.org/10.1146/annurev.arplant.57.032905.105434.

Shin-ichiro, I., Toshinori, K., Atsushi, T., Doi, M. and Ken-ichiro, S. (2008) 'Leaf Positioning of Arabidopsis in Response to Blue Light', *Molecular Plant*, 1(1), pp. 15–26. Available at: https://doi.org/https://doi.org/10.1093/mp/ssm001.

Shin, M., Tagawa, K. and Arnon, D.I. (1963) 'CRYSTALLIZATION OF FERREDOXIN-TPN REDUCTASE AND ITS ROLE IN THE PHOTOSYNTHETIC APPARATUS OF CHLOROPLASTS.', *Biochemische Zeitschrift*, 338, pp. 84–96.

Shook, M.S. and Richards, E.J. (2014) ‘VIM proteins regulate transcription exclusively through the MET1 cytosine methylation pathway’, *Epigenetics*, 9(7), pp. 980–986. Available at: https://doi.org/10.4161/epi.28906.

Shu, H., Nakamura, M., Siretskiy, A., Borghi, L., Moraes, I., Wildhaber, T., Gruissem, W. and Hennig, L. (2014) ‘Arabidopsis replacement histone variant H3.3 occupies promoters of regulated genes’, *Genome Biology*, 15(4). Available at: https://doi.org/10.1186/gb-2014-15-4-r62.

Singh, P., Kaloudas, D. and Raines, C.A. (2008) ‘Expression analysis of the Arabidopsis CP12 gene family suggests novel roles for these proteins in roots and floral tissues’, *Journal of Experimental Botany*, 59(14), pp. 3975–3985. Available at: https://doi.org/10.1093/jxb/ern236.

Slotkin, R.K. (2016) ‘Plant epigenetics: from genotype to phenotype and back again’, in *Genome biology*, p. 57. Available at: https://doi.org/10.1186/s13059-016-0920-5.

Smith, N.G. and Dukes, J.S. (2013) ‘Plant respiration and photosynthesis in global-scale models: Incorporating acclimation to temperature and CO2’, *Global Change Biology*, 19(1), pp. 45–63. Available at: https://doi.org/10.1111/J.1365-2486.2012.02797.X.

Song, Y., Jia, Z., Hou, Y., Ma, X., Li, L., Jin, X. and An, L. (2020) ‘Roles of DNA Methylation in Cold Priming in Tartary Buckwheat’, *Frontiers in Plant Science*, 11, p. 2022. Available at: https://doi.org/10.3389/FPLS.2020.608540/BIBTEX.

Soppe, W.J.J., Jacobsen, S.E., Alonso-Blanco, C., Jackson, J.P., Kakutani, T., Koornneef, M. and Peeters, A.J.M. (2000) ‘The late flowering phenotype of fwa mutants is caused by gain-of-function epigenetic alleles of a homeodomain gene’, *Molecular cell*, 6(4), pp. 791–802. Available at: https://doi.org/10.1016/S1097-2765(05)00090-0.

Steward, N., Ito, M., Yamaguchi, Y., Koizumi, N. and Sano, H. (2002) ‘Periodic DNA methylation in maize nucleosomes and demethylation by environmental stress’, *Journal of Biological Chemistry*, 277(40), pp. 37741–37746. Available at: https://doi.org/10.1074/jbc.M204050200.

Stroud, H., Otero, S., Desvoyes, B., Ramírez-Parra, E., Jacobsen, S.E. and Gutierrez, C. (2012) ‘Genome-wide analysis of histone H3.1 and H3.3 variants in Arabidopsis thaliana’, *Proceedings of the National Academy of Sciences of the United States of America*, 109(14), pp. 5370–5375. Available at: https://doi.org/10.1073/pnas.1203145109.

Studer, A., Zhao, Q., Ross-Ibarra, J. and Doebley, J. (2011) ‘Identification of a functional transposon insertion in the maize domestication gene tb1’, *Nature Genetics 2011 43:11*, 43(11), pp. 1160–1163. Available at: https://doi.org/10.1038/ng.942.

Stuefer, J.F. and Huber, H. (1998) ‘Differential effects of light quantity and spectral light quality on growth, morphology and development of two stoloniferous Potentilla species’, *Oecologia*, 117(1–2), pp. 1–8. Available at: https://doi.org/10.1007/s004420050624.

Suetsugu, N., Kagawa, T. and Wada, M. (2005) ‘An auxilin-like J-domain protein, JAC1, regulates phototropin-mediated chloroplast movement in Arabidopsis’, *Plant*

physiology, 139(1), pp. 151–162. Available at: https://doi.org/10.1104/PP.105.067371.

Sun, S., Zhu, J., Guo, R., Whelan, J. and Shou, H. (2021) 'DNA methylation is involved in acclimation to iron-deficiency in rice (Oryza sativa)', *The Plant journal : for cell and molecular biology*, 107(3), pp. 727–739. Available at: https://doi.org/10.1111/TPJ.15318.

Tamoi, M., Miyazaki, T., Fukamizo, T. and Shigeoka, S. (2005) 'The Calvin cycle in cyanobacteria is regulated by CP12 via the NAD(H)/NADP(H) ratio under light/dark conditions', *Plant Journal*, 42(4), pp. 504–513. Available at: https://doi.org/10.1111/j.1365-313X.2005.02391.x.

Tanaka, Y., Sugano, S.S., Shimada, T. and Hara-Nishimura, I. (2013) 'Enhancement of leaf photosynthetic capacity through increased stomatal density in Arabidopsis', *New Phytologist*, 198(3), pp. 757–764. Available at: https://doi.org/10.1111/nph.12186.

Tang, Y., Liu, Xuncheng, Liu, Xu, Li, Y., Wu, K. and Hou, X. (2017) 'Arabidopsis NF-YCs Mediate the Light-Controlled Hypocotyl Elongation via Modulating Histone Acetylation', *Molecular Plant*, 10(2), pp. 260–273. Available at: https://doi.org/10.1016/J.MOLP.2016.11.007.

Taylor, S.H. and Long, S.P. (2017) 'Slow induction of photosynthesis on shade to sun transitions in wheat may cost at least 21% of productivity', *Philosophical Transactions of the Royal Society B: Biological Sciences*, 372(1730). Available at: https://doi.org/10.1098/RSTB.2016.0543.

Teixeira, F.K. and Colot, V. (2009) 'Gene body DNA methylation in plants: a means to an end or an end to a means?', *The EMBO Journal*, 28(8), p. 997. Available at: https://doi.org/10.1038/EMBOJ.2009.87.

Terashima, I., Hanba, Y.T., Tazoe, Y., Vyas, P. and Yano, S. (2006) 'Irradiance and phenotype: comparative eco-development of sun and shade leaves in relation to photosynthetic CO2 diffusion', *Journal of Experimental Botany*, 57(2), pp. 343–354. Available at: https://doi.org/10.1093/jxb/erj014.

The Arabidopsis Information Resource (2019) *TAIR - Download - TAIR10 genome release*. Available at: https://www.arabidopsis.org/download/index-auto.jsp%3Fdir%3D%252Fdownload_files%252FGenes%252FTAIR10_genome_release (Accessed: 8 April 2022).

Thiebaut, F., Hemerly, A.S. and Ferreira, P.C.G. (2019) 'A Role for Epigenetic Regulation in the Adaptation and Stress Responses of Non-model Plants', *Frontiers in Plant Science*, 10. Available at: https://doi.org/10.3389/fpls.2019.00246.

Thormählen, I., Zupok, A., Rescher, J., Leger, J., Weissenberger, S., Groysman, J., Orwat, A., Chatel-Innocenti, G., Issakidis-Bourguet, E., Armbruster, U. and Geigenberger, P. (2017) 'Thioredoxins Play a Crucial Role in Dynamic Acclimation of Photosynthesis in Fluctuating Light', *Molecular Plant*, 10(1), pp. 168–182. Available at: https://doi.org/10.1016/j.molp.2016.11.012.

Tian, Y., Sacharz, J., Ware, M.A., Zhang, H. and Ruban, A. V. (2017) 'Effects of periodic photoinhibitory light exposure on physiology and productivity of Arabidopsis plants grown under low light', *Journal of Experimental Botany*, 68(15), pp. 4249–

4262. Available at: https://doi.org/10.1093/jxb/erx213.

Tikkanen, M. and Aro, E.-M. (2014) ‘Integrative regulatory network of plant thylakoid energy transduction’, *Trends in Plant Science*, 19(1), pp. 10–17. Available at: https://doi.org/10.1016/j.tplants.2013.09.003.

Tikkanen, M. and Grebe, S. (2018) ‘Switching off photoprotection of photosystem I – a novel tool for gradual PSI photoinhibition’, *Physiologia Plantarum*, 162(2), pp. 156–161. Available at: https://doi.org/10.1111/ppl.12618.

Tiwari, B., Habermann, K., Arif, M.A., Top, O. and Frank, W. (2021) ‘Identification of Small RNAs During High Light Acclimation in Arabidopsis thaliana’, *Frontiers in Plant Science*, 12, p. 1179. Available at: https://doi.org/10.3389/FPLS.2021.656657/BIBTEX.

Tong, W., Li, R., Huang, J., Zhao, H., Ge, R., Wu, Q., Mallano, A.I., Wang, Y., Li, F., Deng, W., Li, Y. and Xia, E. (2021) ‘Divergent DNA methylation contributes to duplicated gene evolution and chilling response in tea plants’, *The Plant Journal*, 106(5), pp. 1312–1327. Available at: https://doi.org/10.1111/TPJ.15237.

Trap-Gentil, M.V., Hébrard, C., Lafon-Placette, C., Delaunay, A., Hagge, D., Joseph, C., Brignolas, F., Lefebvre, M., Barnes, S. and Maury, S. (2011) ‘Time course and amplitude of DNA methylation in the shoot apical meristem are critical points for bolting induction in sugar beet and bolting tolerance between genotypes’, *Journal of experimental botany*, 62(8), pp. 2585–2597. Available at: https://doi.org/10.1093/JXB/ERQ433.

Vaughn, M.W., Tanurdžić, M., Lippman, Z., Jiang, H., Carrasquillo, R., Rabinowicz, P.D., Dedhia, N., McCombie, W.R., Agier, N., Bulski, A., Colot, V., Doerge, R.W. and Martienssen, R.A. (2007) ‘Epigenetic Natural Variation in Arabidopsis thaliana’, *PLOS Biology*, 5(7), p. e174. Available at: https://doi.org/10.1371/JOURNAL.PBIO.0050174.

Veley, K.M., Elliott, K., Jensen, G., Zhong, Z., Feng, S., Yoder, M., Gilbert, K.B., Berry, J.C., Lin, Z.J.D., Ghoshal, B., Gallego-Bartolomé, J., Norton, J., Motomura-Wages, S., Carrington, J.C., Jacobsen, S.E. and Bart, R.S. (2023) ‘Improving cassava bacterial blight resistance by editing the epigenome’, *Nature communications*, 14(1). Available at: https://doi.org/10.1038/S41467-022-35675-7.

Verhoeven, K.J.F., Jansen, J.J., van Dijk, P.J. and Biere, A. (2010) ‘Stress-induced DNA methylation changes and their heritability in asexual dandelions’, *New Phytologist*, 185(4), pp. 1108–1118. Available at: https://doi.org/10.1111/j.1469-8137.2009.03121.x.

Vialet-Chabrand, S., Matthews, J.S.A., Simkin, A.J., Raines, C.A. and Lawson, T. (2017) ‘Importance of fluctuations in light on plant photosynthetic acclimation’, *Plant Physiology*, 173(4), pp. 2163–2179. Available at: https://doi.org/10.1104/pp.16.01767.

Vidal, E., Sayols, S., Moran, S., Guillaumet-Adkins, A., Schroeder, M.P., Royo, R., Orozco, M., Gut, M., Gut, I., Lopez-Bigas, N., Heyn, H. and Esteller, M. (2017) ‘A DNA methylation map of human cancer at single base-pair resolution’, *Oncogene 2017 36:40*, 36(40), pp. 5648–5657. Available at: https://doi.org/10.1038/onc.2017.176.

Villagómez-Aranda, A.L., García-Ortega, L.F., Torres-Pacheco, I. and Guevara-González, R.G. (2021) 'Whole-Genome DNA Methylation Analysis in Hydrogen Peroxide Overproducing Transgenic Tobacco Resistant to Biotic and Abiotic Stresses', *Plants*, 10(1), pp. 1–14. Available at: https://doi.org/10.3390/PLANTS10010178.

Virdi, K.S., Laurie, J.D., Xu, Y.Z., Yu, J., Shao, M.R., Sanchez, R., Kundariya, H., Wang, D., Riethoven, J.J.M., Wamboldt, Y., Arrieta-Montiel, M.P., Shedge, V. and Mackenzie, S.A. (2015) 'Arabidopsis MSH1 mutation alters the epigenome and produces heritable changes in plant growth', *Nature Communications 2015 6:1*, 6(1), pp. 1–9. Available at: https://doi.org/10.1038/ncomms7386.

Virdi, K.S.S., Wamboldt, Y., Kundariya, H., Laurie, J.D.D., Keren, I., Kumar, K.R.S., Block, A., Basset, G., Luebker, S., Elowsky, C., Day, P.M.M., Roose, J.L.L., Bricker, T.M.M., Elthon, T. and Mackenzie, S.A.A. (2016) 'MSH1 Is a Plant Organellar DNA Binding and Thylakoid Protein under Precise Spatial Regulation to Alter Development', *Molecular Plant*, 9(2), pp. 245–260. Available at: https://doi.org/10.1016/J.MOLP.2015.10.011.

Vojta, A., Dobrinic, P., Tadic, V., Bockor, L., Korac, P., Julg, B., Klasic, M. and Zoldos, V. (2016) 'Repurposing the CRISPR-Cas9 system for targeted DNA methylation', *Nucleic Acids Research*, 44(12), pp. 5615–5628. Available at: https://doi.org/10.1093/NAR/GKW159.

Wakao, S. and Benning, C. (2005) 'Genome-wide analysis of glucose-6-phosphate dehydrogenases in Arabidopsis', *The Plant Journal*, 41(2), pp. 243–256. Available at: https://doi.org/10.1111/J.1365-313X.2004.02293.X.

Walker, B.J., South, P.F. and Ort, D.R. (2016) 'Physiological evidence for plasticity in glycolate/glycerate transport during photorespiration', *Photosynthesis Research*, 129(1), p. 93. Available at: https://doi.org/10.1007/S11120-016-0277-3.

Walters, R.G. (2005) 'Towards an understanding of photosynthetic acclimation', *Journal of Experimental Botany*, 56(411), pp. 435–447. Available at: https://doi.org/10.1093/jxb/eri060.

Walters, R.G. and Horton, P. (1994) 'Acclimation of Arabidopsis thaliana to the light environment: Changes in composition of the photosynthetic apparatus', *Planta*, 195(2), pp. 248–256. Available at: https://doi.org/10.1007/BF00199685.

Walters, R.G. and Horton, P. (1995) 'Acclimation of Arabidopsis thaliana to the light environment: changes in photosynthetic function', *Planta*. Springer, pp. 306–312. Available at: https://doi.org/10.2307/23384235.

Wang, F., Wu, N., Zhang, L., Ahammed, G.J., Chen, X., Xiang, X., Zhou, J., Xia, X., Shi, K., Yu, J., Foyer, C.H. and Zhou, Y. (2018) 'Light signaling-dependent regulation of photoinhibition and photoprotection in Tomato', *Plant Physiology*, 176(2), pp. 1311–1326. Available at: https://doi.org/10.1104/pp.17.01143.

Wang, J.W. (2014) 'Regulation of flowering time by the miR156-mediated age pathway', *Journal of Experimental Botany*, 65(17), pp. 4723–4730. Available at: https://doi.org/10.1093/JXB/ERU246.

Wang, P., Hendron, R.W. and Kelly, S. (2017) 'Transcriptional control of photosynthetic capacity: conservation and divergence from Arabidopsis to rice', *New*

Phytologist, 216(1), pp. 32–45. Available at: https://doi.org/10.1111/NPH.14682.

Wang, R.Y., Gehrke, C.W. and Ehrlich, M. (1980) 'Comparison of bisulfite modification of 5-methyldeoxycytidine and deoxycytidine residues.', *Nucleic acids research*, 8(20), pp. 4777–4790. Available at: https://doi.org/10.1093/nar/8.20.4777.

Wang, S., Zhou, Z., Rahiman, R., Lee, G.S.Y., Yeo, Y.K., Yang, X. and Lau, O.S. (2021) 'Light regulates stomatal development by modulating paracrine signaling from inner tissues', *Nature Communications*, 12(1), p. 3403. Available at: https://doi.org/10.1038/s41467-021-23728-2.

Wang, X., Weigel, D. and Smith, L.M. (2013) 'Transposon Variants and Their Effects on Gene Expression in Arabidopsis', *PLOS Genetics*, 9(2), p. e1003255. Available at: https://doi.org/10.1371/JOURNAL.PGEN.1003255.

Wang, Y., Burgess, S.J., de Becker, E. and Long, S.P. (2020) 'Photosynthesis in the fleeting shadows: An overlooked opportunity for increasing crop productivity?', *The Plant Journal*, p. tpj.14663. Available at: https://doi.org/10.1111/tpj.14663.

Wang, Y., Liu, S., Tian, X., Fu, Y., Jiang, X., Li, Y. and Wang, G. (2018) 'Influence of light intensity on chloroplast development and pigment accumulation in the wild-type and etiolated mutant plants of Anthurium andraeanum "Sonate"', *Plant Signaling and Behavior*, 13(8), pp. 1–5. Available at: https://doi.org/10.1080/15592324.2018.1482174.

Wang, Z. and Baulcombe, D.C. (2020) 'Transposon age and non-CG methylation', *Nature Communications*, 11(1), p. 1221. Available at: https://doi.org/10.1038/s41467-020-14995-6.

Ward, B.L., Anderson, R.S. and Bendich, A.J. (1981) 'The mitochondrial genome is large and variable in a family of plants (Cucurbitaceae)', *Cell*, 25(3), pp. 793–803. Available at: https://doi.org/10.1016/0092-8674(81)90187-2.

Ware, M.A., Belgio, E. and Ruban, A. V. (2015) 'Comparison of the protective effectiveness of NPQ in Arabidopsis plants deficient in PsbS protein and zeaxanthin', *Journal of Experimental Botany*, 66(5), pp. 1259–1270. Available at: https://doi.org/10.1093/jxb/eru477.

Waters, M.T., Wang, P., Korkaric, M., Capper, R.G., Saunders, N.J. and Langdale, J.A. (2009) 'GLK Transcription Factors Coordinate Expression of the Photosynthetic Apparatus in Arabidopsis', *The Plant Cell*, 21(4), pp. 1109–1128. Available at: https://doi.org/10.1105/TPC.108.065250.

Wedel, N., Soll, J. and Paap, B.K. (1997) *CP12 provides a new mode of light regulation of Calvin cycle activity in higher plants (chloroplastphotosynthesisglyceraldehyde-3-phosphate dehydrogenaseD-ribulose-5-phosphate kinaseNADPH)*. Available at: www.pnas.org. (Accessed: 17 May 2021).

Wells, J.N. and Feschotte, C. (2020) 'A Field Guide to Eukaryotic Transposable Elements', *Annual review of genetics*, 54, p. 539. Available at: https://doi.org/10.1146/ANNUREV-GENET-040620-022145.

Wenderoth, I., Scheibe, R. and Von Schaewen, A. (1997) 'Identification of the cysteine residues involved in redox modification of plant plastidic glucose-6-phosphate dehydrogenase', *Journal of Biological Chemistry*, 272(43), pp. 26985–

26990. Available at: https://doi.org/10.1074/jbc.272.43.26985.

Wendte, J.M., Zhang, Y., Ji, L., Shi, X., Hazarika, R.R., Shahryary, Y., Johannes, F. and Schmitz, R.J. (2019) 'Epimutations are associated with CHROMOMETHYLASE 3-induced de novo DNA methylation', *eLife*, 8. Available at: https://doi.org/10.7554/eLife.47891.

Wieser, H., Koehler, P. and Scherf, K.A. (2020) 'The Two Faces of Wheat ', *Frontiers in Nutrition* . Available at: https://www.frontiersin.org/articles/10.3389/fnut.2020.517313.

Wild, A. and Wolf, G. (1980) 'The Effect of Different Light Intensities on the Frequency and Size of Stomata, the Size of Cells, the Number, Size and Chlorophyll Content of Chloroplasts in the Mesophyll and the Guard Cells during the Ontogeny of Primary Leaves of Sinapis alba', *Zeitschrift für Pflanzenphysiologie*, 97(4), pp. 325–342. Available at: https://doi.org/10.1016/s0044-328x(80)80006-7.

Williams, B.P. and Gehring, M. (2017) 'Stable transgenerational epigenetic inheritance requires a DNA methylation-sensing circuit', *Nature Communications*, 8(1). Available at: https://doi.org/10.1038/s41467-017-02219-3.

Wyler, M., Stritt, C., Walser, J.C., Baroux, C. and Roulin, A.C. (2020) 'Impact of Transposable Elements on Methylation and Gene Expression across Natural Accessions of Brachypodium distachyon', *Genome Biology and Evolution*, 12(11), p. 1994. Available at: https://doi.org/10.1093/GBE/EVAA180.

Xu, M., Hu, T. and Scott Poethig, R. (2021) 'Low light intensity delays vegetative phase change', *Plant Physiology*, 187(3), pp. 1177–1188. Available at: https://doi.org/10.1093/PLPHYS/KIAB243.

Yan, H., Kikuchi, S., Neumann, P., Zhang, W., Wu, Y., Chen, F. and Jiang, J. (2010) 'Genome-wide mapping of cytosine methylation revealed dynamic DNA methylation patterns associated with genes and centromeres in rice', *The Plant Journal*, 63(3), pp. 353–365. Available at: https://doi.org/10.1111/J.1365-313X.2010.04246.X.

Yan, H., Liu, Y., Zhang, K., Song, J., Xu, W. and Su, Z. (2019) 'Chromatin state-based analysis of epigenetic H3K4me3 marks of Arabidopsis in response to dark stress', *Frontiers in Genetics*, 10(APR). Available at: https://doi.org/10.3389/fgene.2019.00306.

Yang, L., Conway, S.R. and Poethig, R.S. (2011) 'Vegetative phase change is mediated by a leaf-derived signal that represses the transcription of miR156', *Development*, 138(2), pp. 245–249. Available at: https://doi.org/10.1242/DEV.058578.

Yang, L., Lang, C., Wu, Y., Meng, D., Yang, T., Li, D., Jin, T. and Zhou, X. (2022) 'ROS1-mediated decrease in DNA methylation and increase in expression of defense genes and stress response genes in Arabidopsis thaliana due to abiotic stresses', *BMC Plant Biology*, 22(1), pp. 1–10. Available at: https://doi.org/10.1186/S12870-022-03473-4/FIGURES/4.

Yang, Y., Jin, H., Chen, Y., Lin, W., Wang, C., Chen, Z., Han, N., Bian, H., Zhu, M. and Wang, J. (2012) 'A chloroplast envelope membrane protein containing a putative LrgB domain related to the control of bacterial death and lysis is required for chloroplast development in Arabidopsis thaliana', *New Phytologist*, 193(1), pp. 81–

95. Available at: https://doi.org/10.1111/J.1469-8137.2011.03867.X.

Yin, Y., Morgunova, E., Jolma, A., Kaasinen, E., Sahu, B., Khund-Sayeed, S., Das, P.K., Kivioja, T., Dave, K., Zhong, F., Nitta, K.R., Taipale, M., Popov, A., Ginno, P.A., Domcke, S., Yan, J., Schübeler, D., Vinson, C. and Taipale, J. (2017) 'Impact of cytosine methylation on DNA binding specificities of human transcription factors', *Science*, 356(6337). Available at: https://doi.org/10.1126/science.aaj2239.

Yin, Z.H. and Johnson, G.N. (2000) 'Photosynthetic acclimation of higher plants to growth in fluctuating light environments', *Photosynthesis Research*, 63(1), pp. 97–107. Available at: https://doi.org/10.1023/A:1006303611365.

Yokochi, Y., Yoshida, K., Hahn, F., Miyagi, A., Wakabayashi, K.I., Kawai-Yamada, M., Weber, A.P.M. and Hisabori, T. (2021) 'Redox regulation of NADP-malate dehydrogenase is vital for land plants under fluctuating light environment', *Proceedings of the National Academy of Sciences of the United States of America*, 118(6), p. e2016903118. Available at: https://doi.org/10.1073/PNAS.2016903118/SUPPL_FILE/PNAS.2016903118.SAPP.PDF.

Yu, H. and Ong, B.L. (2003) 'Effect of radiation quality on growth and photosynthesis of Acacia mangium seedlings', *Photosynthetica*, 41(3), pp. 349–355. Available at: https://doi.org/10.1023/B:PHOT.0000015458.11643.b2.

Yu, Q.-B., Ma, Q., Kong, M.-M., Zhao, T.-T., Zhang, X.-L., Zhou, Q., Huang, C., Chong, K. and Yang, Z.-N. (2014) 'AtECB1/MRL7, a Thioredoxin-Like Fold Protein with Disulfide Reductase Activity, Regulates Chloroplast Gene Expression and Chloroplast Biogenesis in Arabidopsis thaliana', *Molecular Plant*, 7, pp. 206–217. Available at: https://doi.org/10.1093/mp/sst092.

Yu, X., Zheng, G., Shan, L., Meng, G., Vingron, M., Liu, Q. and Zhu, X.G. (2014) 'Reconstruction of gene regulatory network related to photosynthesis in Arabidopsis thaliana', *Frontiers in Plant Science*, 5(JUN). Available at: https://doi.org/10.3389/FPLS.2014.00273/ABSTRACT.

Yuan, L. and Xu, D.Q. (2001) 'Stimulation effect of gibberellic acid short-term treatment on leaf photosynthesis related to the increase in Rubisco content in broad bean and soybean', *Photosynthesis Research*, 68(1), pp. 39–47. Available at: https://doi.org/10.1023/A:1011894912421/METRICS.

Zabet, N.R., Catoni, M., Prischi, F. and Paszkowski, J. (2017) 'Cytosine methylation at CpCpG sites triggers accumulation of non-CpG methylation in gene bodies', *Nucleic Acids Research*, 45(7), pp. 3777–3784. Available at: https://doi.org/10.1093/nar/gkw1330.

Zaks, J., Amarnath, K., Sylak-Glassman, E.J. and Fleming, G.R. (2013) 'Models and measurements of energy-dependent quenching', *Photosynthesis Research*. Springer, pp. 389–409. Available at: https://doi.org/10.1007/s11120-013-9857-7.

Zeiger, E. and Zhu, J. (1998) 'Role of zeaxanthin in blue light photoreception and the modulation of light-CO 2 interactions in guard cells', *Journal of Experimental Botany*. Oxford University Press, pp. 433–442. Available at: https://doi.org/10.2307/23695976.

Zeller, S.L., Kalinina, O., Brunner, S., Keller, B. and Schmid, B. (2010) 'Transgene ×

Environment Interactions in Genetically Modified Wheat', *PLOS ONE*, 5(7), p. e11405. Available at: https://doi.org/10.1371/JOURNAL.PONE.0011405.

Zhang, C., Qian, Q., Huang, X., Zhang, W., Liu, X. and Hou, X. (2021) 'NF-YCs modulate histone variant H2A.Z deposition to regulate photomorphogenic growth in Arabidopsis', *Journal of Integrative Plant Biology*, 63(6), pp. 1120–1132. Available at: https://doi.org/10.1111/JIPB.13109/SUPPINFO.

Zhang, D.-W., Yuan, S., Xu, F., Zhu, F., Yuan, M., Ye, H.-X., Guo, H.-Q., Lv, X., Yin, Y. and Lin, H.-H. (2016) 'Light intensity affects chlorophyll synthesis during greening process by metabolite signal from mitochondrial alternative oxidase in Arabidopsis', *Plant, Cell & Environment*, 39(1), pp. 12–25. Available at: https://doi.org/10.1111/pce.12438.

Zhang, J.Y., Zhang, Q.H., Shuang, S.P., Cun, Z., Wu, H.M. and Chen, J.W. (2021) 'The Responses of Light Reaction of Photosynthesis to Dynamic Sunflecks in a Typically Shade-Tolerant Species Panax notoginseng', *Frontiers in Plant Science*, 12. Available at: https://doi.org/10.3389/FPLS.2021.718981.

Zhang, M., Cui, G., Bai, X., Ye, Z., Zhang, S., Xie, K., Sun, F., Zhang, C. and Xi, Y. (2021) 'Regulatory Network of Preharvest Sprouting Resistance Revealed by Integrative Analysis of mRNA, Noncoding RNA, and DNA Methylation in Wheat', *Journal of Agricultural and Food Chemistry*, 69(13), pp. 4018–4035. Available at: https://doi.org/10.1021/ACS.JAFC.1C00050/SUPPL_FILE/JF1C00050_SI_018.PDF.

Zhang, T., Maruhnich, S.A. and Folta, K.M. (2011) 'Green light induces shade avoidance symptoms', *Plant Physiology*, 157(3), pp. 1528–1536. Available at: https://doi.org/10.1104/pp.111.180661.

Zhang, X., Sun, J., Cao, X. and Song, X. (2015) 'Epigenetic Mutation of RAV6 Affects Leaf Angle and Seed Size in Rice', *Plant Physiology*, 169, pp. 2118–2128. Available at: https://doi.org/10.1104/pp.15.00836.

Zhao, H., Xu, D., Tian, T., Kong, F., Lin, K., Gan, S., Zhang, H. and Li, G. (2021) 'Molecular and functional dissection of EARLY-FLOWERING 3 (ELF3) and ELF4 in Arabidopsis', *Plant Science*, 303, p. 110786. Available at: https://doi.org/10.1016/J.PLANTSCI.2020.110786.

Zheng, J., Chen, F., Wang, Z., Cao, H., Li, X., Deng, X., Soppe, W.J.J., Li, Y. and Liu, Y. (2012) 'A novel role for histone methyltransferase KYP/SUVH4 in the control of Arabidopsis primary seed dormancy', *New Phytologist*, 193(3), pp. 605–616. Available at: https://doi.org/10.1111/j.1469-8137.2011.03969.x.

Zhou, L., Ng, H.K., Drautz-Moses, D.I., Schuster, S.C., Beck, S., Kim, C., Chambers, J.C. and Loh, M. (2019) 'Systematic evaluation of library preparation methods and sequencing platforms for high-throughput whole genome bisulfite sequencing', *Scientific Reports*, 9(1). Available at: https://doi.org/10.1038/S41598-019-46875-5.

Zhu, X.-G., Ort, D.R., Whitmarsh, J. and Long, S.P. (2004a) 'The slow reversibility of photosystem II thermal energy dissipation on transfer from high to low light may cause large losses in carbon gain by crop canopies: a theoretical analysis', *Journal of Experimental Botany*, 55(400), pp. 1167–1175. Available at: https://doi.org/10.1093/jxb/erh141.

Zhu, X.-G., Ort, D.R., Whitmarsh, J. and Long, S.P. (2004b) 'The slow reversibility of

photosystem II thermal energy dissipation on transfer from high to low light may cause large losses in carbon gain by crop canopies: a theoretical analysis', *Journal of Experimental Botany*, 55(400), pp. 1167–1175. Available at: https://doi.org/10.1093/jxb/erh141.

Zilberman, D., Coleman-Derr, D., Ballinger, T. and Henikoff, S. (2008) 'Histone H2A.Z and DNA methylation are mutually antagonistic chromatin marks', *Nature 2008 456:7218*, 456(7218), pp. 125–129. Available at: https://doi.org/10.1038/nature07324.

Zilberman, D., Gehring, M., Tran, R.K., Ballinger, T. and Henikoff, S. (2007) 'Genome-wide analysis of Arabidopsis thaliana DNA methylation uncovers an interdependence between methylation and transcription', *Nature Genetics*, 39(1), pp. 61–69. Available at: https://doi.org/10.1038/ng1929.

Chapter 8: Supplementary Data

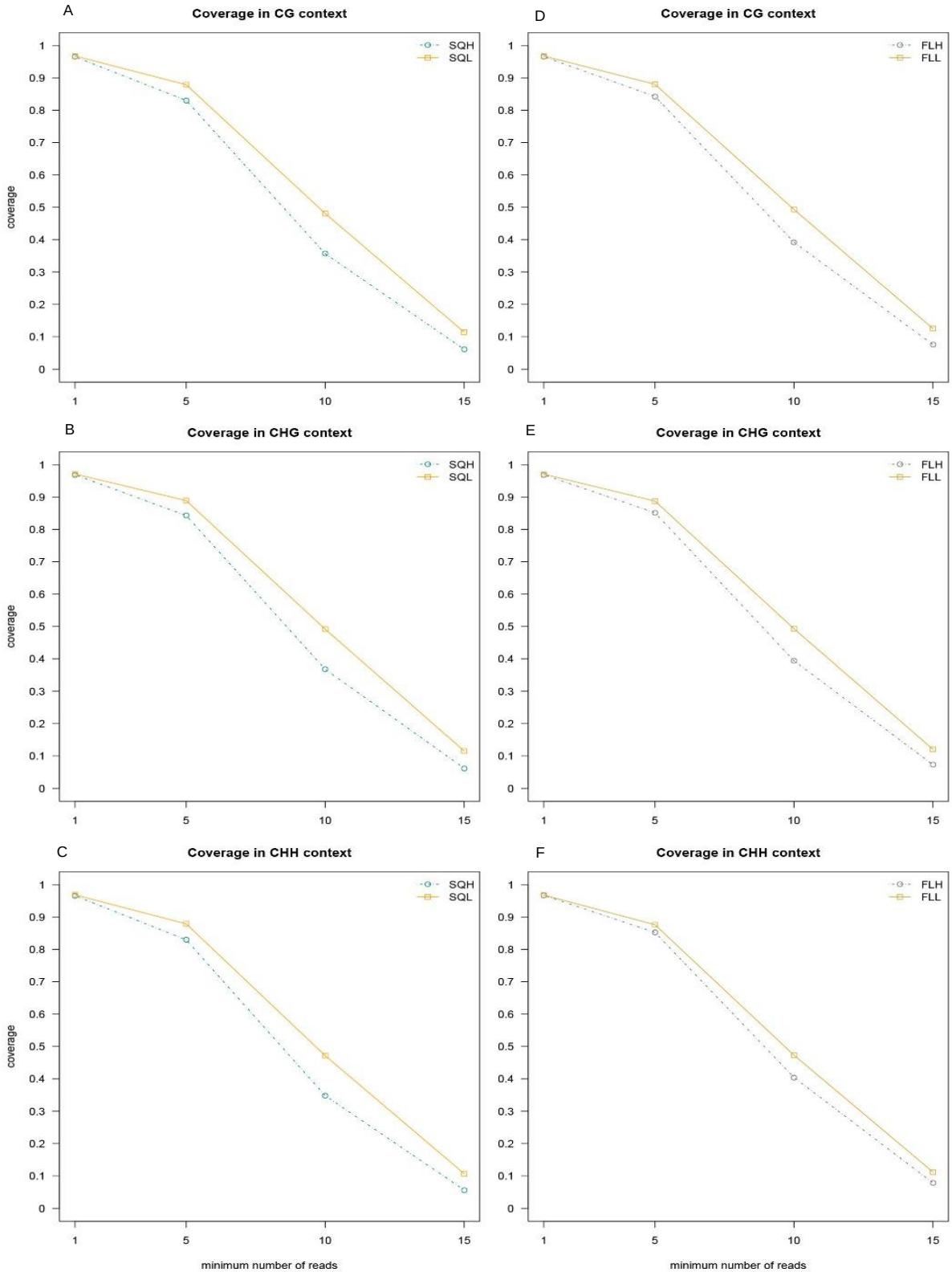

Figure S1: Coverage of whole genome bisulfite sequencing for each sequence context in SQH and SQL samples (**A-C**), and FLH and FLL (**D-F**) samples

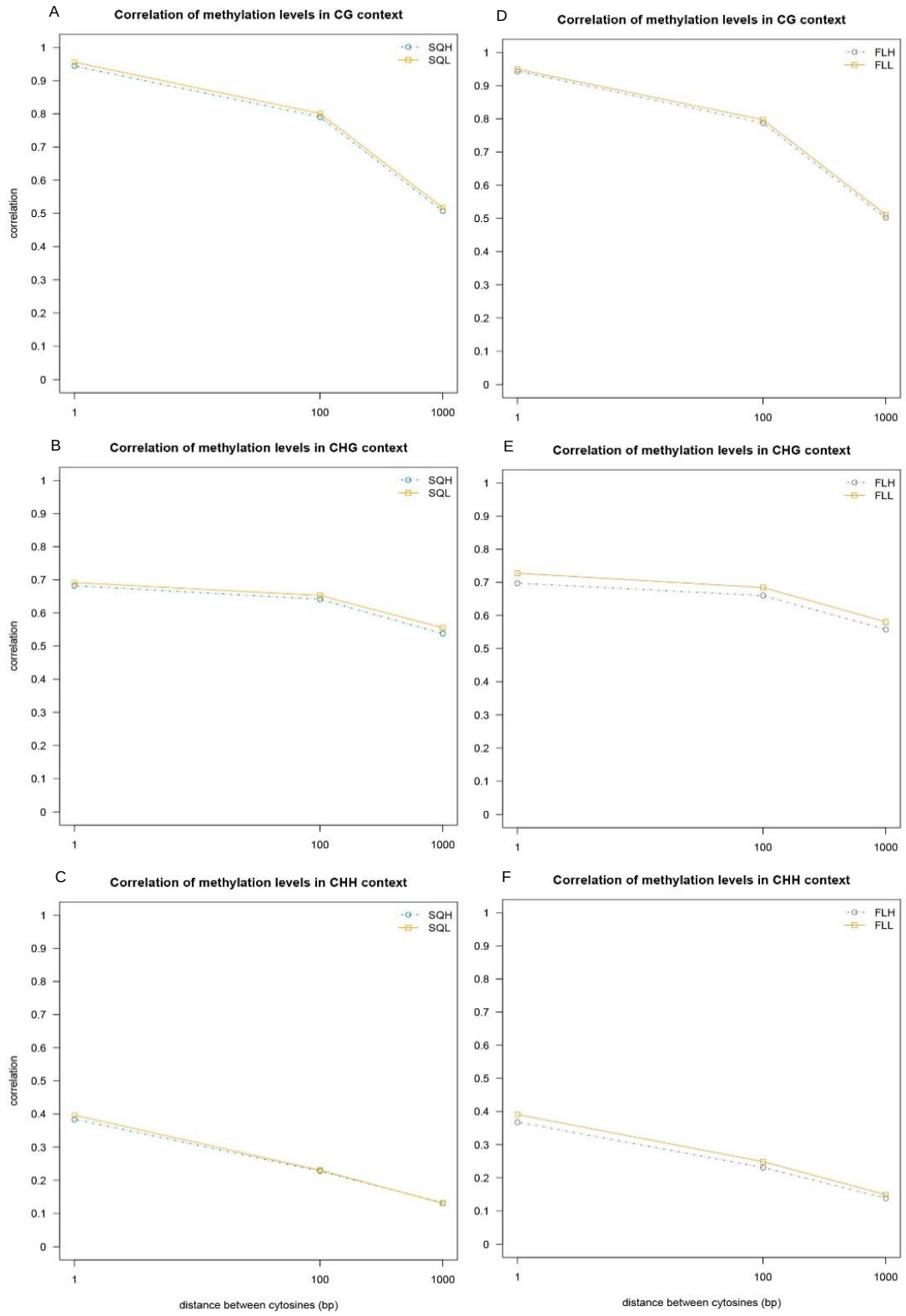

Figure S2: Correlation of methylation in each sequence context for SQH and SQL samples (**A-C**), and FLH and FLL samples (**D-F**).

Table S1: Differentially methylated genes between regime comparisons. SQ=SQHvSQL, FL=FLHvFLL, HL=SQHvFLH, LL=SQLvFLL

Regime comparisons	Differentially methylated genes
SQ	AT1G09486,AT1G27490,AT1G27815,AT1G29620,AT1G30470,AT1G32010,AT1G33100,AT1G33300,AT1G34530,AT1G34620,AT1G36100,AT1G36190,AT1G36230,AT1G36440,AT1G36720,AT1G36950,AT1G37070,AT1G37801,AT1G38149,AT1G38176,AT1G40085,AT1G40093,AT1G40310,AT1G41743,AT1G42160,AT1G42310,AT1G42365,AT1G42410,AT1G42460,AT1G42740,AT1G43200,AT1G43950,AT1G44070,AT1G45080,AT1G47960,AT1G48422,AT1G48953,AT1G50055,AT1G51150,AT1G52960,AT1G54130,AT1G54720,AT1G55700,AT1G55740,AT1G62770,AT1G64440,AT1G66730,AT1G73177,AT1G77815,AT1G77820,AT2G02330,AT2G03080,AT2G04010,AT2G04035,AT2G04310,AT2G05490,AT2G06400,AT2G06500,AT2G07740,AT2G07744,AT2G09890,AT2G10200,AT2G10720,AT2G10960,AT2G11235,AT2G11320,AT2G11640,AT2G11770,AT2G12000,AT2G12500,AT2G12600,AT2G13530,AT2G14190,AT2G14420,AT2G15470,AT2G15770,AT2G16560,AT2G17920,AT2G19140,AT2G22160,AT2G23220,AT2G25370,AT2G25550,AT2G27190,AT2G37370,AT2G41590,AT3G08560,AT3G09960,AT3G11165,AT3G16590,AT3G22940,AT3G25727,AT3G26260,AT3G28157,AT3G28193,AT3G28918,AT3G29615,AT3G30370,AT3G30410,AT3G30413,AT3G30440,AT3G30720,AT3G30780,AT3G30825,AT3G31373,AT3G32093,AT3G32116,AT3G32385,AT3G32895,AT3G32904,AT3G33006,AT3G33175,AT3G42624,AT3G42653,AT3G42700,AT3G42796,AT3G43290,AT3G43433,AT3G43570,AT3G44130,AT3G44210,AT3G44215,AT3G44325,AT3G44755,AT3G45300,AT3G45490,AT3G47320,AT3G50770,AT3G60565,AT4G01240,AT4G03876,AT4G04223,AT4G04270,AT4G05595,AT4G05612,AT4G05613,AT4G05616,AT4G06595,AT4G06686,AT4G06704,AT4G07330,AT4G07492,AT4G08036,AT4G08130,AT4G08262,AT4G08375,AT4G09380,AT4G09875,AT4G09960,AT4G10613,AT4G22650,AT4G26320,AT4G36460,AT5G01080,AT5G18890,AT5G18990,AT5G19015,AT5G24900,AT5G25045,AT5G25320,AT5G26650,AT5G27170,AT5G27250,AT5G27882,AT5G27947,AT5G27965,AT5G28052,AT5G28580,AT5G28627,AT5G29015,AT5G29028,AT5G30218,AT5G31905,AT5G31945,AT5G32053,AT5G32228,AT5G32402,AT5G32488,AT5G32510,AT5G32563,AT5G32800,AT5G33360,AT5G34460,AT5G34810,AT5G34863,AT5G34895,AT5G35046,AT5G35116,AT5G35912,AT5G36005,AT5G36010,AT5G36860,AT5G37875,AT5G38383,AT5G40110,AT5G40780,AT5G41380,AT5G42955,AT5G43285,AT5G45180,AT5G45570,AT5G48595,AT5G48605,AT5G51320,AT5G51650,AT5G53410,AT5G53740,AT5G55250,AT5G55790,AT5G56300,AT5G56605,AT5G62110

FL	AT1G01073,AT1G02890,AT1G04210,AT1G04830,AT1G04970,AT1G05380,AT1G05640,AT1G06590,AT1G06720,AT1G06840,AT1G07110,AT1G10586,AT1G10930,AT1G11310,AT1G11960,AT1G13730,AT1G15020,AT1G16140,AT1G17150,AT1G18120,AT1G18830,AT1G19510,AT1G19830,AT1G21940,AT1G24370,AT1G24686,AT1G26670,AT1G27320,AT1G27980,AT1G28323,AT1G28440,AT1G28460,AT1G28465,AT1G29840,AT1G29910,AT1G30060,AT1G30480,AT1G31850,AT1G32020,AT1G32140,AT1G32350,AT1G32490,AT1G32505,AT1G32720,AT1G32840,AT1G33460,AT1G33970,AT1G34230,AT1G34390,AT1G35186,AT1G35280,AT1G35640,AT1G35735,AT1G35770,AT1G36010,AT1G36140,AT1G36250,AT1G36290,AT1G36395,AT1G36470,AT1G36495,AT1G36590,AT1G36670,AT1G36675,AT1G36690,AT1G36795,AT1G36915,AT1G37000,AT1G37057,AT1G38158,AT1G38410,AT1G38870,AT1G39511,AT1G40103,AT1G40105,AT1G40123,AT1G41730,AT1G41755,AT1G41775,AT1G41795,AT1G41840,AT1G42120,AT1G42393,AT1G42540,AT1G42690,AT1G43270,AT1G43710,AT1G43720,AT1G43770,AT1G43940,AT1G44020,AT1G44750,AT1G44800,AT1G44900,AT1G44970,AT1G47265,AT1G47280,AT1G47950,AT1G48210,AT1G48820,AT1G49070,AT1G49340,AT1G49890,AT1G50610,AT1G54960,AT1G55040,AT1G55120,AT1G56080,AT1G56130,AT1G56520,AT1G56605,AT1G56675,AT1G61080,AT1G61950,AT1G62280,AT1G62695,AT1G62760,AT1G63410,AT1G63730,AT1G63810,AT1G64000,AT1G65020,AT1G65240,AT1G65320,AT1G65940,AT1G66010,AT1G66210,AT1G67300,AT1G67481,AT1G67780,AT1G69070,AT1G69170,AT1G70400,AT1G71692,AT1G71770,AT1G71850,AT1G71920,AT1G73240,AT1G73930,AT1G74040,AT1G74200,AT1G74630,AT1G77390,AT1G77590,AT1G77800,AT1G78070,AT1G78350,AT1G78920,AT1G80070,AT1G80660,AT2G01430,AT2G01905,AT2G01950,AT2G02200,AT2G02210,AT2G02835,AT2G03250,AT2G03270,AT2G03860,AT2G04570,AT2G04760,AT2G04970,AT2G05460,AT2G05500,AT2G05752,AT2G05860,AT2G05890,AT2G06090,AT2G06160,AT2G06235,AT2G06303,AT2G06540,AT2G06550,AT2G06590,AT2G06880,AT2G06885,AT2G06950,AT2G06990,AT2G07215,AT2G07490,AT2G07599,AT2G07747,AT2G07770,AT2G07807,AT2G10070,AT2G10105,AT2G10165,AT2G10232,AT2G10256,AT2G10285,AT2G10370,AT2G10440,AT2G10460,AT2G10480,AT2G10630,AT2G10740,AT2G10980,AT2G11040,AT2G11050,AT2G11120,AT2G11650,AT2G11750,AT2G11773,AT2G11800,AT2G12200,AT2G12430,AT2G12700,AT2G12720,AT2G12860,AT2G12910,AT2G13200,AT2G13240,AT2G14130,AT2G14230,AT2G14288,AT2G14390,AT2G14590,AT2G14595,AT2G14930,AT2G14940,AT2G14950,AT2G15145,AT2G15240,AT2G15930,AT2G16170,AT2G16490,AT2G16530,AT2G16905,AT2G17115,AT2G18100,AT2G18770,AT2G19850,AT2G20290,AT2G20635,AT2G21540,AT2G21800,AT2G22740,AT2G23148,AT2G23710,AT2G24680,AT2G24915,AT2G26080,AT2G26430,AT2G26560,AT2G26770,AT2G26780,AT2G27350,AT2G27870,AT2G28170,AT2G29510,AT2G30090,AT2G30210,AT2G31215,AT2G31970,AT2G32950,AT2G32980,AT2G34130,AT2G34780,AT2G35060,AT2G35530,AT2G35650,AT2G36700,AT2G38010,AT2G38420,AT2G40480,AT2G42120,AT2G43790,AT2G44175,AT2G44570,AT2G44950,AT2G45300,AT2G45650,AT2G47360,AT3G01620,AT3G02160,AT3G02320,AT3G02515,AT3G03140,AT3G03360,AT3G03790,AT3G04740,AT3G05750,AT3G06170,AT3G06250,AT3G06850,AT3G07330,AT3G09450,AT3G10630,AT3G11670,AT3G12710,AT3G13090,AT3G13270,AT3G13290,AT3G13624,AT3G13662,AT3G14075,AT3G14400,AT3G14890,AT3G16090,AT3G16260,AT3G16680,AT3G16820,AT3G17040,AT3G17840,AT3G21170,AT3G21870,AT3G22142,AT3G23380,AT3G23540,AT3G23633,AT3G23660,AT3G24880,AT3G25720,AT3G26020,AT3G26400,AT3G26950,AT3G27

	327,AT3G27328,AT3G27390,AT3G27570,AT3G27930,AT3G28870,AT3G29160,AT3G29252,AT3G29639,AT3G29750,AT3G29775,AT3G30145,AT3G30150,AT3G30450,AT3G30480,AT3G30640,AT3G30655,AT3G30717,AT3G30765,AT3G30790,AT3G30803,AT3G30819,AT3G30836,AT3G30837,AT3G30852,AT3G31320,AT3G31357,AT3G31402,AT3G31406,AT3G31450,AT3G31935,AT3G32080,AT3G32190,AT3G32260,AT3G32389,AT3G32393,AT3G32394,AT3G32425,AT3G32970,AT3G33002,AT3G33073,AT3G33085,AT3G33142,AT3G33169,AT3G33565,AT3G42057,AT3G42236,AT3G42310,AT3G42430,AT3G42535,AT3G42580,AT3G42626,AT3G42645,AT3G42783,AT3G42924,AT3G43050,AT3G43126,AT3G43340,AT3G43420,AT3G43490,AT3G43586,AT3G43864,AT3G43880,AT3G44093,AT3G44115,AT3G44235,AT3G44245,AT3G44274,AT3G44650,AT3G44793,AT3G45420,AT3G45820,AT3G45850,AT3G46960,AT3G47350,AT3G47870,AT3G48526,AT3G49370,AT3G49400,AT3G49510,AT3G49710,AT3G53305,AT3G54280,AT3G54670,AT3G54830,AT3G54890,AT3G55270,AT3G56250,AT3G56990,AT3G57940,AT3G58980,AT3G59660,AT3G61420,AT3G62080,AT3G62240,AT4G00020,AT4G00960,AT4G02120,AT4G02390,AT4G02820,AT4G03580,AT4G03770,AT4G03800,AT4G03816,AT4G03850,AT4G04030,AT4G04070,AT4G04230,AT4G04255,AT4G04375,AT4G04390,AT4G04614,AT4G04635,AT4G05390,AT4G05505,AT4G05550,AT4G05633,AT4G06504,AT4G06506,AT4G06514,AT4G06523,AT4G06528,AT4G06563,AT4G06566,AT4G06590,AT4G06601,AT4G06658,AT4G06660,AT4G06694,AT4G06699,AT4G07350,AT4G07380,AT4G07420,AT4G07480,AT4G07517,AT4G07522,AT4G07524,AT4G07526,AT4G07566,AT4G07580,AT4G07670,AT4G07733,AT4G07868,AT4G08056,AT4G08080,AT4G08091,AT4G08260,AT4G08310,AT4G08336,AT4G08380,AT4G08599,AT4G08970,AT4G09146,AT4G09313,AT4G09360,AT4G10115,AT4G10120,AT4G10140,AT4G10690,AT4G10760,AT4G10870,AT4G11900,AT4G11980,AT4G12020,AT4G12423,AT4G13262,AT4G13460,AT4G13570,AT4G14103,AT4G14140,AT4G15096,AT4G15230,AT4G15320,AT4G15830,AT4G16580,AT4G16860,AT4G16900,AT4G16910,AT4G17410,AT4G18060,AT4G18810,AT4G19560,AT4G20095,AT4G20170,AT4G20370,AT4G21100,AT4G21820,AT4G22450,AT4G22840,AT4G25530,AT4G25692,AT4G25870,AT4G29035,AT4G29300,AT4G29305,AT4G31080,AT4G32920,AT4G33240,AT4G34090,AT4G34110,AT4G34460,AT4G34660,AT4G38040,AT4G39050,AT4G39470,AT5G02860,AT5G03280,AT5G03400,AT5G04885,AT5G05100,AT5G05170,AT5G05350,AT5G06130,AT5G07210,AT5G07660,AT5G07980,AT5G09880,AT5G10270,AT5G10670,AT5G10710,AT5G11340,AT5G11370,AT5G13130,AT5G13300,AT5G13770,AT5G14550,AT5G15680,AT5G16980,AT5G17470,AT5G18480,AT5G18580,AT5G19130,AT5G19200,AT5G19610,AT5G19670,AT5G20320,AT5G20490,AT5G22044,AT5G22220,AT5G22320,AT5G23110,AT5G23490,AT5G23575,AT5G23710,AT5G24065,AT5G24670,AT5G25360,AT5G25430,AT5G25570,AT5G26236,AT5G26240,AT5G26670,AT5G26770,AT5G26800,AT5G26860,AT5G27030,AT5G27705,AT5G27927,AT5G28100,AT5G28120,AT5G28176,AT5G28200,AT5G28253,AT5G28480,AT5G28526,AT5G28605,AT5G28670,AT5G28672,AT5G28673,AT5G28698,AT5G28800,AT5G28845,AT5G28886,AT5G28892,AT5G28930,AT5G29000,AT5G29090,AT5G29408,AT5G29565,AT5G30406,AT5G30410,AT5G30762,AT5G30852,AT5G31651,AT5G31758,AT5G31842,AT5G31919,AT5G31999,AT5G32002,AT5G32017,AT5G32060,AT5G32267,AT5G32404,AT5G32434,AT5G32485,AT5G32495,AT5G32576,AT5G32598,AT5G32605,AT5G32619,AT5G32628,AT5G32678,AT5G32950,AT5G33200,AT5G33226,AT5G33392,AT5G33398,AT5G33410,AT5G33428,AT5G34581,AT5G34686,AT5G34795,AT5G34832,AT5G34835,AT5G34847,AT5G34850,AT5G34858,AT5

	G34880,AT5G34882,AT5G34900,AT5G34990,AT5G35025,AT5G35065,AT5G35070,AT5G35142,AT5G35340,AT5G35354,AT5G3539 0,AT5G35430,AT5G35602,AT5G35603,AT5G35756,AT5G35791,AT5G35805,AT5G35926,AT5G35932,AT5G36296,AT5G36890,AT5G 36905,AT5G37100,AT5G37850,AT5G38005,AT5G38275,AT5G38840,AT5G38870,AT5G39380,AT5G40100,AT5G40210,AT5G40300, AT5G40840,AT5G41310,AT5G41360,AT5G41490,AT5G42010,AT5G42230,AT5G42270,AT5G42635,AT5G43015,AT5G43405,AT5G4 3822,AT5G43960,AT5G44270,AT5G44760,AT5G45030,AT5G46030,AT5G46860,AT5G47040,AT5G48530,AT5G49390,AT5G49430,A T5G49465,AT5G49680,AT5G49930,AT5G50190,AT5G50315,AT5G52170,AT5G52272,AT5G53150,AT5G54203,AT5G54280,AT5G54 380,AT5G54460,AT5G54650,AT5G55580,AT5G55760,AT5G55896,AT5G56020,AT5G56920,AT5G57730,AT5G58040,AT5G58050,AT 5G58410,AT5G58940,AT5G59630,AT5G59640,AT5G59650,AT5G60690,AT5G60930,AT5G60945,AT5G61070,AT5G61970,AT5G619 90,AT5G62165,AT5G63260,AT5G63320,AT5G64860,AT5G65005,AT5G65240,AT5G65820,AT5G67120

HL	AT1G01340,AT1G02120,AT1G02228,AT1G03810,AT1G04400,AT1G04700,AT1G04945,AT1G05200,AT1G05520,AT1G06960,AT1G07390,AT1G09160,AT1G10210,AT1G11130,AT1G11270,AT1G11300,AT1G11410,AT1G11480,AT1G12350,AT1G12480,AT1G13320,AT1G14710,AT1G15780,AT1G17450,AT1G17680,AT1G17690,AT1G18190,AT1G19260,AT1G19420,AT1G20280,AT1G20650,AT1G20890,AT1G20950,AT1G21170,AT1G22920,AT1G23310,AT1G24388,AT1G24390,AT1G26130,AT1G26208,AT1G26390,AT1G27595,AT1G27671,AT1G27790,AT1G28002,AT1G28540,AT1G29900,AT1G30000,AT1G30150,AT1G30820,AT1G31440,AT1G32225,AT1G32270,AT1G33000,AT1G33200,AT1G33450,AT1G34290,AT1G34300,AT1G34460,AT1G34650,AT1G34720,AT1G35330,AT1G35490,AT1G35530,AT1G35535,AT1G35625,AT1G35710,AT1G35745,AT1G35920,AT1G35970,AT1G35990,AT1G36225,AT1G36310,AT1G36400,AT1G36403,AT1G36480,AT1G37040,AT1G37050,AT1G37160,AT1G37210,AT1G38185,AT1G39190,AT1G40081,AT1G41115,AT1G41700,AT1G41740,AT1G41825,AT1G42040,AT1G42170,AT1G42210,AT1G42370,AT1G42396,AT1G42480,AT1G42515,AT1G42525,AT1G42580,AT1G42595,AT1G42650,AT1G42697,AT1G42700,AT1G42705,AT1G42924,AT1G42980,AT1G43150,AT1G43180,AT1G43330,AT1G43723,AT1G45140,AT1G45150,AT1G45191,AT1G45223,AT1G46192,AT1G47480,AT1G47606,AT1G47940,AT1G48290,AT1G48730,AT1G49100,AT1G50060,AT1G50360,AT1G51190,AT1G51460,AT1G51760,AT1G51990,AT1G52380,AT1G53050,AT1G53680,AT1G55045,AT1G55470,AT1G56120,AT1G57390,AT1G57700,AT1G57775,AT1G58470,AT1G59760,AT1G60310,AT1G61320,AT1G62310,AT1G62560,AT1G65550,AT1G66310,AT1G66520,AT1G68905,AT1G70320,AT1G72080,AT1G72180,AT1G73660,AT1G74260,AT1G75100,AT1G76790,AT1G77320,AT1G77405,AT1G78095,AT1G79940,AT2G01022,AT2G01040,AT2G01050,AT2G02160,AT2G02480,AT2G03100,AT2G03120,AT2G03780,AT2G04041,AT2G04060,AT2G04235,AT2G04460,AT2G04675,AT2G04680,AT2G04850,AT2G05020,AT2G05025,AT2G05060,AT2G05475,AT2G05480,AT2G05750,AT2G05914,AT2G06100,AT2G06330,AT2G06340,AT2G06450,AT2G06490,AT2G06510,AT2G06660,AT2G06680,AT2G06780,AT2G06920,AT2G07530,AT2G07570,AT2G07666,AT2G07680,AT2G07682,AT2G07686,AT2G07697,AT2G07728,AT2G07880,AT2G09589,AT2G09862,AT2G09900,AT2G09910,AT2G09953,AT2G10040,AT2G10190,AT2G10220,AT2G10320,AT2G10350,AT2G10490,AT2G10500,AT2G10570,AT2G10670,AT2G10680,AT2G10710,AT2G10790,AT2G10800,AT2G11020,AT2G11100,AT2G11170,AT2G11350,AT2G11440,AT2G11730,AT2G11790,AT2G11810,AT2G11950,AT2G12210,AT2G12380,AT2G12540,AT2G12590,AT2G12680,AT2G12685,AT2G12695,AT2G12770,AT2G12935,AT2G13040,AT2G13150,AT2G13490,AT2G13510,AT2G13520,AT2G13580,AT2G13620,AT2G13750,AT2G13790,AT2G13930,AT2G13980,AT2G13990,AT2G14030,AT2G14370,AT2G14405,AT2G14560,AT2G14720,AT2G14980,AT2G15110,AT2G15120,AT2G15380,AT2G15555,AT2G15815,AT2G16860,AT2G16980,AT2G17020,AT2G17570,AT2G18330,AT2G18810,AT2G18930,AT2G19410,AT2G19910,AT2G20120,AT2G21010,AT2G21120,AT2G22650,AT2G22950,AT2G23945,AT2G24070,AT2G24520,AT2G24720,AT2G24870,AT2G24890,AT2G24990,AT2G25020,AT2G25730,AT2G26215,AT2G26220,AT2G26970,AT2G28290,AT2G29210,AT2G29600,AT2G30720,AT2G30800,AT2G32270,AT2G32410,AT2G32450,AT2G32860,AT2G32970,AT2G33040,AT2G33240,AT2G34300,AT2G34680,AT2G34930,AT2G35110,AT2G35630,AT2G35770,AT2G36360,AT2G36490,AT2G37030,AT2G39890,AT2G40690,AT2G40850,AT2G41220,AT2G41460,AT2G43700,AT2G43865,AT2G44900,AT2G45290,AT2G47220,AT3G01930,AT3G02010,AT3G02130,AT3G02170,AT3G03050,AT3G03

	250,AT3G03620,AT3G03800,AT3G03860,AT3G05630,AT3G06210,AT3G06450,AT3G09370,AT3G10010,AT3G10880,AT3G11290,AT3G11440,AT3G11970,AT3G12012,AT3G12150,AT3G12270,AT3G12980,AT3G13225,AT3G14550,AT3G14840,AT3G15120,AT3G17430,AT3G18100,AT3G18350,AT3G18620,AT3G18820,AT3G18970,AT3G19210,AT3G19960,AT3G20490,AT3G20705,AT3G21100,AT3G21480,AT3G21990,AT3G22270,AT3G22350,AT3G22710,AT3G23590,AT3G23830,AT3G24260,AT3G25680,AT3G25850,AT3G25855,AT3G26440,AT3G26840,AT3G26980,AT3G27230,AT3G27590,AT3G28345,AT3G28410,AT3G28715,AT3G28780,AT3G28855,AT3G29078,AT3G29225,AT3G29360,AT3G29440,AT3G29572,AT3G29660,AT3G29727,AT3G29755,AT3G29792,AT3G30219,AT3G30235,AT3G30320,AT3G30470,AT3G30500,AT3G30560,AT3G30570,AT3G30711,AT3G30744,AT3G30745,AT3G30760,AT3G30763,AT3G30814,AT3G31317,AT3G31330,AT3G31390,AT3G31395,AT3G31425,AT3G31442,AT3G31900,AT3G31940,AT3G31990,AT3G32010,AT3G32092,AT3G32115,AT3G32118,AT3G32130,AT3G32168,AT3G32210,AT3G32240,AT3G32295,AT3G32383,AT3G32397,AT3G32893,AT3G32894,AT3G32897,AT3G33004,AT3G33011,AT3G33106,AT3G33115,AT3G33133,AT3G33157,AT3G33205,AT3G33215,AT3G33293,AT3G33537,AT3G39230,AT3G41768,AT3G42054,AT3G42060,AT3G42115,AT3G42148,AT3G42182,AT3G42252,AT3G42280,AT3G42305,AT3G42330,AT3G42340,AT3G42432,AT3G42475,AT3G42520,AT3G42717,AT3G42718,AT3G42836,AT3G42900,AT3G42916,AT3G42970,AT3G43005,AT3G43100,AT3G43270,AT3G43303,AT3G43370,AT3G43440,AT3G43447,AT3G43460,AT3G43521,AT3G43530,AT3G43563,AT3G43566,AT3G43625,AT3G43680,AT3G44175,AT3G44444,AT3G44530,AT3G44705,AT3G44820,AT3G45095,AT3G45360,AT3G45370,AT3G45638,AT3G45680,AT3G45740,AT3G46375,AT3G46920,AT3G46980,AT3G47230,AT3G47760,AT3G47770,AT3G47920,AT3G48000,AT3G48230,AT3G48630,AT3G48810,AT3G49980,AT3G50240,AT3G50680,AT3G51350,AT3G52260,AT3G52830,AT3G52890,AT3G53342,AT3G55550,AT3G55980,AT3G56190,AT3G56670,AT3G57780,AT3G58790,AT3G59420,AT3G62490,AT3G62500,AT3G63380,AT4G00140,AT4G00190,AT4G00230,AT4G00420,AT4G00620,AT4G02075,AT4G02280,AT4G02300,AT4G02350,AT4G02600,AT4G02650,AT4G03130,AT4G03156,AT4G03640,AT4G03680,AT4G03690,AT4G03795,AT4G03813,AT4G03935,AT4G03977,AT4G04145,AT4G04273,AT4G04394,AT4G04395,AT4G04440,AT4G04525,AT4G04655,AT4G04920,AT4G04940,AT4G04980,AT4G05133,AT4G05410,AT4G05526,AT4G05556,AT4G05560,AT4G05570,AT4G05634,AT4G06477,AT4G06485,AT4G06486,AT4G06488,AT4G06510,AT4G06512,AT4G06531,AT4G06537,AT4G06539,AT4G06547,AT4G06551,AT4G06552,AT4G06556,AT4G06557,AT4G06559,AT4G06576,AT4G06602,AT4G06604,AT4G06606,AT4G06607,AT4G06620,AT4G06626,AT4G06637,AT4G06652,AT4G06674,AT4G06688,AT4G06732,AT4G06734,AT4G07410,AT4G07452,AT4G07496,AT4G07521,AT4G07525,AT4G07605,AT4G07620,AT4G07630,AT4G07690,AT4G07696,AT4G07706,AT4G07780,AT4G07800,AT4G07841,AT4G07890,AT4G07941,AT4G07946,AT4G08020,AT4G08060,AT4G08090,AT4G08100,AT4G08101,AT4G08104,AT4G08131,AT4G08136,AT4G08598,AT4G08650,AT4G08920,AT4G09150,AT4G09290,AT4G09316,AT4G09584,AT4G09760,AT4G09820,AT4G10112,AT4G10340,AT4G10460,AT4G10590,AT4G10695,AT4G10700,AT4G11020,AT4G11050,AT4G11120,AT4G11740,AT4G11820,AT4G11920,AT4G12040,AT4G12330,AT4G12545,AT4G13150,AT4G14135,AT4G14548,AT4G15080,AT4G15242,AT4G15396,AT4G15790,AT4G16010,AT4G16630,AT4G18240,AT4G18420,AT4G20270,AT4G20320,AT4G21180,AT4G22760,AT4G23460,AT4G25270,AT4G25730,AT4G26850,AT4G28970,AT4

	G29010,AT4G29900,AT4G29960,AT4G30090,AT4G30100,AT4G30350,AT4G31110,AT4G31210,AT4G35420,AT4G35740,AT4G3585 0,AT4G36052,AT4G36580,AT4G36910,AT4G36925,AT4G37040,AT4G37570,AT4G37820,AT4G37940,AT4G38180,AT4G38380,AT4G 39420,AT5G02880,AT5G04500,AT5G04853,AT5G05160,AT5G05260,AT5G05920,AT5G06100,AT5G06805,AT5G07850,AT5G08055, AT5G08590,AT5G10090,AT5G11210,AT5G12090,AT5G12430,AT5G13980,AT5G14260,AT5G14610,AT5G14640,AT5G14650,AT5G1 5995,AT5G16630,AT5G16640,AT5G17125,AT5G17730,AT5G17790,AT5G17890,AT5G19165,AT5G19710,AT5G19820,AT5G19950,A T5G20470,AT5G21140,AT5G22920,AT5G24380,AT5G24500,AT5G25420,AT5G25780,AT5G25880,AT5G26270,AT5G26286,AT5G26 290,AT5G26360,AT5G26850,AT5G26910,AT5G26990,AT5G27800,AT5G28170,AT5G28190,AT5G28235,AT5G28310,AT5G28495,AT 5G28524,AT5G28712,AT5G28785,AT5G28910,AT5G28920,AT5G28990,AT5G28993,AT5G29020,AT5G29030,AT5G29032,AT5G290 40,AT5G29046,AT5G29053,AT5G29058,AT5G29100,AT5G29580,AT5G30189,AT5G30207,AT5G30450,AT5G30460,AT5G31412,AT5 G31685,AT5G31752,AT5G31821,AT5G31845,AT5G31855,AT5G31909,AT5G31981,AT5G32071,AT5G32072,AT5G32103,AT5G3224 1,AT5G32433,AT5G32475,AT5G32505,AT5G32513,AT5G32514,AT5G32517,AT5G32518,AT5G32566,AT5G32593,AT5G32594,AT5G 32600,AT5G32610,AT5G32613,AT5G32616,AT5G32622,AT5G32627,AT5G32630,AT5G32654,AT5G32702,AT5G32850,AT5G32900, AT5G33232,AT5G33251,AT5G33253,AT5G33303,AT5G33386,AT5G33388,AT5G33395,AT5G33415,AT5G33441,AT5G34480,AT5G3 4790,AT5G34834,AT5G34841,AT5G34843,AT5G34844,AT5G34846,AT5G34851,AT5G34854,AT5G34883,AT5G34885,AT5G34950,A T5G35076,AT5G35334,AT5G35339,AT5G35604,AT5G35657,AT5G35725,AT5G35737,AT5G35798,AT5G35802,AT5G35860,AT5G35 880,AT5G35920,AT5G35935,AT5G35970,AT5G36050,AT5G36170,AT5G36180,AT5G36223,AT5G36275,AT5G36655,AT5G37017,AT 5G37055,AT5G37410,AT5G38280,AT5G39510,AT5G39550,AT5G40230,AT5G40890,AT5G41320,AT5G41330,AT5G41494,AT5G417 50,AT5G41940,AT5G42170,AT5G42320,AT5G42340,AT5G42565,AT5G42930,AT5G42957,AT5G43035,AT5G43065,AT5G43510,AT5 G43525,AT5G43610,AT5G44415,AT5G44800,AT5G45140,AT5G48960,AT5G49010,AT5G50715,AT5G50940,AT5G50970,AT5G5135 0,AT5G53120,AT5G53510,AT5G53770,AT5G54020

LL	AT1G01040,AT1G01760,AT1G01820,AT1G02140,AT1G02220,AT1G02260,AT1G02470,AT1G03000,AT1G03060,AT1G03200,AT1G03310,AT1G03445,AT1G03520,AT1G03830,AT1G04050,AT1G04200,AT1G04430,AT1G05320,AT1G05470,AT1G06460,AT1G06500,AT1G07200,AT1G08260,AT1G08300,AT1G08340,AT1G08420,AT1G08450,AT1G08490,AT1G08760,AT1G08845,AT1G08860,AT1G08970,AT1G09040,AT1G09230,AT1G09460,AT1G09600,AT1G09870,AT1G10090,AT1G10290,AT1G11330,AT1G11390,AT1G11880,AT1G11905,AT1G12000,AT1G12120,AT1G13170,AT1G13210,AT1G13790,AT1G13880,AT1G14190,AT1G14560,AT1G14570,AT1G14690,AT1G14800,AT1G15160,AT1G15470,AT1G15890,AT1G16110,AT1G16130,AT1G16720,AT1G16860,AT1G17040,AT1G17110,AT1G17145,AT1G17220,AT1G17760,AT1G17920,AT1G18270,AT1G18450,AT1G18480,AT1G18500,AT1G18550,AT1G18690,AT1G18890,AT1G19860,AT1G19870,AT1G20200,AT1G20750,AT1G21080,AT1G21580,AT1G21651,AT1G21835,AT1G21850,AT1G21880,AT1G21930,AT1G22067,AT1G22275,AT1G22280,AT1G22660,AT1G22790,AT1G23470,AT1G23860,AT1G23880,AT1G23940,AT1G24068,AT1G24090,AT1G24280,AT1G24650,AT1G24967,AT1G25320,AT1G25350,AT1G25360,AT1G25580,AT1G26170,AT1G26610,AT1G26620,AT1G26830,AT1G27110,AT1G27470,AT1G27700,AT1G27870,AT1G27900,AT1G29180,AT1G29220,AT1G29490,AT1G30230,AT1G30360,AT1G30890,AT1G30910,AT1G30960,AT1G30980,AT1G31100,AT1G31340,AT1G31470,AT1G31480,AT1G31817,AT1G31983,AT1G31990,AT1G32337,AT1G32440,AT1G32450,AT1G32750,AT1G33010,AT1G33250,AT1G33700,AT1G34130,AT1G34370,AT1G34440,AT1G35190,AT1G35300,AT1G35400,AT1G35460,AT1G35590,AT1G35600,AT1G35660,AT1G35780,AT1G35820,AT1G35860,AT1G35960,AT1G35980,AT1G36110,AT1G36260,AT1G36330,AT1G36360,AT1G36510,AT1G36840,AT1G36990,AT1G37170,AT1G37471,AT1G38340,AT1G38360,AT1G38400,AT1G38416,AT1G38550,AT1G39910,AT1G40075,AT1G40084,AT1G40117,AT1G41600,AT1G41690,AT1G41726,AT1G41797,AT1G41870,AT1G41893,AT1G42080,AT1G42220,AT1G42260,AT1G42390,AT1G42510,AT1G42520,AT1G42600,AT1G42610,AT1G42655,AT1G42852,AT1G42970,AT1G43030,AT1G43060,AT1G43090,AT1G43502,AT1G43755,AT1G43760,AT1G43781,AT1G43870,AT1G43920,AT1G43960,AT1G43997,AT1G44060,AT1G45020,AT1G45070,AT1G45190,AT1G45233,AT1G45249,AT1G47270,AT1G47340,AT1G48370,AT1G48490,AT1G48780,AT1G49550,AT1G49600,AT1G49710,AT1G49740,AT1G49910,AT1G50160,AT1G50500,AT1G50730,AT1G50850,AT1G50860,AT1G51670,AT1G52260,AT1G52570,AT1G52630,AT1G52670,AT1G53840,AT1G54060,AT1G54100,AT1G54150,AT1G54340,AT1G54610,AT1G54775,AT1G54840,AT1G55130,AT1G55200,AT1G55320,AT1G55860,AT1G55960,AT1G56230,AT1G56280,AT1G56450,AT1G56460,AT1G56570,AT1G58050,AT1G58140,AT1G58230,AT1G59650,AT1G59750,AT1G59870,AT1G59980,AT1G60550,AT1G61450,AT1G61520,AT1G61690,AT1G61860,AT1G62130,AT1G62430,AT1G62800,AT1G62970,AT1G63430,AT1G63440,AT1G63940,AT1G63990,AT1G64580,AT1G64585,AT1G64610,AT1G64960,AT1G65080,AT1G65120,AT1G65520,AT1G66140,AT1G66430,AT1G67120,AT1G67140,AT1G67220,AT1G67490,AT1G67500,AT1G67560,AT1G67626,AT1G67820,AT1G67970,AT1G68310,AT1G68580,AT1G68970,AT1G69190,AT1G70250,AT1G70300,AT1G70630,AT1G70840,AT1G70970,AT1G71090,AT1G71320,AT1G71830,AT1G72090,AT1G72131,AT1G72760,AT1G73030,AT1G73410,AT1G73430,AT1G73990,AT1G74370,AT1G74720,AT1G74740,AT1G74790,AT1G74810,AT1G74850,AT1G76270,AT1G76390,AT1G76690,AT1G76705,AT1G76720,AT1G76780,AT1G77030,AT1G77095,AT1G77280,AT1G77310,AT1G77480,AT1G77500,AT1G77620,AT1G78

	330,AT1G78800,AT1G79245,AT1G79380,AT1G79590,AT1G79830,AT1G79840,AT2G01024,AT2G01028,AT2G01031,AT2G01280,AT2G01370,AT2G01440,AT2G01660,AT2G01790,AT2G02260,AT2G02520,AT2G02810,AT2G03150,AT2G03260,AT2G03380,AT2G03600,AT2G03890,AT2G03940,AT2G03980,AT2G03990,AT2G04031,AT2G04042,AT2G04210,AT2G04840,AT2G04920,AT2G05030,AT2G05087,AT2G05120,AT2G05335,AT2G06060,AT2G06080,AT2G06095,AT2G06120,AT2G06270,AT2G06570,AT2G06906,AT2G06910,AT2G06930,AT2G07270,AT2G07330,AT2G07420,AT2G07450,AT2G07560,AT2G07630,AT2G07706,AT2G07760,AT2G07795,AT2G07812,AT2G09930,AT2G10160,AT2G10170,AT2G10223,AT2G10237,AT2G10290,AT2G10300,AT2G10330,AT2G10470,AT2G10540,AT2G11110,AT2G11166,AT2G11180,AT2G11210,AT2G11490,AT2G11510,AT2G12130,AT2G12305,AT2G12320,AT2G12405,AT2G12470,AT2G12570,AT2G12875,AT2G12950,AT2G12980,AT2G12990,AT2G13175,AT2G13280,AT2G13560,AT2G13600,AT2G14120,AT2G14440,AT2G14510,AT2G14535,AT2G14690,AT2G14740,AT2G14770,AT2G14780,AT2G14790,AT2G14990,AT2G15140,AT2G15320,AT2G15530,AT2G15720,AT2G15890,AT2G15910,AT2G16090,AT2G16250,AT2G16820,AT2G16832,AT2G17260,AT2G17890,AT2G18180,AT2G18230,AT2G18470,AT2G18900,AT2G19090,AT2G19190,AT2G19806,AT2G19930,AT2G19960,AT2G20060,AT2G20170,AT2G20240,AT2G21100,AT2G21310,AT2G21655,AT2G22440,AT2G22840,AT2G23200,AT2G23460,AT2G24100,AT2G24240,AT2G24735,AT2G24820,AT2G24900,AT2G24960,AT2G25170,AT2G25530,AT2G26510,AT2G26550,AT2G26580,AT2G26620,AT2G26890,AT2G26910,AT2G26980,AT2G27040,AT2G27050,AT2G27070,AT2G27610,AT2G28150,AT2G28190,AT2G29060,AT2G29065,AT2G30460,AT2G30470,AT2G30910,AT2G30990,AT2G31060,AT2G31290,AT2G32290,AT2G32520,AT2G32910,AT2G33006,AT2G33210,AT2G34020,AT2G34040,AT2G34210,AT2G34220,AT2G34970,AT2G35030,AT2G35340,AT2G36250,AT2G36710,AT2G36850,AT2G37010,AT2G37570,AT2G38040,AT2G38440,AT2G38550,AT2G38760,AT2G38840,AT2G39760,AT2G39910,AT2G39990,AT2G40730,AT2G41210,AT2G41510,AT2G41900,AT2G42500,AT2G42600,AT2G43070,AT2G43970,AT2G44040,AT2G44890,AT2G45240,AT2G45460,AT2G45540,AT2G45810,AT2G46572,AT2G46700,AT2G46730,AT2G46920,AT2G47600,AT2G48110,AT3G01310,AT3G01380,AT3G01450,AT3G01770,AT3G02420,AT3G04240,AT3G04460,AT3G04810,AT3G05280,AT3G05360,AT3G05380,AT3G05685,AT3G05790,AT3G05932,AT3G06330,AT3G06435,AT3G06480,AT3G06530,AT3G06920,AT3G07160,AT3G07600,AT3G07940,AT3G08800,AT3G08943,AT3G09060,AT3G09080,AT3G10070,AT3G10230,AT3G10690,AT3G10770,AT3G11370,AT3G11830,AT3G11945,AT3G12290,AT3G12810,AT3G12940,AT3G13222,AT3G13330,AT3G13750,AT3G13860,AT3G14670,AT3G14790,AT3G15180,AT3G15380,AT3G15970,AT3G16350,AT3G16620,AT3G16830,AT3G16940,AT3G17090,AT3G17410,AT3G17450,AT3G17620,AT3G17660,AT3G17900,AT3G18110,AT3G18290,AT3G18340,AT3G18500,AT3G18640,AT3G18720,AT3G18777,AT3G19050,AT3G19080,AT3G19190,AT3G19250,AT3G19740,AT3G19940,AT3G20200,AT3G20520,AT3G20540,AT3G20720,AT3G20970,AT3G21140,AT3G21250,AT3G21280,AT3G21320,AT3G21351,AT3G22190,AT3G22600,AT3G23020,AT3G23085,AT3G23510,AT3G23640,AT3G23685,AT3G23780,AT3G23790,AT3G24340,AT3G24542,AT3G25410,AT3G25800,AT3G25900,AT3G26030,AT3G26140,AT3G26310,AT3G26560,AT3G26744,AT3G27110,AT3G27320,AT3G27720,AT3G27870,AT3G27940,AT3G28260,AT3G28430,AT3G28450,AT3G28510,AT3G28690,AT3G28860,AT3G28880,AT3G28940,AT3G29090,AT3G29130,AT3G29180,AT3G29270,AT3G29460,AT3G29510,AT3G29515,AT3G29610,AT3

	G29720,AT3G29740,AT3G29768,AT3G29970,AT3G30120,AT3G30190,AT3G30260,AT3G30405,AT3G30510,AT3G30550,AT3G3058 7,AT3G30710,AT3G30737,AT3G30766,AT3G30842,AT3G31005,AT3G31356,AT3G31374,AT3G31410,AT3G31475,AT3G31980,AT3G 31993,AT3G32024,AT3G32043,AT3G32060,AT3G32095,AT3G32164,AT3G32180,AT3G32220,AT3G32250,AT3G33009,AT3G33055, AT3G33097,AT3G33136,AT3G33151,AT3G33193,AT3G33201,AT3G33377,AT3G42140,AT3G42150,AT3G42160,AT3G42179,AT3G4 2186,AT3G42233,AT3G42255,AT3G42360,AT3G42383,AT3G42433,AT3G42434,AT3G42540,AT3G42600,AT3G42640,AT3G42711,A T3G42712,AT3G42770,AT3G42837,AT3G43157,AT3G43175,AT3G43300,AT3G43307,AT3G43330,AT3G43390,AT3G43550,AT3G43 571,AT3G43600,AT3G43684,AT3G43830,AT3G44110,AT3G44200,AT3G44205,AT3G44620,AT3G44880,AT3G45190,AT3G45480,AT 3G45630,AT3G45690,AT3G45720,AT3G46100,AT3G46370,AT3G46420,AT3G46470,AT3G46580,AT3G46740,AT3G47120,AT3G473 10,AT3G47340,AT3G47400,AT3G47460,AT3G47550,AT3G47830,AT3G48131,AT3G48400,AT3G48430,AT3G48770,AT3G48780,AT3 G48890,AT3G49160,AT3G49250,AT3G49420,AT3G50250,AT3G50301,AT3G50370,AT3G50380,AT3G50430,AT3G50720,AT3G5095 0,AT3G51250,AT3G51520,AT3G51632,AT3G51840,AT3G52950,AT3G53050,AT3G53402,AT3G54460,AT3G54870,AT3G57090,AT3G 57140,AT3G57180,AT3G57630,AT3G57660,AT3G58050,AT3G58520,AT3G59020,AT3G59160,AT3G59300,AT3G59410,AT3G59730, AT3G60320,AT3G60800,AT3G60840,AT3G60880,AT3G61260,AT3G61600,AT3G61690,AT3G62060,AT3G62270,AT3G62360,AT3G6 2475,AT4G00060,AT4G00490,AT4G00880,AT4G00920,AT4G01010,AT4G01090,AT4G01190,AT4G01350,AT4G01533,AT4G01700,A T4G01730,AT4G01830,AT4G01883,AT4G02220,AT4G02480,AT4G02560,AT4G02570,AT4G02660,AT4G02690,AT4G02920,AT4G03 090,AT4G03110,AT4G03560,AT4G03723,AT4G03732,AT4G03750,AT4G03826,AT4G03914,AT4G03945,AT4G03981,AT4G04290,AT 4G04392,AT4G04405,AT4G04420,AT4G04423,AT4G04660,AT4G04780,AT4G05076,AT4G05306,AT4G05587,AT4G05620,AT4G064 97,AT4G06515,AT4G06530,AT4G06560,AT4G06561,AT4G06564,AT4G06568,AT4G06571,AT4G06572,AT4G06646,AT4G06654,AT4 G06664,AT4G06678,AT4G06692,AT4G06726,AT4G06750,AT4G07031,AT4G07338,AT4G07440,AT4G07458,AT4G07495,AT4G0754 0,AT4G07570,AT4G07586,AT4G07713,AT4G07740,AT4G07840,AT4G07893,AT4G07917,AT4G07920,AT4G08054,AT4G08070,AT4G 08072,AT4G08078,AT4G08094,AT4G08113,AT4G08390,AT4G08400,AT4G08450,AT4G08480,AT4G08490,AT4G08510,AT4G08630, AT4G08750,AT4G08790,AT4G08810,AT4G08870,AT4G08956,AT4G09565,AT4G09620,AT4G09625,AT4G09700,AT4G10390,AT4G1 0510,AT4G10550,AT4G10710,AT4G10960,AT4G10970,AT4G11370,AT4G11430,AT4G11880,AT4G12420,AT4G12690,AT4G14150,A T4G14190,AT4G14330,AT4G14520,AT4G14700,AT4G14770,AT4G14960,AT4G15233,AT4G15236,AT4G15417,AT4G15440,AT4G15 475,AT4G15560,AT4G15640,AT4G16070,AT4G16130,AT4G16240,AT4G16480,AT4G16680,AT4G16970,AT4G17040,AT4G17300,AT 4G17587,AT4G17880,AT4G18290,AT4G18370,AT4G18440,AT4G19590,AT4G19940,AT4G19970,AT4G20010,AT4G20070,AT4G201 60,AT4G20450,AT4G20910,AT4G21860,AT4G22065,AT4G22350,AT4G23540,AT4G23850,AT4G24020,AT4G24160,AT4G24190,AT4 G24770,AT4G24830,AT4G25040,AT4G25070,AT4G25220,AT4G25540,AT4G25880,AT4G26095,AT4G26740,AT4G26940,AT4G2703 0,AT4G27260,AT4G27300,AT4G28570,AT4G30690,AT4G30780,AT4G30950,AT4G31230,AT4G31300,AT4G31360,AT4G31880,AT4G 31900,AT4G32520,AT4G33670,AT4G33940,AT4G34131,AT4G34690,AT4G35800,AT4G38240,AT4G38552,AT4G38760,AT4G38780,

	AT4G39280,AT4G39672,AT4G39910,AT5G01110,AT5G01185,AT5G01460,AT5G01720,AT5G01780,AT5G01850,AT5G02100,AT5G02130,AT5G02840,AT5G03160,AT5G03250,AT5G03300,AT5G03455,AT5G03720,AT5G03900,AT5G04360,AT5G04460,AT5G04480,AT5G04870,AT5G04895,AT5G04910,AT5G04930,AT5G05140,AT5G05540,AT5G05730,AT5G05740,AT5G05850,AT5G06030,AT5G07940,AT5G08110,AT5G09400,AT5G09740,AT5G10250,AT5G10540,AT5G11040,AT5G11100,AT5G11180,AT5G11440,AT5G11470,AT5G11790,AT5G12360,AT5G13010,AT5G13160,AT5G13205,AT5G13270,AT5G14050,AT5G14960,AT5G15010,AT5G15470,AT5G15546,AT5G15980,AT5G16280,AT5G16300,AT5G16410,AT5G16780,AT5G16890,AT5G17240,AT5G18000,AT5G18050,AT5G18420,AT5G18590

SQvFL	AT1G04425,AT1G19890,AT1G34070,AT1G34580,AT1G35390,AT1G35790,AT1G36610,AT1G39270,AT1G40097,AT1G42695,AT1G47816,AT1G65985,AT2G04470,AT2G04980,AT2G05690,AT2G06335,AT2G06350,AT2G07730,AT2G10640,AT2G11626,AT2G12385,AT2G13190,AT2G13380,AT2G13410,AT2G14380,AT2G15410,AT2G15550,AT2G18660,AT2G24570,AT2G24930,AT2G29605,AT3G20950,AT3G29771,AT3G32033,AT3G42070,AT3G43863,AT3G47165,AT3G47330,AT4G00120,AT4G03980,AT4G04010,AT4G06638,AT4G06708,AT4G07830,AT4G13455,AT4G18000,AT5G20750,AT5G28643,AT5G28715,AT5G28760,AT5G29571,AT5G33310,AT5G34770,AT5G35794,AT5G43755,AT5G45605,AT5G47300
SQvHL	AT1G03240,AT1G17275,AT1G18130,AT1G19392,AT1G20967,AT1G23990,AT1G30030,AT1G30784,AT1G30974,AT1G36035,AT1G36975,AT1G38423,AT1G42745,AT1G43745,AT1G44030,AT1G45063,AT1G46696,AT1G52010,AT1G55560,AT1G57650,AT1G65585,AT1G65750,AT1G66290,AT1G66300,AT1G66570,AT2G03930,AT2G04036,AT2G05000,AT2G05082,AT2G05564,AT2G05635,AT2G06110,AT2G06250,AT2G06410,AT2G06912,AT2G07020,AT2G07620,AT2G10250,AT2G10608,AT2G10610,AT2G10690,AT2G12440,AT2G13250,AT2G13460,AT2G13470,AT2G13540,AT2G13770,AT2G13960,AT2G14400,AT2G14450,AT2G15045,AT2G15420,AT2G16320,AT2G16420,AT2G18610,AT2G22210,AT2G22668,AT2G22890,AT2G40680,AT2G42430,AT2G44470,AT3G20070,AT3G21960,AT3G25130,AT3G26870,AT3G27329,AT3G28956,AT3G29153,AT3G29805,AT3G30160,AT3G30709,AT3G30832,AT3G30844,AT3G30846,AT3G33025,AT3G33154,AT3G33160,AT3G33575,AT3G42155,AT3G42178,AT3G42875,AT3G42980,AT3G43153,AT3G43260,AT3G44212,AT3G44980,AT3G45460,AT3G46120,AT3G51860,AT4G03979,AT4G04840,AT4G05280,AT4G06500,AT4G06516,AT4G06569,AT4G06575,AT4G06579,AT4G06580,AT4G06591,AT4G06748,AT4G07931,AT4G07934,AT4G08022,AT4G08096,AT4G08485,AT4G08600,AT4G08670,AT4G09660,AT4G09710,AT4G10920,AT4G11730,AT4G12426,AT4G12440,AT4G14470,AT4G16195,AT4G16550,AT4G16920,AT4G33300,AT5G07380,AT5G07410,AT5G07430,AT5G15690,AT5G21105,AT5G22420,AT5G24450,AT5G27190,AT5G27300,AT5G27905,AT5G28250,AT5G28593,AT5G28824,AT5G28940,AT5G31807,AT5G32136,AT5G32358,AT5G32481,AT5G32512,AT5G34836,AT5G34965,AT5G35207,AT5G35331,AT5G35336,AT5G35655,AT5G35820,AT5G45082,AT5G47818,AT5G48000,AT5G53775
SQvLL	AT1G06148,AT1G14225,AT1G17390,AT1G25784,AT1G27780,AT1G28120,AT1G38460,AT1G40150,AT1G41680,AT1G43730,AT1G43990,AT1G47360,AT1G49005,AT1G58020,AT1G59885,AT1G63540,AT1G65360,AT1G65681,AT1G67000,AT2G03070,AT2G05190,AT2G07400,AT2G10510,AT2G11330,AT2G11590,AT2G12510,AT2G13310,AT2G13820,AT2G13851,AT2G13860,AT2G13940,AT2G14260,AT2G15520,AT2G15810,AT2G19825,AT2G24755,AT2G24920,AT2G35010,AT2G46130,AT2G46830,AT3G05415,AT3G10900,AT3G17400,AT3G27040,AT3G28820,AT3G30716,AT3G31365,AT3G42436,AT3G42760,AT3G42763,AT3G43640,AT3G43990,AT3G47270,AT3G50320,AT3G55860,AT4G02000,AT4G02700,AT4G03811,AT4G04750,AT4G04820,AT4G05087,AT4G06524,AT4G06720,AT4G06736,AT4G07770,AT4G08890,AT4G19790,AT4G22770,AT4G24300,AT5G03950

FLvHL	AT1G01260,AT1G09060,AT1G11593,AT1G17277,AT1G17745,AT1G18240,AT1G21730,AT1G22770,AT1G24938,AT1G32080,AT1G32680,AT1G33680,AT1G33855,AT1G35035,AT1G35150,AT1G35850,AT1G36300,AT1G36520,AT1G36550,AT1G36600,AT1G36770,AT1G36890,AT1G37060,AT1G37090,AT1G37190,AT1G38350,AT1G40095,AT1G40630,AT1G41896,AT1G42140,AT1G43240,AT1G43763,AT1G44045,AT1G44840,AT1G47550,AT1G47570,AT1G47640,AT1G47650,AT1G47660,AT1G47910,AT1G49440,AT1G49670,AT1G51172,AT1G52990,AT1G54510,AT1G54750,AT1G58300,AT1G58520,AT1G61490,AT1G71010,AT1G72640,AT1G74470,AT1G80490,AT2G01550,AT2G02840,AT2G03690,AT2G03960,AT2G04180,AT2G04770,AT2G04950,AT2G05010,AT2G05090,AT2G05550,AT2G05780,AT2G06170,AT2G06180,AT2G06190,AT2G06790,AT2G07360,AT2G07550,AT2G07635,AT2G07748,AT2G07780,AT2G09838,AT2G09860,AT2G09865,AT2G09870,AT2G09960,AT2G10230,AT2G10605,AT2G10614,AT2G10870,AT2G10890,AT2G10940,AT2G11080,AT2G11130,AT2G11230,AT2G11300,AT2G11450,AT2G11600,AT2G12060,AT2G12820,AT2G12835,AT2G12970,AT2G13140,AT2G13330,AT2G13335,AT2G13400,AT2G13700,AT2G13870,AT2G14140,AT2G14410,AT2G14640,AT2G15480,AT2G15710,AT2G15850,AT2G16150,AT2G16410,AT2G16440,AT2G17010,AT2G18320,AT2G18530,AT2G18590,AT2G21920,AT2G22360,AT2G25350,AT2G25630,AT2G27150,AT2G27320,AT2G31030,AT2G31960,AT2G32500,AT2G39140,AT2G45230,AT2G46930,AT3G02260,AT3G02710,AT3G10330,AT3G14800,AT3G15070,AT3G15290,AT3G17650,AT3G19350,AT3G20700,AT3G23480,AT3G24365,AT3G24495,AT3G24503,AT3G25110,AT3G25230,AT3G25725,AT3G26510,AT3G27140,AT3G28005,AT3G28080,AT3G29032,AT3G29641,AT3G30218,AT3G30400,AT3G30411,AT3G30433,AT3G30703,AT3G30764,AT3G30831,AT3G30838,AT3G30839,AT3G31403,AT3G31540,AT3G31810,AT3G32000,AT3G32021,AT3G32032,AT3G32415,AT3G32964,AT3G32968,AT3G33071,AT3G33072,AT3G33112,AT3G33555,AT3G33585,AT3G42052,AT3G42065,AT3G42100,AT3G42203,AT3G42356,AT3G42386,AT3G42560,AT3G42713,AT3G42715,AT3G42730,AT3G42883,AT3G42993,AT3G42996,AT3G43070,AT3G43142,AT3G43350,AT3G43355,AT3G43356,AT3G43357,AT3G43436,AT3G43444,AT3G43575,AT3G43635,AT3G43723,AT3G44267,AT3G44670,AT3G44730,AT3G45090,AT3G45550,AT3G45780,AT3G45990,AT3G47060,AT3G47260,AT3G47660,AT3G50540,AT3G50670,AT3G50690,AT3G52410,AT3G55060,AT3G56210,AT3G59110,AT4G01930,AT4G02405,AT4G02760,AT4G03780,AT4G03860,AT4G03885,AT4G03970,AT4G04245,AT4G04280,AT4G04380,AT4G04955,AT4G05508,AT4G05583,AT4G05638,AT4G06474,AT4G06509,AT4G06518,AT4G06535,AT4G06536,AT4G06540,AT4G06544,AT4G06585,AT4G06588,AT4G06592,AT4G06593,AT4G06610,AT4G06642,AT4G06656,AT4G06752,AT4G07315,AT4G07339,AT4G07360,AT4G07454,AT4G07500,AT4G07502,AT4G07563,AT4G07725,AT4G07932,AT4G07937,AT4G08050,AT4G08108,AT4G08109,AT4G08112,AT4G08691,AT4G08760,AT4G08990,AT4G09450,AT4G09490,AT4G11670,AT4G12275,AT4G13900,AT4G16340,AT4G17910,AT4G19330,AT4G20700,AT4G21360,AT4G26485,AT4G26610,AT4G27570,AT4G29090,AT4G40100,AT5G02200,AT5G03650,AT5G11770,AT5G13310,AT5G14580,AT5G15420,AT5G17010,AT5G18960,AT5G24270,AT5G24990,AT5G27035,AT5G27890,AT5G27960,AT5G28065,AT5G28415,AT5G28545,AT5G28590,AT5G28692,AT5G29056,AT5G29337,AT5G29574,AT5G30060,AT5G31927,AT5G32042,AT5G32197,AT5G32280,AT5G32471,AT5G33025,AT5G33240,AT5G33252,AT5G33424,AT5G33434,AT5G33806,AT5G34696,AT5G34728,AT5G35280,AT5G35495,AT5G35520,AT5G35555,AT5G35643,AT5G35736,AT5G37150,AT5G37810,AT5G37890,AT5G39

	500,AT5G40280,AT5G41430,AT5G45660,AT5G45760,AT5G46090,AT5G46210,AT5G46645,AT5G46660,AT5G46870,AT5G47430,AT5G48335,AT5G48515,AT5G48860,AT5G49030,AT5G50340,AT5G50717,AT5G51710

FLvLL	AT1G01550,AT1G02080,AT1G02990,AT1G04140,AT1G04620,AT1G04810,AT1G05070,AT1G05270,AT1G05910,AT1G06170,AT1G06910,AT1G09760,AT1G10170,AT1G12260,AT1G13060,AT1G13660,AT1G16710,AT1G18050,AT1G18310,AT1G18700,AT1G19835,AT1G19920,AT1G20960,AT1G21160,AT1G21640,AT1G21660,AT1G21810,AT1G21980,AT1G22870,AT1G22970,AT1G23130,AT1G23180,AT1G23230,AT1G23330,AT1G23480,AT1G23720,AT1G23900,AT1G24190,AT1G24706,AT1G24764,AT1G25375,AT1G26260,AT1G26380,AT1G26520,AT1G26762,AT1G27150,AT1G27220,AT1G27430,AT1G27800,AT1G27850,AT1G27960,AT1G29170,AT1G30630,AT1G30640,AT1G31163,AT1G31210,AT1G31710,AT1G31870,AT1G31993,AT1G32830,AT1G33920,AT1G34090,AT1G34260,AT1G34310,AT1G34320,AT1G34430,AT1G35060,AT1G35146,AT1G35240,AT1G35540,AT1G35614,AT1G35650,AT1G36185,AT1G36630,AT1G36810,AT1G37030,AT1G37200,AT1G37603,AT1G37735,AT1G38270,AT1G38380,AT1G38430,AT1G38440,AT1G38710,AT1G40119,AT1G41723,AT1G41803,AT1G41855,AT1G41900,AT1G42320,AT1G42350,AT1G42736,AT1G43387,AT1G45120,AT1G45130,AT1G47260,AT1G47560,AT1G48090,AT1G48250,AT1G48450,AT1G48870,AT1G49160,AT1G49230,AT1G50030,AT1G51570,AT1G52610,AT1G53390,AT1G53500,AT1G53780,AT1G54370,AT1G55630,AT1G57613,AT1G60020,AT1G62085,AT1G62540,AT1G62830,AT1G64280,AT1G64570,AT1G64790,AT1G64860,AT1G65070,AT1G65810,AT1G65960,AT1G66930,AT1G67190,AT1G68210,AT1G68720,AT1G69480,AT1G69510,AT1G69740,AT1G69770,AT1G72250,AT1G72410,AT1G74170,AT1G75310,AT1G75400,AT1G75700,AT1G75920,AT1G77410,AT1G78940,AT1G79610,AT1G79930,AT2G01010,AT2G01600,AT2G01740,AT2G03932,AT2G04660,AT2G04750,AT2G04990,AT2G05567,AT2G05700,AT2G05930,AT2G05935,AT2G05995,AT2G06140,AT2G06420,AT2G06670,AT2G06720,AT2G06760,AT2G06904,AT2G07010,AT2G07230,AT2G07240,AT2G07380,AT2G07540,AT2G07650,AT2G07681,AT2G09880,AT2G10110,AT2G10140,AT2G10260,AT2G10650,AT2G10660,AT2G10780,AT2G11070,AT2G11165,AT2G11720,AT2G12640,AT2G12650,AT2G12760,AT2G12850,AT2G13160,AT2G13230,AT2G14020,AT2G14200,AT2G15340,AT2G16100,AT2G17460,AT2G19146,AT2G20000,AT2G21550,AT2G23500,AT2G24761,AT2G25160,AT2G26210,AT2G26470,AT2G26840,AT2G27120,AT2G27810,AT2G30505,AT2G31650,AT2G31660,AT2G32400,AT2G32700,AT2G34060,AT2G34110,AT2G38195,AT2G38590,AT2G39340,AT2G39590,AT2G40210,AT2G40310,AT2G41570,AT2G41700,AT2G43330,AT2G43500,AT2G44540,AT2G44610,AT2G44710,AT2G44970,AT2G45100,AT2G45380,AT2G46520,AT2G47020,AT3G01410,AT3G02070,AT3G02350,AT3G03110,AT3G03855,AT3G04130,AT3G04490,AT3G06580,AT3G06820,AT3G07750,AT3G09405,AT3G10380,AT3G12145,AT3G12220,AT3G12680,AT3G13061,AT3G13840,AT3G15980,AT3G17050,AT3G18480,AT3G18524,AT3G19360,AT3G19370,AT3G20220,AT3G22300,AT3G22555,AT3G23450,AT3G24580,AT3G24900,AT3G25485,AT3G26100,AT3G26680,AT3G27170,AT3G27680,AT3G28110,AT3G28120,AT3G29190,AT3G29648,AT3G29787,AT3G29800,AT3G30200,AT3G30436,AT3G30718,AT3G30742,AT3G30811,AT3G30821,AT3G30833,AT3G31340,AT3G31440,AT3G32230,AT3G32280,AT3G32899,AT3G33010,AT3G33077,AT3G33100,AT3G33109,AT3G33121,AT3G33528,AT3G42190,AT3G42253,AT3G42270,AT3G42290,AT3G42313,AT3G42350,AT3G42420,AT3G42794,AT3G42950,AT3G43130,AT3G43251,AT3G43310,AT3G43524,AT3G43546,AT3G43686,AT3G44680,AT3G45270,AT3G45510,AT3G46220,AT3G46400,AT3G46487,AT3G48900,AT3G49740,AT3G50120,AT3G52250,AT3G53930,AT3G55258,AT3G56560,AT3G59100,AT3G59860,AT3G60240,AT3G60570,AT3G62480,AT3G63130,AT3G63

	510,AT4G00570,AT4G00900,AT4G03200,AT4G03390,AT4G03650,AT4G03710,AT4G03810,AT4G04000,AT4G04360,AT4G04550,AT4G05130,AT4G05420,AT4G05592,AT4G06527,AT4G06562,AT4G06567,AT4G06578,AT4G06589,AT4G06632,AT4G06666,AT4G06718,AT4G07334,AT4G07504,AT4G07680,AT4G07738,AT4G07742,AT4G07812,AT4G07935,AT4G07947,AT4G08092,AT4G08093,AT4G08280,AT4G08333,AT4G08395,AT4G08460,AT4G08470,AT4G08660,AT4G08878,AT4G08880,AT4G08995,AT4G09400,AT4G09410,AT4G10180,AT4G10530,AT4G12320,AT4G13470,AT4G13495,AT4G13992,AT4G16870,AT4G17140,AT4G17780,AT4G18520,AT4G19050,AT4G20490,AT4G21650,AT4G22720,AT4G25160,AT4G25630,AT4G27210,AT4G27370,AT4G29380,AT4G30130,AT4G34071,AT4G35870,AT4G36690,AT4G37670,AT4G39170,AT4G39180,AT4G39210,AT5G03430,AT5G04235,AT5G05560,AT5G05660,AT5G06600,AT5G07020,AT5G07740,AT5G11530,AT5G11700,AT5G14120,AT5G14220,AT5G16270,AT5G17370,AT5G17550,AT5G17910
HLvLL	AT1G02500,AT1G03090,AT1G07910,AT1G09910,AT1G11595,AT1G13470,AT1G19450,AT1G22000,AT1G26990,AT1G27570,AT1G27810,AT1G27880,AT1G27940,AT1G31770,AT1G32820,AT1G35870,AT1G36078,AT1G36305,AT1G36570,AT1G36850,AT1G37120,AT1G41790,AT1G41890,AT1G41920,AT1G42727,AT1G42888,AT1G43840,AT1G46120,AT1G49500,AT1G50180,AT1G58602,AT1G61400,AT1G68710,AT1G71710,AT1G72390,AT2G03330,AT2G04160,AT2G04190,AT2G04305,AT2G05390,AT2G05880,AT2G06000,AT2G06810,AT2G07080,AT2G07510,AT2G07600,AT2G09187,AT2G09950,AT2G10860,AT2G11220,AT2G11310,AT2G11740,AT2G12260,AT2G12340,AT2G12920,AT2G13020,AT2G13260,AT2G13363,AT2G14180,AT2G14455,AT2G15070,AT2G15510,AT2G15700,AT2G15800,AT2G15870,AT2G16690,AT2G16830,AT2G23950,AT2G24980,AT2G25050,AT2G29890,AT2G31300,AT2G41600,AT2G44640,AT2G45245,AT3G01610,AT3G02660,AT3G05725,AT3G10530,AT3G12670,AT3G15310,AT3G16560,AT3G19560,AT3G19670,AT3G20100,AT3G25690,AT3G30335,AT3G30465,AT3G30680,AT3G30708,AT3G31630,AT3G31920,AT3G31970,AT3G32035,AT3G32305,AT3G32320,AT3G32340,AT3G32677,AT3G33081,AT3G33130,AT3G42740,AT3G42766,AT3G42886,AT3G42922,AT3G43622,AT3G44045,AT3G44096,AT3G44270,AT3G45140,AT3G47021,AT3G47610,AT3G47740,AT3G49142,AT3G50460,AT3G56940,AT3G61470,AT4G02320,AT4G02960,AT4G03745,AT4G03775,AT4G04105,AT4G04221,AT4G04740,AT4G05586,AT4G05589,AT4G05597,AT4G06479,AT4G06483,AT4G06499,AT4G06503,AT4G06517,AT4G06526,AT4G06584,AT4G06587,AT4G06605,AT4G06609,AT4G06631,AT

	4G06648,AT4G06650,AT4G06682,AT4G07320,AT4G07491,AT4G07510,AT4G07660,AT4G07896,AT4G07960,AT4G08030,AT4G08053,AT4G08099,AT4G08430,AT4G08830,AT4G09595,AT4G10060,AT4G10650,AT4G11340,AT4G13420,AT4G14340,AT4G17450,AT4G22420,AT4G22485,AT4G23120,AT4G27852,AT4G28700,AT4G31160,AT5G03290,AT5G06630,AT5G07570,AT5G13680,AT5G17300,AT5G17320
SQvFLvHL	AT1G07800,AT1G07980,AT1G10745,AT1G15670,AT1G20860,AT1G30340,AT1G33130,AT1G35520,AT1G36940,AT1G41930,AT1G42050,AT1G42060,AT1G43830,AT1G44850,AT1G45163,AT1G54000,AT1G77990,AT2G01029,AT2G05660,AT2G05680,AT2G05800,AT2G06150,AT2G06255,AT2G06840,AT2G06860,AT2G10810,AT2G10921,AT2G11780,AT2G11940,AT2G13080,AT2G13170,AT2G14300,AT2G14430,AT2G14470,AT2G15250,AT2G18480,AT2G20950,AT2G21460,AT2G28640,AT2G28750,AT2G36940,AT2G38220,AT3G10340,AT3G17185,AT3G27400,AT3G28100,AT3G28240,AT3G29643,AT3G30213,AT3G30416,AT3G30418,AT3G30420,AT3G30668,AT3G32110,AT3G33178,AT3G42910,AT3G43020,AT3G43080,AT3G43144,AT3G43870,AT3G45130,AT3G46183,AT3G47280,AT3G52680,AT3G55930,AT3G60140,AT4G03840,AT4G06574,AT4G06597,AT4G06636,AT4G07755,AT4G08560,AT4G08765,AT4G10980,AT4G18410,AT4G21060,AT5G24220,AT5G26580,AT5G26970,AT5G27885,AT5G28165,AT5G28696,AT5G32254,AT5G33624,AT5G35045,AT5G35535,AT5G39245,AT5G47280
SQvFLvLL	AT1G05780,AT1G20390,AT1G20760,AT1G22560,AT1G23930,AT1G24640,AT1G25886,AT1G26558,AT1G35840,AT1G81020,AT2G01918,AT2G05610,AT2G05960,AT2G06240,AT2G10310,AT2G10430,AT2G12330,AT2G13830,AT2G15100,AT2G16180,AT2G18880,AT2G22350,AT2G28980,AT2G31520,AT2G41745,AT3G02610,AT3G29205,AT3G29210,AT3G30810,AT3G31500,AT3G32405,AT3G32902,AT3G33065,AT3G33083,AT3G42553,AT3G49230,AT3G54730,AT3G59720,AT3G62725,AT4G00970,AT4G03310,AT4G04450,AT4G05300,AT4G06491,AT4G06546,AT4G07518,AT4G08105,AT4G09143,AT4G10580,AT4G30740,AT4G31910,AT5G07215,AT5G07505,AT5G09513
SQvHLvLL	AT1G10260,AT1G12725,AT1G13245,AT1G17495,AT1G17900,AT1G21020,AT1G25430,AT1G26860,AT1G33080,AT1G33950,AT1G34240,AT1G35120,AT1G35320,AT1G35647,AT1G36530,AT1G36800,AT1G41835,AT1G42450,AT1G43785,AT1G44140,AT1G46624,AT1G54030,AT1G65450,AT1G67105,AT1G79150,AT2G02103,AT2G04090,AT2G04600,AT2G05130,AT2G05560,AT2G06967,AT2G07160,AT2G07590,AT2G09820,AT2G10100,AT2G10210,AT2G12450,AT2G13060,AT2G14870,AT2G15940,AT2G16080,AT2G19100,AT2G19360,AT2G41640,AT3G23725,AT3G24390,AT3G27883,AT3G28220,AT3G29175,AT3G30330,AT3G31510,AT3G32112,AT3G32120,AT3G33124,AT3G42086,AT3G42256,AT3G42466,AT3G42530,AT3G42720,AT3G42806,AT3G42870,AT3G43675,AT3G43681,AT3G43688,AT3G45775,AT3G48523,AT3G55400,AT4G04140,AT4G04570,AT4G05073,AT4G06581,AT4G07720,AT4G08115,AT4G08780,AT4G13885,AT4G15290,AT4G15370,AT4G17820,AT4G34730,AT4G37705

FLvHLvLL	AT1G01660,AT1G02010,AT1G02520,AT1G03910,AT1G06150,AT1G06630,AT1G07220,AT1G19220,AT1G20160,AT1G24360,AT1G25500,AT1G29750,AT1G30935,AT1G33790,AT1G34550,AT1G35110,AT1G36180,AT1G36540,AT1G37340,AT1G38167,AT1G38450,AT1G40109,AT1G40390,AT1G41710,AT1G41820,AT1G42377,AT1G43250,AT1G43725,AT1G43883,AT1G44510,AT1G44960,AT1G47860,AT1G52940,AT1G55050,AT1G56100,AT1G58190,AT1G59780,AT1G63260,AT1G63750,AT1G64410,AT1G66100,AT1G66783,AT1G67635,AT1G68640,AT1G70620,AT1G74550,AT1G79730,AT2G01973,AT2G02800,AT2G02830,AT2G05040,AT2G05110,AT2G06040,AT2G06290,AT2G06830,AT2G07410,AT2G07660,AT2G07750,AT2G07788,AT2G07789,AT2G09920,AT2G10180,AT2G10240,AT2G10280,AT2G11010,AT2G11430,AT2G11550,AT2G11930,AT2G12360,AT2G12670,AT2G12930,AT2G13850,AT2G14010,AT2G14650,AT2G16676,AT2G16970,AT2G18090,AT2G24880,AT2G24945,AT2G25940,AT2G28470,AT2G32295,AT2G34655,AT2G34790,AT2G39190,AT2G41580,AT2G42730,AT3G05540,AT3G14570,AT3G17360,AT3G19045,AT3G20440,AT3G21180,AT3G21230,AT3G22420,AT3G22770,AT3G24610,AT3G24675,AT3G25460,AT3G28915,AT3G28945,AT3G29080,AT3G29577,AT3G29634,AT3G29796,AT3G30170,AT3G30230,AT3G30630,AT3G30685,AT3G30802,AT3G30830,AT3G30875,AT3G31367,AT3G31375,AT3G31490,AT3G31904,AT3G32195,AT3G32226,AT3G32360,AT3G32966,AT3G33058,AT3G33066,AT3G33070,AT3G33595,AT3G42258,AT3G42431,AT3G42471,AT3G42545,AT3G42622,AT3G42690,AT3G42724,AT3G43148,AT3G43152,AT3G43835,AT3G43867,AT3G44605,AT3G45800,AT3G46490,AT3G46670,AT3G48170,AT3G48200,AT3G48720,AT3G52705,AT3G54823,AT3G54925,AT3G55260,AT3G57410,AT3G59570,AT3G60350,AT4G01975,AT4G02314,AT4G03830,AT4G03920,AT4G04393,AT4G04520,AT4G04530,AT4G05303,AT4G06501,AT4G06522,AT4G06550,AT4G06555,AT4G06573,AT4G06594,AT4G06630,AT4G06640,AT4G06644,AT4G06698,AT4G06742,AT4G07415,AT4G07520,AT4G07530,AT4G07600,AT4G07664,AT4G07856,AT4G09425,AT4G10990,AT4G11375,AT4G18150,AT4G20365,AT4G22415,AT4G26360,AT4G35785,AT4G37100,AT5G10100,AT5G10720,AT5G12210,AT5G14270,AT5G15480,AT5G17165
SQvFLvHLvLL	AT1G12720,AT1G16660,AT1G19090,AT1G20925,AT1G23670,AT1G28230,AT1G29650,AT1G30780,AT1G31030,AT1G31570,AT1G33070,AT1G34080,AT1G34600,AT1G34740,AT1G35370,AT1G36120,AT1G36130,AT1G37405,AT1G40101,AT1G40107,AT1G41850,AT1G42605,AT1G43444,AT1G44880,AT1G47625,AT1G48680,AT1G50050,AT1G51175,AT1G52020,AT1G52850,AT1G53265,AT1G53810,AT1G54040,AT1G54420,AT1G54430,AT1G60987,AT1G61510,AT1G62975,AT1G63870,AT1G64035,AT1G67240,AT1G70010,AT2G01840,AT2G01900,AT2G04670,AT2G05450,AT2G06310,AT2G06555,AT2G07395,AT2G11340,AT2G12370,AT2G12800,AT2G13450,AT2G14040,AT2G15540,AT2G15920,AT2G15990,AT2G16670,AT2G16680,AT2G19840,AT2G23720,AT2G24625,AT2G31080,AT2G32291,AT2G32698,AT2G34100,AT3G25450,AT3G26450,AT3G26483,AT3G26614,AT3G26616,AT3G28153,AT3G28865,AT3G29076,AT3G29480,AT3G29788,AT3G30749,AT3G31945,AT3G32914,AT3G42400,AT3G43302,AT3G43304,AT3G44570,AT3G44796,AT3G45253,AT3G45380,AT3G45520,AT3G47800,AT3G50625,AT3G55670,AT3G57586,AT3G58730,AT3G60170,AT3G62040,AT4G01490,AT4G01525,AT4G01530,AT4G03300,AT4G03380,AT4G03790,AT4G04050,AT4G04130,AT4G04560,AT4G05585,AT4G06487,AT4G06529,AT4G06670,AT4G07355,AT4G07516,AT4G07640,AT4G07942,AT4G08114,AT4G08720,AT4G10830,AT4G14460,AT4G15590,AT4G22040,AT4G22800,AT4G27890,AT4G29200,AT5G01335,AT5G13475

Table S2: List of differentially expressed genes between regime comparisons. SQ=SQHvSQL, FL=FLHvFLL, HL=SQHvFLH, LL=SQLvFLL

Light regime comparison	Differentially expressed genes
SQvFL	AT1G08630,AT1G17830,AT1G31750,AT1G52000,AT1G52040,AT1G61800,AT1G70640,AT2G02990,AT2G19970,AT2G30520,AT2G36750,AT2G45930,AT2G46780,AT2G47750,AT3G01480,AT3G21800,AT3G25290,AT3G43270,AT3G56480,AT4G13110,AT4G21910,AT4G33530,AT5G10300,AT5G16980,AT5G20900,AT5G43420,AT5G48490,AT5G63160,AT5G63450,AT5G65730,AT5G66650
SQvHL	AT1G02380,AT1G02610,AT1G02650,AT1G02920,AT1G03495,AT1G03940,AT1G04040,AT1G04570,AT1G05135,AT1G05810,AT1G06210,AT1G07020,AT1G07510,AT1G08550,AT1G10550,AT1G11380,AT1G12440,AT1G12450,AT1G13700,AT1G14880,AT1G16060,AT1G17060,AT1G19650,AT1G20780,AT1G21440,AT1G22160,AT1G22330,AT1G22400,AT1G22530,AT1G22550,AT1G23390,AT1G23480,AT1G23870,AT1G27290,AT1G27460,AT1G28570,AT1G32870,AT1G33960,AT1G34060,AT1G51680,AT1G51940,AT1G56540,AT1G57680,AT1G58684,AT1G61100,AT1G62620,AT1G66150,AT1G66180,AT1G66390,AT1G66600,AT1G66960,AT1G67050,AT1G69040,AT1G69310,AT1G70290,AT1G70520,AT1G72000,AT1G72150,AT1G72820,AT1G75810,AT1G76090,AT1G76890,AT1G77280,AT1G77920,AT1G78830,AT1G78850,AT1G79970,AT1G80440,AT1G80630,AT2G01850,AT2G01930,AT2G02450,AT2G02950,AT2G03550,AT2G04050,AT2G06850,AT2G14060,AT2G14610,AT2G15090,AT2G16660,AT2G17470,AT2G17550,AT2G18300,AT2G18660,AT2G18700,AT2G20670,AT2G21640,AT2G22200,AT2G22930,AT2G24550,AT2G25200,AT2G25900,AT2G28630,AT2G29440,AT2G30300,AT2G30490,AT2G30930,AT2G31280,AT2G32100,AT2G33020,AT2G34510,AT2G35710,AT2G36050,AT2G36410,AT2G36420,AT2G38820,AT2G39330,AT2G39700,AT2G39950,AT2G41560,AT2G41990,AT2G42580,AT2G44940,AT2G45170,AT2G45180,AT2G46330,AT2G47440,AT2G48030,AT3G02020,AT3G02170,AT3G02800,AT3G04030,AT3G06070,AT3G07060,AT3G10020,AT3G14090,AT3G14700,AT3G15358,AT3G15450,AT3G15630,AT3G15770,AT3G16150,AT3G18773,AT3G18777,AT3G18980,AT3G21240,AT3G21700,AT3G23030,AT3G24400,AT3G24982,AT3G27960,AT3G28080,AT3G28510,AT3G28910,AT3G43430,AT3G44350,AT3G44550,AT3G45260,AT3G46090,AT3G47620,AT3G48100,AT3G49620,AT3G50140,AT3G50450,AT3G50480,AT3G51330,AT3G53980,AT3G56260,AT3G57240,AT3G57680,AT3G58120,AT3G59220,AT3G60200,AT3G61198,AT3G62950,AT4G00670,AT4G00905,AT4G00970,AT4G01330,AT4G01915,AT4G02520,AT4G0354

	0,AT4G10860,AT4G11000,AT4G11300,AT4G11470,AT4G12735,AT4G13340,AT4G13860,AT4G14500,AT4G15690,AT4G15700,AT4G15760,AT4G16447,AT4G17245,AT4G17460,AT4G18130,AT4G18630,AT4G21930,AT4G22360,AT4G23820,AT4G24415,AT4G24800,AT4G27790,AT4G28250,AT4G29070,AT4G29110,AT4G30910,AT4G31000,AT4G31040,AT4G32300,AT4G33040,AT4G34250,AT4G35420,AT4G36730,AT4G36850,AT4G37140,AT4G37240,AT4G37310,AT4G37320,AT4G37610,AT4G38620,AT4G38690,AT4G39780,AT5G02480,AT5G03360,AT5G05390,AT5G06510,AT5G08250,AT5G08280,AT5G08330,AT5G08350,AT5G08520,AT5G09570,AT5G10410,AT5G14120,AT5G14330,AT5G19120,AT5G19190,AT5G20740,AT5G22560,AT5G22920,AT5G23360,AT5G24380,AT5G24640,AT5G25190,AT5G25280,AT5G26690,AT5G28770,AT5G32450,AT5G35777,AT5G37710,AT5G40890,AT5G42200,AT5G42250,AT5G43450,AT5G43760,AT5G44020,AT5G45275,AT5G45490,AT5G49360,AT5G51550,AT5G51910,AT5G52660,AT5G52900,AT5G52940,AT5G54380,AT5G56100,AT5G56700,AT5G57550,AT5G57660,AT5G57790,AT5G58690,AT5G60680,AT5G61440,AT5G62390,AT5G62865,AT5G63470,AT5G63480,AT5G64230,AT5G64620,AT5G65660,AT5G65870,AT5G66350,AT5G66460,AT5G66820,AT5G67330,AT5G67480
SQvLL	AT1G02310,AT1G10970,AT1G12990,AT1G13360,AT1G16500,AT1G19980,AT1G20070,AT1G22882,AT1G23060,AT1G24430,AT1G24530,AT1G29280,AT1G31814,AT1G43590,AT1G47510,AT1G48330,AT1G49450,AT1G49960,AT1G52880,AT1G55850,AT1G56600,AT1G60190,AT1G66920,AT1G71015,AT1G71890,AT1G79160,AT2G04110,AT2G05950,AT2G06255,AT2G17740,AT2G19310,AT2G22710,AT2G23560,AT2G36540,AT2G39350,AT2G42560,AT2G43540,AT3G05640,AT3G07410,AT3G07730,AT3G11340,AT3G11550,AT3G12977,AT3G14020,AT3G20100,AT3G21710,AT3G27220,AT3G47640,AT3G48920,AT3G54363,AT3G59210,AT3G60690,AT3G61630,AT4G03420,AT4G12300,AT4G13660,AT4G14020,AT4G28900,AT4G38060,AT4G39955,AT5G01810,AT5G13180,AT5G15500,AT5G16960,AT5G24080,AT5G43403,AT5G50400,AT5G51670,AT5G53710,AT5G54064,AT5G54230,AT5G54300,AT5G59510,AT5G59760

FLvHL	AT1G01060,AT1G01520,AT1G01560,AT1G02010,AT1G02180,AT1G02400,AT1G03440,AT1G03580,AT1G03650,AT1G03730,AT1G03930,AT1G04350,AT1G04530,AT1G04540,AT1G04550,AT1G05540,AT1G05550,AT1G05575,AT1G05675,AT1G05690,AT1G05750,AT1G05900,AT1G06040,AT1G06200,AT1G07010,AT1G07160,AT1G07450,AT1G07570,AT1G08810,AT1G08920,AT1G09070,AT1G09190,AT1G09680,AT1G09840,AT1G09940,AT1G09970,AT1G10090,AT1G10140,AT1G10155,AT1G10380,AT1G10650,AT1G10850,AT1G11960,AT1G12244,AT1G12610,AT1G12860,AT1G12900,AT1G13080,AT1G13930,AT1G14330,AT1G14480,AT1G14540,AT1G14840,AT1G14870,AT1G15010,AT1G15050,AT1G15290,AT1G15410,AT1G15760,AT1G16370,AT1G16480,AT1G17290,AT1G17630,AT1G18200,AT1G18210,AT1G18300,AT1G18335,AT1G18390,AT1G18470,AT1G18500,AT1G18650,AT1G18710,AT1G18720,AT1G18740,AT1G18810,AT1G19020,AT1G19180,AT1G19270,AT1G19380,AT1G19490,AT1G19950,AT1G20030,AT1G20310,AT1G20440,AT1G20470,AT1G20650,AT1G20693,AT1G20696,AT1G20810,AT1G20870,AT1G21100,AT1G21120,AT1G21550,AT1G21670,AT1G21680,AT1G22190,AT1G22360,AT1G22510,AT1G22610,AT1G23890,AT1G25400,AT1G25682,AT1G26270,AT1G26380,AT1G26560,AT1G26730,AT1G26790,AT1G26820,AT1G27045,AT1G27120,AT1G27770,AT1G28370,AT1G29170,AT1G29340,AT1G30135,AT1G30620,AT1G30720,AT1G30730,AT1G31320,AT1G31420,AT1G31430,AT1G31440,AT1G31650,AT1G32100,AT1G32520,AT1G32740,AT1G32780,AT1G32920,AT1G32928,AT1G33260,AT1G33480,AT1G33600,AT1G33790,AT1G33811,AT1G35510,AT1G42550,AT1G43980,AT1G44000,AT1G44446,AT1G45145,AT1G48315,AT1G48370,AT1G48480,AT1G48610,AT1G49010,AT1G49405,AT1G49580,AT1G49890,AT1G49990,AT1G50180,AT1G50740,AT1G50750,AT1G50890,AT1G51060,AT1G51340,AT1G51620,AT1G52340,AT1G52720,AT1G53090,AT1G53210,AT1G53680,AT1G53885,AT1G54790,AT1G55360,AT1G55960,AT1G56660,AT1G59910,AT1G60590,AT1G60690,AT1G61065,AT1G61210,AT1G61215,AT1G61300,AT1G61340,AT1G61560,AT1G61600,AT1G61670,AT1G61890,AT1G62190,AT1G62250,AT1G62630,AT1G62950,AT1G62960,AT1G63295,AT1G63750,AT1G63830,AT1G63850,AT1G63860,AT1G64065,AT1G64080,AT1G64330,AT1G64440,AT1G64500,AT1G64530,AT1G64625,AT1G64760,AT1G64860,AT1G65070,AT1G65230,AT1G65390,AT1G65870,AT1G66090,AT1G66100,AT1G66160,AT1G66330,AT1G66410,AT1G66460,AT1G66500,AT1G66810,AT1G66840,AT1G67120,AT1G67480,AT1G67710,AT1G67740,AT1G67840,AT1G68570,AT1G68600,AT1G68690,AT1G69370,AT1G69420,AT1G69526,AT1G69700,AT1G69840,AT1G70210,AT1G70250,AT1G70505,AT1G70550,AT1G70610,AT1G70980,AT1G71000,AT1G72416,AT1G72500,AT1G72645,AT1G72900,AT1G73030,AT1G73110,AT1G73170,AT1G73200,AT1G73540,AT1G73660,AT1G73730,AT1G73810,AT1G73860,AT1G74160,AT1G74400,AT1G74450,AT1G74510,AT1G74890,AT1G75100,AT1G76070,AT1G76590,AT1G76600,AT1G76650,AT1G76700,AT1G77080,AT1G77490,AT1G77580,AT1G78230,AT1G78280,AT1G78290,AT1G78460,AT1G78530,AT1G78600,AT1G79110,AT1G79245,AT1G79630,AT1G79680,AT1G80050,AT1G80280,AT1G80520,AT1G80640,AT1G80680,AT1G80760,AT1G80840,AT1G80850,AT2G01260,AT2G01300,AT2G01505,AT2G01730,AT2G02100,AT2G03280,AT2G04100,AT2G04170,AT2G04845,AT2G05310,AT2G06050,AT2G06530,AT2G07680,AT2G12460,AT2G12462,AT2G15280,AT2G15390,AT2G16070,AT2G16500,AT2G16700,AT2G17340,AT2G17480,AT2G17800,AT2G17820,AT2G17840,AT2G18120,AT2G18570,AT2G18690,AT2

	G19580,AT2G19650,AT2G20100,AT2G20570,AT2G20750,AT2G20960,AT2G21320,AT2G21500,AT2G21560,AT2G22240,AT2G22400,AT2G22860,AT2G22880,AT2G23180,AT2G23420,AT2G23430,AT2G23673,AT2G23950,AT2G24240,AT2G24280,AT2G24600,AT2G25250,AT2G25450,AT2G25460,AT2G25480,AT2G26550,AT2G26690,AT2G27310,AT2G27360,AT2G27500,AT2G27690,AT2G28120,AT2G28315,AT2G29360,AT2G29760,AT2G29900,AT2G29910,AT2G30020,AT2G30120,AT2G30170,AT2G30250,AT2G30360,AT2G30460,AT2G30500,AT2G30960,AT2G30990,AT2G31010,AT2G31060,AT2G31380,AT2G31450,AT2G31560,AT2G31750,AT2G32150,AT2G32190,AT2G32430,AT2G32440,AT2G32540,AT2G32690,AT2G32720,AT2G32800,AT2G32950,AT2G32960,AT2G33360,AT2G33580,AT2G34060,AT2G34080,AT2G34360,AT2G34400,AT2G34710,AT2G34720,AT2G34920,AT2G35930,AT2G36380,AT2G36895,AT2G36920,AT2G36970,AT2G37050,AT2G37100,AT2G37720,AT2G38570,AT2G38780,AT2G38790,AT2G38995,AT2G39450,AT2G39470,AT2G39560,AT2G39650,AT2G39730,AT2G40140,AT2G40260,AT2G40540,AT2G40670,AT2G40711,AT2G41290,AT2G41310,AT2G41312,AT2G41350,AT2G41420,AT2G41640,AT2G42975,AT2G42980,AT2G43590,AT2G44490,AT2G44840,AT2G45023,AT2G46225,AT2G46380,AT2G46450,AT2G46660,AT2G46735,AT2G46790,AT2G46810,AT2G46830,AT2G46940,AT2G47150,AT2G47490,AT3G01640,AT3G01830,AT3G01840,AT3G01980,AT3G02010,AT3G02130,AT3G02380,AT3G02830,AT3G02840,AT3G03030,AT3G03450,AT3G04010,AT3G04140,AT3G04720,AT3G04860,AT3G05200,AT3G05345,AT3G05580,AT3G05750,AT3G06410,AT3G06500,AT3G06650,AT3G08505,AT3G08720,AT3G08730,AT3G09040,AT3G09160,AT3G09330,AT3G09390,AT3G09450,AT3G09595,AT3G09600,AT3G10060,AT3G10120,AT3G10230,AT3G10300,AT3G10570,AT3G10760,AT3G10930,AT3G10985,AT3G11460,AT3G11490,AT3G11650,AT3G11670,AT3G11820,AT3G11900,AT3G12320,AT3G12490,AT3G12520,AT3G12920,AT3G13040,AT3G13160,AT3G13404,AT3G13405,AT3G13510,AT3G14050,AT3G14590,AT3G14770,AT3G15115,AT3G15200,AT3G15310,AT3G15354,AT3G15500,AT3G15520,AT3G15530,AT3G16060,AT3G16280,AT3G16860,AT3G17040,AT3G17185,AT3G17640

FLvLL	AT1G01810,AT1G02350,AT1G03760,AT1G06000,AT1G06720,AT1G0851,AT1G10360,AT1G12280,AT1G15440,AT1G17140,AT1G17420,AT1G17745,AT1G18850,AT1G19350,AT1G20190,AT1G24070,AT1G25250,AT1G25370,AT1G26762,AT1G27470,AT1G27920,AT1G29320,AT1G29460,AT1G29940,AT1G31550,AT1G34640,AT1G42430,AT1G48920,AT1G51800,AT1G52930,AT1G53645,AT1G54000,AT1G54010,AT1G54570,AT1G55205,AT1G55210,AT1G56110,AT1G57790,AT1G61120,AT1G61640,AT1G61870,AT1G62710,AT1G63250,AT1G63780,AT1G63810,AT1G64200,AT1G66580,AT1G68740,AT1G69530,AT1G71210,AT1G72310,AT1G72520,AT1G74240,AT1G75700,AT1G76640,AT1G77030,AT1G77520,AT1G78170,AT1G78995,AT1G79530,AT1G80130,AT1G80270,AT2G15690,AT2G17280,AT2G18900,AT2G20490,AT2G20940,AT2G24110,AT2G24210,AT2G24560,AT2G26695,AT2G27770,AT2G27775,AT2G29540,AT2G29710,AT2G30830,AT2G31110,AT2G31390,AT2G34070,AT2G34260,AT2G34357,AT2G35290,AT2G35742,AT2G35790,AT2G38750,AT2G38770,AT2G38980,AT2G40200,AT2G40360,AT2G40610,AT2G41170,AT2G42540,AT2G45000,AT2G45960,AT2G46250,AT2G46710,AT3G03060,AT3G03780,AT3G04485,AT3G05810,AT3G05932,AT3G06530,AT3G07050,AT3G07750,AT3G09350,AT3G09870,AT3G12145,AT3G12270,AT3G12300,AT3G12860,AT3G13310,AT3G15352,AT3G15357,AT3G16330,AT3G16370,AT3G17050,AT3G18600,AT3G19800,AT3G21540,AT3G22310,AT3G23590,AT3G23630,AT3G23830,AT3G23990,AT3G26410,AT3G26445,AT3G28007,AT3G43715,AT3G44750,AT3G44860,AT3G46180,AT3G46210,AT3G47420,AT3G47980,AT3G48250,AT3G48290,AT3G48720,AT3G49230,AT3G49240,AT3G52170,AT3G54510,AT3G55510,AT3G55580,AT3G55940,AT3G56060,AT3G56070,AT3G56830,AT3G56990,AT3G57150,AT3G57490,AT3G57940,AT3G58660,AT3G59670,AT3G63445,AT4G00695,AT4G03440,AT4G04020,AT4G04940,AT4G05410,AT4G05440,AT4G11911,AT4G12600,AT4G13750,AT4G14690,AT4G14750,AT4G15770,AT4G16630,AT4G18950,AT4G19060,AT4G21140,AT4G21320,AT4G23540,AT4G24240,AT4G25340,AT4G25630,AT4G25730,AT4G27435,AT4G27490,AT4G27560,AT4G30410,AT4G30990,AT4G31500,AT4G31790,AT4G32890,AT4G33000,AT4G34200,AT4G34360,AT4G34710,AT4G36830,AT4G38850,AT4G38910,AT5G02050,AT5G02670,AT5G02820,AT5G02840,AT5G04190,AT5G06550,AT5G06970,AT5G09470,AT5G09590,AT5G10250,AT5G10930,AT5G11240,AT5G13830,AT5G14520,AT5G15550,AT5G16750,AT5G17030,AT5G17990,AT5G19110,AT5G20010,AT5G24780,AT5G25390,AT5G27120,AT5G27250,AT5G35935,AT5G38890,AT5G39080,AT5G40540,AT5G40770,AT5G41670,AT5G42150,AT5G42650,AT5G43400,AT5G43980,AT5G44510,AT5G46270,AT5G46500,AT5G48880,AT5G49280,AT5G49560,AT5G50930,AT5G51080,AT5G55920,AT5G56030,AT5G57780,AT5G59240,AT5G59780,AT5G62370,AT5G64470,AT5G64680,AT5G64700,AT5G65080,AT5G65920,AT5G67630

FLLvLL	AT3G18217,AT3G18750,AT3G19010,AT3G19080,AT3G19240,AT3G20270,AT3G20410,AT3G20440,AT3G20600,AT3G21070,AT3G21150,AT3G21390,AT3G21670,AT3G21870,AT3G22104,AT3G22420,AT3G22810,AT3G23000,AT3G23020,AT3G23109,AT3G23250,AT3G23840,AT3G23930,AT3G24460,AT3G25585,AT3G25590,AT3G25780,AT3G26085,AT3G26310,AT3G26782,AT3G26910,AT3G26980,AT3G27210,AT3G27350,AT3G27690,AT3G28040,AT3G28060,AT3G28210,AT3G28345,AT3G28750,AT3G29000,AT3G29760,AT3G29772,AT3G42860,AT3G43250,AT3G43540,AT3G44260,AT3G45040,AT3G45960,AT3G45970,AT3G46200,AT3G46900,AT3G46930,AT3G47100,AT3G47295,AT3G47430,AT3G47500,AT3G47580,AT3G48000,AT3G48240,AT3G48520,AT3G48990,AT3G49120,AT3G49170,AT3G49320,AT3G49530,AT3G49650,AT3G49780,AT3G50260,AT3G50660,AT3G50950,AT3G51150,AT3G52360,AT3G52450,AT3G52890,AT3G52920,AT3G53220,AT3G53240,AT3G53350,AT3G53920,AT3G54020,AT3G54220,AT3G54500,AT3G54690,AT3G55330,AT3G55430,AT3G55990,AT3G56080,AT3G56300,AT3G56370,AT3G56590,AT3G56790,AT3G56880,AT3G56940,AT3G57040,AT3G57360,AT3G58590,AT3G58680,AT3G59140,AT3G59400,AT3G59780,AT3G59820,AT3G60080,AT3G61080,AT3G61190,AT3G61310,AT4G00050,AT4G00070,AT4G01050,AT4G01250,AT4G01360,AT4G02350,AT4G02380,AT4G02425,AT4G02850,AT4G03550,AT4G04850,AT4G05087,AT4G05090,AT4G05460,AT4G08500,AT4G10150,AT4G10650,AT4G11600,AT4G11680,AT4G11780,AT4G12080,AT4G12110,AT4G12390,AT4G13395,AT4G13680,AT4G14096,AT4G14365,AT4G14370,AT4G14430,AT4G14550,AT4G14740,AT4G14820,AT4G15248,AT4G15430,AT4G15545,AT4G15550,AT4G16490,AT4G16740,AT4G17230,AT4G17350,AT4G17490,AT4G17500,AT4G17610,AT4G17615,AT4G18010,AT4G18020,AT4G18520,AT4G18530,AT4G18570,AT4G18880,AT4G18980,AT4G19380,AT4G19520,AT4G19820,AT4G19830,AT4G19960,AT4G19985,AT4G20000,AT4G20070,AT4G20300,AT4G20860,AT4G21390,AT4G21560,AT4G21570,AT4G21680,AT4G22220,AT4G22290,AT4G22560,AT4G22570,AT4G22710,AT4G22730,AT4G22780,AT4G23010,AT4G23180,AT4G23190,AT4G23220,AT4G23680,AT4G24110,AT4G24220,AT4G24700,AT4G24790,AT4G25030,AT4G25290,AT4G25420,AT4G25470,AT4G25490,AT4G25810,AT4G25850,AT4G26055,AT4G26850,AT4G27280,AT4G27360,AT4G27595,AT4G27652,AT4G27654,AT4G28150,AT4G29220,AT4G29440,AT4G29610,AT4G29780,AT4G30270,AT4G30280,AT4G30610,AT4G30980,AT4G31550,AT4G31970,AT4G32710,AT4G33130,AT4G33560,AT4G33920,AT4G33930,AT4G33940,AT4G33985,AT4G34120,AT4G34390,AT4G34410,AT4G34630,AT4G34650,AT4G35050,AT4G35480,AT4G35830,AT4G35985,AT4G36010,AT4G36105,AT4G36230,AT4G36500,AT4G36650,AT4G36670,AT4G36900,AT4G36945,AT4G37080,AT4G37330,AT4G37550,AT4G37560,AT4G37650,AT4G37925,AT4G38092,AT4G38320,AT4G38330,AT4G38430,AT4G38440,AT4G38960,AT4G39330,AT4G39510,AT4G39710,AT4G39830,AT5G01090,AT5G01100,AT5G01260,AT5G01380,AT5G02120,AT5G02830,AT5G03140,AT5G03250,AT5G03555,AT5G03720,AT5G04250,AT5G04660,AT5G04760,AT5G04780,AT5G04870,AT5G05140,AT5G05300,AT5G05330,AT5G05590,AT5G05600,AT5G06790,AT5G07440,AT5G08305,AT5G08430,AT5G08440,AT5G08720,AT5G09270,AT5G09850,AT5G09990,AT5G10695,AT5G11000,AT5G11020,AT5G11260,AT5G11380,AT5G11680,AT5G13190,AT5G13200,AT5G13205,AT5G13360,AT5G13630,AT5G13920,AT5G14470,AT5G14650,AT5G14760,AT5G15050,AT5G15180,AT5G15310,AT5G15430,AT5G15600,AT5G15640,AT5G15790,AT5

	G15830,AT5G15900,AT5G15910,AT5G16540,AT5G16910,AT5G17165,AT5G17230,AT5G17300,AT5G17310,AT5G17460,AT5G17850,AT5G18020,AT5G18030,AT5G18080,AT5G18150,AT5G18400,AT5G18404,AT5G18460,AT5G18470,AT5G18670,AT5G19090,AT5G19230,AT5G19290,AT5G19390,AT5G19500,AT5G19600,AT5G19730,AT5G19970,AT5G20050,AT5G20230,AT5G20410,AT5G20580,AT5G22250,AT5G22390,AT5G22540,AT5G22545,AT5G22690,AT5G22820,AT5G24120,AT5G24590,AT5G25440,AT5G25590,AT5G25930,AT5G26030,AT5G26340,AT5G27420,AT5G27520,AT5G27930,AT5G28530,AT5G30495,AT5G32621,AT5G34800,AT5G34810,AT5G35735,AT5G35740,AT5G35970,AT5G36700,AT5G36910,AT5G36925,AT5G37020,AT5G37540,AT5G37770,AT5G37790,AT5G38410,AT5G38690,AT5G38710,AT5G39350,AT5G39580,AT5G41050,AT5G41070,AT5G41100,AT5G41750,AT5G42760,AT5G42890,AT5G43630,AT5G43870,AT5G44005,AT5G44420,AT5G44430,AT5G44585,AT5G45720,AT5G45750,AT5G45940,AT5G45950,AT5G46080,AT5G46710,AT5G46830,AT5G47070,AT5G47220,AT5G47230,AT5G47240,AT5G47540,AT5G47610,AT5G47620,AT5G47650,AT5G47850,AT5G48380,AT5G48460,AT5G48520,AT5G48545,AT5G48657,AT5G49230,AT5G49300,AT5G49520,AT5G50240,AT5G51390,AT5G51850,AT5G52020,AT5G52120,AT5G52170,AT5G52570,AT5G53900,AT5G54130,AT5G54170,AT5G54650,AT5G54690,AT5G54940,AT5G55380,AT5G55620,AT5G55760,AT5G56840,AT5G56850,AT5G56860,AT5G57210,AT5G57220,AT5G57640,AT5G57710,AT5G57785,AT5G57960,AT5G58090,AT5G58140,AT5G58340,AT5G58380,AT5G58870,AT5G59550,AT5G59660,AT5G60170,AT5G60370,AT5G61370,AT5G61380,AT5G61600,AT5G62520,AT5G62910,AT5G62990,AT5G63530,AT5G63700,AT5G64190,AT5G64260,AT5G64310,AT5G64530,AT5G64660,AT5G64750,AT5G64770,AT5G64840,AT5G64870,AT5G64905,AT5G64940,AT5G65300,AT5G65683,AT5G65685,AT5G65820,AT5G65890,AT5G66070,AT5G66210,AT5G67030,AT5G67080,AT5G67140,AT5G67385,AT5G67640

HLvLL	AT1G01200,AT1G01370,AT1G01640,AT1G01820,AT1G01900,AT1G02640,AT1G02860,AT1G02970,AT1G03090,AT1G04020,AT1G04730,AT1G05890,AT1G06370,AT1G06540,AT1G06550,AT1G07240,AT1G08800,AT1G08900,AT1G08980,AT1G09200,AT1G09390,AT1G09570,AT1G11000,AT1G11280,AT1G11350,AT1G11530,AT1G12200,AT1G12380,AT1G12910,AT1G13245,AT1G13390,AT1G14205,AT1G15380,AT1G15885,AT1G16400,AT1G16410,AT1G17190,AT1G18250,AT1G18590,AT1G18870,AT1G19610,AT1G20010,AT1G20950,AT1G21810,AT1G21830,AT1G23190,AT1G23450,AT1G23880,AT1G23960,AT1G25510,AT1G26580,AT1G26665,AT1G27660,AT1G27880,AT1G28330,AT1G30220,AT1G30250,AT1G30330,AT1G30600,AT1G31790,AT1G32090,AT1G33050,AT1G35290,AT1G35530,AT1G35612,AT1G36370,AT1G36980,AT1G43700,AT1G45201,AT1G47900,AT1G49032,AT1G49240,AT1G49720,AT1G49730,AT1G51070,AT1G51140,AT1G51270,AT1G52710,AT1G53170,AT1G53780,AT1G53785,AT1G54385,AT1G54680,AT1G54730,AT1G55320,AT1G55690,AT1G56010,AT1G56140,AT1G56200,AT1G56280,AT1G57540,AT1G58030,AT1G58190,AT1G62260,AT1G62540,AT1G62560,AT1G62870,AT1G63650,AT1G63690,AT1G63800,AT1G64230,AT1G64380,AT1G64720,AT1G65060,AT1G65470,AT1G65480,AT1G66370,AT1G67750,AT1G67980,AT1G68050,AT1G68430,AT1G68470,AT1G69580,AT1G69588,AT1G70420,AT1G71060,AT1G71865,AT1G72970,AT1G74670,AT1G75490,AT1G76705,AT1G77145,AT1G78130,AT1G78370,AT1G78430,AT1G78570,AT1G78895,AT1G79700,AT1G80160,AT1G80180,AT1G80340,AT1G80570,AT1G80960,AT2G01340,AT2G02400,AT2G04780,AT2G05520,AT2G05540,AT2G06002,AT2G06025,AT2G10980,AT2G11150,AT2G11780,AT2G13680,AT2G14050,AT2G14170,AT2G15440,AT2G15830,AT2G15960,AT2G16380,AT2G16850,AT2G17036,AT2G17705,AT2G18290,AT2G18390,AT2G19450,AT2G20740,AT2G20980,AT2G21660,AT2G22250,AT2G22450,AT2G22980,AT2G24490,AT2G25730,AT2G25850,AT2G25880,AT2G25930,AT2G26300,AT2G26530,AT2G27402,AT2G27830,AT2G28260,AT2G28740,AT2G28790,AT2G30230,AT2G30600,AT2G31270,AT2G31945,AT2G32090,AT2G32940,AT2G32990,AT2G33340,AT2G33830,AT2G34150,AT2G34655,AT2G34690,AT2G35120,AT2G35810,AT2G36060,AT2G36570,AT2G36885,AT2G37040,AT2G37130,AT2G37260,AT2G38400,AT2G39200,AT2G39400,AT2G39570,AT2G40080,AT2G40480,AT2G41180,AT2G42040,AT2G42890,AT2G43100,AT2G44060,AT2G44480,AT2G44690,AT2G45360,AT2G45900,AT2G46490,AT2G46535,AT2G46650,AT2G47460,AT2G47485,AT2G47800,AT3G01520,AT3G01770,AT3G03180,AT3G03380,AT3G04020,AT3G04910,AT3G05160,AT3G05800,AT3G06433,AT3G07010,AT3G07274,AT3G07280,AT3G07560,AT3G07650,AT3G07720,AT3G07880,AT3G08770,AT3G10185,AT3G11020,AT3G11100,AT3G13450,AT3G14395,AT3G15680,AT3G15820,AT3G16640,AT3G16770,AT3G19370,AT3G20200,AT3G20260,AT3G21190,AT3G21780,AT3G21790,AT3G22460,AT3G23085,AT3G23150,AT3G23480,AT3G23510,AT3G23530,AT3G24000,AT3G24420,AT3G25130,AT3G25150,AT3G25990,AT3G26165,AT3G26180,AT3G26280,AT3G26740,AT3G27640,AT3G27770,AT3G28840,AT3G28850,AT3G28945,AT3G29035,AT3G29590,AT3G30775,AT3G41979,AT3G43600,AT3G44730,AT3G44798,AT3G44960,AT3G44970,AT3G45090,AT3G45590,AT3G45930,AT3G46320,AT3G46370,AT3G46640,AT3G46670,AT3G47160,AT3G47340,AT3G47360,AT3G48780,AT3G49580,AT3G50500,AT3G50830,AT3G50840,AT3G51380,AT3G52630,AT3G53210,AT3G53800,AT3G53830,AT3G53880,AT3G53990,AT3G54366,AT3G54390,AT3G54560,AT3G54600,AT3G54750,AT3

	G56050,AT3G56960,AT3G57630,AT3G58990,AT3G59010,AT3G59765,AT3G60160,AT3G60290,AT3G60300,AT3G61160,AT3G61210,AT3G62150,AT3G62290,AT3G62650,AT3G62740,AT3G63200,AT3G63250,AT4G00020,AT4G00335,AT4G00480,AT4G00720,AT4G01060,AT4G01440,AT4G02060,AT4G02110,AT4G04330,AT4G04410,AT4G04760,AT4G04925,AT4G06746,AT4G09820,AT4G09830,AT4G11360,AT4G11521,AT4G11910,AT4G12440,AT4G14040,AT4G14200,AT4G14270,AT4G14680,AT4G15260,AT4G15280,AT4G15610,AT4G15620,AT4G15780,AT4G16190,AT4G16380,AT4G16520,AT4G17140,AT4G17486,AT4G17680,AT4G17970,AT4G19890,AT4G20370,AT4G20930,AT4G21620,AT4G23250,AT4G24520,AT4G26050,AT4G26940,AT4G26960,AT4G27130,AT4G28040,AT4G28220,AT4G28240,AT4G28310,AT4G29150,AT4G29820,AT4G30110,AT4G30240,AT4G30690,AT4G31050,AT4G31060,AT4G31820,AT4G31840,AT4G32150,AT4G32340,AT4G33980,AT4G34240,AT4G35030,AT4G35110,AT4G35640,AT4G38660,AT4G38932,AT4G38950,AT4G39210,AT4G39400,AT4G39940,AT4G40070,AT5G01340,AT5G01370,AT5G01500,AT5G01940,AT5G02020,AT5G03240,AT5G03730,AT5G04220,AT5G05060,AT5G05435,AT5G05480,AT5G05690,AT5G05790,AT5G06690,AT5G06870,AT5G07100,AT5G07460,AT5G08020,AT5G08500,AT5G10170,AT5G10390,AT5G10400,AT5G10860,AT5G11230,AT5G12110,AT5G13060,AT5G13110,AT5G14180,AT5G14200,AT5G16410,AT5G16420,AT5G17590,AT5G17800,AT5G18170,AT5G18525,AT5G18640,AT5G19260,AT5G20520,AT5G20850,AT5G21020,AT5G21970,AT5G22090,AT5G22270,AT5G22880,AT5G23380,AT5G23420,AT5G23890,AT5G24105,AT5G24160,AT5G24610,AT5G25350,AT5G26330,AT5G27860,AT5G35926,AT5G37980,AT5G39160,AT5G39190,AT5G40450,AT5G41260,AT5G41700,AT5G42190,AT5G42720,AT5G42825,AT5G42860,AT5G43060,AT5G43745,AT5G44720,AT5G45310,AT5G46240,AT5G46330,AT5G46860,AT5G47590,AT5G48385,AT5G48412,AT5G48850,AT5G49640,AT5G49810,AT5G52630,AT5G53486,AT5G54080,AT5G54670,AT5G55480,AT5G56750,AT5G56870,AT5G57340,AT5G57420,AT5G57565,AT5G57655,AT5G58000,AT5G58787,AT5G58920,AT5G59070,AT5G59680,AT5G59690,AT5G59720,AT5G59870,AT5G60490,AT5G61000,AT5G61930,AT5G62360,AT5G62900,AT5G63370,AT5G63550,AT5G63620,AT5G63800,AT5G63980,AT5G65360,AT5G66790,AT5G67180
SQvFLvHL	AT1G02660,AT1G05170,AT1G05870,AT1G06160,AT1G07000,AT1G07135,AT1G08930,AT1G11700,AT1G12820,AT1G15960,AT1G16130,AT1G18570,AT1G19700,AT1G27100,AT1G27370,AT1G32240,AT1G33610,AT1G48100,AT1G51440,AT1G57990,AT1G63260,AT1G64390,AT1G69890,AT1G69900,AT1G72490,AT2G01180,AT2G01190,AT2G16600,AT2G23810,AT2G25735,AT2G26560,AT2G31230,AT2G32200,AT2G35658,AT2G40475,AT2G41430,AT2G44500,AT3G01290,AT3G04640,AT3G10150,AT3G24750,AT3G28070,AT3G48360,AT3G51550,AT3G52400,AT3G55980,AT3G57520,AT3G57930,AT3G59350,AT3G60260,AT3G62720,AT4G00300,AT4G09920,AT4G13100,AT4G16500,AT4G17880,AT4G23810,AT4G26950,AT4G32295,AT4G32480,AT5G02290,AT5G05440,AT5G06320,AT5G08150,AT5G11460,AT5G17600,AT5G25250,AT5G45110,AT5G61590,AT5G67200
SQvFLvLL	AT5G49100

SQvHLvLL	AT1G11260,AT1G19370,AT1G30160,AT1G50040,AT1G75580,AT2G15890,AT2G18050,AT2G23290,AT2G29300,AT2G37870,AT2G43290,AT2G46730,AT3G13600,AT3G14720,AT3G18950,AT3G50410,AT3G53790,AT4G00270,AT4G03210,AT4G08040,AT4G20260,AT4G27450,AT4G33467,AT5G06280,AT5G07990,AT5G11070,AT5G20250,AT5G24880,AT5G25240,AT5G37300,AT5G47050
FLvHLvLL	AT1G10070,AT1G11440,AT1G22500,AT1G23205,AT1G62030,AT1G71340,AT1G73010,AT1G73870,AT1G76240,AT1G80800,AT2G01150,AT2G15020,AT2G20880,AT2G21510,AT2G22500,AT2G25820,AT2G27080,AT2G30890,AT2G32210,AT2G32410,AT2G34600,AT2G36220,AT2G40960,AT2G43465,AT3G02070,AT3G02880,AT3G04310,AT3G05937,AT3G06868,AT3G09590,AT3G12110,AT3G17510,AT3G53190,AT3G54810,AT3G57450,AT4G02330,AT4G15490,AT4G16563,AT4G19390,AT4G20830,AT4G24540,AT4G24570,AT4G27070,AT4G28140,AT4G30400,AT4G31800,AT4G31875,AT4G35770,AT5G03670,AT5G05410,AT5G06270,AT5G09440,AT5G13220,AT5G13700,AT5G15650,AT5G16380,AT5G18290,AT5G28237,AT5G38140,AT5G42900,AT5G44568,AT5G46730,AT5G52050,AT5G62040,AT5G66052,AT5G67300
SQvFLvHLvLL	AT1G04220,AT1G08250,AT1G11210,AT1G13260,AT1G15100,AT1G21910,AT1G25560,AT1G29690,AT1G33760,AT1G35140,AT1G70090,AT1G75220,AT1G77640,AT2G17230,AT2G22420,AT3G19680,AT3G25600,AT3G28140,AT3G28340,AT3G50060,AT3G55840,AT3G59080,AT4G01950,AT4G08950,AT4G11280,AT4G11990,AT4G24780,AT4G35270,AT4G37260,AT4G39070,AT5G03552,AT5G05190,AT5G22380,AT5G23130,AT5G43740,AT5G45340,AT5G54470,AT5G57560,AT5G67450

Table S3: Complete table of differentially methylated and expressed genes between growth light regimes. Coloured according to light regime comparison- Red= SQHvSQL, Orange= FLHvFLL, Purple= SQHvFLH, Blue= SQLvFLL. *P*-adj<0.05, n=3.

Gene code	Context	Methylation	log2FC	Gene	Function
AT1G62770	CHH	loss	3.03	PMEI9	PMEI9 pectin methylesterase inhibitor.
AT2G06255	CHH	loss	1.33	EFL3	DUF1313 domain containing protein, involved in photoperiodism
AT2G22710	CG, CHG	gain	2.24		Transposable element (guard cell)
AT1G33950	CHH	loss	-4.97	IAN7	Avirulence induced gene (AIG1) family protein
AT2G18660	CHH	loss	-3.34	ATPNP-1	Encodes PNP-A (Plant Natriuretic Peptide A), exact role unknown but is stress responsive
AT4G00970	CHG	gain	-2.25	CRK41	Encodes a cysteine-rich receptor-like protein kinase.
AT1G02010	CG	gain	-1.21	SEC1A	member of KEULE Gene Family
AT1G06720	CG	gain	2.21		P-loop containing nucleoside triphosphate hydrolases superfamily protein
AT1G11960	CG	loss	2.89	OSCA1.3	Calcium channel that is phosphorylated by BIK1 in the presence of PAMPS and required for stomatal immunity.
AT1G17745	CHH	loss	1.89	PGDH2	encodes a 3-Phosphoglycerate dehydrogenase
AT1G26380	CG	loss	2.25	FOX1	Functions in the biosynthesis of 4-hydroxy indole-3-carbonyl nitrile (4-OH-ICN), a cyanogenic phytoalexin in *Arabidopsis*
AT1G26762	CHH	gain	-2.53		Transmembrane protein
AT1G28230	CHH	gain	1.96	ATPUP1	Encodes a transporter that transports purines, cytokinins and other adenine derivatives
AT1G29170	CG	gain	-1.42	WAVE2	Encodes a member of the SCAR family. These proteins are part of a complex (WAVE) complex. The SCAR subunit activates the ARP2/3 complex which in turn act as a nucleator for actin filaments
AT1G31420	CG	loss	-0.81	FEI1	Encodes a plasma membrane localized leucine-rich repeat receptor kinase that is involved in cell wall elongation
AT1G33790	CG	loss	1.63		jacalin lectin family protein

AT1G49890	CG	loss	-0.64	QWRF2	Together with QWRF1 redundantly modulates cortical microtubule arrangement in floral organ growth and fertility
AT1G54000	CHH	gain	3.10	GLL22	GDSL-motif esterase/acyltransferase/lipase
AT1G63260	CG	loss	-1.14	TET10	Member of TETRASPANIN family
AT1G63750	CHH	gain	1.30		miR825-5p target proposed as a phasiRNA producing locus
AT1G63810	CG	loss	2.27		nucleolar protein
AT1G64860	CG	loss	-1.60	SIGA	Subunit of chloroplast RNA polymerase, confers the ability to recognize promoter sequences on the core enzyme
AT1G65070	CG	gain	-1.60		DNA mismatch repair protein MutS, type 2
AT1G66100	CHG	loss	-2.74		Predicted to encode a PR (pathogenesis-related) protein. Belongs to the plant thionin (PR-13) family
AT1G69170	CG	gain	-0.87	SPL6	Required for the resistance mediated by the TIR-NB-LRR RPS4 against Pseudomonas syringae carrying the avrRps4 effector.
AT1G75700	CG	gain	-2.35	HVA22G	HVA22-like protein G
AT2G10940	CG	loss	-1.90		Bifunctional inhibitor/lipid-transfer protein/seed storage 2S albumin superfamily protein
AT2G26560	CG	gain	3.24	PLP2	Encodes a lipid acyl hydrolase with wide substrate specificity that accumulates upon infection by fungal and bacterial pathogens. Protein is localized in the cytoplasm in healthy leaves, and in membranes in infected cells. Plays a role in cell death and differentially affects the accumulation of oxylipins. Contributes to resistance to virus.
AT2G32950	CG	loss	-1.00	COP1	Represses photomorphogenesis and induces skotomorphogenesis in the dark.
AT2G34060	CHH	gain	-2.44		Peroxidase superfamily protein
AT3G02070	CG	gain	0.65		Cysteine proteinases superfamily protein
AT3G03360	CG	loss	-0.91		F-box/RNI-like superfamily protein
AT3G05750	CG	loss	-0.85	TRM6	Encodes a member of the TRM superfamily, which plays a role in preprophase band formation during plant cell division and controls the robustness of the orientation of that cell division
AT3G07750	CG	gain	3.16	RRP42	3-5-exoribonuclease family protein

AT3G09450	CG	loss	-5.63		fusaric acid resistance family protein
AT3G11670	CG	gain	-1.09	DGD1	Responsible for the final assembly of galactolipids in photosynthetic membranes. Provides stability to the PS I core complex (e.g., subunits PsaD, PsaE).
AT3G12145	CHH, CG	loss, gain	1.53	FLOR1	A novel leucine-rich repeat protein. Interacts directly with MADS domain transcription factor.
AT3G17040	CG	loss,gain	-1.09	HCF107	It is an RNA tetratricopeptide repeat-containing protein required for normal processing of transcripts from the polycistronic chloroplast psbB-psbT-psbH-petB-petD operon coding for proteins of the photosystem II and cytochrome b6/f complexes.
AT3G17050	CG	loss	-1.43		Transposable element, pseudogene
AT3G17185	CHH	loss,gain	-3.90	ATTAS3	Encodes a trans-acting siRNA (tasi-RNA) that regulates the expression of auxin response factor genes (ARF2, ARF4, ETT). One of 3 genomic loci that encode the TAS3 siRNA. Has been identified as a translated small open reading frame by ribosome profiling
AT3G20440	CG	loss	3.30	BE1	a putative glycoside hydrolase. Involved in organogenesis and somatic embryogenesis by regulating carbohydrate metabolism
AT3G21870	CHH	loss	-2.47	CYCP2;1	cyclin p2
AT3G22420	CG	loss	-1.40	WNK2	Encodes a member of the WNK family (9 members in all) of protein kinases, the structural design of which is clearly distinct from those of other known protein kinases, such as receptor-like kinases and mitogen-activated protein kinases. Its transcription is under the control of circadian rhythms.
AT3G27170	CG	loss	-2.86	CLC-B	member of anion channel protein family
AT3G48720	CHH	gain, loss	-1.32	DCF	Encodes a hydroxycinnamoyl-CoA: v-hydroxy fatty acid transferase involved in cutin synthesis
AT3G49230	CHH	gain	5.04	DEG1	Transmembrane protein
AT3G56990	CG	loss	2.16	EDA7	embryo sac development arrest 7
AT3G57940	CG	loss	2.55		GNAT acetyltransferase (DUF699)
AT4G00960	CHG	loss	-3.18		protein kinase superfamily protein

AT4G17610	CG	gain	1.79	TRM3	tRNA/rRNA methyltransferase (SpoU) family protein
AT4G18520	CG	loss	1.60	PDM1	Encodes a PPR (pentatricopeptide repeat) protein PDM1/SEL1. Involved in RNA editing and splicing of plastid genes
AT4G25630	CG	loss	4.73	FIB2	encodes a fibrillarin, a key nucleolar protein in eukaryotes which associates with box C/D small nucleolar RNAs (snoRNAs) directing 2'-O-ribose methylation of the rRNA.
AT5G13770	CG	gain	-1.79		Pentatricopeptide repeat (PPR-like) superfamily protein
AT5G16980	CG	gain	2.52		Zinc-binding dehydrogenase family protein
AT5G17165	CHH	gain	-2.32		hypothetical protein, expressed in guard cell
AT5G28237	CHH	loss,gain	5.35		Pyridoxal-5-phosphate-dependent enzyme family protein
AT5G34800	CG	loss	-1.36	VANDAL20	Transposable element
AT5G35495	CG, CHG	loss, gain/loss	-2.51	ATLINE1_4	Transposable element, Class I
AT5G46920	CG	gain	1.53		Intron maturase, type II family protein in plastids
AT5G52170	CG	loss	-4.39	HDG7	Encodes a homeobox-leucine zipper family protein belonging to the HD-ZIP IV family
AT5G54650	CG	gain	0.73	FH5	Encodes a protein with similarity to formins that is involved in cytokinesis. FH5 was shown to be a maternally expressed imprinted gene.
AT5G55760	CG	loss	-0.75	SRT1	a member of the SIR2 (sirtuin) family HDAC (histone deacetylase)
AT5G65820	CG	loss	-1.16		Pentatricopeptide repeat (PPR) superfamily protein
AT1G02010	CG	loss	1.19	SEC1A	member of KEULE gene family
AT1G03090	CG	loss	-3.89	MCCA	MCCA is the biotinylated subunit of the dimer MCCase, which is involved in leucine degradation. Both subunits are nuclear coded, and the active enzyme is located in the mitochondrion
AT1G04400	CG	loss	-2.14	CRY2	Blue light receptor mediating blue-light regulated cotyledon expansion and flowering time
AT1G06630	CG	loss	-1.44		F-box/RNI-like superfamily protein
AT1G10210	CG	loss	-1.23	MPK1	Mitogen activated protein kinase, functions in auxin-activated signalling
AT1G11410	CG	gain	0.86		S-locus lectin protein kinase family protein

AT1G13245	CHH	gain	-1.38	RTFL17	Involved in negative regulation of cell proliferation
AT1G15670	CHH	loss	-3.28	KFB01	Encodes a member of a family of F-box proteins, called the KISS ME DEADLY (KMD) family, that targets type-B ARR proteins for degradation and is involved in the negative regulation of the cytokinin response. Also named as KFB1, a member of a group of Kelch repeat F-box proteins that negatively regulate phenylpropanoid biosynthesis by targeting the phenylpropanoid biosynthesis enzyme phenylalanine ammonia-lyase.
AT1G20650	CG	loss	1.61	ASG5	Protein kinase superfamily protein
AT1G20890	CG	gain	-0.95		caveolin-1 protein
AT1G20950	CG	loss	1.25		Phosphofructokinase family protein
AT1G27880	CG	loss	1.84		DEAD/DEAH box RNA helicase family protein
AT1G27940	CG	loss	2.89	PGP13	P-glycoprotein 13
AT1G30820	CG	loss	-2.72	CTP SYNTHASE1	Cytidine triphosphate synthase
AT1G31420	CG	gain	0.71	FEI1	a plasma membrane localized leucine-rich repeat receptor kinase that is involved in cell wall elongation
AT1G31440	CG	gain	1.42	SH3P1	SH3-domain containing protein
AT1G31570	CHH	loss,gain	2.17	ATENSPM3	CACTA-like TE
AT1G31770	CG	loss	1.94	ABCG14	ATP-binding cassette 14
AT1G32080	CG	loss	1.62	LRGB	Encodes a plant LrgAB/CidAB protein localized to the chloroplast envelope that is involved in chloroplast development, carbon partitioning, ABA/drought response, and leaf senescence
AT1G33080	CHH	loss	0.82		MATE efflux family protein
AT1G33790	CG	gain	-1.64		jacalin lectin family protein
AT1G34300	CG	loss	-1.42		lectin protein kinase family protein
AT1G35530	CG	gain	1.73	FNACM	highly conserved helicase that functions as a major factor limiting meiotic crossover formation

AT1G42980	CG	loss	-2.26		Actin-binding FH2 (formin homology 2) family protein
AT1G47640	CG	loss	-0.73		seven transmembrane spanning domains
AT1G49500	CHH	loss	-2.98		transcription initiation factor TFIID subunit 1b-like protein
AT1G50180	CG	gain	1.55	CAR1	Host immune receptor
AT1G53680	CG	loss	2.33	ATGSTU28	Encodes glutathione transferase belonging to the tau class of GSTs.
AT1G57650	CHH	loss	-3.61		ATP binding protein
AT1G58190	CG	loss	-5.00	ATRLP9	receptor-like protein 9
AT1G58520	CHH	loss	3.61	RXW8	GDSL-like lipase/acylhydrolase superfamily protein
AT1G61490	CG	gain	-1.11		S-locus lectin protein kinase family protein
AT1G62290	CG	gain	-7.37	ATPASPA2	Saposin-like aspartyl protease family protein
AT1G62310	CG	gain	-1.63	JMJ29	A probable H3K9me2 demethylase
AT1G62560	CHH	loss	3.42	FMO GS-OX3	belongs to the flavin-monooxygenase (FMO) family, encodes a glucosinolate S-oxygenase that catalyzes the conversion of methylthioalkyl glucosinolates to methylsulfinylalkyl glucosinolates
AT1G63260	CG	gain	-0.87	TET10	member of TETRASPANIN family
AT1G63470	CG	gain	1.07	AHL5	AT hook motif DNA-binding family protein;
AT1G63750	CHH	loss	-1.78		miR825-5p target proposed as a phasiRNA producing locus
AT1G66100	CHG	loss	2.13		Predicted to encode a PR (pathogenesis-related) protein
AT1G67980	CG	gain	-5.43	CCOAMT	Encodes S-adenosyl-L-methionine: transcaffeoyl Coenzyme A 3-O-methyltransferase. Methyltransferase in the lignin biosynthetic pathway
AT1G68470	CG	gain	2.12		exostosin family protein
AT1G72180	CG	loss	-1.26	CEPR2	Encodes a leucine-rich repeat receptor kinase that functions as a receptor for CEP1 peptide. Mediates nitrate uptake signaling
AT1G73660	CG	loss	1.16	SIS8	Encodes a protein with similarity to MAPKKKs. May function as a negative regulator of salt tolerance

AT1G75100	CG	loss	1.86	JAC1	Required for the chloroplast accumulation response, but not for the avoidance response. No molecular function known. Influences the composition of photosynthetic pigments, the efficiency of photosynthesis, and the CO2 uptake rate
AT1G77990	CHH	gain	1.26	AST56	A low-affinity sulfate transporter
AT2G02160	CG	loss	-0.77	C3H17	Non-tandem CCCH zinc finger protein
AT2G04305	CG	loss	-0.72		Magnesium transporter CorA-like family protein
AT2G05025	CG	loss	6.36	ATIS112A	AT2TE08160, DNA/Harbinger TE
AT2G05040	CG	loss	2.45	ATGP3	AT2TE08225, LTR/Gypsy TE
AT2G06510	CG	gain	-1.22	RPA1A	Encodes a homolog of Replication Protein A that is involved in meiosis I in pollen mother cells
AT2G07680	CHG	gain	1.70	ABCC13/MRP11	a member of the multidrug resistance associated protein MRP/ABCC subfamily. Its expression is induced by gibberellic acid and downregulated by naphthalene acetic acid, abscisic acid, and zeatin
AT2G11780	CG	loss	-5.66		TE, pseudogene
AT2G13790	CG	loss	-1.65	ATSERK4	Receptor-like protein kinase that plays a role in myriad processes such as cell death, defense response, stomatal movement,and brassinosteroid signalling
AT2G15480	CG, CHH	gain	-1.45	UGT73B5	UDP-glucosyl transferase 73b5
AT2G17570	CG	loss	-0.93	ATCPT1	Cis-prenyltransferase involved in dolichol accumulation.
AT2G20120	CG	gain	-1.24	COV1	Encodes an integral membrane protein of unknown function, highly conserved between plants and bacteria; is likely to be involved in a mechanism that negatively regulates the differentiation of vascular tissue in the stem
AT2G22890	CG, CHH	loss	-2.02		Kua-ubiquitin conjugating enzyme hybrid localization domain-containing protein
AT2G23950	CG	loss	1.33	CIK2	Encodes an LLR receptor kinase that is expressed in protophloem and is required for CLE peptide sensing in roots
AT2G25730	CG	gain	-3.34		zinc finger FYVE domain protein

AT2G32295	CG	gain	1.51		ERD1/XPR1/SYG1 family protein
AT2G32410	CG	loss	1.03	AXL1	Involved in chiasma distribution, affects expression of key DNA repair and meiotic genes, signifcant role in DNA repair
AT2G33240	CG	loss	2.47	ATSID	member of Myosin-like proteins
AT2G34655	CHH	loss	2.59		hypothetical protein
AT2G39140	CG	gain	-1.47	RSUA1	Suppressor of var2 variegation phenotype. Chloroplast localized. Loss of function mutant has defects in chloroplast protein translation and rRNA processing
AT2G39890	CG	gain	1.08	ATPROT1	Encodes a proline transporter with affinity for gly betaine, proline and GABA. Protein is expressed in the vascular tissue, specifically the phloem.
AT2G41640	CG	gain	-1.46	GT61	Glycosyltransferase family 61 protein
AT2G44900	CG	loss	-0.80	ARABIDILLO-1	Promotes lateral root development
AT3G02010	CG	loss	-2.37		Pentatricopeptide repeat (PPR) superfamily protein
AT3G02130	CG	gain	-1.06	RPK2	Functions as a regulator of meristem maintenance
AT3G02170	CG	loss	-1.26	LNG2	Regulates leaf morphology by promoting cell expansion in the leaf-length direction
AT3G10340	CHH	gain	1.45	PAL4	A putative a phenylalanine ammonia-lyase
AT3G12980	CG	loss	-0.95	HAC5	Encodes an enzyme with histone acetyltransferase activity that can use both H3 and H4 histones as substrates
AT3G15290	CG	loss	-0.90		3-hydroxyacyl-CoA dehydrogenase family protein
AT3G15310	CG	loss,gain	7.33	ATSI112A	AT3E21700, DNA/Harbinger TE
AT3G16560	CG	loss	1.10		Protein phosphatase 2C family protein
AT3G17185	CHH	gain	3.66	ATTAS3	Encodes a trans-acting siRNA (tasi-RNA) that regulates the expression of auxin response factor genes (ARF2, ARF4, ETT)
AT3G18820	CG	gain	-1.00	ATRAB7B	Interacts with VPS35 to function as checkpoint in control of traffic towards the vacuole
AT3G18970	CG	loss	-1.70	MEF20	Encodes a pentatricopeptide repeat protein (PPR) protein involved in mitochondrial mRNA editing

AT3G20440	CG	gain	-3.97	BE1	a putative glycoside hydrolase. Involved in organogenesis and somatic embryogenesis by regulating carbohydrate metabolism. Mutation in BE1 has pleotrophic effect on the whole plant development
AT3G20490	CG	gain	1.40	KNO1	Involved in DNA repair
AT3G22420	CG	gain	1.33	WNK2	Member of WNK family protein kinases
AT3G23480	CG	gain	-1.64		Cyclopropane-fatty-acyl-phospholipid synthase
AT3G25130	CHH	gain	2.13		Acidic leucine-rich nuclear phosphoprotein 32 family B protein
AT3G26450	CG	loss	1.00		Polyketide cyclase/dehydrase and lipid transport superfamily protein
AT3G26510	CG	loss	-1.38		Octicosapeptide/Phox/Bem1p family protein
AT3G26980	CG	gain	-1.92	MUB4	membrane-anchored ubiquitin-fold protein 4 precursor
AT3G28080	CHH	gain	1.56	UMAMIT47	nodulin MtN21-like transporter family protein
AT3G28345	CG	gain	4.42	ABCB15	Encodes an ATP-binding cassette (ABC) transporter. Expressed in the vascular tissue of primary stem
AT3G28945	CHG	gain	-2.35	TA11	AT3TE45620, LINE/L1
AT3G44730	CG	gain	1.06	ATKP1	kinesin-like protein 1
AT3G44820	CG	loss	0.84		Phototropic-responsive NPH3 family protein
AT3G45090	CG	gain	1.02		P-loop containing nucleoside triphosphate hydrolases superfamily protein
AT3G46670	CG	loss	1.32	UGT76E11	UDP-glucosyl transferase 73E11
AT3G47800	CHH	loss	-5.34		Galactose mutarotase-like superfamily protein
AT3G48000	CG	gain	-0.80	ALDH2A	Encodes a putative (NAD+) aldehyde dehydrogenase
AT3G48523	CHG, CHH	gain	4.90	ATCOPIA44	AT3TE72850, LTR/Copia
AT3G48630	CHH	gain	-2.87		hypothetical protein
AT3G49142	CG	gain	-2.26		Tetratricopeptide repeat (TPR)-like superfamily protein
AT3G52890	CG	loss	1.00	KIPK	KCBP-interacting protein kinase interacts specifically with the tail region of KCBP
AT3G55980	CG	loss	-3.32	ATSZF1	salt-inducible zinc finger

AT3G56190	CG	gain	-0.90	ASNAP	Encodes one of two alpha-SNAPs (soluble NSF attachment protein) in *Arabidopsis*, involved in SNARE complex disassembly
AT3G56940	CG	loss	0.92	CRD1	Encodes a putative ZIP protein with varying mRNA accumulation in leaves, stems and roots. Has a consensus carboxylate-bridged di-iron binding site
AT3G57410	CG	loss	-1.25	ATVLN3	Encodes a protein with high homology to animal villin. VLN3 is a Ca2+-regulated villin involved in actin filament bundling
AT3G58730	CG	loss	-0.59	VHA-D	Member of V-ATPase family. Vacuolar-type H + -ATPase (V-ATPase) is a multisubunit proton pump located on the endomembranes
AT3G63380	CG	loss	-2.26	AUTO-INHIBITED CA2+ ATPASE 12	ATPase E1-E2 type family protein / haloacid dehalogenase-like hydrolase family protein
AT4G01490	CG, CHH	loss,gain	3.29	ATLINE1_6	AT4TE03295, LINE/L1
AT4G01525	CHH	gain	3.42	SADHU5-1	AT4TE03410, TE
AT4G02350	CG	loss	-1.40	SEC15B	Encodes a member of the exocyst complex gene family. The exocyst is a protein complex involved in tethering vesicles to the plasma membrane during regulated or polarized secretion
AT4G06477	CG	loss	3.52	ATLANTYS1	AT4TE14185, LTR/Gypsy
AT4G09820	CHG	gain	5.06	ATTT8	TT8 is a regulation factor that acts in a concerted action with TT1, PAP1 and TTG1 on the regulation of flavonoid pathways, namely proanthocyanidin and anthocyanin biosynthesis. Affects dihydroflavonol 4-reductase gene expression
AT4G10650	CG	gain	-3.53		P-loop containing nucleoside triphosphate hydrolases superfamily protein
AT4G12440	CHH	loss	5.01	APT4	adenine phosphoribosyl transferase 4
AT4G15790	CG	loss	1.33		uveal autoantigen with coiled coil/ankyrin
AT4G17610	CG	loss	-1.93	ATTRM3	tRNA/rRNA methyltransferase (SpoU) family protein

AT4G21060	CG	gain	0.91	ATGALT2	Encodes an endomembrane system-localized, hydroxyproline-O-galactosyltransferase specific for arabinogalactan-protein biosynthesis
AT4G26850	CG	loss	2.98	GDP-L-GALACTOSE PHOSPHORYLASE	Encodes a novel protein involved in ascorbate biosynthesis, which was shown to catalyze the transfer of GMP from GDP-galactose to a variety of hexose-1-phosphate acceptors. Recessive mutation has a reduced amount of vitamin C, lower level of non-photochemical quenching, and reduced rate of conversion of violaxanthin to zeaxanthin in high light.
AT4G28700	CG	loss	2.68	AMMONIUM TRANSPORTER1;4	ammonium transporter 1
AT4G29010	CG	gain	-1.33	AIM1	Functions in beta-oxidation of fatty acids, similar to CuMFP with L-3-hydroxyacyl-CoA hydrolyase , L-3-hydroxyacyl-dehydrogenase, D-3-hydroxyacyl-CoA epimerase, and 3, 2-enoyl-CoA isomerase activities
AT4G29900	CG	gain	-1.48	ACA10	one of the type IIB calcium pump isoforms. encodes an autoinhibited Ca(2+)-ATPase that contains an N-terminal calmodulin binding autoinhibitory domain
AT4G30090	CG	gain	-1.89		golgin family A protein
AT4G33300	CHH	loss	-1.83	ADRL1-L1	Encodes a member of the ADR1 family nucleotide-binding leucine-rich repeat (NB-LRR) immune receptors
AT4G35420	CG	gain	-1.43	DRL1	A closely related homolog of the rice anther-specific gene OsDFR2. DRL1 may be involved in a metabolic pathway essential for pollen wall development and male fertility
AT4G36910	CG	gain	1.13	CBSX1	Encodes a single cystathionine beta-synthase domain-containing protein. Modulates development by regulating the thioredoxin system
AT4G37100	CG	gain	0.73		Pyridoxal phosphate (PLP)-dependent transferases superfamily protein
AT5G12210	CHH	gain	-0.87	ATRGTB1	Encodes the Rab geranylgeranyl transferase beta subunit that is essential for embryo and seed development
AT5G14270	CG	gain	-1.75	BET9	Bromodomain protein that functions as a negative regulator of sugar and ABA signaling.
AT5G14650	CG	gain	1.49	PGLR	Encodes a cell wall localized endo-polygalacturonase
AT5G17165	CHH	loss,gain	2.66		hypothetical protein

AT5G17300	CG	loss	3.58	RVE1	Myb-like transcription factor that regulates hypocotyl growth by regulating free auxin levels in a time-of-day specific manner
AT5G22920	CG	loss	-6.75	ATRZPF34	Encodes a protein with sequence similarity to RING, zinc finger proteins. Loss of function mutations show reduced (15%) stomatal aperture under non stress conditions
AT5G24270	CHH	gain	-2.10	ATSOS3	encodes a calcium sensor that is essential for K+ nutrition, K+/Na+ selectivity, and salt tolerance
AT5G24380	CG	loss	3.61	ATYSL2	closest *Arabidopsis* homolog of Zea maize metal-phytosiderophore/metal-nicotianamine transporter ZmYS1
AT5G25240	CHH	gain	-2.49		stress induced protein
AT5G25370	CHH	loss	1.93	PHOSPHOLIPASE D ALPHA 3	Member of C2-PLD subfamily, involved in hyperosmotic response
AT5G26360	CG	gain	-0.81	CCT3	TCP-1/cpn60 chaperonin family protein
AT5G28237	CHH	loss	-1.98	CMT2	Encodes a plant DNA methyltransferase that methylates mainly cytosines in CHH contexts
AT5G34790	CHG	gain	1.61		CACTA-like TE
AT5G34800	CHG	loss	1.64	VANDAL20	AT5TE46165, DNA/MuDR TE
AT5G35970	CG	loss	2.10		P-loop containing nucleoside triphosphate hydrolases superfamily protein
AT5G38096	CG	gain	5.17		
AT5G40890	CG	loss	-2.55	ATCLC-A	Encodes a member of the voltage-dependent chloride channel. Also functions as a NO3-/H+ exchanger that serves to accumulate nitrate nutrient in vacuoles
AT5G41750	CHG	gain	-3.05		disease resistance protein (TIR-NBS-LRR class) family
AT5G45660	CG	gain	-1.43		Pseudogene of AT5G38100; methyltransferase-related protein
AT5G47430	CG	gain	-0.69		DWNN domain, a CCHC-type zinc finger
AT5G53550	CG	gain	-1.68	YSL3	YELLOW STRIPE like 3

AT5G54380	CG	gain	-2.16	THESEUS1	a receptor kinase regulated by Brassinosteroids and required for cell elongation during vegetative growth
AT5G59650	CG	gain	-2.16		Leucine-rich repeat protein kinase family protein
AT5G59660	CG	gain	2.23		Leucine-rich repeat protein kinase family protein
AT1G01820	CG	loss	-0.82	PEX11C	Integral to peroxisome membrane, controls peroxisome proliferation
AT1G03090	CG	gain	-2.48	MCCA	MCCA is the biotinylated subunit of the dimer MCCase, which is involved in leucine degradation. Both subunits are nuclear coded, and the active enzyme is located in the mitochondrion
AT1G09910	CG	gain	-1.46		Rhamnogalacturonate lyase family protein
AT1G12000	CG	loss	1.53		Phosphofructokinase family protein
AT1G13245	CHH	loss	-1.72	RTFL17	ROTUNDIFOLIA like 17
AT1G20160	CG	loss	-1.14	SBT5.2	Encodes two isoforms. One (SBT5.2(a)) is a secreted, cell wall localized subtilisin-like serine protease that is involved in regulation of stomatal development. The second isoform (SBT5.2(b) is localized to endosomes
AT1G21810	CG	loss	1.79	VETH2	Encodes a protein that localizes at motile vesicle-like small compartments in differentiating xylem cells that is associated with microtubule plus-ends
AT1G23880	CG	loss	0.94		NHL domain-containing protein
AT1G25350	CG	loss	0.92	OVA9	Glutamine-tRNA ligase, putative / glutaminyl-tRNA synthetase, putative / GlnRS
AT1G25430	CG	loss	-1.48		AT1TE28830, LINE TE
AT1G26762	CHH	gain	-2.35		Transmembrane protein
AT1G27150	CG	gain	-1.80		Tetratricopeptide repeat (TPR)-like superfamily protein
AT1G27470	CG	loss	2.18		transducin family protein / WD-40 repeat family protein
AT1G27880	CG	loss	2.26		DEAD/DEAH box RNA helicase family protein
AT1G53780	CG	gain	-1.37		26S proteasome regulatory complex ATPase
AT1G53840	CG	loss	-0.80	ATPME1	Encodes a pectin methyltransferase
AT1G55320	CG	loss	1.50	AAE18	Encodes a protein with similarity to acyl activating enzymes. AAE18 is localized to the peroxisome where it may be involved in metabolism of auxin precursors to active auxins

AT1G56280	CG	gain	-2.42	DIL9	Encodes a gene whose transcript level in root and leaves increases to progressive drought stress. The increase in transcript level is independent from abscisic acid level. Sequence is not similar to any protein of known function. It appears to be a member of plant-specific gene family. It's phosphorylated by AtCPK11 in a Ca(2+)-dependent manner at Thr105 and Ser107 within the AtDi19 bipartite nuclear localization signal
AT1G58190	CG	gain	-4.08	RLP9	Receptor-like protein 9
AT1G61860	CG	loss	2.02	PBL41	Protein kinase superfamily protein
AT1G62540	CG, CHH	loss, gain	1.86	FMO GS-OX2	belongs to the flavin-monooxygenase (FMO) family, encodes a glucosinolate S-oxygenase that catalyzes the conversion of methylthioalkyl glucosinolates to methylsulfinylalkyl glucosinolates
AT1G75700	CG	gain	-2.89	HVA22G	HVA22-like protein G
AT1G76705	CG	loss	-2.79		calmodulin binding protein
AT1G77030	CG	loss	2.34	RH29	Required for functional maturation of male and female gametophytes
AT1G77310	CG	loss	1.89	UBN2	wound-responsive family protein
AT1G79150	CHH	gain	2.73	ATNOC3	Nucleolar complex binding protein
AT2G15890	CG	loss	-3.39	CBP1	a regulator of transcription initiation in central cell-mediated pollen tube guidance
AT2G22710	CG	loss	-2.15		Transposable element (guard cell)
AT2G29065	CG	gain	-1.26		GRAS family transcription factors
AT2G34655	CHH	gain	1.34		Hypothetical protein
AT2G41510	CG	loss	-2.01	ATCKX1	encodes a protein whose sequence is similar to cytokinin oxidase/dehydrogenase, which catalyzes the degradation of cytokinins. Acts on zeatin 9-riboside-50-triphosphate substrate
AT2G46730	CG	loss	-0.97		pseudogene of galacturonosyltransferase-like protein
AT3G01770	CG	gain	-1.36	GTE11	Global transcription factor, Bromodomain protein that functions as a negative regulator of sugar and ABA signaling
AT3G02070	CG	gain	-0.68		Cysteine proteinases superfamily protein
AT3G05932	CG	gain	-0.93		Potential natural antisense gene, locus overlaps with AT3G05930

AT3G06530	CG	loss	3.29		ARM repeat superfamily protein
AT3G07750	CG	gain	2.68	RRP42	3-5 exoribonuclease family protein
AT3G10770	CG	loss	-1.20		Single-stranded nucleic acid binding R3H protein
AT3G12145	CHH	loss	1.68	FLOR1	A novel leucine-rich repeat protein. Interacts directly with MADS domain transcription factor.
AT3G17050	CG	loss	-1.84		Pseudogene, TE
AT3G18524	CG	loss	0.96	ATMSH2	Encodes a DNA mismatch repair homolog of human MutS gene, MSH6. MSH2 is involved in maintaining genome stability and repressing recombination of mismatched heteroduplexes
AT3G19370	CG	gain	2.20		filament-like protein (DUF869)
AT3G20100	CG	loss	-1.39	CYP705A19	Cytochrome P450 from family CYP705A
AT3G20200	CG	loss	1.93		kinase with adenine nucleotide alpha hydrolases-like domain-containing protein
AT3G22300	CG	loss	1.51	RPS10	Nuclear-encoded gene for mitochondrial ribosomal small subunit protein S10
AT3G23085	CHH	gain	-3.90		hAT-like transposase family, TE
AT3G23510	CG	loss	3.25		Cyclopropane-fatty-acyl-phospholipid synthase
AT3G23640	CG	gain	-1.92	HGL1	heteroglycan glucosidase 1
AT3G27940	CG	gain	-1.04	LBD26	LOB domain-containing protein 26
AT3G28945	CG, CHH	gain	-2.36	TA11	AT3TE45620, LINE/L1 TE
AT3G29180	CG	loss	-1.22		DUF1336 family protein
AT3G30842	CG	gain	-5.50	ABCG38	ATP-binding cassette G38, pleiotropic drug resistance 10
AT3G43600	CG	loss	1.69	AAO2	Encodes an aldehyde oxidase. AAO2 does not appear to act on abscisic aldehyde in vitro but it is possible that it may function in abscisic acid biosynthesis when the activity of At2g27150 (AAO3), the primary abscisic aldehyde oxidase, is lost
AT3G46370	CG	loss	-1.58		Leucine-rich repeat protein kinase family protein

AT3G46670	CG	gain	1.46	UGT76E11	UDP-glucosyl transferase 76E11
AT3G47340	CG	loss	-5.30	ASN1	encodes a glutamine-dependent asparagine synthetase, the predicted ASN1 peptide contains a purF-type glutamine-binding domain, and is expressed predominantly in shoot tissues, where light has a negative effect on its mRNA accumulation.
AT3G48720	CHH	loss/gain	-1.24	DCF	Encodes a hydroxycinnamoyl-CoA: v-hydroxy fatty acid transferase involved in cutin synthesis
AT3G48780	CG	loss	-0.91	ATSPT1	Encodes one of the two LCB2 subunits (LCB2a and LCB2b) of serine palmitoyltransferase, an enzyme involved in sphingolipid biosynthesis. LCB2a and LCB2b are functional redundant
AT3G49230	CHH	gain	6.28	DEG1	Transmembrane protein
AT3G57630	CG	loss	1.38	EXAD	Encodes a glycoprotein glycosyl transferase ExAD. Knockout mutants show truncated root hair phenotype
AT3G57660	CG	loss	2.54	NRPA1	Encodes a subunit of RNA polymerase I
AT3G59020	CG	loss	0.73		ARM repeat superfamily protein
AT4G01190	CG	loss	1.84	PIP5K11	Type I phosphatidylinositol-4-phosphate 5-kinase, subfamily A. Preferentially phosphorylates PtdIns4P
AT4G01440	CG	loss	1.39	UMAMIT31	nodulin MtN21-like transporter family protein
AT4G01700	CG	gain	1.82		Chitinase family protein
AT4G02960	CG	loss	4.85	ATRE2	a copia-type retrotransposon element containing LTRs and encoding a polyprotein
AT4G03560	CG	loss/gain	-1.24	ATCCH1	Encodes a depolarization-activated Ca(2+) channel
AT4G04360	CG	loss	-0.91	ELMO3	transmembrane protein, putative (DUF1068)
AT4G08390	CG	gain	1.76	SAPX	Encodes a chloroplastic stromal ascorbate peroxidase Sapx
AT4G10580	CHH	gain	-3.84	ATGP1	AT4TE27915, LTR/Gypsy TE
AT4G17140	CG	gain	-1.92		pleckstrin homology (PH) domain-containing protein
AT4G23540	CG	loss	1.86		ARM repeat superfamily protein

AT4G25630	CG	loss	4.37	FIB2	encodes a fibrillarin, a key nucleolar protein in eukaryotes which associates with box C/D small nucleolar RNAs (snoRNAs) directing 2'-O-ribose methylation of the rRNA.
AT4G26940	CG	loss	0.87	CAGE2	Putative beta 1,3-galactosyltransferase that acts redundantly with CAGE1 during primary and secondary cell wall biosynthesis
AT4G30690	CG	gain	-1.93	ATIF3-4	Ribosome disassembly in chloroplast, cytoplasm, cell wall, and plasma membrane
AT4G39210	CG	gain	1.85	APL3	Encodes the large subunit of ADP-Glucose Pyrophosphorylase which catalyzes the first, rate limiting step in starch biosynthesis
AT4G39280	CG	loss	1.00		phenylalanyl-tRNA synthetase, putative / phenylalanine-tRNA ligase
AT5G02840	CG	loss	-1.78	RVE4	a homolog of the circadian rhythm regulator RVE8, involved in heat shock response
AT5G11790	CG	gain	2.07	NDL2	Plays a role in dehydration stress response
AT5G14050	CG	loss	2.48		Transducin family protein / WD-40 repeat family protein
AT5G15470	CG	gain	0.81	GAUT14	Encodes a protein with putative galacturonosyltransferase activity
AT5G16410	CG	loss	-2.88		HXXXD-type acyl-transferase family protein
AT5G23380	CG	loss	-2.51		hypothetical protein (DUF789)
AT5G25240	CHH	gain	2.26		Stress induced protein
AT5G25560	CG	gain	-0.98		CHY-type/CTCHY-type/RING-type Zinc finger protein
AT5G27030	CG	gain	1.27	TRP3	TOPLESS family member involved in the negative regulation of SNC1-dependent phenotypes
AT5G28237	CG	loss/gain	2.63		Pyridoxal-5-phosphate-dependent enzyme family protein
AT5G38140	CG	loss	-0.79	NF-YC12	nuclear factor Y, subunit C12. Involved in regulation of transcription
AT5G41260	CG	gain	-1.95	BSK8	BRASSINOSTEROID-SIGNALING KINASE 8, kinase with tetratricopeptide repeat domain-containing protein
AT5G48880	CG	loss	3.03	PKT1	Encodes a peroxisomal 3-keto-acyl-CoA thiolase 2 precursor. EC2.3.1.16 thiolases
AT5G49580	CG	gain	-0.63		Chaperone DnaJ-domain superfamily protein
AT5G50940	CG	loss	-1.73		RNA-binding KH domain-containing protein

AT5G54100	CG	gain	2.15	ATSLP2	SPFH/Band 7/PHB domain-containing membrane-associated protein family
AT5G55480	CG	loss	1.08	GDPDL4	Glycerophosphoryl diester phosphodiesterase-like protein involved in cell wall cellulose accumulation and pectin linking. Impacts root hair, trichome and epidermal cell development
AT5G63550	CG	loss	0.92		DEK domain-containing chromatin associated protein
AT5G10250	CG	gain	-2.38	DOT3	Encodes a protein with an N-terminal BTB/POZ domain and a C-terminal NPH3 family domain. dot3 mutants have defects in shoot and primary root growth and produce an aberrant parallel venation pattern in juvenile leaves.

Table S4: List of photosynthetic-related genes used for mining of RNA sequencing data

GENE CODE	ABBREVIATION
AT1G01060	LHY
AT1G02340	HFR1/REP1
AT1G64860	SIG
AT2G20570	GLK1/2
AT2G25930	ELF3/4
AT2G36270	ABI5
AT2G37678	FHY1/FHL
AT2G39730	RCA
AT2G40080	ELF3/4
AT2G43010	PIF4/5
AT2G46790	PRR
AT3G01500	CA1
AT3G03450	DELLA
AT3G06483	PDK
AT3G17609	HY5/HYH
AT3G53920	SIG
AT3G54620	BZIP25
AT4G36730	GBF1
AT5G02810	PRR
AT5G03720	HSFA
AT5G11260	HY5/HYH
AT5G11670	NADP-ME2
AT5G24120	SIG
AT5G28770	BZIP63
AT5G38410	RBCS3B
AT5G39610	ORE1
AT5G56860	GNC/CGA1
AT5G61380	TOC1
AT2G05070	LHCB2.2
AT3G08940	LHCB4.2
AT3G27690	LHCB2.4
AT1G80280	HYDROLASE, A-B
AT1G44446	CAO
AT5G54270	LHCB3
AT5G35490	MRU1
AT5G48490	LTP
AT4G27440	PORB
AT1G15820	LHCB6
AT2G42540	COR15A
AT1G76100	PLASTOCYANIN

AT2G39030	GNAT FAMILY
AT3G56940	CRD1
AT2G42220	RHODANESE-LIKE DOMAIN
AT2G35260	BCM1
AT2G34430	LHCB1.4
AT4G05180	PSBQ2
AT1G68190	ZINC FINGER FAMILY
AT1G05085	HYPOTHETICAL PROTEIN
AT4G32800	ABI4
AT5G62000	ARF2
AT3G16857	ARR
AT4G31920	ARR
AT2G25180	ARR
AT1G49190	ARR
AT1G01720	ATAF1
AT4G16780	ATHB2
AT2G44910	ATHB4
AT1G75080	BZR1
AT1G19350	BZR2
AT2G46830	CCA1
AT4G34530	CIB
AT5G48560	CIB
AT3G07340	CIB
AT1G10120	CIB
AT1G26260	CIB
AT5G37190	CIP4
AT4G27430	CIP7
AT1G29160	COG1
AT4G23750	CRF2
AT1G14920	DELLA
AT2G01570	DELLA
AT1G66350	DELLA
AT3G20770	EIN3/EIL1
AT2G27050	EIN3/EIL2
AT1G18330	EPR1
AT4G15090	FAR1
AT3G22170	FHY3
AT5G02200	FHY1/FHL
AT3G13960	GRF5
AT5G44190	GLK1/2
AT4G26150	GNC/CGA1
AT1G32330	HSFA

AT2G26150	HSFA
AT1G26945	KDR
AT4G25560	LAF1
AT1G32640	MYC2
AT5G20730	ARF7(NPH4)
AT3G55370	OBP3
AT5G48150	PAT1
AT2G20180	PIF1
AT1G09530	PIF3
AT3G59060	PIF4/5
AT2G46970	PIL1/2
AT3G62090	PIL1/2
AT5G60100	PRR
AT5G24470	PRR
AT5G35210	PTM
AT1G32230	RCD1
AT1G08540	SIG
AT5G13730	SIG
AT2G36990	SIG
AT1G27730	ZAT10
AT3G21175	ZML1
AT1G51600	ZML2
AT1G67090	RBCS1A
AT2G28000	
AT3G04550	RAF1
AT4G04330	RBCX1
AT4G27600	NARA5
AT5G38420	RBCS2B
AT5G38430	RBCS1B
AT5G51110	SDIRIP1
AT2G47400	CP12-1
AT3G62410	CP12-2
AT1G76560	CP12-3
AT3G26650	GAPA
AT3G55800	SBPASE
AT5G46110	APE2
AT1G42960	GAPB
AT1G43670	ATCFBP
AT5G35790	G6PD1
AT5G40760	G6PD6
AT1G24280	G6PD3
AT5G13110	G6PD2

AT5G26751	SK11
AT1G03680	TRX-M1
AT4G03520	TRXM2
AT3G02730	TRXF1
AT5G16400	TRXF2
AT5G42980	TRXH3
AT5G39950	TRXH2
AT3G08710	TRXH9

Table S5: Raw data for overlaps in photosynthetic genes (see Table S2) with RNAseq data.) represents where no log2FC was seen at the cut off of 0.5. *p-adj<0.05, n=3*

Gene	SQHvSQL	FLHvFLL	SQHvFLH	SQLvFLL
AT1G01060	0	-8.16237	7.18597	0
AT1G02340	0	0	-2.63934	0
AT1G64860	0	-1.59728	1.299956	0
AT2G20570	0	-0.84017	1.147865	0
AT2G25930	0	0	-3.61615	-2.3308
AT2G36270	0	0	-3.25662	0
AT2G37678	0	0	-2.50891	0
AT2G39730	0	-1.8336	1.62851	0
AT2G40080	0	0	-4.93568	-4.76683
AT2G43010	0	0	-1.95969	0
AT2G46790	0	-3.24966	2.999301	0
AT3G01500	0	0	1.843175	0
AT3G03450	0	-3.51097	3.569479	0
AT3G06483	0	0	-0.83417	0
AT3G17609	0	0	3.470579	0
AT3G53920	0	-0.83299	1.003498	0
AT3G54620	0	0	-1.10057	0
AT4G36730	-0.84817	0	-1.26595	0
AT5G02810	0	0	-0.80587	0
AT5G03720	0	2.328598	-2.56924	0
AT5G11260	0	-2.66581	2.6411	0
AT5G11670	0	0	-2.01082	0
AT5G24120	0	-3.1886	3.537145	0
AT5G28770	-2.36326	0	-2.21106	0
AT5G38410	0	-1.18926	1.361976	0
AT5G39610	0	0	-3.95258	0
AT5G56860	0	-2.20149	1.812306	0
AT5G61380	0	2.199197	-4.44559	0
AT2G05070	0	-1.46944	0	0
AT3G27690	0	-3.04477	1.982501	0
AT1G80280	0	-2.15096	2.151435	0
AT1G44446	0	-1.77321	1.222085	0
AT5G48490	-3.23022	-4.04212	0	0
AT2G42540	0	4.614446	0	3.740651
AT3G56940	0	-1.17322	0.921517	0
AT2G34430	0	0	-3.13535	0
AT4G32800	0	2.77571	0	0
AT1G19350	0	-0.82906	0	-0.94789
AT2G46830	0	-5.7643	5.140496	0
AT4G27430	0	0	1.043669	0
AT1G66350	0	0	0	-1.35107

AT3G20770	0	0	-1.10142	0
AT1G18330	0	0	-1.15549	0
AT5G44190	0	-1.24243	0	0
AT1G26945	0	-1.71519	0	0
AT1G32640	1.933862	0	0	0
AT5G48150	0	0	0	-1.33438
AT4G04330	0	0	-4.88257	-2.7321
AT5G38420	0	0	1.842029	0
AT2G47400	0	0	-0.77174	0
AT1G76560	0	0	-1.94323	0
AT3G26650	0	-1.43045	0	0
AT3G55800	0	0	1.696628	0
AT5G40760	0	0	0	1.361307
AT5G13110	0	0	1.48659	1.260598
AT5G26751	0	0	-0.71611	0
AT4G03520	0	0	-0.54877	0